

FenFlux: The Short Term Climate  
Response of Carbon Dioxide and Methane  
Fluxes from a Regenerating and a  
Semi-Natural Fen in East Anglia  
United Kingdom

---

Thesis submitted for the degree of

Doctor of Philosophy

at the University of Leicester

by

Gong Pan (MSc.)

Department of Geography

University of Leicester

2017

This work was carried out under the supervision of:

**Dr. Jörg Kaduk**

Senior Lecturer in Physical Geography

Department of Geography, University of Leicester, United Kingdom

**Prof. Heiko Balzter**

Professor of Physical Geography

Director of the Centre for Landscape and Climate Research

Holder of the Royal Society Wolfson Research Merit Award

Holder of the Royal Geographical Society's Cuthbert Peek Award

Department of Geography, University of Leicester, United Kingdom

**Prof. Susan Page**

Professor of Physical Geography

Department of Geography, University of Leicester, United Kingdom

“路漫漫其修远兮，吾将上下而求索”

“The road ahead will be long; our climb will be steep;  
I shall search step by step”

Extracts from “Li Sao (The Lament)” by Qu Yuan (340 - 278 B.C.)

To my parents, my wife (张亮霞) and my son (Jemmy)

# Abstract

FenFlux: The Short Term Climate Response of Carbon Dioxide and Methane Fluxes from a Regenerating and a Semi-Natural Fen in East Anglia, United Kingdom

Gong Pan

---

Peatlands store ~30% of global soil organic carbon (SOC) and are frequently carbon dioxide (CO<sub>2</sub>) sinks, while also being sources of methane (CH<sub>4</sub>) due to anaerobic decomposition under waterlogged soil conditions. Hence, the role of peatlands in the radiative forcing of the Earth's atmospheric system and their impact on the global climate system is complex. This study presents the first long-term direct flux measurements of land-atmosphere CO<sub>2</sub> and CH<sub>4</sub> exchange at a temperate lowland fen peatland in East Anglia, UK. The dynamics and magnitude of CO<sub>2</sub>, H<sub>2</sub>O, CH<sub>4</sub> and energy fluxes were quantified using the eddy covariance (EC) technique at two sites: a former-arable regenerating site (Baker's Fen, BF) and a semi-natural fen (Sedge Fen, SF) at Wicken Fen NNR. This allowed investigation and comparison of ecosystem responses to climate variability and restoration. EC measurements at BF covered three annual cycles (2013 - 2015), and at SF two and a half cycles (August 2013 - December 2015). BF acted as a net CO<sub>2</sub> source in all years, emitting  $161.03 \pm 12.51$ ,  $83.61 \pm 11.53$  and  $98.39 \pm 13.31$  g CO<sub>2</sub>-C m<sup>-2</sup>yr<sup>-1</sup> in 2013, 2014 and 2015, respectively; it was a net CH<sub>4</sub> source of  $6.067 \pm 0.096$  g CH<sub>4</sub>-C m<sup>-2</sup>yr<sup>-1</sup> in 2013 and  $2.009 \pm 0.087$  g CH<sub>4</sub>-C m<sup>-2</sup>yr<sup>-1</sup> in 2015, and of  $2.845 \pm 0.103$  g CH<sub>4</sub>-C m<sup>-2</sup> (8<sup>th</sup> April - 31<sup>st</sup> December 2014). The annual carbon balance for BF was lower than average carbon losses from arable fens, indicating that restoration can achieve net carbon emissions reduction. SF was also a net CO<sub>2</sub> source of  $297.59 \pm 9.16$  g CO<sub>2</sub>-C m<sup>-2</sup> (1<sup>st</sup> August - 31<sup>st</sup> December 2013), and a large net CO<sub>2</sub> sink of  $-356.86 \pm 49.13$  g CO<sub>2</sub>-C m<sup>-2</sup>yr<sup>-1</sup> in 2014 and of  $-243.78 \pm 15.25$  g CO<sub>2</sub>-C m<sup>-2</sup>yr<sup>-1</sup> in 2015. Large inter-annual variability in CO<sub>2</sub> exchange at SF indicates sensitivity to climatic conditions, and highlights the need to maintain an appropriate water level height to prevent or reduce soil carbon losses to the atmosphere as CO<sub>2</sub>.

# Acknowledgements

Firstly, I would like to express my deepest appreciation to my supervisors, Dr. Jörg Kaduk, Prof. Heiko Balzter and Prof. Susan Page for the patient guidance, incessant encouragement and wisdom that you provided throughout. I'm grateful for the free and creative environment you provided during my Ph.D. research. I really enjoyed working with you and won't forget the interesting discussions and crazy field trips with you.

My Ph.D. project benefited from quite a lot of help by many people; the project would have been a "mission impossible" without you guys. Especially I would like to thank Alex Cumming and Simon Benson for all your support, efforts and humour during field work, rain or shine, summer or winter. I also want to thank Adam Cox for assisting with raw data management, and providing solid computer technical support. I greatly appreciate and acknowledge all the assistance given by the department technical team and general office, Bill Hickin, Gary Hancox, Gemma Black, Gemma Ollerenshaw, Vanessa Greasley and Charlotte Langley. It is you who made my days so much easier!

Huge thanks to Prof. Håkan Rydin and Dr. Gustaf Granath from Uppsala University (Sweden) for bringing me to the world of peatland; I miss the snow, the mires, the *Sphagnum*, the *Fika* and all the memories of Sweden. Many thanks to Dr. Jiahong Li from LI-COR Ltd. (U.S.A.) for pointing me the right way to get familiar with the instruments and providing lots of useful advice for data processing. I'm grateful that Dr. Marta Galvagno shared her experiences with wavelet coherence analysis and EC measurement during her Ph.D. research. Thanks to Prof. QuanFa Zhang, Prof. XiaoLi Cheng, Prof. GuiRui Yu, Prof. ShuLi Niu, Dr. HaiQiang Guo and Dr. XianJin Zhu from the Chinese Academy of Science (CAS) for sharing experiences in carbon flux research in China, and inviting me to the 10<sup>th</sup> Ecology Seminar in Fudan University (Shanghai, China). Many thanks to Prof. XiaoLi Cheng, Dr. YanChang Wang and Dr. XianJin Zhu for comments on the thesis draft.

Thanks to Dr. Michael Peacock from the Open University for all your help and interesting discussions during field trip encounters. I also would like to express my sincere appreciation to the staff and volunteers from the National Trust (NT) at Wicken Fen NNR for helping with various things along the way. Especially, many thanks to John Bragg for providing hourly water level data from the NT installed dip-wells on both study sites and maps of Wicken Fen NNR, and allowing me to use these data in my dissertation. Many thanks to Martin Lester, Carol Laidlaw and John Hughes from the NT for all your continual support and assistance with instrument maintenance.

I also would like to thank Dr. Jon Kelvin, Prof. Michael Acreman and Prof. Richard J. Harding from the Centre of Ecology and Hydrology (CEH, UK) for building the EC system and initiating the research at Sedge Fen, and continual support throughout my project. Thanks also to Dr. Ross Morrison (CEH, UK) for sharing experiences from his previous work. I am grateful for the guidance of and discussions with many colleagues working in the DEFRA-funded lowland peatland GHG emissions project.

I was glad to meet many carbon flux people at the 5<sup>th</sup> annual flux course at Niwot Ridge, U.S.A. in 2012. Special thanks to Prof. Russel Monson, Dr. David Moore and Dr. Paul Stoy for hosting the interesting course and providing such a unique opportunity to join the community. It was my honour to have interesting talks with Prof. Dennis Baldocchi and Dr. George Burba during the flux course. I won't forget the lovely cabin, night talks and beer at the mountain station. Also thanks to my supervisors for providing the means for me to join the course. I also would like to thank Prof. Nigel Roulet, Prof. Juul Limpens, Prof. Mats Nilsson and Prof. Patrick Crill for giving me quite a lot of useful advice for my Ph.D. during the "Carbon dynamics and exchange in peatlands" course at Umeå, Sweden in summer 2012.

This project was supported by the DEFRA grant SP1210 "Lowland peatland systems in England and Wales - evaluating greenhouse gas fluxes and carbon balances" and equipment was funded by the Department of Geography, University of Leicester. My PhD. was funded by a studentship from College of Science, University of Leicester. The scholarship also supported training courses and conferences. I'm also grateful for

the efforts of my supervisor Dr. Jörg Kaduk and the DEFRA project for funding the field trips.

Personally, I would like to give a big hug to all my fellows from the CLCR family (Centre for Landscape and Climate Research, UoL), especially thanks Dr. Virginia Nicola-Perea for taking care of all of us. Thanks to David Ackerley, Dr. Bashir Adamu, Dr. Paul Arellano, Dr. Beth Cole, Alex Cumming, Dr. Prem Pandey, Dr. Pedro Rodriguez-Veiga, Hao Wang and Dr. James Wheeler for making me feel like at home, sharing experiences and all the support.

Finally and the most importantly, I want to say a simple word THANK YOU to my family and friends far away in China. This thesis is dedicated to my beloved parents, my wife and my son, my mates in Wuhan and my Leicester families. I would never have been able to start, never mind finish my Ph.D. without your love, your give, your sacrifice, and your patience.

**Thank you all!**

**由衷感谢!**

**潘功**

# Table of Contents

<b>Abstract</b> .....	<b>i</b>
<b>Acknowledgements</b> .....	<b>ii</b>
<b>Table of Contents</b> .....	<b>v</b>
<b>List of Figures</b> .....	<b>ix</b>
<b>List of Tables</b> .....	<b>xii</b>
<b>List of Acronyms and Abbreviations</b> .....	<b>xiii</b>
<b>Chapter 1</b>	
<b>Introduction and Thesis Overview</b> .....	<b>1</b>
1.1. Research Context .....	2
1.2. Research Aims and Specific Objectives .....	9
1.3. Research Questions .....	10
1.4. Thesis Structure.....	11
<b>Chapter 2</b>	
<b>Peatland and Climate Change</b> .....	<b>15</b>
2.1. Carbon Storage in Peatland Ecosystems .....	16
2.1.1. Peatland Ecosystems.....	16
2.1.2. Plant Diversity in Peatland Ecosystems.....	18
2.1.3. The Global Peat Carbon Store .....	18
2.2. Carbon Cycling in Peatlands.....	20
2.2.1. Peatlands and Greenhouse Gases.....	20
2.2.2. Net Ecosystem Carbon Dioxide Exchange in Peatlands .....	22
2.2.3. Land-atmosphere Methane Exchange in Peatlands .....	24
2.2.4. Dissolved Organic Carbon in Peatlands .....	27
2.2.5. Water Budget in Peatlands.....	29
2.3. Response of Peatlands to Environmental Changes .....	32
2.4. Related Research.....	34
2.5. Summary .....	37
<b>Chapter 3</b>	

<b>Study Sites .....</b>	<b>39</b>
3.1. Wicken Fen .....	40
3.1.1. Wicken Fen National Nature Reserve .....	40
3.1.2. History of Wicken Fen.....	44
3.1.3. Conservation and Restoration at Wicken Fen.....	46
3.2. Study Site One: Baker's Fen .....	48
3.3. Study Site Two: Sedge Fen .....	50
3.4. Summary .....	52
<b>Chapter 4</b>	
<b>Methods, Data Collection and Processing .....</b>	<b>54</b>
4.1. The Eddy Covariance System .....	55
4.1.1. Eddy Covariance Theory .....	55
4.1.2. Quality Control .....	62
4.1.3. Data Gap-filling .....	62
4.1.4. Flux Partitioning .....	63
4.1.5. Energy Balance Closure.....	64
4.2. Instrumentation .....	65
4.2.1. Instrumentation at Baker's Fen.....	65
4.2.2. Instrumentation at Sedge Fen .....	68
4.2.3. Output Variables of Instruments.....	71
4.3. Data Processing and Analysis .....	73
4.3.1. Software .....	73
4.3.2. Eddy Covariance Data Processing .....	73
4.3.3. Quality Control .....	75
4.3.4. Data Coverage.....	77
4.3.5. Data Gap-filling and Partitioning .....	79
4.3.6. Uncertainty Estimation for Annual Sums.....	80
4.3.7. Energy Balance Closure.....	81
4.3.8. Regression Analysis of Environmental Factors.....	83
4.3.9. Light Response Curves .....	84
4.3.10. Multi-scale Analysis of Environmental Controls .....	85
4.4. Summary .....	87
<b>Chapter 5</b>	

<b>Short-term Climate Response of Carbon Dioxide and Methane Fluxes in a Regenerating Fen (Baker’s Fen).....</b>	<b>88</b>
5.1. Environmental Conditions at Wicken Fen Nature Reserve .....	89
5.1.1. Meteorology.....	89
5.1.2. Ground Water Levels at Baker’s Fen .....	97
5.2. Temporal Dynamics of Carbon Fluxes at Baker’s Fen.....	100
5.2.1. Wind Rose Plots.....	100
5.2.2. Fingerprint Plots .....	102
5.2.3. Mean Diurnal Patterns .....	105
5.2.4. Seasonal Trends in Daily Carbon Budgets .....	109
5.2.5. Annual Carbon Budgets.....	114
5.3. Response of Carbon Flux to Major Environmental Factors.....	118
5.3.1. Effects of Environmental Factors .....	118
5.3.2. Light Response Curves .....	120
5.3.3. Multi-scale Analysis of Environmental Controls on CO <sub>2</sub> Fluxes.....	123
5.4. Discussion and Conclusion .....	126
5.4.1. EC Measurement Performance .....	126
5.4.2. Carbon Dioxide Fluxes .....	127
5.4.3. Methane Fluxes.....	134
<b>Chapter 6</b>	
<b>Short-term Climate Response of Carbon Dioxide Fluxes in a Semi-natural Fen (Sedge Fen) .....</b>	<b>137</b>
6.1. Environmental Conditions .....	138
6.1.1. Ground Water Levels at Sedge Fen .....	138
6.2. Temporal Dynamics of Carbon Fluxes .....	140
6.2.1. Wind Rose Plots.....	140
6.2.2. Fingerprint Plots .....	142
6.2.3. Mean Diurnal Patterns .....	145
6.2.4. Seasonal Trends in Daily Carbon Budgets .....	148
6.2.5. Annual Carbon Dioxide Budget .....	152
6.3. Response of Carbon Flux to Environmental Factors .....	156
6.3.1. Effects of Environmental Factors .....	156
6.3.2. Light Response Curves .....	158

6.3.3.	Multi-scale Analysis of Environmental Controls .....	161
6.4.	Discussion and Conclusion .....	165
6.4.1.	EC Measurement Performance .....	165
6.4.2.	Carbon Dioxide Fluxes .....	166
<b>Chapter 7</b>		
<b>Comparison of Carbon Dioxide Fluxes between Two Temperate Lowland Fens with Different Land-use Types .....</b>		
		<b>170</b>
7.1.	Environmental Conditions .....	171
7.1.1.	Ground Water Levels.....	171
7.2.	Seasonal Patterns of Carbon Dioxide Fluxes .....	173
7.3.	Annual Carbon Dioxide Budget.....	179
7.4.	Discussion and Conclusion .....	180
<b>Chapter 8</b>		
<b>Conclusions, Research Limitations and Outlook.....</b>		<b>186</b>
8.1.	Thesis Conclusions.....	187
8.2.	Research Limitations and Future Research Outlook.....	191
8.2.1.	Ancillary Measurements .....	191
8.2.2.	Other Carbon and GHG Fluxes .....	192
8.2.3.	Station Maintenance .....	193
8.2.4.	Spatial Heterogeneity and Representativeness .....	193
8.2.5.	Up-scaling of Observation Results .....	194
<b>Reference .....</b>		<b>195</b>

# List of Figures

<b>Figure 1:</b> Peat and peaty soil of United Kingdom. Peat map is based on the Hydrology of Soil Types classification. ....	4
<b>Figure 2:</b> Annual average precipitation in United Kingdom from 1981 to 2010.....	6
<b>Figure 3:</b> Precipitation anomalies for the year 2011 in UK comparing to 1971 - 2000 annual average.....	7
<b>Figure 4:</b> Sections and subsections comprising the thesis structure. ....	12
<b>Figure 5:</b> Simplified conceptual diagram of carbon cycling in peatland ecosystem. ....	22
<b>Figure 6:</b> Conceptual diagram of the net carbon balance in peatland ecosystem.....	24
<b>Figure 7:</b> A conceptual diagram of methane fluxes in peatland ecosystems.....	26
<b>Figure 8:</b> A conceptual model of DOC production.....	28
<b>Figure 9:</b> Generalized peatland water budget. ....	31
<b>Figure 10:</b> A recent map of Wicken Fen Vision plan and the adjacent area of Wicken Fen.....	41
<b>Figure 11:</b> An old map of Wicken Fen. ....	42
<b>Figure 12:</b> Map of Wicken Fen. ....	43
<b>Figure 13:</b> Konik Pony at Baker's Fen and Highland Cattle at Baker's Fen .....	47
<b>Figure 14:</b> A view at Baker's Fen from the south-west (dominant wind direction) to the flux station with Highland Cattle standing on the site.....	49
<b>Figure 15:</b> A view at Sedge Fen to the west (dominant wind direction) from the top of the flux tower... ..	50
<b>Figure 16:</b> a) Schematic representation of the surface layer above a homogeneous land surface divided into inertial sub-layer and roughness sub-layer; b) Schematic representation of the eddy covariance tower and the control volume with which the expression of the gas exchange is determined .....	56
<b>Figure 17:</b> Footprint of Baker's Fen eddy covariance site. ....	66
<b>Figure 18:</b> Setup of the EC station at Baker's Fen.....	67
<b>Figure 19:</b> Footprint of Sedge Fen eddy covariance site .....	68
<b>Figure 20:</b> Setup of the AWS at Sedge Fen .....	69
<b>Figure 21:</b> Setup of the EC station at Sedge Fen.....	71
<b>Figure 22:</b> Data coverage for different periods in different years .....	78
<b>Figure 23:</b> Energy balance closure for Baker's Fen .....	81
<b>Figure 24:</b> Energy balance closure for Sedge Fen .....	82
<b>Figure 25:</b> Monthly meteorological variables.....	92
<b>Figure 26:</b> Comparison of cumulative monthly precipitation during 2013 to 2015 against the 1981 to 2010 average. ....	95
<b>Figure 27:</b> Comparison of ground water levels at Baker's Fen. ....	97
<b>Figure 28:</b> Comparison of groundwater levels at Baker's Fen during measurement period .....	99

<b>Figure 29:</b> Distribution of direction and source strength of the measured (non-gap-filled) net ecosystem CO <sub>2</sub> exchange (NEE, left panels) and methane (CH <sub>4</sub> , right panels) fluxes in different years during the measurement period (2013 to 2015) at Baker's Fen .....	101
<b>Figure 30:</b> Net ecosystem CO <sub>2</sub> exchange (NEE, top panels), air temperature (T <sub>air</sub> , lower left), and photosynthetic photon flux density (PPFD, lower right) at Baker's Fen during the measurement period (2013 to 2015) .....	104
<b>Figure 31:</b> Comparison of monthly mean diurnal cycles of net ecosystem CO <sub>2</sub> exchange (NEE) and CH <sub>4</sub> fluxes at Baker's Fen during measurement period (2013 - 2015). .....	107
<b>Figure 32:</b> Seasonal change in daily CO <sub>2</sub> and CH <sub>4</sub> budget and environmental variables at Baker's Fen during the measurement period (2013 to 2015). .....	110
<b>Figure 33:</b> Annual cumulative net ecosystem CO <sub>2</sub> exchange (NEE) at Baker's Fen during measurement period (2013 to 2015), with cumulative daily range as uncertainties. ....	114
<b>Figure 34:</b> Annual cumulative net ecosystem CO <sub>2</sub> exchange (NEE), ecosystem respiration (R <sub>eco</sub> ) and gross primary production (GPP) .....	115
<b>Figure 35:</b> Annual cumulative CH <sub>4</sub> fluxes at Baker's Fen during measurement period (2013 to 2015)..	116
<b>Figure 36:</b> Light response curves of GPP plotted for different months during the growing season from 2013 to 2015 at Baker's Fen .....	122
<b>Figure 37:</b> Wavelet coherence analysis between gross primary production (GPP) and photosynthetic photon flux density (PPFD) during the measurement period (2013 to 2015) at Baker's Fen .....	124
<b>Figure 38:</b> Wavelet coherence analysis between gross primary production (GPP) and air temperature (T <sub>air</sub> ) during the measurement period (2013 to 2015) at Baker's Fen. ....	125
<b>Figure 39:</b> Wavelet coherence analysis between gross primary production (GPP) and vapour pressure deficit (VPD) during the measurement period (2013 to 2015) at Baker's Fen. ....	125
<b>Figure 40:</b> Wavelet coherence analysis between ecosystem respiration (R <sub>eco</sub> ) and vapour pressure deficit (VPD) during the measurement period (2013 - 2015) at Baker's Fen .....	126
<b>Figure 41:</b> Monthly water level range 1994 - 2008 (grey) and 2013 (yellow), 2014 (blue), 2015 (red) monthly mean water levels relative to the fen surface measured at SF dipwell NW07 .....	139
<b>Figure 42:</b> Mean daily position of water levels relative to the fen surface measured at SF dipwell NW07. ....	140
<b>Figure 43:</b> Distribution of direction and source strength of the measured (non-gap-filled) net ecosystem CO <sub>2</sub> exchange (NEE) in separate years during the measurement period (2013 to 2015) at Sedge Fen. .	141
<b>Figure 44:</b> Fingerprint plots of net ecosystem CO <sub>2</sub> exchange (top panels), air temperature (lower left), and global radiation (R <sub>g</sub> , lower right) at Sedge Fen during the measurement period (August 2013 to 2015). .....	143
<b>Figure 45:</b> Comparison of monthly mean diurnal cycles of net ecosystem CO <sub>2</sub> exchange at Sedge Fen during measurement period (August 2013 to 2015). .....	146
<b>Figure 46:</b> Seasonal change in daily CO <sub>2</sub> budget and environmental variables at Sedge Fen during the measurement period (August 2013 to 2015). .....	150

<b>Figure 47:</b> Annual cumulative net ecosystem CO <sub>2</sub> exchange (NEE) at Sedge Fen in 2014 and 2015, with cumulative daily range as uncertainties. ....	153
<b>Figure 48:</b> Annual cumulative net ecosystem CO <sub>2</sub> exchange (NEE), ecosystem respiration (R <sub>eco</sub> ) and gross primary production (GPP). ....	154
<b>Figure 49:</b> light response curves of GPP plotted for different months during the growing season from August 2013 to 2015 at Sedge Fen .....	160
<b>Figure 50:</b> Wavelet coherence analysis between gross primary production (GPP) and photosynthetic photon flux density (PPFD) during the measurement period (August 2013 to 2015) at Sedge Fen.....	162
<b>Figure 51:</b> Wavelet coherence analysis between gross primary production (GPP) and air temperature (T <sub>air</sub> ) during the measurement period (August 2013 to 2015) at Sedge Fen. ....	163
<b>Figure 52:</b> Wavelet coherence analysis between gross primary production (GPP) and vapour pressure deficit (VPD) during the measurement period (August 2013 to 2015) at Sedge Fen .....	164
<b>Figure 53:</b> Wavelet coherence analysis between ecosystem respiration (R <sub>eco</sub> ) and vapour pressure deficit (VPD) during the measurement period (August 2013 to 2015) at Sedge Fen.....	164
<b>Figure 54:</b> Ground water levels at Baker's Fen and Sedge Fen during measurement period. ....	172
<b>Figure 55:</b> Comparison of monthly total net ecosystem CO <sub>2</sub> exchange (NEE), ecosystem respiration (R <sub>eco</sub> ) and gross primary production (GPP).....	174
<b>Figure 56:</b> Comparison of accumulative net ecosystem CO <sub>2</sub> exchange (NEE), ecosystem respiration (R <sub>eco</sub> ) and gross primary production (GPP).....	177

# List of Tables

<b>Table 1:</b> Main theoretical assumptions for eddy covariance theory .....	58
<b>Table 2:</b> Summary of main processing procedures for calculation fluxes from raw eddy covariance data .....	60
<b>Table 3:</b> General comparison between eddy covariance method and chamber techniques .....	61
<b>Table 4:</b> Main output variables from all the instruments which have been used in this study in EC system. ....	72
<b>Table 5:</b> Data coverage for different period in year .....	78
<b>Table 6:</b> Monthly total gross primary production, ecosystem respiration and net ecosystem CO <sub>2</sub> exchange estimated for Baker’s Fen during measurement period (2013 to 2015). ....	112
<b>Table 7:</b> Monthly total methane flux at Baker’s Fen during measurement period (2013 to 2015) .....	113
<b>Table 8:</b> CO <sub>2</sub> -equivalent comparison based on GWP for measurement period 2013 - 2015 at Baker’s Fen .....	117
<b>Table 9:</b> Pearson coefficients (r) of fluxes (NEE, GPP, R <sub>eco</sub> and F <sub>CH4</sub> ) on environmental factors at Baker’s Fen .....	117
<b>Table 10:</b> Stepwise regression analysis of fluxes (NEE, GPP, R <sub>eco</sub> and F <sub>CH4</sub> ) against significantly related environmental factors at Baker’s Fen .....	117
<b>Table 11:</b> Comparison of annual carbon dioxide budgets for managed and restored temperate and boreal peatlands with permanent vegetation cover reported in literature. ....	129
<b>Table 12:</b> Monthly total gross primary production, ecosystem respiration and net ecosystem CO <sub>2</sub> exchange estimated for Sedge Fen during measurement period (August 2013 to 2015). ....	151
<b>Table 13:</b> The comparison of carbon balance at Sedge Fen during the measurement period.....	155
<b>Table 14:</b> Pearson coefficients (r) of fluxes (NEE, GPP and R <sub>eco</sub> ) on environmental factors at Sedge Fen .....	155
<b>Table 15:</b> Stepwise regression analysis of fluxes (NEE, GPP and R <sub>eco</sub> ) against significantly related environmental factors at Sedge Fen. ....	175
<b>Table 16:</b> Comparison of monthly total gross primary production, ecosystem respiration and net ecosystem CO <sub>2</sub> exchange between Baker’s Fen and Sedge Fen during measurement period. ....	175
<b>Table 17:</b> The comparison of carbon balance between Baker’s Fen and Sedge Fen during the measurement period. ....	178
<b>Table 18:</b> Potential changes in soil carbon storage resulting from land use change.....	183

# List of Acronyms and Abbreviations

AGC	Parameter of cleanness of the LI-7500A optical path
amsl	Above mean sea level
ATP	Adenosine triphosphate
AWS	Automatic Weather Station
BF	Baker's Fen
C	Carbon
CH <sub>4</sub>	Methane
CH <sub>2</sub> O	Carbohydrate
CLCR	Centre for Landscape and Climate Research (University of Leicester)
CO	Carbon monoxide
CO <sub>2</sub>	Carbon dioxide
DIC	Dissolved Inorganic Carbon
DOC	Dissolved Organic Carbon
EBC	Energy Balance Closure
EC	Eddy Covariance
ET	Evapotranspiration
G	Soil heat flux
GEP	Gross Ecosystem Photosynthesis
GHG	Greenhouse gas
GMT	Greenwich Mean Time
GPP	Gross Primary Production
GWI	Ground Water Inflow
GWO	Ground Water Outflow
GWP	Global Warming Potential
ha	Hectare
H	Sensible heat flux
H <sub>2</sub> O	Water vapour
HOST	Hydrology of Soil Types classification
Hz	Hertz
IPCC	Intergovernmental Panel on Climate Change
IRGA	Infrared Gas Analyser
LE	Latent heat flux

LiDAR	Light Detection and Ranging
Ltd.	Limited company
LUT	Look Up Tables method
MAD	Median Absolute Deviation
MDC	Mean Diurnal Cycle
MDS	Marginal Distribution Sampling
MDV	Mean Diurnal Variation
MODIS	Moderate Resolution Imaging Spectrometer
N	Nitrogen
NECB	Net Ecosystem Carbon Budget
NEE	Net Ecosystem Exchange
NEP	Net Ecosystem Production
NGO	Non-Governmental Organisations
NIR	Near-infrared
NNR	National Nature Reserve
NOAA	National Oceanic and Atmospheric Administration (USA)
N <sub>2</sub> O	Nitrous oxide
NPP	Net Primary Production
NT	The National Trust
NVC	National Vegetation Classification
O <sub>2</sub>	Oxygen
O <sub>3</sub>	Ozone
P	Precipitation
PAR	Photosynthetically Active Radiation
PBL	Planetary Boundary Layer
PC	Particulate Carbon
POC	Particulate Organic Carbon
PPFD	Photosynthetic Photon Flux Density
PSI, PSII	Photosystem I, II
QC	Quality Control
QCL	Quantum Cascade Laser
QF	Quality Flags
$R_{eco}$	Ecosystem respiration
$R_g$	Global radiation
$R_n$	Net radiation
$RH$	Relative humidity
$s$	Mixing ratio of the interest gas
SAT	Sonic Anemometer Title
SD	Standard Deviation
SF	Sedge Fen

SO <sub>4</sub>	Sulphate ion
SOC	Soil Organic Carbon
SOM	Soil Organic Matter
SSSI	Site of Special Scientific Interest
SWI	Surface Water Inflow
SWO	Surface Water Outflow
$T_{air}$	Air temperature
TDL	Tuneable Diode Laser spectrometer
$u$	Mean horizontal wind speed
$u^*$	Friction velocity
UK	The United Kingdom
UNFCCC	United Nations Framework Convention on Climate Change
UoL	The University of Leicester
v	Volts
VOC	Volatile Organic Carbon
VPD	Vapour Pressure Deficit
W	Watts
$w$	Vertical wind speed
WPL	Webb, Pearman and Leuning correction
WT	Water Table
$X_{max}$	Peak footprint distance from tower
$Z_m$	EC tower measurement height
3-D	3 dimensions

***Greek Letters***

$\alpha$	Ecosystem apparent quantum yield
$\rho_a$	Air density
$\rho_c$	Gas density
$\Delta S$	Energy storage in the ecosystem

# **Chapter 1**

## **Introduction and Thesis Overview**

## 1.1. Research Context

Peatlands are wetland ecosystems that store approximately 30% of global soil carbon (C) stocks and are, in a natural state, frequently carbon dioxide (CO<sub>2</sub>) sinks (Strack, 2008). At the same time, they are a source of methane (CH<sub>4</sub>) to the atmosphere because of reduced rates of aerobic decomposition in a perennially waterlogged soil environment (Baird *et al.*, 2009). It is recognized that peatlands have a significant role in the global C balance and climate regulation (Charman, 2002). However, peatland ecosystems are also particularly sensitive to climate change.

The atmospheric concentration of greenhouse gases (GHGs) has been increased significantly by human activities since 1850 (i.e. by 30% for CO<sub>2</sub>, 150% for CH<sub>4</sub> and 17% for N<sub>2</sub>O) which has caused an enhanced global warming effect of the Earth (Bonan, 2008; IPCC, 2014a; Walther *et al.*, 2002). It is suggested that the major contributions toward anthropogenic GHG emissions are fossil fuel combustion and land management / land use change (Canadell *et al.*, 2010; Raupach & Canadell, 2010). The global surface temperature increased by  $0.74 \pm 0.18$  °C during 1906 - 2005 (Trenberth *et al.*, 2007), while Solomon *et al.* (2007) predict that, by 2100, the global surface temperature rise could reach 1.4 to 5.8 °C. Anthropogenic changes to peatland ecosystems and the resulting changes in GHG fluxes (e.g. Roulet, 2000; Sirin *et al.*, 2008; Turetsky *et al.*, 2002) can make a contribution to the observed increase in the concentration of GHGs in the atmosphere and, thereby, to global climatic change.

Peatland ecosystems are vulnerable to a range of land use pressures, including drainage, agriculture, forestry, peat harvesting and fire (Joosten & Clarke, 2002; Page *et al.*, 2002). As a result, for example, a large quantity of C is now being released to the atmosphere in the form of CO<sub>2</sub> due to the drainage of peatland following a long period of historical accumulation (Couwenberg, 2011; Couwenberg *et al.*, 2011). Changes in climate and land use can alter the hydrology of peatlands, local geomorphology, and vegetation production and subsequently the vegetation cover of the peat surface

(Limpens *et al.*, 2008), therefore, reducing or reversing the peatland C sink capacity (Oechel *et al.*, 2000; Page *et al.*, 2011). There is also concern that current and future global warming caused by modern human activities can drive a C storage loss in peatlands, leading to large C emissions into the atmosphere (Charman, 2002). As a result, peatland ecosystems have a significant influence on past, present and future climates due to climate feedbacks associated with GHG emissions into the atmosphere and their role in global warming (Denman *et al.*, 2007).

Peatland ecosystems are the largest semi-natural ecosystem and terrestrial C store in the UK, storing up to  $3200 \pm 300$  Mt C, and hosting a variety of nationally important species and habitats (Smith *et al.*, 2007) (Figure 1). They are also crucially important for biodiversity and other ecosystem services (Wilson & Carpenter, 1999). However, 10 Mt CO<sub>2</sub>-C yr<sup>-1</sup> are lost to the atmosphere from the UK's damaged peatlands (i.e. as a result of drainage, agriculture, forestry, peat harvest and burning) (Worrall *et al.*, 2011). On the global scale, it is estimated that some 500,000 km<sup>2</sup> of degraded peatlands emit around 2 Gt CO<sub>2</sub>-C yr<sup>-1</sup> due to drainage, fire and peat extraction (Joosten, 2009).

Fens are minerotrophic peatlands of global importance for huge storage of soil C and high biodiversity (Lamers *et al.*, 2002). Lowland fen peatlands in England occupy 958 km<sup>2</sup>, store large amounts of C and are subject to very high levels of land use pressure because of their high agricultural productivity (Thompson, 2008). Drained fen peatland is among the most profitable and productive soil types in the UK (Morris *et al.*, 2000; 2010). Therefore, in England, nearly all of the original fens have been drained and cultivated for intensive agricultural land use (Baird *et al.*, 2009). In the fenland region of East Anglia (The Fens), this has resulted in an oxidative loss of peat at a rate of about 1 cm yr<sup>-1</sup> (Thompson, 2008).



Schöfl *et al.*, 2011). Thus, more study of the detailed effects of peatland rewetting on the GHG emissions over the longer term is needed.

To gain a better quantitative understanding of the relationships between climate variability and peatland ecosystems, accurate measurements of GHG fluxes are needed to compile a full ecosystem C and energy balance. In recent decades researchers have tried to measure C, water and energy fluxes between ecosystems and the atmosphere by using different techniques, such as the chamber technique, eddy covariance method, and remote sensing techniques (Baldocchi, 2003; Lee *et al.*, 2004). The results of these on-going studies have the potential to inform future conservation and restoration policies for peatland ecosystems.

On UK peatlands, to date, most measurements of GHG fluxes have been collected on upland blanket bogs (mainly located in the northern and central parts of the country). However, there is a lack of quantitative evidence on the C fluxes on lowland temperate fen ecosystems (Couwenberg, 2011; Teh *et al.*, 2011). Moreover, very limited data exist on C flux for any types of fen ecosystem that are undergoing restoration following intensive arable land use (Baird *et al.*, 2009). There is also a concern about whether the research findings on blanket bog GHG fluxes (both degraded and restored) can simply be assumed to apply to lowland fens, since there are very large differences between the two ecosystems in terms of vegetation, the physical and chemical characteristics of the peat soil, hydrology, climate and land use. Therefore, this lack of data and knowledge of the large areas of degraded lowland temperate fen ecosystems in the country must be systematically addressed.

The fenland region of East Anglia contains the largest contiguous area of temperate lowland fens in the British Isles (Baird *et al.*, 2009). The area is one of the driest regions of the UK (Figure 2). It also is under great pressure from the agricultural sector and from an increasing population, both of which place a demand on available water resources (Anglian Water, 2007). Moreover, in 2012, the inherent variability of the climate of England and Wales was unusually extreme which emphasised the impact that climatic irregularities can pose for peatland restoration schemes in this part of the UK. From April 2010 to March 2012, large parts of southern, central and eastern

England (especially lowland England) were declared to be experiencing one of the ten most significant droughts of one- to two-years duration in the last 100 years (Kendon *et al.*, 2013) (Figure 3). The drought led to visible impacts on the lowland peat soils in the Fens, where road surfaces started to crack due to peat contraction. However, in spring 2012 the prolonged severe drought was dramatically terminated by the wettest April to July period over England and Wales in almost 250 years (Parry *et al.*, 2013). The unusual hydrological climate in the last few years provides an opportunity to investigate the impacts of climate variability on the GHG emissions from lowland fenland ecosystems in the UK which is the central objective of this thesis.

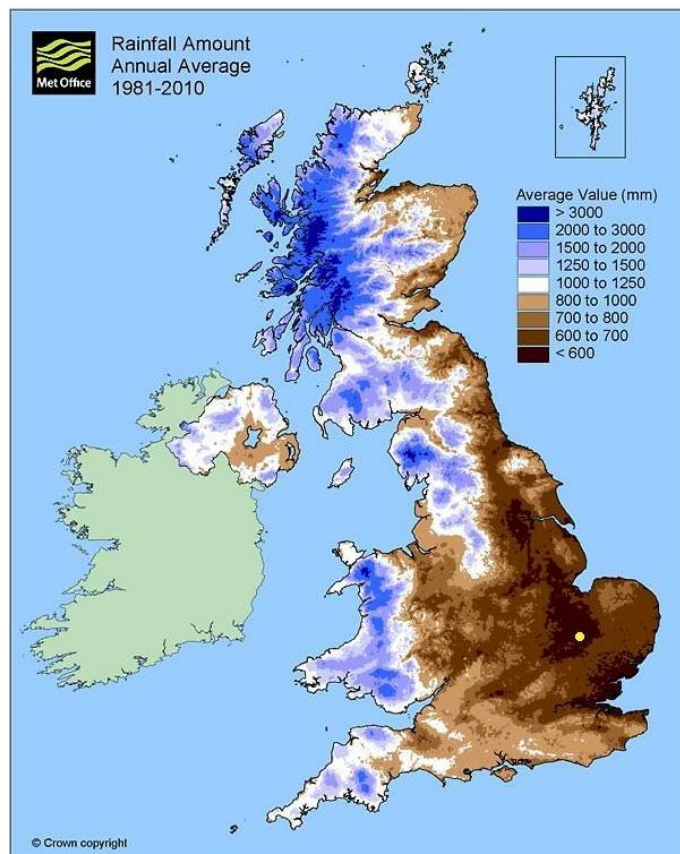


**Figure 2:** Annual average precipitation in United Kingdom from 1981 to 2010. The map also indicates the location of the study site (Wicken Fen) with the yellow dot (edited from Met Office UK actual climate maps, for more information see: <http://www.metoffice.gov.uk/climate/uk/summaries/anomacts> ).

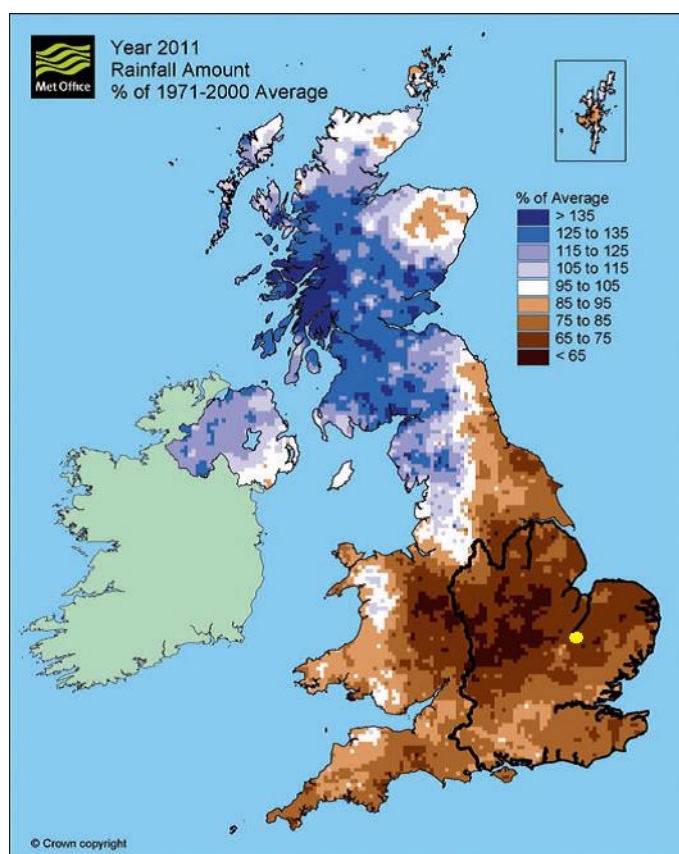


**Figure 3:** Precipitation anomalies for the year 2011 in UK comparing to 1971 - 2000 annual average, also delineating 'Lowland England' area in solid black line, the yellow dot indicates the location of the study site (Wicken Fen) (Kendon et al., 2013; edited from Met Office UK climate anomaly maps, for more information see: <http://www.metoffice.gov.uk/climate/uk/summaries/anomacts> ).

Two study sites were identified in the Fenland region of East Anglia. The first study site is located at Baker's Fen (BF). This is a rewetting temperate lowland fen located at Wicken Fen National Nature Reserve (NNR). It has been drained and was formerly under intensive agricultural use from around the mid-19<sup>th</sup> Century. The peat soils of the study site are highly degraded compared to the semi-natural areas in the same nature reserve owing to drainage and agricultural cropping which have promoted peat oxidation. The site has undergone restoration by the landowner, the National Trust (NT), since 1995 who undertook ditch blocking to raise the ground water table. During the restoration, it was replanted with several locally common graminoid species. Since 2003, the site has been subject to conservation grazing by Konik ponies and Highland cattle that are free-roaming over the site and the neighbouring area of the Adventurer's Fen.

The second study site is located close-by in the same fenland landscape on the Wicken Fen NNR. Sedge Fen (SF) is a near-pristine temperate lowland fen, a remnant of the former East Anglia floodplain fens in the UK, which has never been drained or used for agriculture or peat extraction. SF lies about 2 m above the adjacent drained farmland where BF is located, with peat lost due to compaction and wastage. There are numerous ditches (lodes) around / on the site; therefore the SF is hydrologically isolated because of the management regime with the ditches. The NT installed a wind mill in 2011 to supply (pump) minerotrophic water from the Wicken Lode to the site. The dominant species of SF are giant sword sedge (*Cladium mariscus*) together with common reed (*Phragmites australis*). Both species can typically be found in waterlogged environments, and both can supply oxygen internally to their root systems and, by the same passive diffusion process, transport CH<sub>4</sub> to the atmosphere. The fen vegetation has historically been harvested commercially and is currently being harvested in sections every 3 or 4 years for conservation purposes. This vegetation management regime produces a mosaic of vegetation stands of varying ages, and arrests the natural process of ecosystem succession towards scrub and woodland.

In earlier scientific studies, most biosphere-atmosphere exchange measurements in ecological studies relied on chamber enclosure techniques. The chamber technique uses a sealed chamber that is gas tight to the atmosphere to calculate the flux rate of non-reactive gaseous compounds by monitoring changes in concentration over time (enrichment or depletion) in the enclosure (Livingston & Hutchinson, 1995). The data obtained from studies using chamber techniques are limited in terms of continuity, repeatability and measurement period. In the last few decades, micrometeorological techniques have been introduced into geophysical and ecological research, including the flux-gradient method, the mass balance technique, and the eddy covariance method. Among these micrometeorological methods, the eddy covariance (EC) technique is considered to be one of the most direct tools for quantifying vertical exchanges of trace gases, energy and water between the atmosphere and biosphere at an ecosystem scale, providing continuous long-term measurements without introducing significant measurement artefacts (Baldocchi, 2003). Long-term measurements make it possible to detect not only daily variations but also seasonal and inter-annual variations of C fluxes in response to environmental conditions (Lee *et al.*, 2004). Recently, globally, EC has

become one of the main and standard flux measurement methods (Aubinet *et al.*, 2012). FluxNet, the global long-term flux micrometeorological measurement network, has been established in order to evaluate C, water and energy exchange dynamics in different ecosystems and to co-ordinate global scale studies for synthesis and modelling (Baldocchi *et al.*, 2001a).

In 2009, the Centre for Landscape and Climate Research (CLCR) / Department of Geography, University of Leicester (UoL), along with the Centre for Ecology and Hydrology (CEH, Wallingford) established two EC towers, with one located at BF and one at SF. These were the first such measurement stations to be installed on temperate lowland fen peatlands in the UK. A third EC tower has subsequently been installed on fenland used for horticultural production; this is in the northern Fens, on the Norfolk and Lincolnshire border, some 40 km north from Wicken Fen NNR. Thus, a complete GHG flux measurement system for UK lowland fens has been established, covering three different temperate lowland fen ecosystems under different land uses and hydrological conditions (i.e. regenerating fen, semi-natural fen, and agricultural fen).

## 1.2. Research Aims and Specific Objectives

The FenFlux project is a collaborative project between the University of Leicester and the CEH, Wallingford. The aim of the FenFlux project, to which this study contributes, is to understand the climate change impact on lowland peatland C stocks, and the response of CO<sub>2</sub> / CH<sub>4</sub> and energy fluxes to seasonal / inter-annual climatic and hydrological variability. Moreover, the research programme aims to investigate whether the lowland peatland ecosystem functions as a net CO<sub>2</sub> / CH<sub>4</sub> sink or source according to different land management conditions (i.e. regenerating and semi-natural).

Specifically, the main objectives of this thesis are to (i) quantify the CO<sub>2</sub> and CH<sub>4</sub> exchanges between the two different types of fen ecosystems and the atmosphere, and investigate their daily, seasonal and inter-annual variability using the EC technique; (ii) determine the role of seasonal and inter-annual climatic variability (e.g. temperature,

hydrology, ecosystem soil and plant processes *etc.*) on CO<sub>2</sub> and CH<sub>4</sub> fluxes in lowland fen ecosystems; (iii) assess the effect of land use changes (specifically restoration) on C cycling in fen peatlands. However, the CH<sub>4</sub> measurement instruments on SF were supported by another funding source. Therefore, the results of the CH<sub>4</sub> measurements on SF will be published in a collaboration paper (i.e. Kaduk *et al.*, 2015) but not in this thesis.

### 1.3. Research Questions

In light of the general research context described and the objectives detailed in the previous sections, this thesis seeks to address the following research questions with reference to lowland fens in the East Anglian region of the UK.

- i. What is the magnitude of land / atmosphere CO<sub>2</sub> and CH<sub>4</sub> exchanges at the rewetting (regenerating) ex-arable site? Does this site function as either a net CO<sub>2</sub>/ CH<sub>4</sub> sink or source during the measurement period? Does this site present a positive or negative radiative forcing to the atmosphere?
- ii. What is the diurnal, seasonal and annual pattern of land / atmosphere CO<sub>2</sub> and CH<sub>4</sub> exchange at the rewetting (regenerating) ex-arable site? What are the main environmental drivers influencing the land / atmosphere CO<sub>2</sub> and CH<sub>4</sub> exchanges at this site?
- iii. What is the magnitude of land / atmosphere CO<sub>2</sub> exchange at the semi-natural (near-pristine) site? Does this site function as a net CO<sub>2</sub> sink or source during the measurement period? Does this site present a positive or negative radiative forcing to the atmosphere?
- iv. What is the diurnal, seasonal and annual pattern of land / atmosphere CO<sub>2</sub> exchange at the semi-natural (near-pristine) site? What are the main environmental drivers influencing the land / atmosphere CO<sub>2</sub> exchange at this site?

- v. Based on the results, what is the likely impact of land use change on land / atmosphere CO<sub>2</sub> exchange at lowland fen ecosystems?

The outcomes of this research will provide an improved understanding of the role of lowland temperate fen ecosystems in terms of the UK's terrestrial C budget. The results will help understand the impact of land-use type on the C balance of lowland fen peatland ecosystems and highlight which climatic / hydrological factors play an important role in influencing the C budget, thereby providing information to support policy making on land management and ecosystem restoration to mitigate land-based GHG emissions.

## 1.4. Thesis Structure

The chapters in this thesis are grouped into three sections (Figure 4). The first section including chapters one through four presents the general research context and background information, introduces the study sites, also describes the methodology employed in the research, and outlines the underlying theory. The following section, chapters five and six, present and discuss the results of the research undertaken at the two study sites. Chapter seven presents and discusses the results of the comparison study of the two sites. The last section, chapter eight provides a summary of the research described in the thesis, highlighting the main achievements and concluding with the key findings and recommendations for future research arising from the findings of this study.

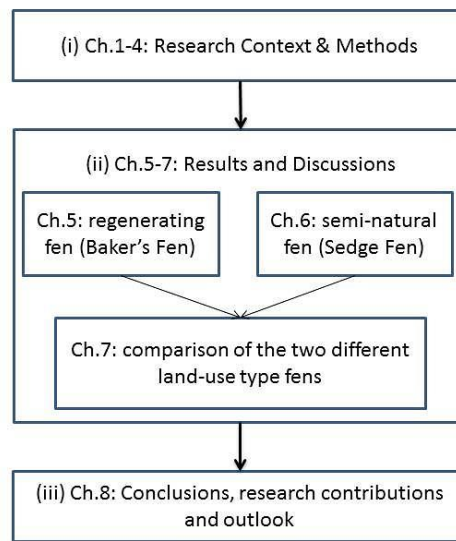


**Figure 4:** Sections and subsections comprising the thesis structure.

**Chapter 1. Introduction and Thesis Overview**

This chapter presents the general context, background and the broader field of the study, outlines the thesis structure, and brings out the research questions. The aims and objectives of the thesis are clarified as well.

**Chapter 2. Peatland and Climate Change**

This chapter gives an introduction to peatland ecosystems, especially peatlands in the UK, as well as providing a conceptual understanding of the role of peatlands in the natural climate system and the impact of environmental changes (climate changes and anthropogenic effects) on peatland ecosystem C cycling. Ecosystem restoration on peatlands is also discussed in this chapter.

**Chapter 3. Study Sites**

This chapter provides an introduction to the Wicken Fen NNR where this study was undertaken. The history of and the vegetation on the site are described, and the

ecosystem restoration activities are presented. This provides an intensive understanding of the whole study area to gain a clear picture of the study locations, namely Baker's Fen (BF) and Sedge Fen (SF).

#### ***Chapter 4. Methods, Data Collection and Processing***

This chapter describes the measurement instruments and methods employed in this study to collect the data upon which subsequent analyses are based. It also gives an introduction to the underlying theory of the methodology - eddy covariance. The flux data processing routines, quality control, statistical analyses, gap filling and all aspects relating to the manipulation of the data are presented as well.

#### ***Chapter 5. Short-term climate response of carbon dioxide and methane fluxes in a regenerating fen (Baker's Fen)***

This chapter presents the seasonal and inter-annual dynamics and magnitude of land / atmosphere CO<sub>2</sub> and CH<sub>4</sub> exchanges at a rewetting ex-arable lowland temperate fen (BF), and addresses research questions 1 and 2.

#### ***Chapter 6. Short-term climate response of carbon dioxide fluxes in a semi-natural fen (Sedge Fen)***

In this chapter, the seasonal and inter-annual dynamics and magnitude of land / atmosphere CO<sub>2</sub> exchange at a semi-natural lowland temperate fen (SF) are analysed, and research questions 3 and 4 are addressed.

#### ***Chapter 7. Comparison of carbon dioxide fluxes between two temperate lowland fens with different land-use types***

This chapter compares the influence of the two different land-use types of temperate lowland fen on the dynamics and magnitude of land / atmosphere CO<sub>2</sub> exchange under similar climate conditions over the same period, and addresses research question 5.

## ***Chapter 8. Conclusions, Research Limitations and Outlook***

This chapter provides a synopsis of the thesis work, highlighting the main achievements, summarising the key findings, and a critical review of the research describing the limitation *etc.* in the study. Recommendations for future research arising from the study are also included in the last chapter.

## **Chapter 2**

# **Peatland and Climate Change**

## 2.1. Carbon Storage in Peatland Ecosystems

### 2.1.1. Peatland Ecosystems

Peatland ecosystems are unique wetland ecosystems in which slow accumulation of peat has occurred due to incomplete decomposition of plant litter under more or less water-saturated conditions (Rydin & Jeglum, 2013). Long-term or seasonal inundated conditions create the poorly aerated soil with low soil temperature amplitude and the anoxic conditions preferred by anaerobic bacteria (Holden *et al.*, 2004). Peat formation is the accumulation of organic material due to incomplete decomposition of plant debris (i.e. litter fall, dead roots; Rydin *et al.*, 1999). However, due to the slow decomposition and compaction processes, the net peat accumulation rate is only about 0.5 to 1 mm yr<sup>-1</sup> in the northern hemisphere (Quinty & Rochefort, 2003). Therefore, deep peat soil formation is the result of thousands of years of decomposition and compaction processes.

Normally, peatlands can be classified into two main ecosystem types (fens and bogs) based on hydrological and nutrient gradients. Fens (minerotrophic peatlands) are a type of peatland with a water table close to the surface, which are fed by precipitation together with surface runoff water. As a result, they can be rich in base cations (alkaline), and have relatively high pH (4 - 8.5) (Glenn *et al.*, 2006; Sonnentag *et al.*, 2010). Fen ecosystems can be further classified along the pH gradient as poor (pH 4 - 5), intermediate (pH 5 - 6), rich (pH 6 - 7) and extremely rich (pH 7 - 8.5) fens (Worrall *et al.*, 2011). Fens often support a relatively high diversity of vegetation species (Baird *et al.*, 2009); with the dominant peat forming species changing from mosses to vascular plant communities along the fen pH gradient (Pan, 2010). In the UK, the most common types of fens are basin and floodplain fens (Baird *et al.*, 2009).

Another type of peatland - bogs are ombrotrophic peatlands with a peat surface that is above and isolated from ground water, and which can only receive water and nutrients from rainfall and atmospheric inputs, creating a plant species and mineral poor

ecosystem, also lower in pH (3.5 - 4). Peat mosses (*Sphagnum* spp.) are the dominant peat forming species on bogs (Granath *et al.*, 2010; Rydin *et al.*, 1999). Bog ecosystems can be further classified as raised (lowland) and blanket (upland) bogs (Baird *et al.*, 2009).

In peatlands, the slow accumulation of peat soil deposits gradually raises the surface vegetation above the influence of groundwater, altering the environmental conditions of the substrate and changing the vegetation distribution. Moreover, some bog species of peat moss (*Sphagnum* spp.) also can acidify the environment to favour themselves over the vascular plants by producing an acid decay-resistant litter and forming a drier habitat (Pan, 2010; van Breemen, 1995). These autogenic factors cause a slow and unidirectional transition, expressed as the typical peatland ecosystem succession, from a fen community gradually to a bog environment (Granath *et al.*, 2010). Therefore, the water level plays an important role in peatland ecosystem succession (Rydin, 1985). However, this ecosystem succession also can be reversed due to water level changes by allogenic processes (i.e. climate change, rewetting management) (Hughes & Dumayne-Peaty, 2002; Magyari *et al.*, 2001).

In comparison with other terrestrial ecosystems (e.g. forests, grasslands), peatlands are minor terrestrial ecosystems that only cover an estimated 400 million ha, which accounts for about 3% of the Earth's total land surface (Gorham, 1991). Yet their role in C storage and land surface GHG exchange exceeds that of these other systems. They are estimated to store up to one third of the global soil C pool (300 - 600 Pg C; Turunen *et al.*, 2002). The distribution of peatland ecosystems is closely associated with the hydrological climate, depending on the balance between precipitation and evaporation. Thus, climate is a major determinant of the distribution and character of peatland ecosystems, determining the location and diversity of the peatlands in the world (Tanneberger & Wichtmann, 2011). Most peatlands occur in the boreal zone of the northern hemisphere, mainly in North America, Russia and Northern Europe. For example, peatlands cover 11% of Canadian territory (Quinty & Rochefort, 2003). There are significant amounts of tropical peatlands (30 - 45 million ha) occurring in Southeast Asia, the Caribbean, Central America and Southern China, while temperate peatlands

are distributed more sparsely in Central Europe and Asia, mostly in low-lying areas (Page *et al.*, 2011; Strack, 2008).

### 2.1.2. Plant Diversity in Peatland Ecosystems

Peatlands exhibit highly characteristic ecological traits, hosting a variety of globally important species and habitats. Therefore peatland ecosystems are of global importance for biodiversity and comprise a wide spectrum of rare, threatened and endangered plants, animals and habitats (Tanneberger & Wichtmann, 2011).

Peatland ecosystems have a narrow range of environmental conditions; many species in peatlands are peatland specialists and therefore have restricted distributions (Gunnarsson *et al.*, 1999). Because of the low nutrient availability as well as flooding and anoxic conditions, the more nutrient poor and lower pH side of the peatland range (bog and poor fen systems) are normally dominated by *Sphagnum* species (Snäll *et al.*, 2003). Bryophytes in general, particularly the brown mosses, benefit from better adaptability to high pH and mineral rich conditions, and thus substitute for *Sphagnum* species to dominate in rich fen ecosystems (Pan, 2010). There are, however, several *Sphagnum* species that can be found in rich fen ecosystems and which are indicators of relatively high pH, such as *Sphagnum warnstorffii*, *S. contortum* and *S. teres* (Rydin & Jeglum, 2013). Along the water and nutrient gradients, the nutrient and mineral richer fen ecosystems (i.e. intermediate and rich fens) are characterized by dense swards of graminoids, such as sedges (*Cladium* spp., *Carex* spp., *Eriophorum* spp., Poaceae and other Cyperaceae) (Pedrotti *et al.*, 2014). Moreover, there are a considerable number of herb species (e.g. orchids) that occur in intermediate and rich fens (Rydin & Jeglum, 2013).

### 2.1.3. The Global Peat Carbon Store

Where peat soils remain water-saturated throughout the growing season, creating anoxic conditions that inhibit decomposition, organic matter accumulates over years to

millennia (Lafleur *et al.*, 2001). Thus, peatland ecosystems represent globally significant soil C stocks, many of which have been accumulating since the era of the last glaciation, i.e. a period of around 12,000 years (Drösler *et al.*, 2008). Currently, around a third of the global soil organic C is stored in peatlands (about 550 Pg of C), an amount that is more than half of the C stored in the atmosphere (approximately 750 Pg) (Smith, 2004; Strack, 2008). At UK level, peatlands (including upland blanket bogs, lowland raised bogs, fens and shallow peaty soils) store about 5.1 billion tonnes of C (Smith *et al.*, 2007), which contain more than half of the total amount of C stored in all kinds of soils in the country ( $9.8 \pm 2.4$  billion tonnes) (Dawson & Smith, 2007). However, it is reported that the UK peatlands are currently a net source of 5.73 Mt CO<sub>2</sub>-C yr<sup>-1</sup> (Worral *et al.*, 2011). And for high-latitude global peatlands, there is a concern that modern anthropogenic forcing will drive the climate towards warming, and as a result, these peatlands will become permafrost-free, emitting stored C into the atmosphere (Cai *et al.*, 2010; Sagerfors *et al.*, 2009; Sottocornola & Kiely, 2010). On the other hand, since peatland ecosystems store such large quantities of C, even small changes in C fluxes could have a significant impact on the global climate system (Frolking & Roulet, 2007). Therefore, when considering the potential effects of climate change on the ecosystem-atmosphere C exchange and hydrological regimes in peatlands, it is critical to gain a better understanding of how CO<sub>2</sub> and CH<sub>4</sub> fluxes, the energy balance and hydrological processes in peatland ecosystems are linked to climate, and how climate might respond to the changes in peatland ecosystems.

In very simple terms, the C lost from peatland ecosystems is principally due to net ecosystem exchange of CO<sub>2</sub>, emissions of CH<sub>4</sub>, and aquatic losses of Dissolved Organic Carbon (DOC), Dissolved Inorganic Carbon (DIC) and Particulate Organic Carbon (POC) (Dawson & Smith, 2007). The GHG balance of a peatland ecosystem is particularly affected by the uptake or efflux of CO<sub>2</sub> and CH<sub>4</sub> (Dawson & Smith, 2007) which, in turn are influenced by a series of complex physical, biological and hydrological processes.

## 2.2. Carbon Cycling in Peatlands

### 2.2.1. Peatlands and Greenhouse Gases

The greenhouse gases (GHGs) are the gases that affect the radiative forcing of the atmosphere and are responsible for causing the Earth's greenhouse effect. GHGs absorb and re-emit the infrared radiation emitted from the Earth's surface (Chapin *et al.*, 2002). The main GHGs are water vapour (H<sub>2</sub>O), CO<sub>2</sub>, CH<sub>4</sub> and nitrous oxide (N<sub>2</sub>O) (IPCC, 2008). Since the mid-18<sup>th</sup> Century, the atmospheric concentrations of GHG have increased strongly (IPCC, 2014a). The total global emission of GHG increased from 29 Gt CO<sub>2</sub> equivalents in 1970 to 50 Gt CO<sub>2</sub> equivalents in 2004 of which 77% is attributed to CO<sub>2</sub> and 14% to CH<sub>4</sub> (Olivier *et al.*, 2005). The fast rise of GHG atmospheric concentration has contributed significantly to a 0.6 °C increase of global mean temperature in the last 100 years (IPCC, 2014a). Thus, the increase of the GHG atmospheric concentration is considered as the main factor causing anthropogenic climate change (Pan *et al.*, 2012). Therefore, an international agreement (the Kyoto Protocol) was adopted in 1997 aiming to reduce GHG emissions globally (UNFCCC, 1997). In the last few decades, the attention of the scientific community has been focused on assessing the role of different ecosystems on GHG emissions as well as global C and water cycling (Baldocchi, 2008).

Chapin *et al.* (2006) proposed that, at an ecosystem scale, the net ecosystem carbon budget (NECB) presents the total rate of organic C flux in the ecosystem. The net flux of several forms of C contributing to NECB are the flux of CO<sub>2</sub>, CO, CH<sub>4</sub>, DOC, dissolved inorganic carbon (DIC), volatile organic carbon (VOC) and the net lateral transfer of particulate (non-dissolved, non-gaseous) carbon (PC) (Equation 1). In the equation, a positive NECB indicates a net C source. In peatland ecosystems, the GHG flux accounts for most of the ecosystem C flux (Limpens *et al.*, 2008).

$$NECB = NEP + F_{CO} + F_{CH_4} + F_{VOC} + F_{DIC} + F_{DOC} + F_{PC} \quad (\text{Eq. 1})$$

There is a large body of previous and on-going research suggesting that natural peatlands may function as a net sink or a small net source for atmospheric CO<sub>2</sub>, and generally as a source of atmospheric CH<sub>4</sub> (Gorham, 1991; Limpens *et al.*, 2008; Pastor *et al.*, 2002; Roulet *et al.*, 2007; Waddington & Roulet, 2000; Walter *et al.*, 2001). In general, N<sub>2</sub>O emissions are quite low from natural peatlands, but there is evidence to suggest that peatlands under agricultural use could release significant amounts of N<sub>2</sub>O (Augustin *et al.*, 1996; Martikainen *et al.*, 1993; Roobroeck *et al.*, 2010). Frey and Smith (2005) also suggested that peatlands are important sources of DOC to downstream ecosystems. DOC, although not in itself a GHG, can be converted to CO<sub>2</sub> as a result of bacterial decomposition in waterways (Frey & Smith, 2005). However, at the current time, studies of NECB of peatland ecosystems are still rare globally (Hendriks *et al.*, 2007; Koehler *et al.*, 2011; Nilsson *et al.*, 2008) and in most studies, the components of the NECB of peatland ecosystems are considered individually (Levy *et al.*, 2012; Sagerfors *et al.*, 2009; Warburton, 2003).

Both CO<sub>2</sub> and CH<sub>4</sub> are potent GHGs and their exchange is strongly determined by peatland ecosystem function (Figure 5). Studies have suggested that peatlands might act as a CO<sub>2</sub> sink in some years and a source in others, the response being related to regional and local differences in ecology, hydrology and climate. Emission of CH<sub>4</sub> is similarly variable in space and time (Blodau & Moore, 2003; Moore *et al.*, 1998).

The mode of gas fluxes in peatland ecosystems strongly differs between drained and water saturated conditions (Hooijer *et al.*, 2010). In drained peatlands, diffusion is responsible for more than 90% of the total gas fluxes due to the presence of permanently air-filled pores. However, in water saturated peat soils, a substantial part of the gases are transferred to the atmosphere by ebullition, with the bubbles containing comparatively high concentrations of CH<sub>4</sub> (10 - 90%) and CO<sub>2</sub> (Chanton & Whiting, 1995).

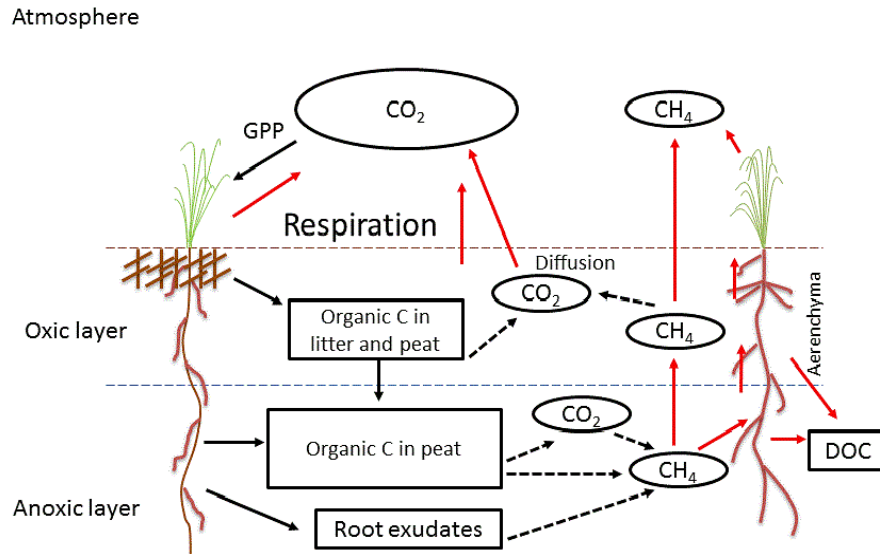
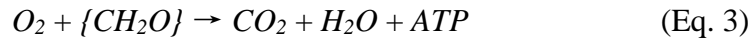
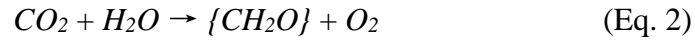


**Figure 5:** Simplified conceptual diagram of carbon cycling in peatland ecosystem. Dashed arrows show microbial processes (edited from Parish et al., 2008; Rydin & Jeglum, 2013).

### 2.2.2. Net Ecosystem Carbon Dioxide Exchange in Peatlands

Like in all other ecosystems, the  $\text{CO}_2$  exchange between a terrestrial ecosystem and the atmosphere includes both  $\text{CO}_2$  taken up by plants via photosynthesis and that released to the atmosphere through ecosystem respiration ( $R_{eco}$ ; including autotrophic respiration and heterotrophic respiration) (Heimann & Reichstein, 2008). Carbon dioxide is absorbed from the atmosphere by plants (and other autotrophs) through gross ecosystem photosynthesis (GEP) when sunlight is available as a source of energy, where oxygen ( $\text{O}_2$ ) and carbohydrate ( $\{\text{CH}_2\text{O}\}$ ) are produced during the process (Taiz & Zeiger, 2010; Equation 2). A fraction of these carbohydrates is consumed within the ecosystem through autotrophic respiration during day and night time in aerobic conditions (Winegardner, 1995; Equation 3). The remainder of the carbohydrates is stored in the biosphere and can be converted to  $\text{CO}_2$  and  $\text{H}_2\text{O}$  by heterotrophic respiration (Winegardner, 1995; Equation 3).



The net ecosystem exchange (NEE) is defined as the difference between  $R_{eco}$  and GPP (Valentini *et al.*, 2000; Equation 9). Therefore, negative values of NEE indicate net CO<sub>2</sub> uptake by the ecosystem which means the net CO<sub>2</sub> accretion is to be maintained over time (Page *et al.*, 2011). An imbalance would affect the CO<sub>2</sub> concentration in the atmosphere, which plays an important role in influencing global climate (Taneva & Gonzalez-Meler, 2011). Therefore, measurements of CO<sub>2</sub> flux are used to define whether an ecosystem is a net source or sink of CO<sub>2</sub> at different temporal scales. As already discussed, peatland ecosystems are a potential CO<sub>2</sub> sink due to the typically waterlogged and anoxic conditions, which result in low ecosystem respiration rates and hence low rates of organic matter decomposition (Byrne *et al.*, 2004).

Theoretically, the amount of CO<sub>2</sub> taken up and stored in a peatland ecosystem results from the difference between CO<sub>2</sub> uptake by GEP and CO<sub>2</sub> release through  $R_{eco}$  (Figure 6; Rydin & Jeglum, 2013). The balance can be broken in either way. On one side, the primary productivity rate (productivity of organic components from atmospheric CO<sub>2</sub>) of plants is related to the vegetation community type, which is driven by insolation duration, temperature, nutrient availability and hydrology (Frolking *et al.*, 1998; Griffis *et al.*, 2000; Malmer, 1986; Waddington *et al.*, 1998). Similarly, on the other side,  $R_{eco}$  is also related to vegetation communities, both due to the inclusion of autotrophic respiration in  $R_{eco}$  and the varying decomposability of organic matter of different peat substrates and vegetation types (Moore & Basiliko, 2006). However,  $R_{eco}$  also can be affected directly by temperature, substrate composition and hydrology. For example, low water levels could result in an increased  $R_{eco}$  rate since the decomposition rate is faster under aerobic conditions compared to anaerobic conditions (Moore & Dalva, 1993). Environmental variations may result in peatlands acting as a CO<sub>2</sub> sink in some years and as a source in others (Chimner & Cooper, 2003).

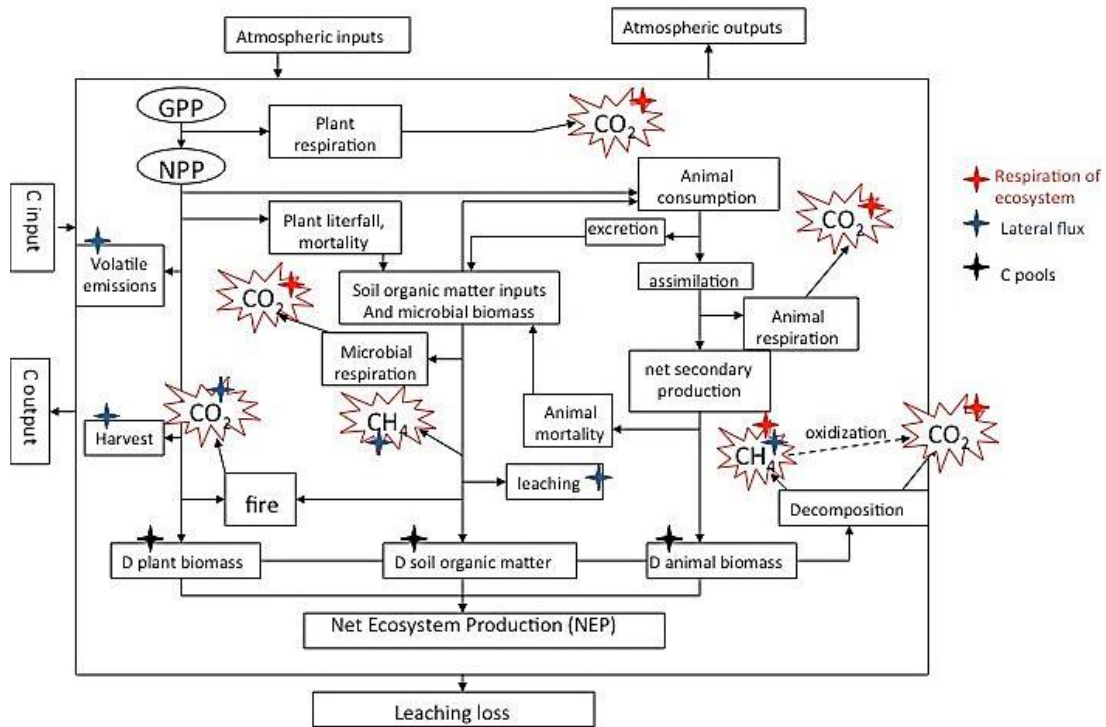


**Figure 6:** Conceptual diagram of the net carbon balance in peatland ecosystem.

### 2.2.3. Land-atmosphere Methane Exchange in Peatlands

Methane (CH<sub>4</sub>) is the second most potent greenhouse gas after CO<sub>2</sub>. The relative global warming potential (GWP) for a 100-year horizon is 25 for CH<sub>4</sub> and the radiative forcing of CH<sub>4</sub> is  $0.48 \pm 0.05 \text{ W m}^{-2}$ , which means CH<sub>4</sub> is about 25 times more efficient as a GHG than CO<sub>2</sub> (IPCC, 2014a; NOAA, 2010). Methane can also react with other atmospheric pollutants (i.e. dichlorodifluoro methane) in the troposphere producing other GHG (i.e. ozone (O<sub>3</sub>), carbon monoxide (CO) and CO<sub>2</sub>). Atmospheric CH<sub>4</sub> accounts for 15% - 20% of the total warming effect of GHGs (IPCC, 2014a). However, the interactions of CH<sub>4</sub> in the climatic system are still poorly understood, and the global budget of CH<sub>4</sub> is also very uncertain (Kirschke *et al.*, 2013).

During last few centuries, the atmospheric CH<sub>4</sub> concentration increased dramatically (from  $1.06 \times 10^{-12}$  in 1750 to  $1.75 \times 10^{-12}$  in 1998); especially after the Industrial Revolution, it increased more than 10% per decade before the 1980s (IPCC, 2001).

However, more recent reports indicate that the CH<sub>4</sub> atmospheric concentration has been quite stable over the period 1999 - 2007 (IPCC, 2008). The underlying reasons for this stabilization of CH<sub>4</sub> concentration in the atmosphere are still not clear, but several studies have suggested that the response of global wetlands to recent climate variability and rice agriculture policy changes have both played a role (Heimann, 2011; Kai *et al.*, 2011). Over the last decade since 2007, however, the atmospheric CH<sub>4</sub> concentration has started to increase rapidly again, with some suggesting that global wetlands may play an important role in this change (Kirschke *et al.*, 2013; Montzka *et al.*, 2011). Globally, 80% of CH<sub>4</sub> emissions come from biogenic sources (Teh *et al.*, 2005). Wetlands are the largest natural source of CH<sub>4</sub>, contributing 70% of natural biogenic CH<sub>4</sub> emissions, an amount equal to 20% of global CH<sub>4</sub> fluxes (IPCC, 2014a). Using ecosystem modelling, Kirschke *et al.* (2013) estimated that the natural wetland emission of CH<sub>4</sub> is 217 Tg yr<sup>-1</sup> for 2000 - 2009 based on their bottom-up approach.

In peatlands (as well as in other wetlands), the production of CH<sub>4</sub> results from slow anaerobic biomass decomposition under strictly anaerobic conditions by methanogens in the saturated zone of peat soil (Lai, 2009). Once CH<sub>4</sub> is produced, it can be oxidised by methanotrophs in the upper aerated peat soil layer and in the rhizosphere (rooting-zone) of vascular vegetation, or transported to the atmosphere via molecular diffusion, ebullition (as gas bubbles) or as simple molecular diffusion or convective gas flow through vascular plants (Meronigal *et al.*, 2004; Reddy & Delaune, 2008) (Figure 7). Theoretically, CH<sub>4</sub> could be effectively consumed in a sufficiently thick aerobic layer as methanotrophs have higher metabolic activity than methanogens under suitable temperature conditions. Thus, methanotrophs modulate the CH<sub>4</sub> emission from soils by diffusion depending on the thickness of the aerobic layer (Hornibrook *et al.*, 2009; Whalen, 2005). In addition to diffusion from the surface, CH<sub>4</sub> is also released by ebullition, gas bubbles released from soil or water (Chanton & Whiting, 1995; Glaser *et al.*, 2004), and flow through vascular plants acting as a gas conduit (Chanton *et al.*, 1993; Whalen, 2005) thereby bypassing any surface aerobic layer and methanotrophism. As a consequence, wetland CH<sub>4</sub> release to the atmosphere is strongly dominated by active or passive vascular plant transport (Hornibrook *et al.*, 2009; Whalen, 2005). Moreover, a considerable amount of CH<sub>4</sub> can be stored in plants (e.g. *Sphagnum* species) that lack aerenchyma or in the saturated zone of peat soil where the

peat surface is barely covered by vascular plants (Chanton & Whiting, 1996). Thus, peatland CH<sub>4</sub> emissions have been found to be closely related to water level (thickness of the aerobic soil layer), vascular plant coverage and peat soil temperature (Bubier *et al.*, 1995; Kellner *et al.*, 2006; Roulet *et al.*, 1992; Stamp *et al.*, 2013; Vitt, 2006).

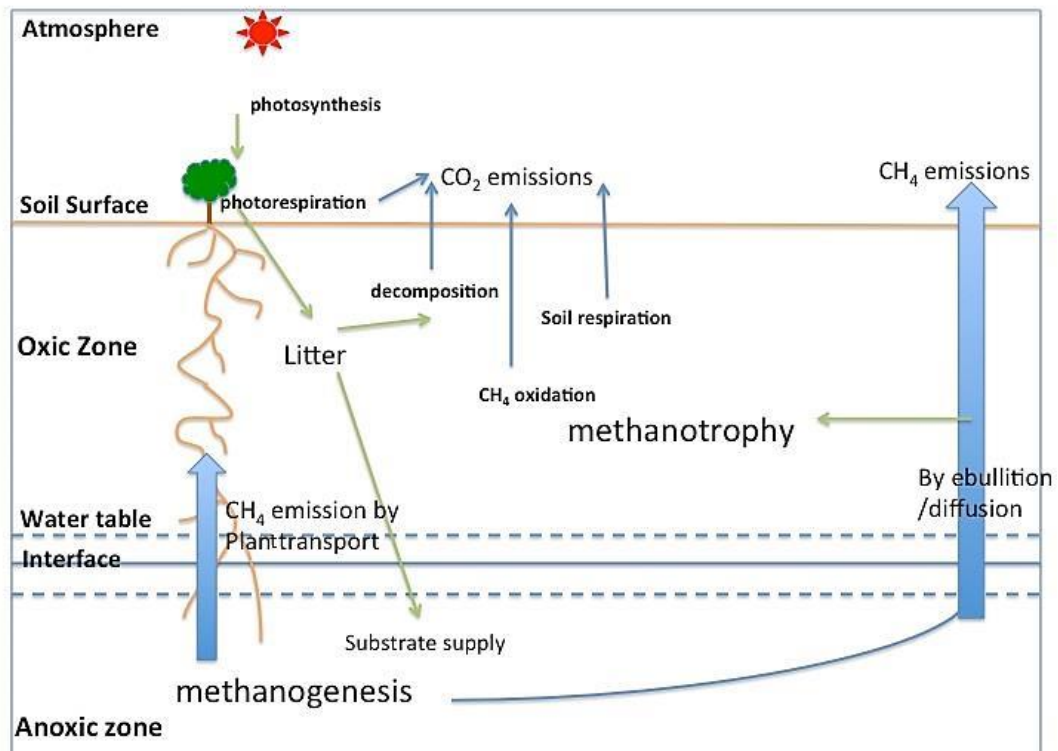


*Figure 7: A conceptual diagram of methane fluxes in peatland ecosystems.*

Theoretically, drainage turns peat soils from a source to a weak sink of CH<sub>4</sub> as a result of reduced CH<sub>4</sub> production in the drier peat soil and enhanced consumption of CH<sub>4</sub> in the aerated zone of the surface peat (Byrne *et al.*, 2004). However, obviously, a drained peatland has a larger oxidic zone that increases organic matter decomposition resulting in large quantities of CO<sub>2</sub> being released into the atmosphere. Harriss *et al.* (1982) found that swamp forest can be a CH<sub>4</sub> sink during drought conditions by consuming atmospheric methane at rates of 0.001 to 0.005 g CH<sub>4</sub> m<sup>-2</sup>day<sup>-1</sup>. While these results cannot be extrapolated to all peatlands, they illustrate the potential complexity of processes that regulate net flux of CH<sub>4</sub> between peatland soil and the atmosphere. The oxidation of CH<sub>4</sub> in soil can be found across a range of other ecosystems in tropical,

temperate and even arctic regions (Mosier *et al.*, 1991; Seiler *et al.*, 1984; Whalen & Reeburgh, 1990). Globally, soil as a sink of CH<sub>4</sub> can assimilate approximately 30 Tg CH<sub>4</sub> per year (Wang *et al.*, 2002). Dörr *et al.* (1992) and Kruse *et al.* (1996) have suggested that soil porosity is the main soil physical property affecting soil CH<sub>4</sub> oxidation rate by influencing the air transported within the soil layer. Czepiel *et al.* (1995) also found that the CH<sub>4</sub> oxidation process is closely related to soil moisture, since water may reduce the air transport rate by reducing the air-filled porosity of soil. It is also worth mentioning that both CH<sub>4</sub> production and oxidation, as microbial processes, are positively related to peat soil temperature, with Dunfield *et al.* (1993) suggesting that production rates are more sensitive than the rates of CH<sub>4</sub> oxidation to soil temperature.

On the other hand, rewetting is often cited as a beneficial peatland restoration method in terms of GHG emissions (Limpens *et al.*, 2008). A rewetted peatland has a relatively high water table that increases the C storage capacity of the peatland due to a smaller oxic zone. However, there is a concern that while the larger anoxic zone can reduce peat surface CO<sub>2</sub> emissions it may lead to increased CH<sub>4</sub> emissions to the atmosphere contributing to the global greenhouse effect (Levy *et al.*, 2012). Moreover, the increase in evapotranspiration (ET) caused by rewetting might change the local climate (Dinsmore *et al.*, 2010).

#### 2.2.4. Dissolved Organic Carbon in Peatlands

During the last few decades, the Dissolved Organic Carbon (DOC) concentration in a large area of freshwaters in the Northern Hemisphere has increased dramatically (Monteith *et al.*, 2007). For example, in England, Evans *et al.* (2006) found that DOC concentrations have almost doubled in eight streams and ten lakes in southern England from 1988 to 2003. Research has suggested that wetlands, especially peatlands, have a significant impact on the DOC concentration in most of the freshwaters in the Northern Hemisphere, because of the high rates of organic matter production in these ecosystems (Urban *et al.*, 1989). Thus, the dynamics of DOC export from peatlands influenced by

global climate changes have been considered as one of the main reasons for the dramatic increase in the DOC concentration of freshwaters in the Northern Hemisphere (Roulet & Moore, 2006).

DOC plays an important role in the overall C cycling in peatlands, by representing a significant part of the C released from decomposition. The production of DOC in peatland can be associated with desorption of peat soil organic C arising from the decomposition of plant tissues by micro-organisms, and the exudation of organic C from the plant rhizosphere (Figure 8). Particularly, in minerotrophic peatlands (fens), underground water DOC inflow counts for a considerable proportion of the DOC intake into the ecosystem.

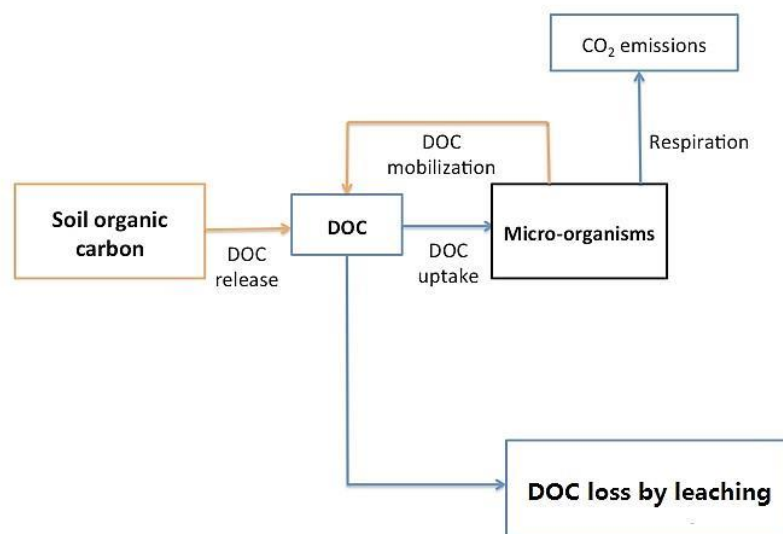


**Figure 8:** A conceptual model of DOC production (modified from Bengtson & Bengtsson, 2007).

There have been several hypotheses suggested by researchers to explain the increase in the concentration of DOC exported from peatlands. First, the increase of temperature and moisture might increase the rates of decomposition of organic litter in peat soil (Freeman *et al.*, 2001). Freeman *et al.* (2001) also noticed that the proportion of phenolics (the main component of DOC) might increase with increasing temperature, which could enhance the effective export of DOC in peatlands by decreasing the

biodegradability of DOC during the export process. Second, the elevated atmospheric CO<sub>2</sub> concentration may have a fertilising effect stimulating plant primary production. Increasing exudation of DOC from the plant rhizosphere may trigger priming promoting further peat soil decomposition, thereby increasing the concentration of DOC exported from peatland ecosystems (Freeman *et al.*, 2004). Hydrological change is another important factor in influencing DOC discharge from peatlands. As mentioned, the dynamics of water level have significant impacts on redox state and biogeochemistry in peatlands therefore altering the production and retention of DOC in the ecosystem. However, it should be noted that the increased water flow from peatlands could result from an increase in runoff without any changes in DOC concentration, whereas the increased DOC concentration can occur with no changes in hydrology (Roulet & Moore, 2006). It is also worth mentioning that Evans *et al.* (2006) suggested that the relatively recent decrease in sulphur deposition following regulations on air pollution might be another important explanation for the increase in DOC being exported from peatlands. Reductions in soil solution SO<sub>4</sub> have raised the acidity of the soil solution and ionic strength, thereby increasing DOC mobilization from the peat causing significant increases in surface water DOC concentration in peatlands (Evans *et al.*, 2006).

All in all, DOC plays a significant part in C release from peat soil decomposition, and thus, along with CO<sub>2</sub> and CH<sub>4</sub>, is an important part of the overall C cycle in peatland ecosystems.

### 2.2.5. Water Budget in Peatlands

Peatland is one of the most important ecosystems occurring in the headwater areas of many freshwaters. It plays an important role in influencing the quantity and quality (i.e. of nutrients, organic matters) of the receiving waters. The hydrological dynamics also have large impacts on the C cycling and energy balance within the ecosystem (Brooks, 1992).

As mentioned earlier, there are significant differences between the hydrological processes in bogs and fens. Here the focus is on fen ecosystems. Carter (1986) produced a general water balance formula for fen ecosystems as (Equation 4):

$$P + SWI + GWI = ET + SWO + GWO + \Delta S \quad (\text{Eq. 4})$$

The water inputs into a fen ecosystem include precipitation ( $P$ ), surface water inflow ( $SWI$ ) and groundwater inflow ( $GWI$ ), while the water outflow from a fen ecosystem includes evapotranspiration ( $ET$ ), surface water outflow ( $SWO$ ) and ground water outflow ( $GWO$ ). The difference between the in- and outflow is the storage in the ecosystem  $\Delta S$  (Carter, 1986) (Figure 9). As a function of the capacity of peatland water storage, water level, is the key hydrological parameter of peatland, which is affected by landscape morphology, geology, soil physical properties and the balance between the inflows and outflows of water. The changes in storage, reflected by the changes in water level, have significant impacts on  $\text{CO}_2$  and  $\text{CH}_4$  fluxes, and DOC production and transport in peatland ecosystems. It is important to note that the water chemistry changes resulting from surface groundwater exchanges between ecosystems also have impacts on the overall C cycling in peatlands.

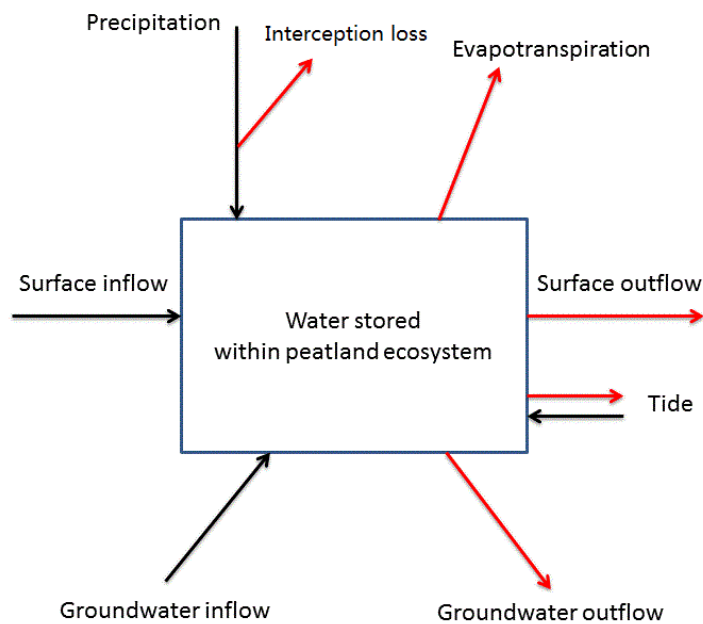


**Figure 9:** Generalized peatland water budget (modified from Mitsch & Gosselink, 2000).

Evapotranspiration (ET) may be one of the most important hydrological fluxes at peatland sites. This is especially so where the ecosystem is hydrologically isolated from the groundwater by impervious soil layers, in which case ET might become the major loss pathway of water from the ecosystem, accounting for more than 80% of water losses during the summer season (Acreman & Jos   2000). It is suggested that wetland ecosystems tend to have higher ET rates than other terrestrial ecosystems (e.g. forests, grasslands *etc.*) due to their long-term waterlogged condition and dense vegetation cover (Bullock & Acreman, 2003). However, the actual ET rates vary between different peatland ecosystems due to the differences in land cover vegetation types and the proportion of open water on the site (Acreman *et al.*, 2003). A high ET rate may cause a large water loss from the peatland ecosystem and thus have an influence on downstream water resources. Therefore, it is important to quantify the ET rate on a peatland site in order to better support the hydrological management of the ecosystem and to determine regional available water resources at the larger scale (Kelvin, 2011).

Conservation and restoration management of peatland ecosystems may also involve the active manipulation of the water storage of the ecosystem by control over either the

inflows to or outflows from the ecosystem by using ditches, sluices and pumps. As a result, particular water levels will be controlled by management operations; however, there may still be seasonal variations (Acreman *et al.*, 2003; 2007; Gasca-Tucker *et al.*, 2007). Drainage for forestry, peat extraction and agriculture substantially decreases the water storage in peatland ecosystems. Thus, the major objective of peatland restoration is limiting water loss from the ecosystem (e.g. by using ditches blocking, straw mulches on the peat surface *etc.*; Quinty & Rochefort, 2003).

### 2.3. Response of Peatlands to Environmental Changes

Large-scale environmental changes (i.e. climate changes, land-use changes, drainage, and peat extraction) are associated with significant impacts on peatland C balances (Byrne *et al.*, 2004; Joosten & Clarke, 2002). There are numerous environmental factors which limit or stress vegetation differently; among these, temperature, radiation, water availability and nutrient availability, and atmospheric gas concentration generally exert the most important roles in peatland ecosystems (Rydin & Jeglum, 2013; Taiz & Zeiger, 2010). When one of these environmental factors is beyond the optimal range for plant growth, it becomes a stress factor (Galvagno, 2011).

Considering the peatland ecosystem, one of the most important environmental changes, a lowered water table (e.g. due to climate change or drainage management) will yield a deeper oxic layer leading to increased aerobic decomposition and enhanced rates of CO<sub>2</sub> release and DOC losses (Holden *et al.*, 2004). However, lowered water levels favour methanotrophs and trigger a strong reduction or even complete cessation of CH<sub>4</sub> emission (Limpens *et al.*, 2008). In some cases, peatlands drained for forestry may still act as an ecosystem C sink, although this may not happen over a short period of afforestation and not at all sites (Laine *et al.*, 1996). Conversely, rewetting of peatland for restoration may decrease the rate of peat decomposition, thus increasing the C uptake, but increase the rate of CH<sub>4</sub> emission owing to the re-establishment of anaerobic conditions in the surficial peat layer (Hughes *et al.*, 2011; Renger *et al.*,

2002). In general, peat harvesting after drainage and drainage for agriculture usually convert peatlands to C sources (Kasimir-Klemedtsson *et al.*, 1997; Rodhe & Svensson, 1995). However, the CH<sub>4</sub> emissions from harvested peatlands are low and may stay at a low level for a long period until methanogen populations recover (Tuittila *et al.*, 2000). Hence, responses of peatland ecosystem C budgets to restoration rewetting have emerged as a relevant and complex question.

In terms of the response of peatland ecosystems to climate change, previous research has indicated that temperature and water level are the two main factors influencing the C cycling processes in peatlands (Blodau, 2002; Vasander & Kettunen, 2006). Generally, warmer conditions and a lowered water table may lead to an increase in  $R_{eco}$ , a reduction in GPP or a combination of the two, causing the net loss of CO<sub>2</sub> (Aurela *et al.*, 2009; Bubier *et al.*, 2003; Griffis *et al.*, 2000; Leppäälä *et al.*, 2011). It has been suggested that an increased temperature could increase peat decomposition (Updegraff *et al.*, 2001) and CH<sub>4</sub> emission (Fowler *et al.*, 1995a) directly, and may significantly alter C budgets in temperate and boreal peatland ecosystems. Furthermore, changes in temperature (i.e. air temperature, soil temperature), hydrological climate (i.e. precipitation, humidity) and irradiance could alter the distribution, coverage rate and even the dominant species of the vegetation on a site, thereby affecting the C cycling process in the ecosystem (Rydin & Jeglum, 2013). The concomitant changes in water table as a result of climate warming or drainage may increase the rate of CO<sub>2</sub> emission and, in most cases, lead to a strong reduction in CH<sub>4</sub> emission (Laine *et al.*, 1996). It has been suggested by previous research that an increase of 2 °C could increase CO<sub>2</sub> emissions by up to 30%, whilst a 15 - 20 cm lowering of the WT would increase the CO<sub>2</sub> emission by 50 - 100% (Silvola *et al.*, 1996). However, it is still unclear how GHG exchanges will respond to the increasing frequency of meteorological extremes rather than the climatic changes in average conditions alone (Ciais *et al.*, 2005; Reichstein *et al.*, 2007; Rogiers *et al.*, 2008).

The role of a single environmental factor on influencing an ecosystem is often complex. Environmental factors and ecosystems interact over multiple temporal scales from seconds to years, and act differently on complex biological processes (Stoy *et al.*, 2009). For instance, fast changes in sunlight, temperature or precipitation may influence the

daily CO<sub>2</sub> and water exchanges. Over the longer term, phenology and water level changes influence the ecosystem processes on monthly to seasonal scales, while long-term climate changes have an impact on the timing of phenological events annually and inter-annually (Baldocchi *et al.*, 2001b).

The influence of climate change is likely, therefore, to be complex and the impacts on peatland ecosystem C cycle processes are likely to be interacting and synergistic. Yet, the impact of climate changes on peatland C stocks and GHG exchanges remain poorly understood and quantified.

## 2.4. Related Research

In order to quantify and understand the GHG flux in peatland ecosystems, techniques that allow for accurate and continuous monitoring of the net exchange of GHG over prolonged periods of time are required. Most early biosphere-atmosphere exchange measurements in ecological studies relied on chamber techniques which are inherently limited in terms of continuity, repeatability, measurement period and statistical significance (Lenschow, 1995; Moncrieff *et al.*, 1997). Moreover, the physical perturbation of the site, such as damage to vegetation and compaction of the ground soil, are also concerns when conducting chamber measurements (Baldocchi *et al.*, 1988). Therefore, more and more micrometeorological techniques have been introduced into geophysical and ecological research in the last few decades, including the flux-gradient method, the mass balance technique and the EC method (Baldocchi, 2003). Among these micrometeorological methods, the EC technique is considered one of the most direct and defensible ways to quantify trace gas exchange rates by measuring fluxes within the lower atmospheric boundary layer, and also benefiting in terms of providing a continuous long-term measurement record without adverse disturbance to the environment under study. Long-term flux measurements make it possible to detect not only daily variations but also seasonal and inter-annual variations. Recently, globally, EC has become one of the main and standard flux measurement

methods. FluxNet, the global long-term flux measurement network, is built up for global scale studies on biosphere-atmosphere exchanges (Baldocchi *et al.*, 2001a).

During the last few years, the EC method has been commonly used for CO<sub>2</sub> flux measurements on peatland ecosystems. Benefiting from continuous long-term measurement collection, Lafleur *et al.* (2005a) conducted a five year long CO<sub>2</sub> flux measurement study by EC on a boreal bog in Canada from 1998 to 2003. Lafleur *et al.* (2001) focused on seasonal variation of CO<sub>2</sub> fluxes during the first year of measurement, and found the bog functioned as a sink of CO<sub>2</sub> during the summer growing season and a source during the winter. A subsequent four year measurement period (Lafleur *et al.*, 2003) suggested the ecosystem was sensitive to inter-annual climatic variance (acting as a sink of CO<sub>2</sub> for the first three years but barely in the fourth year as a result of a summer drought). Lafleur *et al.* (2005a; 2005b) also suggested that the ecosystem respiration of the bog may be sensitive to peat temperature, but not to the water level and that ET was not significantly related to water table variations due to a persistently low water level in the bog. Aurela *et al.* (2002) suggested that wintertime efflux may play an important role in influencing the peatland ecosystem annual CO<sub>2</sub> flux by showing that CO<sub>2</sub> fluxes for the winter period (105 g CO<sub>2</sub> m<sup>-2</sup>) were even greater than the absolute value of the total annual fluxes (-68 g CO<sub>2</sub> m<sup>-2</sup>). The advantage, therefore, of continuous long-term measurement records has been shown distinctly here compared to the short-term static technique that might only be conducted during the growing season.

Previous studies on peatland ecosystems have shown high spatial and temporal variability in land / atmosphere CO<sub>2</sub> exchanges (Lindroth *et al.*, 2007; Riutta *et al.*, 2007; Teh *et al.*, 2011). In the last few decades, most of the C flux studies on peatlands have focused on the natural (undisturbed) ecosystems of the arctic and boreal climates (Teh *et al.*, 2011). However, most temperate peatland ecosystems show some degree of anthropogenic disturbance and therefore might be large sources of CO<sub>2</sub> (Billett *et al.*, 2010). Only very limited recent studies have reported net CO<sub>2</sub> fluxes at temperate peatlands (e.g. Hatala *et al.*, 2012; Jacobs *et al.*, 2007; Lloyd, 2006; Nieveen *et al.*, 2005; Veenendaal *et al.*, 2007). There is a concern that the research findings on near-pristine boreal peatlands are unlikely to reflect the dynamics of NEE operating in

managed temperate peatland ecosystems since there are very large differences between the two ecosystems in terms of vegetation, the physical and chemical characteristics of the peat soil, hydrology, climate and land use (Teh *et al.*, 2011). The EC measurement conducted on a site changing from peatland to agricultural land indicates that the land use change might cause a huge amount of annual C loss ( $1061 \pm 500 \text{ kg C ha}^{-1}\text{yr}^{-1}$ ) (Nieveen *et al.*, 2005). A flux measurement study on tropical peatland also suggested that drainage disturbance may convert the peatland ecosystem into a CO<sub>2</sub> source (Hirano *et al.*, 2007). However, Hargreaves *et al.* (2003) witnessed a newly drained peatland for afforestation become a source of CO<sub>2</sub>, but then a sink again when ground vegetation recolonized (2 - 4 years) in a fen in Scotland. Conversely, Lohila *et al.* (2004) argued that land use change might cause the peat to decompose more rapidly even after more than 100 years of cultivation activity. These results could be explained by the different vegetation community recolonized on the peat soil.

In the UK, to date, most measurements of GHG fluxes have been collected on ombrogenous peatlands (mainly located in the northern and central parts of the country) (Billet *et al.*, 2010; Dinsmore *et al.*, 2010; Koehler *et al.*, 2011; Sottocornola & Kiely, 2010), while there is a lack of quantitative evidence on C fluxes on lowland temperate fen ecosystems (Couwenberg, 2011; Teh *et al.*, 2011). Moreover, very limited data exist on C flux for fen ecosystems that are regenerating after intensive arable land use (Baird *et al.*, 2009). The lowland fen ecosystems were only included in reporting of UK peatland C budgets recently (Billet *et al.*, 2010). There has been one report on the C balance of grazed and mown lowland fen in the Somerset Levels which reported a small net emission of  $59 \text{ g CO}_2\text{-C m}^{-2}\text{yr}^{-1}$  from the ecosystem for only one year measurements (Lloyd, 2006). But the current CO<sub>2</sub> sink / source status of the large areas of degraded lowland temperate fen ecosystems in other parts of the country remains largely unquantified (Evans *et al.*, 2011).

Earlier studies on CH<sub>4</sub> fluxes were mostly conducted by chamber techniques owing to the limitations in the measurement equipment (a high-frequency sensor is needed). The implementation of EC measurements of CH<sub>4</sub> started to become successful only in the late 1990s using closed-path systems with tuneable diode laser (TDL) spectrometers. The quantum cascade laser (QCL) spectrometers have been developed subsequently

and used recently for the same purpose (Kroon *et al.*, 2010). Fowler *et al.* (1995b) have tried to combine flux gradient, EC and relaxed eddy accumulation methods to measure the CH<sub>4</sub> emission on a peatland in Scotland, and found that CH<sub>4</sub> emission may be over-estimated on high latitude wetlands. Hargreaves & Fowler (1998) also conducted another measurement of CH<sub>4</sub> fluxes on a temperate peatland by using a combination of micrometeorology methods to discuss the relationships between CH<sub>4</sub> emission and peat temperature and water level. These were pioneer studies using micrometeorology methods to measure CH<sub>4</sub> fluxes. Heikkinen *et al.* (2002) compared the measurement of CO<sub>2</sub> and CH<sub>4</sub> fluxes by the static chamber and the EC methods, and found that the static chamber results showed lower CO<sub>2</sub> and higher CH<sub>4</sub> fluxes than those estimated from EC measurements (the CH<sub>4</sub> flux was measured by a fast response TDL spectrometer added to the EC system).

## 2.5. Summary

This chapter reviewed the scientific and policy literature relative to the project (2.4). The importance of peatland ecosystem in terms of C storage and climate change was outlined (2.1). The C cycling (physical and biological processes) in peatland ecosystems was described (2.2). The current state of knowledge relating to lowland fen ecosystems, peatlands restoration was reviewed (2.1) and the impacts of anthropogenic activities on peatland ecosystems were discussed (2.3).

At the current time, very limited observation data exist on GHG fluxes from lowland temperate fen ecosystems in the UK. Until now, the best estimates of CO<sub>2</sub> losses from arable fens in East Anglia were represented by Bradley (1997) and Gauci (2008). The scarcity of GHG flux research at lowland peatland sites has been identified as a key evidence gap (Evans *et al.*, 2011). Moreover, there is a lack of quantitative evidence on the change in GHG fluxes from rewetting / regenerating peatland ecosystems on which to base a description of the detailed effects of peatland restoration on GHG emissions in the longer-term. Understanding the current and potential future roles of the large areas of lowland temperate fens in the UK requires quantification of GHG fluxes and

all climate relevant C budgets across different land-use status and site types. The novel knowledge of the dynamics of land / atmosphere GHG exchanges is essential for designing effective conservation and restoration policies on peatland ecosystems.

The two EC stations in this project were the first such measurement stations to be installed on temperate lowland fen peatlands in the UK, and can provide continuous direct measurements on a rewetting / regenerating fen and a semi-natural fen in the same geographic location. The field observation measurements of GHG fluxes at an ecosystem scale represent a first step towards full land C budget accounting. The continuous direct measurements on a rewetting / regenerating fen compared to those from a near-by semi-natural fen provide long term quantitative evidence to explore the detailed effects of rewetting-restoration on peatlands GHG emissions. This research therefore makes an important step towards filling the current gaps in knowledge and longer-term direct observation data.

## **Chapter 3**

### **Study Sites**

## 3.1. Wicken Fen

### 3.1.1. Wicken Fen National Nature Reserve

This Ph.D. project focuses on research undertaken at Wicken Fen NNR, Cambridgeshire, UK (52°18' N, 0°16' E). Both of the study sites are located in this NNR, namely at Baker's Fen (BF), and at Sedge Fen (SF). The Wicken Fen NNR is one of the oldest nature reserves in the country, located to the south of Wicken village and approximately 26 km north east of Cambridge. It is within the original great East Anglian Fenland Region (Rowell & Harvey, 1988; Figure 1) and situated in an area of low relief (McCartney *et al.*, 2001). Whilst originally part of an extensive wetland, the nature reserve is now surrounded by arable land on peat soils and is an isolated semi-natural peatland ecosystem (Friday & Colston, 1999; National Trust, 2007).

Due to the large demand for farmland by the increasing UK population, the great drainage of the Fens in the 17<sup>th</sup> Century resulted in the conversion of former wet fen to agricultural uses, resulting in an enormous loss of natural fen habitats, which could be described as the greatest ecological disaster in the history of the country (Rotherham, 2013). However, small parts of the Fens, including much of Wicken Fen NNR, avoided drainage (Rowell & Harvey, 1988). Therefore, Wicken Fen NNR is one of the few remaining, well preserved fragments of East Anglian fenland, thereby providing a unique habitat for many characteristic wetland species. The NNR has an exceptionally diverse flora and fauna; over 8000 species have been recorded making the site one of the most species rich nature reserves in Great Britain (Warrington *et al.*, 2009). The site also is one of the most important wetland habitats in Europe, famous for the presence of unusual *Molinia caerulea-Cirsium dissectum* and *Phragmites australis-Peucedanum* plant communities (Friday, 1997). Wicken Fen is protected under UK law as a Site of Special Scientific Interest (SSSI), and is also on the list of Wetlands of International Importance under the terms of the RAMSAR Convention (RAMSAR, 2014).

Wicken Fen NNR was established by the NT as the first UK nature reserve in 1899. The NT, a Non-Governmental Organisation (NGO), manages the site and has expanded

the reserve area from an original 0.6 ha to a current area of *circa* 930 ha (Hughes *et al.*, 2011; McCartney *et al.*, 2001; Warrington *et al.*, 2009). A further expansion plan for a landscape scale wetland restoration project - Wicken Fen Vision, has been set up in 1999, aiming to create a maximum of 5,300 ha of wetland nature reserve by 2100 by bringing more adjacent land into conservation management through restoration of fen and wetland habitats (Warrington *et al.*, 2009; Figure 10). However, the reserve area is still under tremendous pressure from intensive farming, increasing populations and other human activities on adjacent areas. It is anticipated that over 44% of the proposed restoration will target the degraded peat soil currently used for agriculture (National Trust, 2007). There is, however, concern about the feasibility of reserve expansion due to the availability of adequate water for rewetting in this agriculturally dominated landscape (Ness & Procter-Nicholls, 2008). Further concerns relate to the isolation of the reserve area which is quite some distance from other wetland reserves, thus limiting species dispersals.

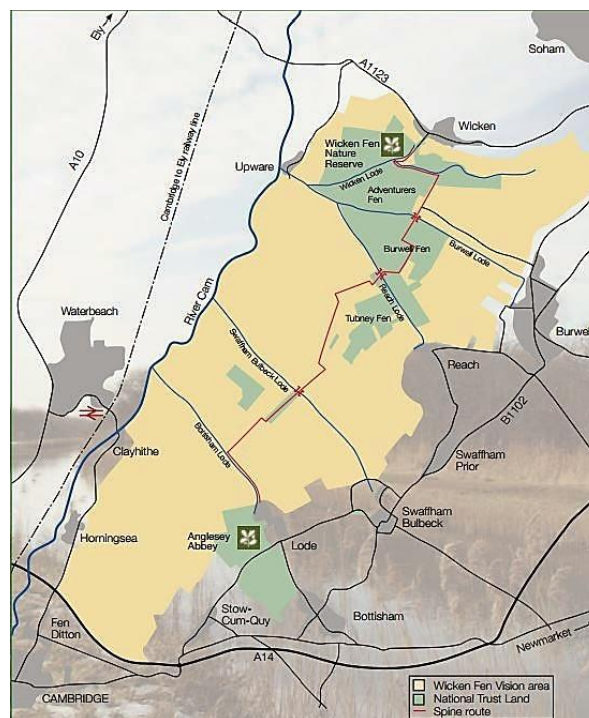


**Figure 10:** A recent map of Wicken Fen Vision plan and the adjacent area of Wicken Fen (edited from Warrington *et al.*, 2009).

The Wicken Fen area receives an average yearly precipitation of 560 mm yr<sup>-1</sup> and the mean annual temperature has been recorded at 10.4 °C (1979 to 2008) (Morrison *et al.*,

2013). The annual potential ET rate is about 594 mm on average; the precipitation is evenly distributed throughout a typical year (McCartney & de la Hera, 2004; Stroh *et al.*, 2012). The growing season lasts from March to October in this region (Kelvin, 2011). During most of the growing season the ET is more than the precipitation in the area (McCartney *et al.*, 2001; McCartney & de la Hera, 2004). The dominant wind direction is south-west throughout the year (Stroh *et al.*, 2012).

The peat depth on the site ranges from about 0.75 m to more than 4 m; the south-western part of Wicken Fen NNR has deeper peat profiles, whereas the north-eastern part is shallower. The underlying impermeable Gault clay is about 15 - 23 m thick which could inhibit vertical drainage (McCartney & de la Hera, 2004). Due to land drainage, peat harvesting, and intensive farming, the fen is now perched 2 - 3 m above the adjacent farmland.

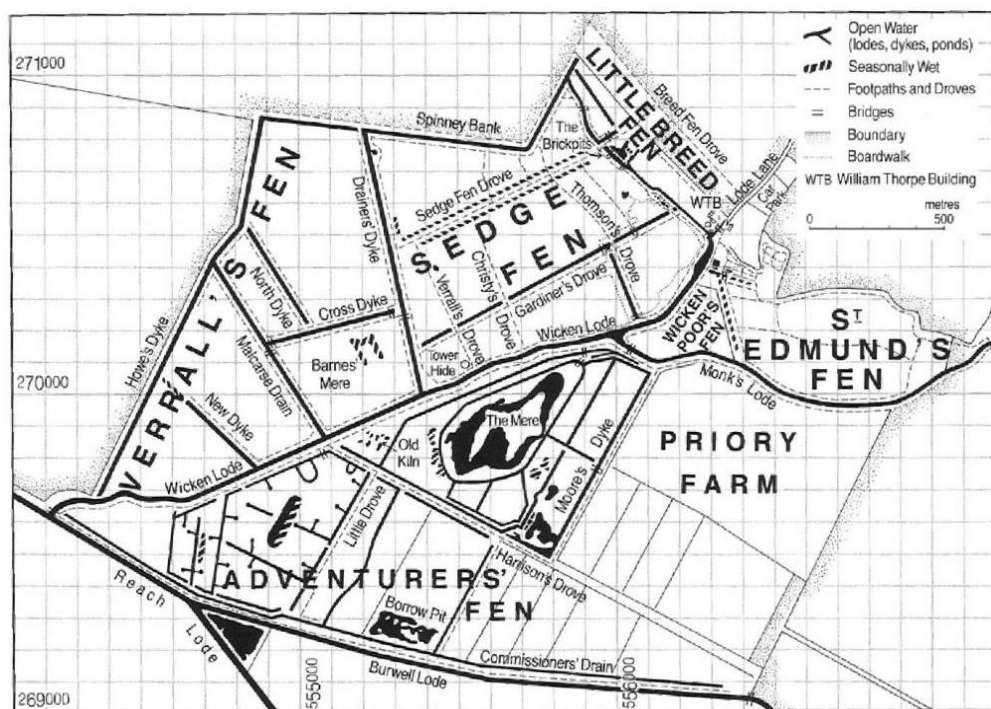


**Figure 11:** An old map of Wicken Fen (from Friday, 1997). The Priory Farm is rewetted and called Baker's Fen nowadays.

Wicken Fen has been sub-divided into several isolated areas by lodes or ditches and into different management units during the 17<sup>th</sup> and the 18<sup>th</sup> Centuries (Figure 11). The vegetation communities in different areas present different stages of the fenland

ecological succession reflecting differences in the land use history. The diverse vegetation communities in the area are characteristic of moderate to low fertility floodplain fens and high pH peat soils (McCartney & de la Hera, 2004). The shallow open waters, such as the lodes, ditches and meres, represent the very early stages of the hydrosere, and are distributed sporadically in the area. The subsequent successional stage is the reed-beds stage which can be found in the southern part of the reserve (the Adventurer's Fen) (Figure 12). The establishment of sedge communities is the next successional stage (e.g. the SF) and woody vegetation (fen "carr") is the final stage which can be found at the edge of the SF (Figure 12).



**Figure 12:** Map of Wicken Fen, indicating the location of the two study sites Sedge Fen and Baker's Fen (map provided by John Bragg from the NT).

### 3.1.2. History of Wicken Fen

Wicken Fen is a lowland temperate fen located on the southern edge of the original East Anglian Great Fenland region which formed between the uplands of Lincolnshire, Cambridgeshire, Suffolk and Norfolk (Moore, 1997).

In the 17<sup>th</sup> Century, the East Anglian Great Fenland covered around 3,367 km<sup>2</sup>, running north to south from Lincoln to near Cambridge, and east to west from Brandon to Peterborough (Darby, 1983). Frequent but irregular flooding events from the North Sea and the Great Fenland rivers created this waterlogged flooded plain. The deposition of silts from the incursions of seawater formed the low-lying base, and the incomplete decay of the dead vegetation formed the peat soils in the frequently waterlogged conditions in the areas further from the sea in the southern part of the Fenland expanse (Moore, 1997).

In the Romano-British period, the waterlogged conditions provided little opportunity for large scale human settlement in this vast flooded plain area. Only the drained coastal region of the northerly siltlands, and the margin or the isolated islands of the southern peatland area (e.g. Ely) were developed for human settlement and grazing land during this period. By contrast, no prosperous settlement or large scale land transformation could be found in the southern peatland area during this time. In the southeast corner of the Fenland, several lodes (i.e. Reach Lode, Swaffham Bulbeck Lode, Bottisham Lode; Figure 10) that represent ancient waterways still exist to this day. These are believed to have been dug by the Romans for transport but not for drainage purposes. After the Roman period, most of the area of the Fenland was held as ecclesiastical property for quite a long time. During this period, due to the lack of technology, only small-scale drainage schemes were conducted for generating revenue. The land became Crown property in the mid-16<sup>th</sup> Century after the dissolution of the monasteries in 1539 (Darby, 1956; 1983; Kelvin, 2011; Rowell, 1997).

Large-scale extensive drainage schemes of the peatland area were initiated in the early 17<sup>th</sup> Century in the Great Fens region. The largest drain plan called the Fen Project was proposed by the Crown in 1620. Initially, the project was aimed at preventing flooding

as a priority, since the region suffered from flooding both from upland water and the sea quite often during this period. Several catastrophic floods happened in 1607 and 1613, which were probably the greatest disasters since the flood of 1236. With the help of the Dutch engineer Cornelius Vermuyden, an extensive drainage network in the region was built, and the natural watercourses and the artificial Roman lodes were strengthened. The project was completed in 1663, and greatly improved the life of the settlers, and brought large areas of land into agricultural production (Darby, 1956; 1983; Harris, 1953).

Turf (peat) digging also prevailed in the Great Fen region in the 17<sup>th</sup> Century. The first documented turbary was built in 1091 in the neighbourhood of a cropland area, but by the 12<sup>th</sup> and 13<sup>th</sup> Centuries turbaries started to be widespread in the region. After the large-scale drainage in the 17<sup>th</sup> Century, the turf digging activities increased dramatically due to an increase in the demand for fuel in the Fenland areas where wood and other fuel sources were in short supply. Another important reason for this was probably that it was much easier to harvest peat after the great drainage. Turf digging appeared to decline from the late 18<sup>th</sup> Century onwards on both Baker's Fen and St. Edmunds Fen (Figure 12), and certainly by the time of the establishment of the Wicken Fen nature reserve. However, Burwell Fen and Adventurers' Fen (Figure 10) still supported the largest turbary for commercial digging until cessation of these workings in the mid-20<sup>th</sup> Century after the Second World War (Lohoar & Ballard, 1990).

Many documents note that the SF is the only area in the Great Fen region which had not been allotted to be drained during the Fen Project in the 17<sup>th</sup> Century (Gardiner & Tansley, 1923). As a result of this supposition, there are reasonable grounds to believe that the original SF area has never been drained (Rowell & Harvey, 1988). The giant sword sedge (*Cladium mariscus*) is the dominant species on the SF. This sedge had been harvested commercially as the cut material could be used for fuel, thatching, domestic and agricultural litter and fodder. The sedge cutting was not an annual event, but only took place once in perhaps three to five years. The high commercial value of the sedge is believed to be the main reason for keeping this area away from the drainage efforts. However, due to the drainage and the peat extraction in the

neighbouring area, the total area of sedge only now covers 8% of the site (Rowell, 1997).

In the early 20<sup>th</sup> Century, the establishment of the Wicken Fen nature reserve combined the subdivisions of the Wicken Fen under a single ownership. Both drainage and peat digging in the neighbourhood area ceased during this period as well. This landmark progress successfully protected the enclosed area from further disturbance. Even though the commercial value of sedge dramatically declined in the late 19<sup>th</sup> Century, the SF had fortunately survived from the collapse of the sedge industry by being recognised as a site of ecological and historical importance. The nature reserve initially only covered part of the SF, but has since been expanded to its present extent for conservation purposes (Rowell, 1997).

### 3.1.3. Conservation and Restoration at Wicken Fen

The conservation value of Wicken Fen was recognised as a result of the diverse flora, fauna and habitats found at the site, and also the presence of many endangered plant species such as fen violet (*Viola persiciflora*) and milk-parsley (*Peucedanum palustre*) (Kelvin, 2011). It was designated as a NNR in 1993 (Lock *et al.*, 1997).

Under current management by the NT, the plan is to use a more naturally sustainable approach to create a mosaic of mostly self-regenerating wetland habitats, including diverse micro-ecosystems such as wet grasslands, reed beds, marsh, fen and shallow ponds and ditches, chalk grassland and woodlands (National Trust, 2009). This natural regenerating restoration approach lets the species assemblages change over time under appropriate controls in environmental conditions and requires less intensive and costly management. The exact composition and distribution of the self-regenerating mosaic habitats is less predictable but will be more sustainable both in the short and long term. The NT is deliberately aiming for a “lighter touch”, also, for those parts of the site under restoration management, only sometimes supplementing with some seeding of

appropriate vegetation species, reducing the infield water losses and introducing conservation grazing (Warrington *et al.*, 2009).

As on the reclaimed agricultural land under restoration management and elsewhere in the nature reserve, the NT has used ditch sluice and pump mechanisms in order to maintain water levels and reduce the infield water losses. Different types of pump technology have been used in the last few decades, such as wind-driven pumps, steam-driven pumps and modern electrically powered pumping mechanisms (Kelvin, 2011). The water levels in soil and ditches have been controlled appropriately by the modern electrically powered pumping mechanisms nowadays on the site, although seasonal variations can occur. Ditch sluice and impermeable membranes are also employed for preventing infield drainage in order to allow the appropriate permanent wetland vegetation to develop (Friday, 1997). In some particular areas of the nature reserve, the land is allowed to become much wetter to encourage birds, wildflowers, and insects.



**Figure 13:** Konik Pony at Baker's Fen (photo taken by © Mike Peacock) and Highland Cattle at Baker's Fen (photo taken by © Hugh Venables).

Conservation grazing was introduced to Wicken Fen in 2003 at BF and Adventurer's Fen (the area between the Wicken Lode and Burwell Lode; Figure 10). This grazing compartment covers over 155 ha; the naturalistic grazing system allows animals free-roaming over the whole available area throughout the year. The Konik Pony, an eastern European breed of primitive pony, is one of the species chosen to graze on the site (Figure 13). Another grazing animal chosen for the site is the Highland Cattle which originates from the Highlands and Islands of Scotland (Figure 13). The Konik Pony

was introduced from a nature reserve in the Netherlands with a similar management system; and the Highland Cattle were from a similar free-range system on the Isle of Mull, so both of them quickly settled in at Wicken Fen. Both the Konik Pony and Highland Cattle are tough, robust animals which are well-adapted to and thrive in wetland habitats and have been used successfully to help manage nature reserves right across Europe. There is wide acceptance that conservation grazing can be a valuable tool to influence the developing vegetation in the regenerating wetland ecosystems, since the grazers can keep the landscape open and help the vegetation to become established (Laidlaw, 2011). The large animals also can create other habitats such as trodden paths, dusty hollows, water-filled hoof prints and piles of dung, making the animals act as catalysts for the introduction of new flora and fauna to the ecosystem. The grazing wardens from the NT only provide necessary help to the herds (e.g. regular inspections, monitoring, recording *etc.*) under the “hands-off” approach to avoid any further disruption to the animals by human intervention (Laidlaw, 2011; National Trust, 2011; personal conversation with Carol Laidlaw, the grazing warden at Wicken Fen NNR).

### 3.2. Study Site One: Baker’s Fen

The study site at BF is located in the southern part of Wicken Fen NNR, covering an area of about 55 ha (Priory Farm in Figure 11). BF is a rewetting temperate lowland fen that was formerly under intensive agricultural use from around the mid-19<sup>th</sup> Century (Figure 14). The site, called “Priory Farm” in the last centuries, was initially drained in 1840 and used for intensive row crop production in the years prior to restoration (Friday & Colston, 1999). The site was recently initially restored in 1994 and rewetted in 1998 by ditch blocking to raise the ground water table. Calcareous water is abstracted from Monks Lode to the site only between November and April due to the summer water rights being fully allocated to the surrounding agricultural land use (M. Lester, personal communication; Figure 11). During the restoration, it was replanted with some native common grass and rush species (i.e. *Poa trivialis*, *Agrostis stolonifera* and *Juncus inflexus*) (Friday, 1997). Today, there still is quite a large area of arable

land to the south-west side of BF, but on the other sides it abuts onto the established, original fenland features of the nature reserve.



**Figure 14:** A view at Baker's Fen from the south-west (dominant wind direction) to the flux station with Highland Cattle standing on the site (photo taken by © Ajay Tegala).

Conservation grazing with Konik Pony and Highland Cattle was introduced to BF and the neighbouring Adventurer's Fen in 2003. There were 29 Konik Ponies and 29 Highland Cattle on the site at the end of 2008. Today, there are 31 Konik Ponies and 28 Cattle on the site (C. Laidlaw, personal communication). The number of animals has fluctuated over the years because of breeding, animal social behaviour or management. However, the grazing pressure is controlled at a flexible population density of roughly one animal for every 1.5 ha (Laidlaw, 2011).

The surface of BF is a mosaic of semi-natural grassland communities and consists of ~ 60% relatively dry areas with rough grassland, ~ 30% perennially saturated areas and ~ 5% drainage ditches at variable spacing (Morrison, 2012). The relatively dry areas are dominated by rough bluegrass (*Poa trivialis*), creeping bent (*Agrostis stolonifera*), couch grass (*Elytrigia repens*), cocksfoot (*Dactylis glomerata*) and false oat-grass (*Arrhenatherum elatius*); perennially wet areas are dominated by soft rush (*Juncus inflexus*), hairy sedge (*Carex hirta*) and creeping bent (*A. stolonifera*); and the drainage ditches are dominated by common reed (*Phragmites australis*) (Morrison, 2012).

Peat soils at BF are highly degraded Adventurer's series (sedge) fen peats of about 0.55 m in depth, overlying 15 - 23 m impervious grey Gault clay. The soil organic matter (SOM) in the top 0.3 m of the peat profile is about 34% (Morgan, 2005; Stroh *et al.*, 2012) and peat bulk density is approximately  $1.1 \text{ g cm}^{-3}$  (Ness & Procter-Nicholls, 2008). The growing season lasts from March to October (Morrison, 2012).

### 3.3. Study Site Two: Sedge Fen

The second study site SF is located in the north of Wicken Lode in the Wicken Fen NNR, covering an area of 137.7 ha (Figure 15). Documents suggest that this original SF is one of the very few remnants of the original fens in the great East Anglian Fenland region in the sense that it has never been drained or used for agriculture or peat extraction in its history (Rowell & Harvey, 1988). It is a rich calcareous fen (pH ~7) which forms the nucleus of the Wicken Fen NNR (Kelvin, 2011).



**Figure 15:** A view at Sedge Fen to the west (dominant wind direction) from the top of the flux tower (photo taken by © Jörg Kaduk).

The peat soil at SF is Adventurer's series (sedge) fen peat which is more than 4 m deep at the south-western end, and less than 1 m deep in the north-eastern corner, overlying on 15 - 23 m thick impervious grey Gault clay (Friday *et al.*, 1997). The peat depth is *circa* 2 m at the location of the flux tower. The SF lies about 2 m above the adjacent drained farmland, between 3 - 5 m above the sea level. The SOM is about 77% in the top 0.5 m of the peat profile, and the bulk density is about 0.2 g cm<sup>-3</sup> to a depth of 0.5 m (Morgan, 2005; Stroh *et al.*, 2012).

There are numerous ditches / lodes on the site (Figure 11). The primary source of calcareous water to the SF is the Wicken Lode (Kelvin, 2011; Figure 11). Historically, SF was subject to winter flooding from Wicken Lode and a drought period in summer (Godwin, 1931). In the 1940s, a sluice and pump were installed upstream to maintain the lode water levels and prevent the site from flooding (Lock *et al.*, 1997). Thus, the ditches are employed as drainage channels during winter and irrigation channels during summer. To limit water loss from SF to the adjacent agriculture land at a lower elevation, an impermeable membrane was installed along the northern boundary to the agricultural area in the late 1980s (Friday, 1997). Therefore, the SF is hydrologically isolated by the impermeable membrane within the northern boundary, a ridge of clay to the Northeast and the Wicken Lode to the South and West, as well as the impermeable Gault clay layer beneath the peat layer (McCartney & de la Hera, 2004). In the early investigations of the hydrological regime at the SF, Godwin & Bharucha (1932) determined that the ditch water levels only affect soil water levels outside of the ditch. As the site presents an isolated hydrological unit, further research suggested that the main factor producing the lower water table in summer was the enhanced summer transpiration loss from the vegetation surface, rather than the rainfall observed at the site or the ditch water level fluctuations (Gilman, 1988; Gowing, 1977). However, its isolated hydrological condition meant that there was no minerotrophic water supply to the site and, therefore, the site showed signs of drying (McCartney & de la Hera, 2004). In response to this finding, a wind mill to pump minerotrophic water from the Wicken Lode into the fen was installed by the NT in 2011, aiming to abstract additional calcareous water from Monks Lode and delivers it to the fen during the winter months (Kaduk *et al.*, 2015; Figure 11).

In SF, the sedge has historically been harvested commercially for fuel, thatching, domestic and agricultural litter and fodder, enabling the site to persist as open fen habitat (Rowell, 1994). By the mid-15<sup>th</sup> Century, the established standard practice was for the 3 or 4 year old sedge to be harvested in summer. This practice ceased in the late 19<sup>th</sup> Century when the site was placed under conservation management by the NT. Instead of summer harvesting, an intermittent winter cutting regime was implemented during the early 20<sup>th</sup> Century which led to a decline of sedge communities and the colonisation of the fen by carr woodland (Rowell & Harvey, 1988). Therefore, the traditional summer cutting was re-implemented following an extensive scrub clearance programme to restore open fen vegetation (Friday, 1997). Nowadays, the sedge is harvested in sections every 3 or 4 years and scrub clearance takes place when needed to preserve the sedge plant communities (Kaduk *et al.*, 2015).

The human management practices such as controlling soil water levels and the sedge cutting regime have maintained diverse vegetation communities and arrested the natural process of ecological succession towards carr vegetation. Giant sword sedge (*Cladium mariscus*) has historically been the dominant species together with common reed (*Phragmites australis*) (Figure 15); this vegetation type corresponds with the *Symphytum officinale* sub-community of *Phragmites australis*-*Peucedanum palustre* tall herb fen of the National Vegetation Classification (NVC S24c) (Rodwell, 1995). Both species can typically be found in waterlogged environments as they have an internal air space system to supply oxygen to the submerged parts of the plant (Conway, 1936; 1938). Therefore they have been capable of persisting at the site, despite winter flooding. Moreover, these dominant species can transport CH<sub>4</sub> from the soil to the atmosphere via their internal channels thus forming a CH<sub>4</sub> emission pathway that bypasses the methanotrophic zone in the soil or surface water (Brix *et al.*, 1996; Figure 7).

### 3.4. Summary

This chapter provides an overview of the flux measurement sites at the Wicken Fen NNR (3.1.1). The ecological and edaphic conditions (3.1.1), together with the history

(3.1.2), the current management practices and ecosystem restoration activities (3.1.3) employed at the two study sites (3.2 and 3.3) were presented separately. This provides an intensive understanding of the study region and a detailed picture of the study locations.

## **Chapter 4**

# **Methods, Data Collection and Processing**

## 4.1. The Eddy Covariance System

The ground-based EC system is the primary instrumentation system used in this research to measure land-atmosphere CO<sub>2</sub> and CH<sub>4</sub> exchanges at the two study sites. In this section the EC theory is introduced, summarising the most important elements from detailed reviews of the EC techniques that are available in the literature (e.g. Aubinet *et al.*, 2000; Baldocchi, 2003; Baldocchi *et al.*, 1988; 2012; Burba & Anderson, 2010; Foken *et al.*, 2012; Monson & Baldocchi, 2014).

### 4.1.1. Eddy Covariance Theory

Flux density can be defined as transport of a scalar or vector quantity expressed through a unit area per unit time, which can be used for mass, heat, momentum *etc.* (Burba & Anderson, 2010). Therefore, the measurement of the appropriate flux density is widely used to estimate the exchanges of trace gases, heat or water in an area of interest. Over the last decades, the EC technique as a method to measure the flux density has been widely used as one of the most direct and reliable methods available to quantify the land-atmosphere trace gas fluxes over relatively large “footprint” areas (ecosystem-scale) in different ecosystems continuously (Baldocchi *et al.*, 1988; Laine *et al.*, 2006). EC can also be used to measure the fluxes of sensible heat, latent heat and momentum (Aubinet *et al.*, 2012; Baldocchi *et al.*, 2001a). The EC method has been recently widely used for studies of plant physiology and role of environmental factors on ecosystem functions (Aubinet *et al.*, 2000). Currently, there are over 500 EC sites all over the world (Monson & Baldocchi, 2014).

EC measurements rely on sensing the turbulent airflow within the planetary boundary layer (PBL) at the interface between the atmosphere and the biosphere. The turbulent motion within the surface boundary layer can be imagined as a horizontal flow of numerous eddies of various frequencies rotating in 3 dimensions (3-D; Figure 16) (Stull,

1988). Each eddy is characterised by a specific temperature, concentration of water vapour and gases such as CO<sub>2</sub>, and has a vertical wind component. Therefore the concentration, temperature, humidity and vertical wind speed of eddies can be measured by EC instrumentation installed at a fixed height ( $Z_m$ ) to determine the difference between the amount of mass and energy that is moving upwards to the atmosphere and downwards to the biosphere, i.e. the net flux (Foken *et al.*, 2012; Figure 16).

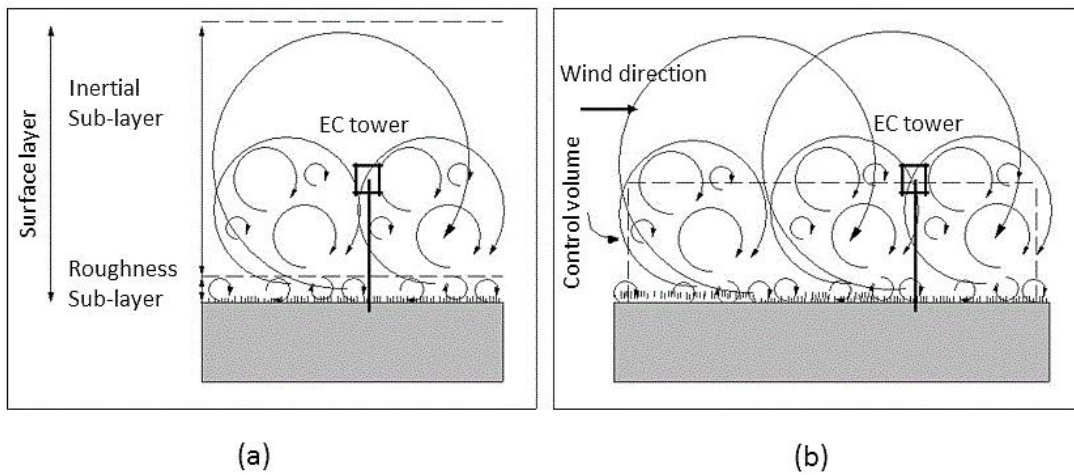


**Figure 16:** a) Schematic representation of the surface layer above a homogeneous land surface divided into inertial sub-layer and roughness sub-layer; b) Schematic representation of the eddy covariance tower and the control volume with which the expression of the gas exchange is determined (edited from Kroon, 2010).

In mathematical terms, in turbulent airflow, the vertical flux ( $F$ ) can be presented by the equation as (Burba, 2013; Equation 5):

$$F = \overline{\rho_a w s} \quad (\text{Eq. 5})$$

In the Equation 5, flux computed as the mean product of the air density ( $\rho_a$ ), vertical wind speed ( $w$ ) and the mixing ratio of the interest gas ( $s$ ). The Equation 5 can be broken into means and deviations by Reynolds decomposition and simplified as (Burba, 2013; Equation 6):

$$F = \left( \overline{\rho_a w s} + \overline{\rho_a w' s'} + \overline{w \rho_a' s'} + \overline{s \rho_a' w'} + \overline{\rho_a' w' s'} \right) \quad (\text{Eq. 6})$$

To further simplify Equation 6, an important assumption has been made in the EC method: in conventional EC measurements, the terrain has been assumed to be horizontal flat and uniform, which means the average fluctuation is assumed to be zero (Baldocchi, 2003; Foken, 2008; Horst & Weil, 1993). In other words, the conventional EC measurements should be used over a flat and vast ground layer with homogenous vegetation type, under atmospheric turbulence conditions which do not change over the averaging time period (i.e. 30 or 60 minutes). Therefore, the air density fluctuation, and flow divergence can be considered negligible (absence of horizontal advection) (Burba, 2013; Leuning, 2004). Based on these assumptions, the eddy flux can be computed as in Equation 7, where the overbar denotes the temporal averaging (i.e. 30 or 60 minutes), and the prime denotes the deviation from the mean of air density ( $\rho_a$ ), vertical wind speed ( $w$ ) and the mixing ratio of the interest gas ( $s$ ) respectively (Equation 7).

$$F \approx \overline{\rho_a w' s'} \quad (\text{Eq. 7})$$

However, most instruments usually do not measure mixing ratio of the interest gas ( $s$ ) but the gas density ( $\rho_c$ ), so a more practical formula is presented as (Burba, 2013; Equation 8):

$$F \approx \overline{\rho_a w' s'} \approx \overline{w' \rho_c'} \quad (\text{Eq. 8})$$

Thus, the eddy flux can be presented as the mean covariance between deviations in instantaneous vertical wind speed ( $w$ ) and the gas density ( $\rho_c$ ) (Equation 8). Based on these theoretical principles, the EC method assesses the gas exchanges across the biosphere-atmosphere interface by sampling the turbulent motions along with their scalar concentrations over a time integral under the assumptions made in the method proposed by Baldocchi *et al.* (1996).

There are also several other assumptions that have been made in the EC method, which should be considered carefully during the site selection and instrument installation phases (Table 1): i) the measurement point (tower position) should represent an upwind area; ii) the measured fluxes are originating from the surface of interest (Burba & Anderson, 2012; Scheupp *et al.*, 1990); iii) the measurements should be done inside of the boundary layer of interest and only from the interest area (Malhi *et al.*, 2004); iv) the EC instruments used can respond to small changes at very high frequency (10 Hz or 20 Hz) (Moore, 1986; Munger *et al.*, 2012); v) the turbulent exchange should be stationary and fully developed (Foken *et al.*, 2004; 2012).

**Table 1:** Main theoretical assumptions for eddy covariance theory (edited from Morrison, 2012; Burba & Anderson, 2010)

Theoretical Assumptions	Reference
Sensor can respond to high frequency variations in turbulence and scalar concentrations	Moore, 1986 Munger <i>et al.</i> , 2012
Measurements are made within the surface (constant flux) layer	Malhi <i>et al.</i> , 2004
A flat homogeneous surface (or fetch) with a uniform source/sink status exists for an extended upwind distance from the tower	Foken, 2008 Horst & Weil, 1994
Absence of horizontal advection	Leuning, 2004
Fluctuations average to zero over time	Baldocchi, 2003 Foken, 2008
Turbulent exchange is stationary (e.g. steady-state) and fully developed	Foken & Wichura, 1996 Foken <i>et al.</i> , 2004; 2012
Atmospheric density fluctuations are negligible	Webb, Pearman & Leuning, 1980 Burba & Anderson, 2012

However, due to these theoretical assumptions being rarely fully met in practice, as well as the physical phenomena, instrument systematic errors, specificities of terrain

and experimental setup, and other uncertainties, there are a number of potential measurement errors (Moncrieff *et al.*, 2004; Ruppert *et al.*, 2006; Table 1). It should be noted that none of the flux measurement errors are trivial (they may combine to over 100% of the initial measured flux value). To minimize or avoid such errors, it is very important to install the instruments properly and maintain instruments carefully (Rebmann *et al.*, 2012). There are also a number of corrections possible during data processing and data quality control that serve to minimize the errors (Burba & Anderson, 2010; Table 2). For example, most of the frequency response errors due to the instruments can be partially reduced by proper instrumental setup, and further corrected by frequency response corrections. The proper instrument maintenance with a spike removal procedure and filtering of raw (20 Hz) EC data can minimize the effect of spikes and noise to a large degree (Vickers & Mahrt, 1997). There are also a series of corrections that can be done during the data processing, such as (Table 2): i) coordinate rotation correction for unlevelled instrument flux (sonic anemometer) (Lee *et al.*, 2004; Wilczak *et al.*, 2001); ii) Webb-Pearman-Leuning correction related to temperature and humidity fluctuations (Webb, Pearman & Leuning, 1980); iii) sonic heat correction for sonic temperature errors affecting sensible heat flux measurements (Schotanus *et al.*, 1983); iv) time lag corrections between sonic anemometer and scalar sensors (Foken, 2008); v) coefficient corrections of LE and H (Mauder *et al.*, 2008); vi) storage corrections in the air column below  $Z_m$  (Papale *et al.*, 2006); and vii) high frequency co-spectral loss corrections (Moore, 1986).

Some errors are most severe in specific types of EC instrument. For example, time delay errors and tube attenuation errors are observed mostly in closed-path analyzers. However, missing data always occur during use of open-path analyzers due to rain or snow. A number of different mathematical methods (e.g. Monte Carlo Method) can be used for data gap filling by testing what the error is for a specific data set (Aubinet *et al.*, 2000). Comparing the closed-path and open-path analyzers, closed-path analyzers require more power supply than the open-path analyzers do. The relatively new open-closed path (enclosed) (e.g. LI-7200) analyzer may minimize the disadvantages both from the open-path and closed-path analyzers to some degree, but it requires more power than an open-path system due to the power requirement for pumping the intake air into the analyzer (Aubinet *et al.*, 2012).

**Table 2:** Summary of main processing procedures for calculation fluxes from raw eddy covariance data (LI-COR, 2015c)

Processing Procedure	Description
De-trending of raw time series	Applied to eliminate non-stationary behaviour (i.e. trend) of the measured variables during the averaging period (Mauder <i>et al.</i> , 2008)
Coordinate rotation for sonic anemometer title (SAT) correction	Applied to align instrumental coordinate system with the local terrain to the mean streamlines of the wind to remove contamination of the vertical component of wind speed by the other two horizontal components (Foken, 2008)
Angle-of-attack dependent correction (Gill's only)	Applied only for vertical mounted omni-directional SAT to compensate the effects of flow distortion induced by the transducer self-shading by frame on the turbulent flow field (Gash & Dolman, 2003; Nakai & Shimoyama, 2012)
Time lags compensation	Applied to compensate measurements time lags between SAT and any other high frequency instrument due to spatial separation and passage of air into sampling lines (Foken, 2008)
Statistical analysis and spike removal	Applied to screen raw data statistically due to instrument and electrical noise, remove spikes, drop-outs, data exceeding absolute limits, poor amplitude resolution and skewness and kurtosis issues from any further flux computation (Mauder <i>et al.</i> , 2013; Rebmann <i>et al.</i> , 2012; Vickers & Mahrt, 1997)
Data conversion and computation	Applied to convert sonic temperature to true temperature for calculation H; compute of the averages of all measured variables with a half time stamp (Schotanus <i>et al.</i> , 1983)
High frequency response corrections	Applied to compensate high frequency flux contribution losses due to finite sensors separation, signal attenuation, path averaging, time constants of EC system (Baldocchi, 2003)
Low frequency response corrections	Applied to compensate low frequency flux contribution losses due to finite averaging length and de-trending (Massman & Clement, 2004; Moncrieff <i>et al.</i> , 2004).
Atmospheric density fluctuation correction (WPL correction, open-path only)	Molar density measurements are influenced by fluctuations of temperature, humidity and pressure that generate expansion and contraction of air volume. The Webb, Pearman and Leuning (WPL) correction applied to adjust these effects on measured fluxes (Leuning, 2004; Webb, Pearman & Leuning, 1980)
Storage corrections	The storage term need to be counted during periods of weak turbulent mixing, the fluxes from surface may accumulate and not reach the measurement height ( $Z_m$ ). Generally, the storage term is negligible over short vegetation with low $Z_m$ (Aubinet <i>et al.</i> , 2012; Papale <i>et al.</i> , 2006).
Random uncertainty estimation	Calculate flux random uncertainty due to sampling error (Finkelstein & Sims, 2001; Mann & Lenschow, 1994)
Footprint estimation	Applied to calculate the distance from the EC tower contribution to the measured fluxes, which will use for quality control (Burba & Anderson, 2011; Kormann & Meixner 2001)
Quality control test	Flag data quality based on steady-state and developed turbulence tests (Foken <i>et al.</i> , 2004)

On the spatial scale, the EC method represents an intermediate vacancy between (i) the leaf / single plant measurements (i.e. leaf cuvettes) or small scale measurements (i.e. soil chambers) and (ii) regional assessments (i.e. remote sensing). Comparing with the other intermediate-scale ground based GHG flux measurement techniques (i.e. chamber measurement); both methods have some advantages and disadvantages (Table 3). However, the ground based measurements are restricted to spatially discrete observations. A current strategy to use optical remote sensing techniques based on Earth observation data to create a consistent global dataset of primary production estimates is advocated widely in the future work, emphasizing the value of multi-scale observations for modelling (Friend *et al.*, 2007; Heinsch *et al.*, 2006).

**Table 3:** General comparison between eddy covariance method and chamber techniques (edited from Drösler *et al.*, 2008)

Characteristics	Methods		
	Eddy covariance	Automatic chamber	Manual chamber
Undisturbed gas exchange	++	+/-	+/-
Integration over spatial variability	++	-	-
Direct measurement of small-scale spatial variability and management	--	+	++
Tracking temporal variability	++	++	-
Costs	--	--	++
Workload	++	+	--
Performance under all climatic conditions	+/-	+/-	++

“+” means advantage, “-” means disadvantage

### 4.1.2. Quality Control

Quality control (QC) is a data filtering procedure to check the processed half-hour dataset quality and exclude the flux data of suspect quality due to unfavourable micro-meteorological conditions and to instrument malfunctioning (Foken, 2003). The QC procedures are site specific, but typical QC steps include: a) remove data flagged as being in a low quality class, during precipitation, snow, and frost events (Foken, 2003; Foken *et al.*, 2004; Göckede *et al.*, 2004; Mauder & Foken, 2011); b) removal of statistical outliers (above or below thresholds) in half-hour flux dataset (Elbers *et al.*, 2011; Papale *et al.*, 2006); c) friction velocity ( $u^*$ ) filtering (statistical tests for turbulence conditions) (Foken *et al.*, 2004; Ruppert *et al.*, 2006); d) footprint modelling for spatial assessment of flux measurements (Hsieh *et al.*, 2000; Kljun *et al.*, 2004; Kormann & Meixner, 2003).

One of the important challenges relates to the EC measurements during nocturnal periods (Aubinet *et al.*, 2012). During the night and under thermally stable conditions, when NEE represents exclusively respiratory processes, low turbulence conditions can cause the respired CO<sub>2</sub> to accumulate below  $Z_m$  (Aubinet *et al.*, 2012; Papale *et al.*, 2006). In such conditions, horizontal advection may transport CO<sub>2</sub> away from the site of production therefore the assumptions underlying the EC theory are not fully met. As a consequence nocturnal NEE could be underestimated and the further cumulative CO<sub>2</sub> sequestration overestimated (Aubinet *et al.*, 2012; Goulden *et al.*, 1996). This issue is addressed by filtering flux data obtained during the stable stratification periods under a certain  $u^*$  threshold, with the generated gaps being replaced using the gap-filling procedure described below (Goulden *et al.*, 1996; Lohila *et al.*, 2011; Papale *et al.*, 2006).

### 4.1.3. Data Gap-filling

Together with unavoidable original gaps in EC measurements due to system downtime, artificial gaps after QC procedures affect the flux dataset (Papale, 2012). Normally,

typical EC data coverage is 40% to 60% at annual timescales (Falge *et al.*, 2001). Although processed available data with gaps is unproblematic for obtaining a defensible annual budget and is adequate for analyses of functional relationships, a gap-filling procedure is required to produce daily, seasonal and annual sums of CO<sub>2</sub> exchange (Papale, 2012).

A range of gap-filling methods have been reported and compared, and can be divided into several main types: non-linear regression (Desai *et al.*, 2005); look-up table types (Reichstein *et al.*, 2005); artificial neural networks (Papale & Valentini, 2003) and others (e.g. mean diurnal variation; Moffat *et al.*, 2007). All these gap-filling methods have advantages and disadvantages; method choice ultimately depends on amount and distribution of gaps, availability of meteorological data and the balance between implementation costs and gap-filling performance (Moffat *et al.*, 2007; Richardson & Hollinger, 2007; Richardson *et al.*, 2008). An online high performance gap-filling method of Reichstein *et al.* (2005) as one of the standardized methods has been made available and widely adopted by the whole EC flux measurement community (i.e. Carboeurope-IP project and FluxNet).

#### 4.1.4. Flux Partitioning

The EC measurement only provides direct measurement of NEE, while GPP and  $R_{eco}$  cannot be discriminated from the measurements of daytime NEE (Reichstein *et al.*, 2005; 2012). Therefore, a modelling approach needs to be used to partition the measured NEE into its component fluxes (Lasslop *et al.*, 2010; Reichstein *et al.*, 2005; 2012).

From an ecosystem aspect, a negative NEE indicates existence of a sink of CO<sub>2</sub> when a net uptake of CO<sub>2</sub> appears in the ecosystem; while a positive NEE means the ecosystem is acting as a source of CO<sub>2</sub> when CO<sub>2</sub> is away from the surface to the atmosphere. The net CO<sub>2</sub> flux can be expressed as (Equation 9):

$$NEE = R_{eco} - GPP \quad (\text{Eq. 9})$$

Nowadays, many different flux partitioning algorithms have been developed (Desai *et al.*, 2005; Lasslop *et al.*, 2010; Reichstein *et al.*, 2005). One of the most widely used algorithms in the community is based on extrapolating measurement of nocturnal NEE to NEE during daytime as  $T_{air}$ , with GPP estimated by difference (Reichstein *et al.*, 2005). An alternative approach is estimation of daytime  $R_{eco}$  as the y-intercept of the light response to daytime NEE (Smith *et al.*, 2010).

#### 4.1.5. Energy Balance Closure

The evaluation of the energy balance closure (EBC) is commonly used to assess EC estimate performance (Leuning *et al.*, 2012; Wilson *et al.*, 2002). Wilson *et al.* (2002) defined that “EBC is an expression of the first law of thermodynamics, which requires the sum of the turbulent energy fluxes measured with the EC system (the sensible heat flux,  $H$  and the latent heat flux,  $LE$ ) to balance the sum of all other energy terms”. In simple terms, the energy balance can be defined as “the turbulent fluxes  $H$  and  $LE$  against the available energy which can be approximated by the difference between net radiation ( $R_n$ ) and ground heat flux ( $G$ )” (Oke, 1987) (Equation 10):

$$R_n - G \approx H + LE \quad (\text{Eq. 10})$$

where  $R_n$  is measured using a net radiometer,  $G$  is measured by soil heat flux plates, and  $H$  and  $LE$  are EC measurements (for all terms, units are expressed in  $\text{W m}^{-2}$ ). As a plausibility test, the smaller the difference between the two terms, the higher is the quality of the data used. However, in reality, full EBC is rarely attained in observation, mostly around 70% to 90% across a range of ecosystems (Foken *et al.*, 2006; Jacobs *et*

*al.*, 2008). There are various potential reasons that can cause an imbalance in EBC, some of which may influence the flux measurements; however, it should not be used to correct the trace gas flux measurements (Foken *et al.*, 2011; Twine *et al.*, 2000).

## 4.2. Instrumentation

### 4.2.1. Instrumentation at Baker's Fen

An EC system consists of multiple sensors making simultaneous measurements of all flux terms, as well as the relevant meteorological instruments. The Baker's Fen EC station is located at 52°18'15"N, 0°17'27"E, at Wicken Fen NNR. The station is based at 4 m above mean sea level (amsl) with a clear fetch over BF, over 600 m along the dominant (southwest) wind directions, about 300 - 400 m in all other directions (Figure 17). The instruments are mounted on the tripod arm at about 2.3 m above the ground level, about 1.5 m above the vegetation surface (i.e. over twice the maximum summer vegetation height; Foken, 2008). The EC system is composed of the following instruments (Figure 18). All meteorology measurements were logged on a datalogger CR1000, the datalogger clock was synchronised during each field work visit. The whole system was set to Greenwich Mean Time (GMT) during the whole measurement period. The power system was provided by an array of four 250 W solar panels and a bank of four 6 v car batteries (Solar-wind Ltd., Ipswich, UK). The power control system and the batteries were housed in a box located north of the EC tower. The station was within a fenced enclosure to protect damage by / to grazing animals. The vegetation within the enclosure was cut intermittently to maintain similar conditions to the grazed site. Dip wells were installed and maintained by the NT; water level data from 107-1 (location marked on the map) which was used in this study was provided by John Bragg from the NT (Figure 17).



**Figure 17:** Footprint of Baker's Fen eddy covariance site. The red marker indicates the location of the EC station. The green marker labeled 107-1 points to the location of the automatic dipwell managed by the NT of which the data are used in this study. The red lines show 100 m distance to the North, East, South and West of the EC tower.

High frequency measurements (20 Hz) were taken by:

- 1 × CSAT3 Three Dimensional Sonic Anemometer (Campbell Scientific Ltd., Shepshed, UK) at 2.24 m height
- 1 × LI-COR LI-7500A Open-Path CO<sub>2</sub> and H<sub>2</sub>O Infrared Gas Analyser (IRGA) (LI-COR Ltd., Lincoln, Nebraska, USA) at 2.24 m height
- 1 × LI-COR LI-7700 Open-Path CH<sub>4</sub> IRGA (LI-COR Ltd., Lincoln, Nebraska, USA) at 2.26 m height
- 1 × LI-COR LI-7550 Analyser Interface Unit (LI-COR Ltd., Lincoln, Nebraska, USA)



**Figure 18:** Setup of the EC station at Baker's Fen with sonic anemometer, the IRGAs, radiometers, relative humidity and temperature probe, solar panels and the power control system in the green box within a fence enclosure (© G. Pan).

Meteorology measurements were taken every 10 seconds and averaged to 30 min means by:

- 1 × CR1000 Data Logger (Campbell Scientific Ltd., Shepshed, UK)
- 1 × CNR1 Net Radiometer (Kipp & Zonen Ltd., Delft, The Netherlands)
- 1 × SKP215 Quantum Sensor (Skye Instruments Ltd., Powys, UK)
- 1 × HMP45C Relative Humidity and Temperature Probe (Campbell Scientific Ltd., Shepshed, UK)
- 4 × HFP01SC Soil Heat Flux Plates (Hukesflux Ltd., Delft, The Netherlands) at 8 cm below the ground surface
- 1 × ARG100 Tipping Bucket Rain-gauge (Environmental Measurements Ltd., North Shields, UK)

#### 4.2.2. Instrumentation at Sedge Fen

The SF station is located at  $52^{\circ}18'35''\text{N}$ ,  $0^{\circ}16'47''\text{E}$ , within the old Sedge Fen area in Wicken Fen NNR. At this station, there is an automatic weather station (AWS) and an EC station mounted on separate tripods. Both the AWS and the EC station are at 4 m amsl with a clear fetch over SF of 150 m to the north of the EC tower by an area of woodland, but at least 400 m in all other wind directions (Kaduk *et al.*, 2015; Figure 19). The instruments on the AWS and the EC station are mounted at about 4 m above the ground level, about 2.5 m above the sedge canopy (about double the mean vegetation height) (Foken, 2008). Meteorology measurements of the EC station and the AWS were logged on separate dataloggers. The datalogger clocks were synchronised during each field work visit. The whole system was set to Greenwich Mean Time (GMT) during the whole measurement period. The system power was similar as BF with an array of four 250 W solar panels and a bank of four 6 v car batteries (Solarwind Ltd., Ipswich, UK). There is a box located north of the EC tower housed the power control system and batteries.



**Figure 19:** Footprint of Sedge Fen eddy covariance site. The red marker indicates the location of the AWS and EC station. The green marker labeled NW07 points to the location of the automatic dipwell managed by the NT of which the data are used here. The red lines show 100 m distance to the North, East, South and West of the flux tower. The remaining blue and green markers are further dipwells managed by the NT (from Kaduk *et al.*, 2015).

The AWS was equipped with the following instruments (Figure 20). Measurements were taken every 10 seconds and averaged to 30 minute means. Dip wells were installed and maintained by the NT, water level data from NW07 (location marked on the map) which was used in this study was provided by John Bragg from the NT (Figure 19).

- 1 × CR1000 Data Logger (Campbell Scientific Ltd., Shepshed, UK)
- 1 × HMP45C Relative Humidity and Temperature Probe (Campbell Scientific Ltd., Shepshed, UK)
- 2 × HFP01 Soil Heat Flux Plates (Hukseflux Ltd., Delft, The Netherlands) at 5 cm below the ground surface
- 2 × Cup Anemometers



**Figure 20:** Setup of the AWS at Sedge Fen with the relative humidity and temperature probe, two cup anemometers and radiation sensor, white weatherproof boxes house datalogger and instrument control units (© G. Pan).

The instrumentation setup of the EC station was composed of the following instruments (Figure 21):

Meteorology measurements were taken every 10 seconds and averaged to 30 minute means by:

- 1 × CR3000 Data Logger (Campbell Scientific Ltd., Shepshed, UK)
- 1 × CNR1 Net Radiometer (Kipp & Zonen Ltd., Delft, The Netherlands)
- 1 × HMP45C Relative Humidity and Temperature Probe (Campbell Scientific Ltd., Shepshed, UK)
- 2 × HFP01 Soil Heat Flux Plates (Hukseflux Ltd., Delft, The Netherlands) at 8 cm below the ground surface

High frequency measurements (20 Hz) were taken by:

- 1 × Gill R3-50 Ultrasonic Anemometer (Gill Instruments Ltd., Lymington, UK) at 3.94 m height
- 1 × LI-COR LI-7500A Open-Path CO<sub>2</sub> and H<sub>2</sub>O IRGA (LI-COR Ltd., Lincoln, Nebraska, USA) at 3.79 m height
- 1 × LI-COR LI-7700 Open-Path CH<sub>4</sub> IRGA (LI-COR Ltd., Lincoln, Nebraska, USA) at 3.6 m height
- 1 × LI-COR LI-7550 Analyser Interface Unit (LI-COR Ltd., Lincoln, Nebraska, USA)

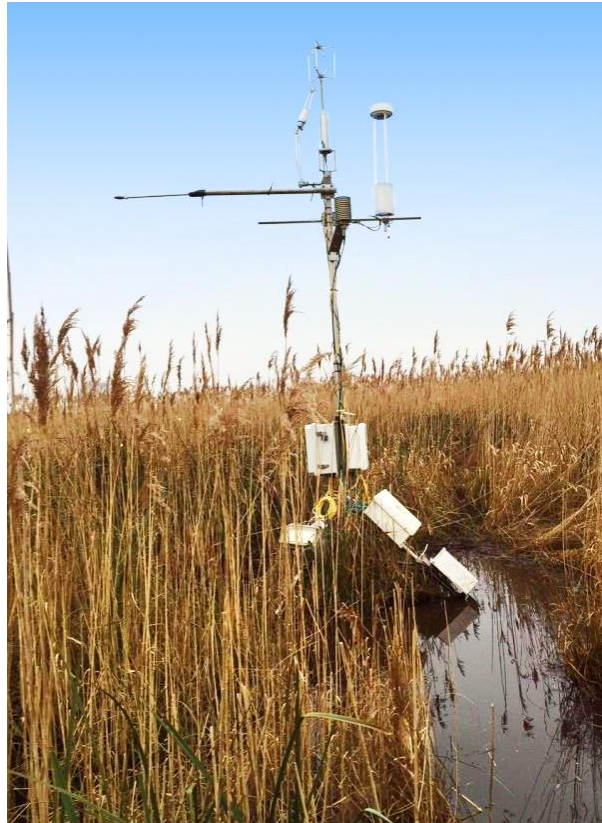


**Figure 21:** Setup of the EC station at Sedge Fen with the sonic anemometer, the IRGAs, radiometer and second relative humidity and temperature probe, white weatherproof boxes house datalogger, instrument control units and washer water storage tank (© G. Pan).

#### 4.2.3. Output Variables of Instruments

The output variables of and further information about all the instruments which have been used in this study at each study site are presented in the Table 4.

**Table 4:** Main output variables from all the instruments which have been used in this study in the EC system. Further information about the instruments is also indicated as reference.

Instrument	Measured Variables (notation)	Site	Reference
CSAT3 Three Dimensional Sonic Anemometer	Horizontal wind velocity: $u'$ ( $\text{m s}^{-1}$ ); $v'$ ( $\text{m s}^{-1}$ ) Vertical wind velocity: $w'$ ( $\text{m s}^{-1}$ ) Speed of sound: $c$ ( $\text{m s}^{-1}$ )	BF	(Campbell Scientific, 2015a)
Gill R3-50 Ultrasonic Anemometer	Horizontal wind velocity: $u'$ ( $\text{m s}^{-1}$ ); $v'$ ( $\text{m s}^{-1}$ ) Vertical wind velocity: $w'$ ( $\text{m s}^{-1}$ ) Speed of sound: $c$ ( $\text{m s}^{-1}$ )	SF	(Gill Instruments, 2007)
LI-COR LI-7500A Open-Path CO <sub>2</sub> and H <sub>2</sub> O IRGA	CO <sub>2</sub> concentration density: CO <sub>2</sub> ( $\mu\text{mol m}^{-2}\text{s}^{-1}$ ) H <sub>2</sub> O concentration density: H <sub>2</sub> O ( $\text{mmol m}^{-2}\text{s}^{-1}$ )	BF/ SF	(LI-COR, 2015a)
LI-COR LI-7700 Open-Path CH <sub>4</sub> IRGA	CH <sub>4</sub> concentration density: CH <sub>4</sub> ( $\mu\text{mol m}^{-2}\text{s}^{-1}$ ) Air temperature: CH <sub>4</sub> temperature ( $^{\circ}\text{C}$ ) Air pressure: CH <sub>4</sub> pressure (kPa)	BF/ SF	(LI-COR, 2015b)
Li-COR LI-7550 Analyser Interface Unit	Temperature measured at LI-7550: Temperature ( $^{\circ}\text{C}$ ) Barometric pressure measured in LI-7550: Pressure (kPa)	BF/ SF	(LI-COR, 2015a)
CNR1 Net Radiometer	Solar radiation (shortwave): $SW_{\text{in}}$ ( $\text{W m}^{-2}$ ) Reflected solar radiation (shortwave): $SW_{\text{out}}$ ( $\text{W m}^{-2}$ ) Far Infrared incoming radiation (longwave): $LW_{\text{in}}$ ( $\text{W m}^{-2}$ ) Far Infrared radiation from soil surface (longwave): $LW_{\text{out}}$ ( $\text{W m}^{-2}$ ) CNR1 temperature: CNR1T (K) Net Radiation: $R_n$ ( $\text{W m}^{-2}$ )	BF/ SF	(Campbell Scientific, 2011)
SKP215 Quantum Sensor	Photosynthetically active radiation: PAR (PPFD, $\mu\text{mol m}^{-2}\text{s}^{-1}$ )	BF	(Campbell Scientific, 1996)
HMP45C Relative Humidity and Temperature Probe	Relative humidity: RH (%) Air temperature: $T_{\text{air}}$ ( $^{\circ}\text{C}$ )	BF/ SF	(Campbell Scientific, 2009)
HFP01SC Soil Heat Flux Plate	Ground heat flux: $G$ ( $\text{W m}^{-2}$ )	BF/ SF	(Campbell Scientific, 2012)
ARG100 Tipping Bucket Rain-gauge	Rainfall intensity: Rain (mm)	BF	(Campbell Scientific, 2010)

## 4.3. Data Processing and Analysis

### 4.3.1. Software

Data loggers ran Campbell Scientific CRBASIC (Campbell Scientific, 2013) to calculate 30 min averages of meteorological data. The LI-7550 ran embedded software version 5.0.1 from 01/01/2013 to 16/08/2013, version 6.5.5 from 16/08/2013 to 10/09/2014 and from then on version 7.0.1. Raw EC measurements were processed with EddyPro 6.1.0 (LI-COR, 2015c) which also read in the meteorological data as external biomet data files for flux computation. The output, 30-minute fluxes and meteorology data were inputted into R version 3.1.3 (R Core Team, 2014) for QC, flux partitioning, data analysis and visualization mostly with self-developed code. For data gap-filling and some visualization the R package REddyProc developed by the Max Planck Institute for Biogeochemistry in Jena was used (MPI Biogeochemistry, 2014), which is based on Reichstein *et al.* (2005).

### 4.3.2. Eddy Covariance Data Processing

High frequency (10 and 20 Hz) raw EC measurement data was processed by EddyPro software package (version 6.1.0) to calculate half-hour turbulent fluxes of CO<sub>2</sub>, CH<sub>4</sub>, latent and sensible heat and momentum. A half-hour interval is recognised to be adequate to capture low frequency contributions without affecting diurnal changes in the measured variables (Burba & Anderson, 2010). Negative fluxes denote uptake from the atmosphere to the biosphere and the positive fluxes represent losing from the ecosystem.

In particular, the main procedures implemented in this study by using EddyPro (version 6.1.0) include:

- De-trending: all deviations were calculated as block averages over half-hour averaging interval. Obeys Reynolds decomposition rule (the mean value of fluctuations is identically zero). Block average method retains the largest portion of low frequency content (Mauder *et al.*, 2008).
- Coordinate rotation: A double rotation was applied to each 30-minute data set of raw measurements.
- Angle-of-attack dependent correction: angle-of-attack errors in the measured wind speed were corrected according to Nakai *et al.* (2006) for site SF only (using Gill's SAT).
- Time lag compensation: sonic anemometer and IRGA measurements were synchronized using covariance maximisation to account for sensor separation and electronic delays.
- Statistical analysis and spike removal: the raw data were statistically screened for the detection and removal of spikes, drop-outs, data exceeding absolute limits, poor amplitude resolution and skewness and kurtosis issues based on Vickers & Mahrt (1997).
- Density fluctuation correction: density fluctuations were corrected according to Webb, Pearman & Leuning (1980).
- Frequency response corrections: High and low frequency losses were estimated following Moncrieff *et al.* (2004) and Moncrieff *et al.* (1997), respectively.
- Storage correction: storage of CO<sub>2</sub> below the measurement height ( $Z_m$ ) was estimated from successive CO<sub>2</sub> concentration measurement (Papale *et al.*, 2006)
- Random uncertainty estimation: the flux random uncertainty due to sampling error was estimated with the method Finkelstein & Sims (2001).
- Footprint estimation: in the first instance the footprint model of Kljun *et al.* (2004) was implemented in Eddypro was used to estimate spatial representativeness of the fluxes, and switch to the footprint model of Kormann & Meixner (2001) if the requirements of the model of Kljun *et al.* (2004) are not fulfilled.
- Quality control test: the fluxes were assigned quality flags (QF) for QC using the 0-1-2 system described by Mauder & Foken (2004).

### 4.3.3. Quality Control

#### 4.3.3.1. Low Quality Data, Outlier, Spikes Removal

This step of QC of the half-hour turbulent fluxes involved removal of statistic outliers, data flagged as low quality, values outside a likely range and de-spiking.

The QC procedures implemented in this study include:

- All flux data were removed if quality flagged as 2 in the 0-1-2 flag system (Mauder & Foken, 2004).
- All flux data were filtered using the median absolute deviation (MAD) method, data were treated separately for daytime and night-time period using a moving window of 13 days and the recommended z-value of 5.5 (Papale *et al.*, 2006).
- All flux data were removed when it was raining and the half-hour after rain (unfavourable meteorological conditions).
- CO<sub>2</sub> and LE flux data were discarded when LI-7500A AGC (parameter of the cleanness of the LI-7500A optical path) increased above 80 or LI-7500A signal strength dropped below 85%. CH<sub>4</sub> flux data were removed when LI-7700 signal strength dropped below 15%.
- The CO<sub>2</sub> fluxes were removed if they were outside the range observed in similar ecosystems (-50 to 50  $\mu\text{ mol m}^{-2}\text{s}^{-1}$ ); LE fluxes were removed if out of the range -50 to 500  $\text{W m}^{-2}$ ; H fluxes were removed if out of the range -200 to 500  $\text{W m}^{-2}$ .
- The CH<sub>4</sub> fluxes were removed if they were outside the range observed in forests, wetlands, croplands and pasture (-0.1 to 2.5  $\mu\text{ mol m}^{-2}\text{s}^{-1}$ ) (Nicolini *et al.*, 2013).
- The CO<sub>2</sub> and CH<sub>4</sub> flux data were removed if either H or LE were removed because the density correction requires H and LE.

#### 4.3.3.2. Friction Velocity Threshold

The periods of low turbulence condition and limited air mixing were identified using a friction velocity ( $u^*$ ) threshold for  $u^*$  filtering (Gu *et al.*, 2005). The assumption of the  $u^*$  filtering approach is that the night-time CO<sub>2</sub> fluxes represent respiratory processes only and do not depend on turbulence regimes. The measured CO<sub>2</sub> fluxes will only be accepted when they are independent from changes of  $u^*$  when the  $u^*$  value is above the threshold (Massman & Lee, 2002). The  $u^*$  threshold value is site-specific and varies from 0.0 to 0.6 m s<sup>-1</sup> in different ecosystems (Gu *et al.*, 2005; Massman & Lee, 2002).

In this study, the  $u^*$  threshold was calculated for different years at the two study sites respectively based on Reichstein *et al.* (2005) and Papale *et al.* (2006). The nocturnal NEE data (when global radiation  $R_g < 20 \text{ W m}^{-2}$ ) were split into six temperature classes of equal size and each temperature class has been divided into 20  $u^*$  classes. For each temperature class, the  $u^*$  threshold was identified as the  $u^*$  class where the mean was less than 95% of the mean of higher  $u^*$  class (Papale *et al.*, 2006). As  $u^*$  varies across the different seasons and years considered, the  $u^*$  threshold was calculated on different time aggregations in separate years. At both sites, the  $u^*$  filtering was finally performed using the growing season (May to October) threshold which was the highest value found on both sites on this basis.

The  $u^*$  threshold was set to 0.32 m s<sup>-1</sup> for BF 2013; 0.28 m s<sup>-1</sup> for BF 2014; 0.28 m s<sup>-1</sup> for BF 2015; 0.26 m s<sup>-1</sup> for SF 2013; 0.39 m s<sup>-1</sup> for SF 2014; 0.39 m s<sup>-1</sup> for SF 2015. All flux data were filtered using these  $u^*$  thresholds for different years / sites separately.

#### 4.3.3.3. Flux Footprint Estimates

Footprint analysis allows an assessment of the spatial representativeness of the flux measurements, i.e. “the field of view” of the EC system. In particular, the footprint model provides a measurement of relative contribution from one upwind point during each half-hour period (Scheupp *et al.*, 1990). There are various methods available in the community for modelling footprints (Burba & Anderson, 2011). In this study, in the

first instance the footprint model of Kljun *et al.* (2004) was implemented and then switched to the footprint model of Kormann & Meixner (2001) if the requirements of the model of Kljun *et al.* (2004) were not fulfilled.

The  $X_{\max}$  (maximum upwind distance from the tower) allows identification of the part of the source area affecting the measured fluxes. The flux data originating from further than the  $X_{\max}$  were assumed to originate from outside of the target area.

The  $X_{\max}$  was set at 200 m for BF and 150 m for SF based on Eddypro footprint outputs. All the flux data originating from further than 200 m at BF and 150 m at SF were removed.

#### 4.3.4. Data Coverage

At the BF station, the EC measurement data collected for this thesis started on 1<sup>st</sup> Jan. 2013 and ended on 31<sup>st</sup> Dec. 2015. At the SF station, data collection started on 1<sup>st</sup> Aug. 2013 and ended on 31<sup>st</sup> Dec. 2015. In total, there are about 5.5 site years of data included in this study. There was a long gap in continuous measurements between 3<sup>rd</sup>. January and 14<sup>th</sup>. February 2014 at BF due to batteries being stolen from the station; and a long gap between 15<sup>th</sup> Mar 2014 and 8<sup>th</sup> May 2014 at SF due to system malfunction.

Together with significant data gaps due to instrumental failure during the data acquisition phase, the QC procedure also further reduced the amount of available data. In general, data coverage during winter and night was inferior compared to summer and daytime data acquisitions because of more frequent power or instrument malfunctions, and low quality data on the basis of  $u^*$  threshold. This is particularly so for methane due to its low atmospheric concentration and hence complexities of high frequency measurements with low maintenance and low instruments (Rinne *et al.*, 2007). Many studies have reported low data coverage after QC that is mainly caused by data lost during winter and at night (Jackowicz-Korczynski *et al.*, 2010; Rinne *et al.*, 2007).

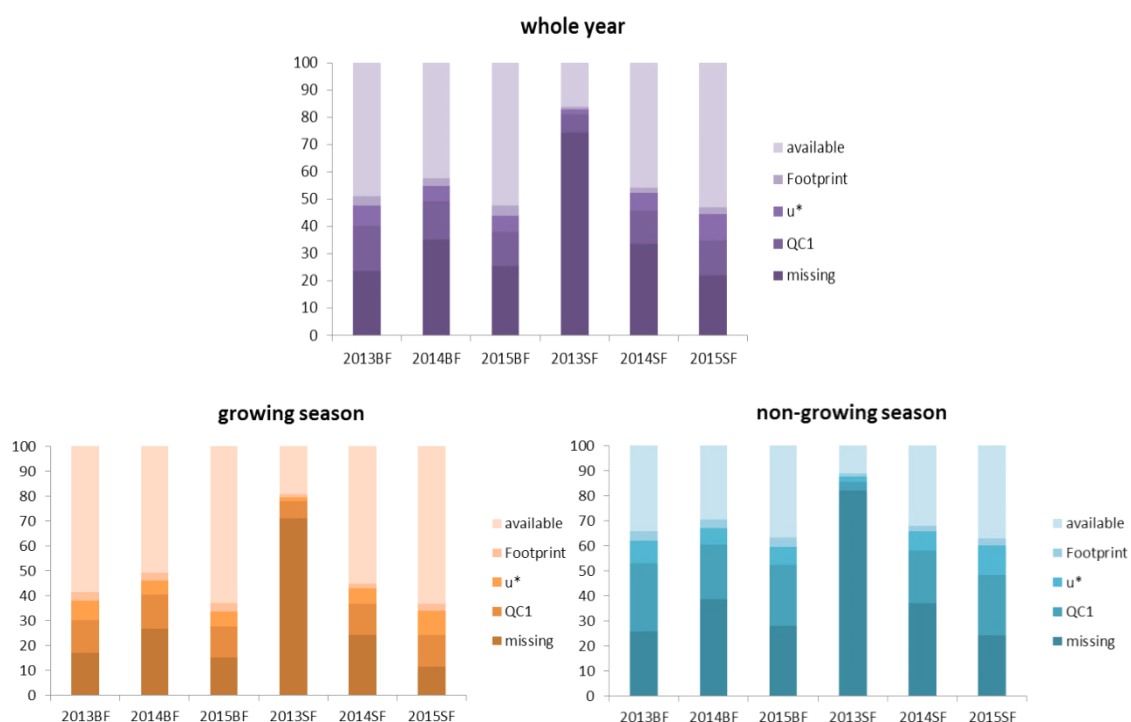


**Figure 22:** Data coverage for different periods in different years. From left to right, the complete dataset (whole year), the growing season (May to October) and the non-growing season (rest of year). Data coverage calculated using all flux data ( $CO_2$ ,  $CH_4$ ,  $H_2O$ ,  $LE$  and  $H$ ). Original gaps (missing) and the gaps generated by different QC procedures are outlines by the colour palette.

After the QC, the available data retained for two sites in different years are (Table 5):

**Table 5:** Data coverage for different periods in different years (% of valid data). 2013 SF only covers data from August to December 2013.

Year / Site	Whole Year	Growing Season	Non-growing season
2013 BF	49%	59%	39%
2014 BF	42%	51%	34%
2015 BF	53%	63%	42%
2013 SF (Aug. - Dec.)	16%	19%	13%
2014 SF	46%	55%	37%
2015 SF	53%	63%	42%

The data coverage during the growing season (May to October) on both sites was similar as shown in other studies in similar ecosystems (Wohlfahrt *et al.*, 2008; Zeeman *et al.*, 2010; Table 5). As expected, data coverage during the non-growing season was much lower than the coverage during the growing season in the same year (Figure 22). Most of the missing data can be attributed to the non-growing season or to night-time measurement periods when biological activity is very low. Nevertheless, it was concluded that the data set was sufficient for the reconstruction of an annual cycle.

#### 4.3.5. Data Gap-filling and Partitioning

The 30-minute turbulent flux data after the QC were gap-filled using the Marginal Distribution Sampling (MDS) method (Reichstein *et al.*, 2005) to produce daily, seasonal and annual sums. MDS is a variant of the Mean Diurnal Variation (MDV) approach (Falge *et al.*, 2001), and is widely adopted by the community (i.e. Carboeurope-IP project and FluxNet). The gap-filling algorithm is derived from covariance and temporal auto-correlation of the fluxes. The gaps have been substituted by the data measured under the similar meteorological conditions according to its types (Look up tables, LUT) within a time window  $\pm 7$  to 14 days, or substituted with data measured at the same time of the year (MDV).

The CO<sub>2</sub> fluxes were filled using  $R_g$ ,  $T_{air}$  and water vapour pressure deficit (VPD) as meteorological variables in the algorithm; latent heat fluxes were filled using  $R_n$ , VPD and  $T_{air}$ ; sensible heat fluxes using  $R_n$ ,  $T_{air}$  and VPD; and CH<sub>4</sub> fluxes were filled using  $R_n$ , water table (WT) and  $T_{air}$ . The selection of the variables used for gap filling was based on an exploration of the co-variation of the variables and the R<sup>2</sup> of the predictions from the gap filling for the existing measurements.

The partitioning of NEE into CO<sub>2</sub> flux components (GPP and  $R_{eco}$ ) was performed by the modelling approach used widely by the community (e.g. Moffat *et al.*, 2007; Reichstein *et al.*, 2005). The Reichstein *et al.* (2005) partitioning approach uses only original data to model nocturnal NEE (representing solely respiratory process nocturnal

$R_{eco}$ ) as a function of temperature. The nocturnal NEE data are therefore used to fit the Lloyd & Taylor (1994) respiration model (Equation 11):

$$R_{eco}(T) = R_{eco,ref} \cdot e^{E_0 \cdot \left\{ \frac{1}{T_{ref}-T_0} - \frac{1}{T-T_0} \right\}} \quad (\text{Eq. 11})$$

where  $R_{eco,ref}$  is basal ecosystem respiration at reference temperature ( $T_{ref}$ ) set to 10 °C;  $E_0$  (K) is the activation-energy;  $T$  is either air or soil temperature and  $T_0$  is the temperature where  $R_{eco}$  reaches zero (set constant at - 46.02 °C). This function is applied over small window periods assuming model parameters are time-varying with changes in ecosystem properties. For each period, the best values of the regression parameters are used to estimate daytime  $R_{eco}$  and missing  $R_{eco}$  values, and GPP is estimated by the difference (Equation 12):

$$GPP = R_{eco} - NEE \quad (\text{Eq. 12})$$

#### 4.3.6. Uncertainty Estimation for Annual Sums

The uncertainty of the annual sums was explored using a Monte-Carlo simulation procedure assuming a normal distribution for each single 30 minute flux datum. For original data, it was assumed that their random error calculated according to Finkelstein & Sims (2001) approximates their standard deviation (SD). For gap-filled fluxes the SD as reported by the gap-filling procedure was used. For each 30 minute flux, uncertainties were generated assuming a normal distribution of the measurement with the mean of the measurement and the assigned SD. Using these distributions 1000 flux time series were generated by drawing randomly from the normal distributions for each

of the 30 minute fluxes. The SD and the 95% confidence interval of these 1000 realisations were taken to indicate the uncertainty of the annual sums.

#### 4.3.7. Energy Balance Closure

The EBC was evaluated by linear regression of the sum of the turbulent energy fluxes (LE + H) measured with the EC system against energy fluxes ( $R_n - G$ ) obtained by independent methods. In this study, EBC evaluation was performed on 30 minute time scale with quality controlled (not gap-filled) data and on daily scale by using daily averages of the turbulent and available energy fluxes (gap-filled) (Leuning *et al.*, 2012).

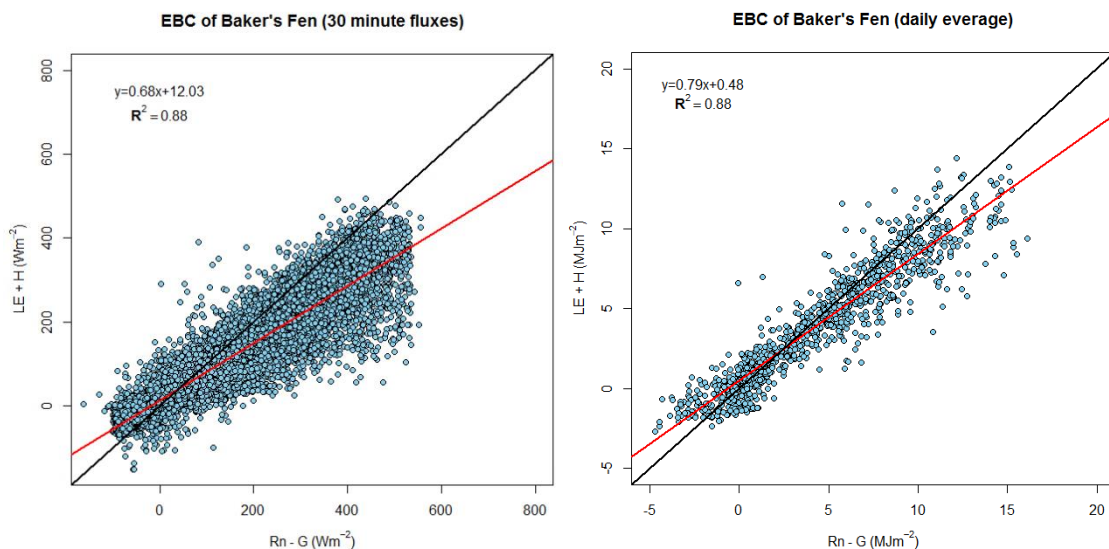


**Figure 23:** Energy balance closure for Baker's Fen. The left panel shows the measured (non-gap-filled but quality controlled) 30 min latent (LE) and sensible (H) heat fluxes plotted against measured net radiation ( $R_n$ ) reduced by the ground heat flux (G) at Baker's Fen during the whole measurement period. The right panel shows energy balance closure evaluated using daily averages (with gap-filled data). Regression equations, coefficients of determination are provided.

As shown in the Figure 23 and Figure 24, the turbulent energy fluxes were well correlated with the available energy at 30 minute scale and with daily averages on both sites ( $R^2$  of 0.88, 0.88, 0.88 and 0.76, correspondingly). The EBCs of both sites were within the range of values reported across a range of wetland ecosystems globally (68%, 88% at 30 minute scale; 79%, 86% with daily averages, respectively; Merbold *et al.*, 2009; Veenendaal *et al.*, 2007). The EBC at SF was higher than at BF at both time

scales. However, the imbalance of regression equations indicated the turbulent fluxes were overestimated during the period of low available energy (e.g. winter night-time) whereas they were underestimated during the high available energy period (e.g. summer daytime) (Figure 23 and 24). There are several reasons to explain the lack of energy balance closure measured using the EC technique: i) the footprint mismatch between the net radiometers, soil heat flux plates and the time-varying EC system (Foken, 2008); ii) surface heterogeneities within the footprint or advection that are not sampled by the EC system (Foken, 2008); iii) high or low frequency spectral loss due to instrument geometry limitations and use of finite averaging periods (Wilson *et al.*, 2002); iv) underestimation of G or other heat storage terms (S) (Jacobs *et al.*, 2008); v) instrument bias caused by study site environments (e.g. soil heat flux plates may be inaccurate in dry organic soils; Laurila *et al.*, 2012). It is also worth commenting that the heat flux plates perform poorly in peat substrates and neglected storage term could be the explanation for the relative imbalance EBC in this study (Harding & Lloyd, 2008; Jacobs *et al.*, 2008).

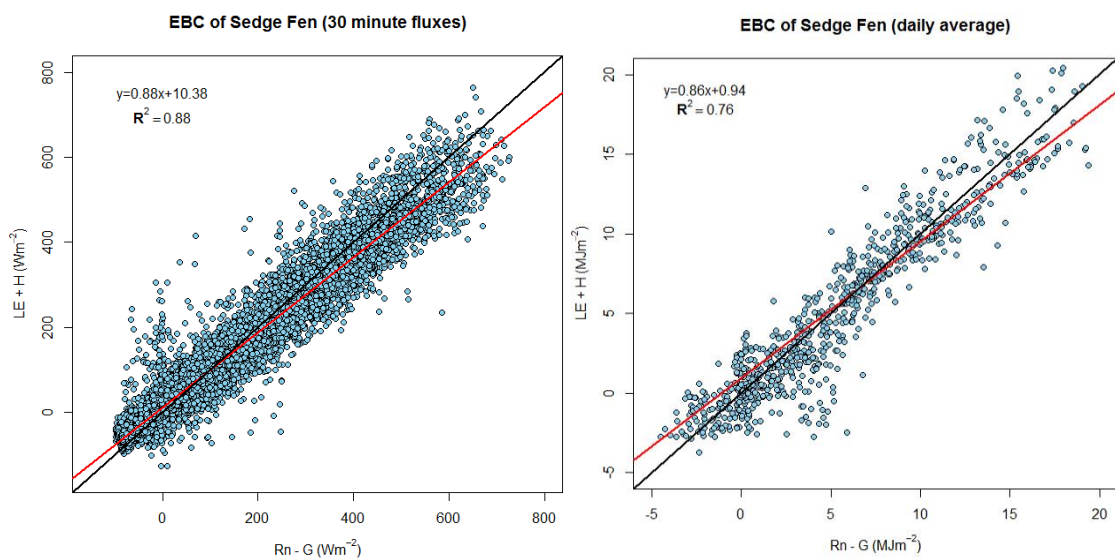


**Figure 24:** Energy balance closure for Sedge Fen. The left panel shows the measured (non-gap-filled but quality controlled) 30 min latent (LE) and sensible (H) heat fluxes plotted against measured net radiation ( $R_n$ ) reduced by the ground heat flux (G) at Sedge Fen during the whole measurement period. The right panel shows energy balance closure evaluated using daily averages (with gap-filled data). Regression equations, coefficients of determination are provided.

The EBC have been improved significantly at BF when assessed with daily averages indicating closure of 68% and 79% respectively (Figure 23). The daily EBC at SF is similar as the EBC assessed with 30 minute flux data, with slightly lower regression

slope at 0.86 and 0.88 correspondingly but with much smaller intercept of 0.94 W m<sup>-2</sup> compared to 10.38 W m<sup>-2</sup> (Figure 24). The improvement in daily EBC is consistent with results from a multisite evaluation across a range of FluxNet sites (Leuning *et al.*, 2012), suggesting the fact that daily integrals account to a large extent for short term phase shifts between measured cause and effect, for example lag in the soil heat flux as it responds to surface warming.

As an alternative method, the energy balance ratio (EBR) was also applied to evaluate the EBC in this study (Equation 13; Wilson *et al.*, 2002):

$$EBR = \frac{\sum(H+LE)}{\sum(R_n - G)} \quad (\text{Eq. 13})$$

The EBR compared turbulent fluxes and available energy with cumulative energy terms over a large time scale. Small scale (half hour) changes in energy storage tend to be elided by summation over the considered period. The EBR based on the quality controlled measured data was 0.88 and 0.98 for BF and SF correspondingly; whereas the one based on the gap-filled data was 0.90 and 1.04 for BF and SF correspondingly. The results of EBR further indicated the high quality of the EC measurements on both study sites.

#### 4.3.8. Regression Analysis of Environmental Factors

To test the effects of measured environmental factors on the variations of CO<sub>2</sub> and CH<sub>4</sub> fluxes, the Pearson correlation analysis and the stepwise multivariate regression analysis were conducted by SPSS version 17.0 (SPSS Inc., 2008). Before data were selected to conduct such analyses, the non-parametric test was run by using the Kolmogorov-Smirnov test to validate the normality of selected data distribution. The Levene's test was explored to test the homogeneity of variances. The significance level was set to 0.05, which indicates that a lower p-value than 0.05 was statistical significance. In the stepwise multivariate regression, the minimum p-value for a variable to be suggested for adding to and removing from the model was set to 0.1.

#### 4.3.9. Light Response Curves

Photosynthesis process is driven by light; however, the way NEE responds to changes in photosynthetic photon flux density (PPFD) could vary within vegetation types and seasons. In this study, the light response curve was analysed to describe the correlations between NEE and PPFD at two study sites during the study period in the growing seasons. There are several different functions to describe this relation exist (e.g. rectangular hyperbola, linear function with saturation, and non-rectangular hyperbola; Blackman, 1905; Rabinowitch, 1951; Tamiya, 1951). The rectangular hyperbolic light response function has been frequently used (known as Michaelis-Menten type model, Aubinet *et al.*, 2001; Falge *et al.*, 2001; Froelking *et al.*, 1998; Equation 14):

$$NEE = \frac{\alpha F_{max} PPFD}{\alpha PPFD + F_{max}} + R_{eco} \quad (\text{Eq. 14})$$

Where  $F_{max}$  ( $\mu\text{mol CO}_2 \text{ m}^{-2}\text{s}^{-1}$ ) is the maximum  $\text{CO}_2$  flux at infinite light (also referred as maximum assimilation,  $A_{max}$ ),  $\alpha$  ( $\text{mol mol}^{-1}$ ) is the ecosystem apparent quantum yield (the initial slope of the light response curve).

Photosynthetic  $\text{CO}_2$  assimilation increases with the increase of PPFD. NEE values change from positive to negative, passing through a point where  $\text{CO}_2$  uptake exactly balances  $\text{CO}_2$  release. It is normally called the light compensation point. Photosynthetic assimilation increased linearly with PPFD when NEE lies above the light compensation point, and the velocity of this rise (i.e. the slope of the linear relation between NEE and PPFD) is the maximum quantum yield of photosynthesis. Quantum yields vary from 0 to 1, during which the absorbed light used for photosynthesis is increasing. In the intact leaf, measured quantum yields for  $\text{CO}_2$  fixation vary around 4% to 6% (Taiz & Zeiger, 2010). At higher PPFD, the photosynthetic response to light reaches saturation level, and  $\text{CO}_2$  assimilation assumes its maximum value,  $F_{max}$ . Further increases in incident light do not affect the photosynthetic rate.

Light response curves were calculated by daytime half-hour NEE ( $R_g > 20 \text{ W m}^{-2}$ ) measured during the growing season (May to October) during the measurement period. Model parameters were estimated using the simulated annealing algorithm implemented by the function *nls* () in R stats package (version 3.1.3; R Core Team, 2014).

#### 4.3.10. Multi-scale Analysis of Environmental Controls

In this study, the spectral approach of wavelet analysis was applied to analysis the correlations between C fluxes and measured environmental factors in multiple temporal scales. The wavelet analysis has been employed widely throughout science and engineering since past decades (Cazelles *et al.*, 2008). It has been used quite often in climatology recently (Torrence & Compo, 1998), but poorly represented in C flux studies (Vargas *et al.*, 2010). It has been well known that ecosystem processes are affected by environmental oscillations at multiple temporal scales, simple linear relationships between ecological processes and environmental factors are often weakly able to reveal the underlying ecological mechanisms (Stenseth *et al.*, 2002). The analysis in time frequency domain (i.e. wavelet coherence analysis) has been demonstrated could help us to interpret multi-scale non-stationary time-series data and explain the correlations between the periodicities of time-series of ecosystem processes and those of environmental factors (Cazelles *et al.*, 2008; Vargas *et al.*, 2011).

By using wavelet analysis, the spectral characteristics of interest time series are analysed as independent parts divided through a fully scalable modulated window which continuously shifted the scale and time, for every signal position the spectrum is calculated (Galvagno, 2011). It provides a collection of time frequency representations of signal with different time resolutions as the final result (Galvagno, 2011). Therefore, this approach can track how the different temporal scales related to the periodic components of the signal change over time, allowing identifying regions of local

correlations between two time series as a function of frequency (Cazelles *et al.*, 2008). The continuous wavelet transform has been used in this study because of its ability to produce a smooth picture in time-scale domain of a non-stationary process (i.e. ecosystem C fluxes) and discern discontinuous events present in the signal (i.e. heat waves, rain pulses) (Vargas *et al.*, 2010).

The continuous wavelet transform can be defined as the convolution integral (Equation 15):

$$W_n(s) = \left(\frac{\delta_t}{s}\right) \sum_{n^i=0}^{N-1} x_n \psi_0^* \left(\frac{n-n^i}{s/\delta_t}\right) \quad (\text{Eq. 15})$$

where  $x_n$  is a discrete wavelet transform signal of length  $N$  sampled at  $\delta_t$  interval,  $\psi_0^*$  is the complex conjugate of the translated and scaled basic (mother) wavelet, and  $s$  is the wavelet scale at which the transform is applied (Vargas *et al.*, 2010).

The ability of wavelet analysis to detect small intervals of scales (i.e. spectral resolution) depends on the choice of the mother wavelet which is the base function from which transformations are calculated (Vargas *et al.*, 2010). Different type of mother wavelet exist, wavelets with better frequency resolution have poorer temporal resolution and vice versa (Vargas *et al.*, 2010). One of the most-used basic (mother) wavelet for geophysical applications is the Morlet wavelet (Grinsted *et al.*, 2004).

In this study, wavelet coherence analysis was applied to investigate coherence between the periodicities of CO<sub>2</sub> flux components with  $T_{air}$ , PPF and VPD, the measured environmental variables, at multiple temporal scales. The 30-minutes time series of CO<sub>2</sub> flux and environmental variables measured during the measurement period were used.

The wavelet analysis was operated using function  $wco$  () in the R package ‘‘Sowas’’ (Maraun *et al.*, 2007). This function inputs time-series data to calculate the wavelet coherence of two variables, based on the Morlet wavelet to evaluate correlations

between the two interest time series with respect to time and scale. Correlations varied between 0 (absence on coherence) and 1 (full coherence) (Galvagno, 2011).

## 4.4. Summary

The Chapter 4 has provided an overview of the underlying theory of the micrometeorological EC technique (4.1). The details of the theoretical assumptions of the EC method, and the corrections and post-processing of the raw data to meet the theoretical assumptions were described (4.1.1). The station instrumental systems deployed at the two flux measurement sites were introduced (4.2). A summary of the flux raw data processing routines and site-specific QC protocols was presented (4.3.2 & 4.3.3). The details of the methods used to fill unavoidable gaps in EC flux data (4.1.3 & 4.3.5), to partition NEE into CO<sub>2</sub> flux components (i.e. GPP and  $R_{eco}$ ; 4.1.4) and to estimate the measurement uncertainties (4.3.6) were provided. The methods of flux data processing routines, QC, gap filling and flux partitioning were based on the standardised method protocols of the FluxNet community. The methods of flux results analysis (i.e. regression analysis; light response curves; multi-scale analysis of environmental controls) were presented as well (4.3.8, 4.3.9 & 4.3.10).

The total data coverage after QC procedures was provided (4.3.4). The data coverage was compared for different periods (i.e. growing seasons, non-growing seasons) in different years. As a result, the total data coverage during the growing seasons at both study sites is better than in the non-growing seasons. The total data coverage at both sites was within the range reported from other EC measurement studies.

The role of EBC as a means of assessing the plausibility of the EC flux measurements was evaluated by reconstructing the surface energy budget (4.3.7). The EBC was higher at SF than for BF. The EBC improved for both study sites when using the daily average in the analysis. The EBC was within the normal range reported from other studies.

## **Chapter 5**

# **Short-term Climate Response of Carbon Dioxide and Methane Fluxes in a Regenerating Fen (Baker's Fen)**

## 5.1. Environmental Conditions at Wicken Fen Nature Reserve

### 5.1.1. Meteorology

The UK is located in the mid-latitude westerly wind belt on the edge of the Atlantic Ocean. As a result of variations in climate, topography, and land use, the eastern and southern parts of the UK are drier, warmer, sunnier and less windy than those further west and north (Jenkins, 2009).

The fenland region of East Anglia covers the largest region of low, flat land in the UK. The climate of the area is generally dry and mild. The region is one of the driest regions in the country with many areas receiving less than 600 mm of rainfall per year (Murphy *et al.*, 2009; Figure 2). Farming is an important activity in East Anglia; therefore, the area also is under great pressure from the agricultural land use sector and an increasing human population for limited available water sources (Anglian Water, 2007).

Prior to the measurement period, the UK experienced a cold and dry year in 2010 which was the coldest year in the country since 1986. The December of 2010 was one of the coldest calendar months in the last 100 years. It also was the driest year since 2003, and the period January to June in 2010 was particularly dry, the driest such period since 1953 (Met Office, 2013a). The year 2011 had a warm spring and autumn contrasting with a cool summer. April 2011 was the warmest April in overall UK records as well as for central England. However the summer in 2011 was the coolest summer since 1993. In 2011, much of central, eastern and southern England had a persistent rainfall deficiency, with parts of the east Midlands and East Anglia recording less than 400 mm precipitation, whilst the northern parts of the country received almost 4000 mm rainfall. East Anglia had the second driest year on record, eclipsed only by 1921. In contrast, Scotland had its wettest year on record from 1910 (Met Office, 2013b). 2012 was a year of dramatic contrast. The first three months in 2012 were

relatively warm and dry; however, the weather abruptly shifted from April onwards to an exceptionally wet period lasting through much of the summer. Similarly to 2011, the early spring in 2012 was quite warm; the month of March was the 3<sup>rd</sup> warmest March on record for the UK. However, the 2012 summer was the second coolest summer since 1998 followed by 2011, and the autumn was the coolest autumn since 1993 (Met Office, 2013c). In 2012, the prolonged drought periods in large parts of southern, central and eastern England (especially lowland England) from April 2010 to March 2012 were declared to be one of the ten most significant droughts of one- to two-year duration in the last 100 years (Kendon *et al.*, 2013) (Figure 3). The drought led to visible impacts on East Anglia lowland peat soils in the fens, where road surfaces started to crack due to peat contraction. However, the severe prolonged drought was dramatically terminated by the wettest April to July in 2012 over England and Wales in almost 250 years (Parry *et al.*, 2013). Thus lowland England was characterised by strong seasonal variations in hydrological / climate conditions prior to the measurement period, with the unusual weather conditions in the last few years providing an opportunity to investigate the impacts of climate on the GHG emissions from lowland fenland ecosystems.

In order to compare the climate conditions during the measurement period to longer-term climatic patterns, monthly average  $T_{air}$  and precipitation sums (2013 to 2015) are presented together with longer-term meteorological observations. However, there is no long-term meteorological record available for the Wicken Fen NNR study location. Therefore, additional meteorological data were obtained from the nearest UK Met Office NIAB station in Soham (52°33' N, 0°34' E, 6 m amsl) located approximately 10 km from Wicken Fen NNR. The additional meteorological data including monthly average air temperature, precipitation, air frost days and the duration of sunshine for the thirty year period from 1981 to 2010 were used to define baseline climatic conditions. The monthly average data on the number of days with air frost and sunshine hours in separate years during the measurement period (2013 to 2015) obtained from the Soham station were used to infer the weather conditions at the study site.

Monthly average meteorological data observed during 2013 to 2015 on Wicken Fen NNR (using data from BF) are compared against 1981 to 2010 climate averages, and

the monthly anomalies are also shown. The Wicken Fen NNR study area was characterised by strong seasonal variation in climate / hydrological conditions during the measurement period from 2013 to 2015 (Figure 25). Significant annual variations, inter-annual differences and departures from baseline climatic conditions (thirty year average 1981 to 2010) were observed from the comparison.

#### 5.1.1.1. Air Temperature

The monthly average air temperature ( $T_{air}$ ) showed a symmetrical seasonal pattern in all years (top left panel in Figure 25), increased from the start of the year, peaked during the summer months, and declined throughout the autumn. Annual mean temperature of the study area in 2013 was 9.78 °C, 0.3 °C below the 1981 - 2010 long term average (10.1 °C). Whereas 2014 was much warmer, and 2015 was slightly warmer than average, at annual mean temperature of 11.45 °C and 10.78 °C respectively (Figure 25).

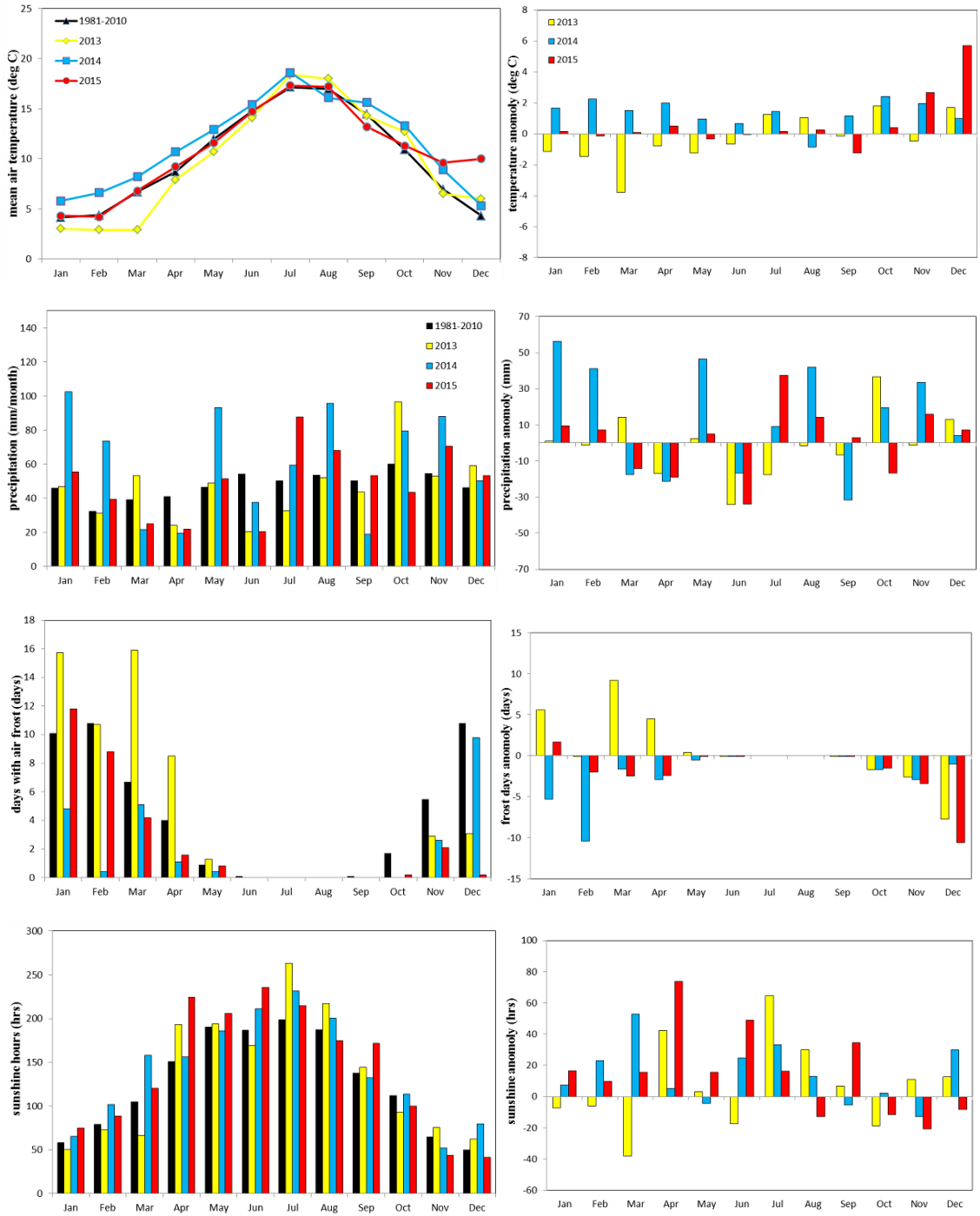


**Figure 25:** Monthly meteorological variables (mean air temperature, precipitation, air frost days and sunshine hours) measured in Wicken Fen NNR during the measurement period 2013 to 2015 (left panels). Thirty years average as baseline climatic conditions are for the period 1981 to 2010. Monthly anomalies are shown on the right panels. 1981 to 2010 average data are from the Met Office station at Soham station. Data supplied by the Met Office.

In general, the study period experienced one of the coldest winter-spring periods in last few decades during the first half year of 2013, and one of the warmest years in the 2014 compared to the long-term average. Until mid-November, 2015 saw mostly quiet weather, generally near the average (Figure 25). Conditions were colder than normal during the whole first half year of 2013, however relatively warmer during the summer in 2013 (Figure 25). It has been reported that 2014 was the warmest year on record for the whole country (ahead of 2006) except for Northern Ireland where it was third warmest behind 2007 and 2006 (Kendon *et al.*, 2015). It is worth noting that the eight warmest years in the country have all occurred since 2002 (Met Office, 2015). The whole year of 2014 was warmer than normal except for August. March of 2013 was the coldest March in the area for at least the last three decades; the monthly average  $T_{air}$  (2.9 °C) was almost 4 °C (> 2 SD cooler) lower than the long-term average and accompanied by the largest number of frost days during the study period (Figure 25). It has been reported that both March and spring overall in 2013 were the coldest in the UK records since 1962. In contrast, the July of 2013 was the third warmest in the records and it was the warmest summer since 2006 (Met Office, 2014). February and March in 2014 were some of the warmest months in the area during the same period of the last few decades, accompanied by the fewest days with air frost in February 2014 during the study period (Figure 25). Under the influence of ex-hurricane Bertha, August 2014 was the coldest August of the last few decades. The November and December of 2015 were exceptionally warm in the region as well as most parts of the country, with December the mildest in the records from 1659 (Met Office, 2015; 2016). Remarkably, there were almost no air frosts during December 2015 (Figure 25).

To compare the three years in the measurement period, the first half year of 2015 (from January to July) showed very similar  $T_{air}$  as the long-term average, which was cooler than 2014 and warmer than 2013 during the same period. Most of the months of 2014 were warmer than 2013 and 2015, excluding August and December which were warmer in 2013 and 2015 than in 2014. The growing season (May to October) was warmer in 2014 than in 2013 and 2015 with mean  $T_{air}$  of 15.3 °C, 14.7 °C and 14.2 °C respectively (Figure 25).

Spring (March to May) air temperatures were warmer than the thirty year average in

2014 whereas they were colder than average in 2013. In the spring of 2015, the temperatures were close to average with fewer days of frost. The late spring of 2013 (April and May) showed a dramatic temperature increase close to the long-term average after a cold March, although April experienced more frost days than average. 2014 experienced one of the warmest springs in the last three decades with mean spring  $T_{air}$  at 10.7 °C (Figure 25).

All summer months (June to August) in 2013 and 2014 were warmer than the 1981 to 2010 average, excluding June 2013 and August 2014. All three months in 2015 were close to but warmer than normal. 2013 showed a continuing increase in summer months temperatures with only June average  $T_{air}$  below the normal average, reached the warmest month of the year was July which was close to the average  $T_{air}$  in July 2014. 2013 also experienced the warmest August comparing to the other two years and the average. August 2014 was the only month in the year when average  $T_{air}$  was below the normal average, consistent with the high rainfall during this month (Figure 25).

Considerable differences in autumn (September to November) temperatures were observed in all three years. Monthly temperature was statistically warmer than normal during all autumn months in 2014 (Mann-Whitney U tests,  $p < 0.05$ ). All autumn months in 2014 were about 2 °C ( $> 1$  SD) warmer than the thirty years average. During autumn 2013, mean monthly temperature was normal in September and November, but was more than 2 °C ( $> 1$  SD) warmer in October and December (winter) than the thirty years average. September 2015 was the only month in the year when average  $T_{air}$  was below the average, whereas the months of November and December (winter) were exceptionally warmer than during the other two years as well as the average. The mean  $T_{air}$  of November and December in 2013 were more than 2 °C ( $> 1$  SD) warmer than the thirty years average (Figure 25).

The duration of sunshine and the presence of frost are closely related to  $T_{air}$ . The variation in length of day means that the duration of sunshine shows marked variation throughout the measurement period. On average, in the study area, December is the month with the least sunshine and July is the sunniest month. In general, most of the months during the measurement period had longer sunshine duration than the long-term

average, except the first three months and June, September in 2013, November in 2014, August and the last three months in 2015 (Figure 25). It is not exceptional that 2013 was mostly dull during January to March with relatively low  $T_{air}$  during the same period. However, surprisingly, November 2015 was reported as provisionally dullest in the records for the country scale whereas it was much warmer than average till the end of the year (Met Office, 2016; Figure 25). Most of the months had fewer frost days during the measurement period compared to the long-term average. Only the first five months in 2013 had more frost days than the average which is not surprisingly so, while the January in 2015 had two more days with frost than the average (Figure 25).

#### 5.1.1.2. Precipitation

The thirty-year average showed the rainfall is fairly evenly distributed throughout the year in the region. However, large annual and inter-annual variation in the seasonal distribution of rainfall was observed in all three measurement years at the study area (Figure 25; Figure 26).

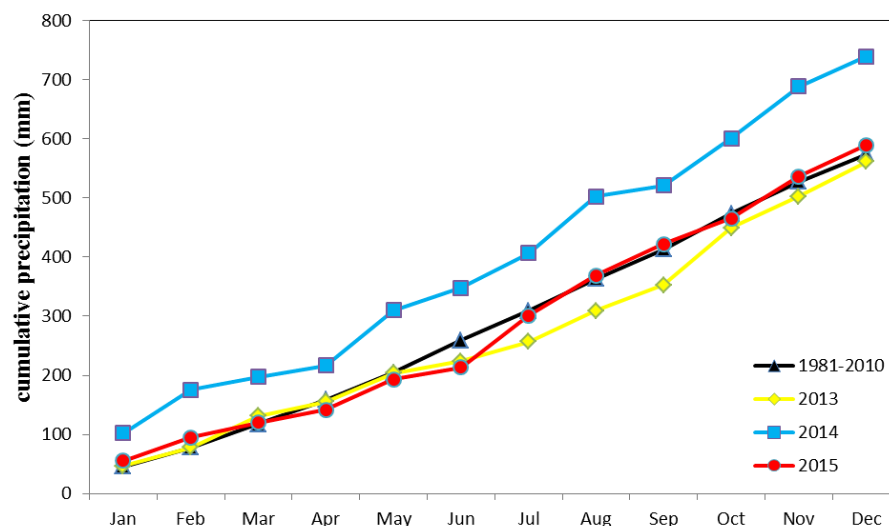


**Figure 26:** Comparison of cumulative monthly precipitation during 2013 to 2015 against the 1981 to 2010 average. 1981 to 2010 average monthly precipitation data are from the Met Office station at Soham. Data supplied by the Met Office.

On an annual basis, 2013 was slightly drier and 2015 was slightly wetter than long-term average; whereas 2014 was distinctly wetter than the average (Figure 26). The total annual precipitation of 2013 was lower but close to the thirty-year average, at 561.6 mm yr<sup>-1</sup> in 2013 comparing to an average of 574 mm yr<sup>-1</sup> for the last three decades. However, in 2014, the total annual precipitation was statistically higher than the thirty-year mean, at 739.2 mm yr<sup>-1</sup> (>1 SD). The total annual precipitation of 2015 was slightly higher than the average at 589.4 mm yr<sup>-1</sup> (Figure 26).

The year 2013 experienced a prolonged drought period during the summer starting from June, with all the summer months drier than the long term average (June to September), receiving 35% less precipitation than the average during the same period (Figure 25). However, this condition abruptly shifted from October. The October of 2013 was the wettest month in the year, as well as the wettest October compared to the other two years and the long term average. December 2013 also recorded above average rainfall (Figure 25). It has been reported that some parts of the UK even received over twice the normal amount of rainfall in the months of October and December in 2013, and 2013 December was the wettest of any calendar month on the record in Scotland since 1910 (Met Office, 2014).

The total annual precipitation for 2014 was 739.2 mm, 129% of the 1981 - 2010 average in the region. For the whole country, 2014 was the fourth wettest year in the UK records from 1910, behind 2012, 2000 and 1954. It is worth mentioning that five of the six wettest years in UK records have occurred since 2000 (Kendon *et al.*, 2015). A large contribution to the high total annual precipitation came from very wet weather in January, February, May, August and November in 2014. However, March, April, June and September were drier than average in the area, and September 2014 was the driest September for the whole country average since 1910 (Met Office, 2015; Figure 25).

The annual statistics for 2015 rainfall in the study area are generally near average. However, it experienced an exceptionally dry June with only 20.3 mm (same as June 2013), less than 40% of the 1981 - 2010 average rainfall in June. The condition shifted rapidly in July with the highest precipitation compared to the other two summer months as well as the long term average in the same period, receiving 87.7 mm in the month,

174% of the 1981 - 2010 average (Figure 25; 26). It is worth mentioning that 2015 was one of the wettest years at the whole country scale, coming after 2014, 2012, 2000. It has been reported that December 2015 was the wettest calendar month in the UK in the last few decades (Met Office, 2016).

### 5.1.2. Ground Water Levels at Baker's Fen

The monthly ground water levels during the measurement period are presented and compared to the maxima and minima for the period prior to the measurement period (i.e. from 2008 to 2012) in Figure 27. Changes of meteorological conditions had a strong influence on ground water levels at BF (Figure 27). During winter, water from the adjacent river, the Monks Lode, is transferred onto the site, leading to rapid recharge of the water table in late autumn of each year, and near-surface water levels during the winter (Evans *et al.*, 2015). The site is thus subject to highly variable hydrological conditions over the year, with active water management maintaining wet conditions in winter, but with exposure to most or all of the surviving peat to aeration during much of the growing season.

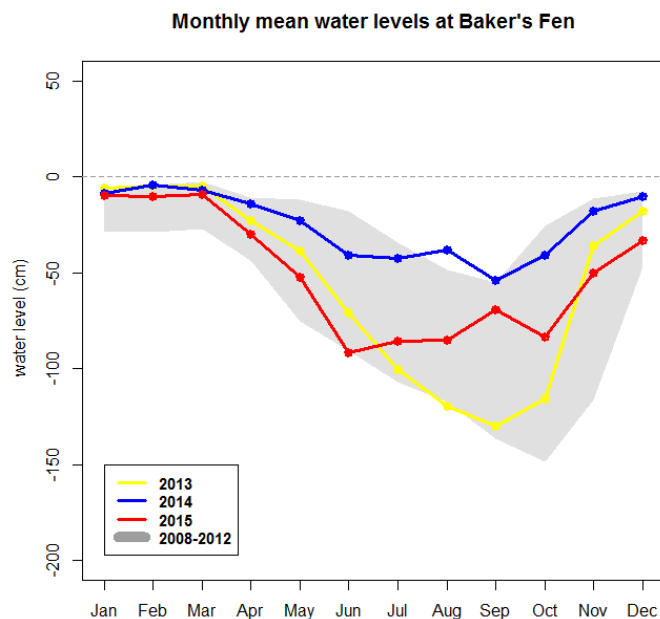


**Figure 27:** Comparison of ground water levels at Baker's Fen. Data show monthly water level range 2008 - 2012 (grey) and 2013(yellow), 2014(blue), 2015 (red) monthly mean water levels relative to the fen surface measured at BF dipwell 107-1. Data supplied by John Bragg @ the NT.

In general, almost all months during the measurement period lie within the range observed during the period 2008 - 2012, except the mean water table in August 2014 was about 10 cm above the historical maximum whereas that in August 2013 was slightly below the historical minima (Figure 27). This is most likely explained by the monthly rainfall amount in August 2014 which was about 100 mm whereas it was only about half this amount in August 2013 (53 mm) during the year's warm and dry summer (Figure 25). As one of the wettest years in the UK records, the ground water table across the whole year of 2014 at BF was close to or even above the historical maximum water level on the site. However, the dry summer in 2013 and the driest month in 2015 (June) had distinct low water table very close to the historical minimum water levels (Figure 27).

The daily mean water levels at BF during the measurement period are presented in Figure 28. The ground water levels were close to the fen surface at the start of the year (January to April) in all years during the measurement period. In 2013, the water levels fluctuated at around -50 cm during relatively wet condition in the year between April and early May, before declining steadily starting from mid-May through to October (Figure 28). This situation, in which the entire remaining peat mass was aerated, continuously through the dry summer persisted until November in 2013. The water level reached a seasonal minimum of about -140 cm in early October. The Site then recovered dramatically following addition of the water onto the site from the adjacent lode, after which water levels have remained close to the ground surface again at the end of the year (Evans *et al.*, 2014; Figure 28).

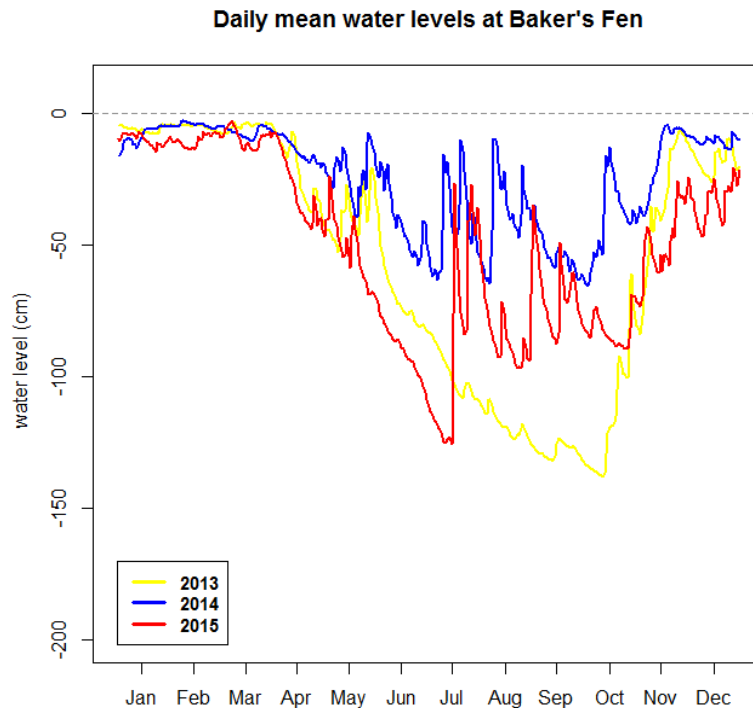


**Figure 28:** Comparison of groundwater levels at Baker's Fen during measurement period. Data show the mean daily position of water levels relative to the fen surface measured at BF dipwell 107-1. Data supplied by John Bragg @ the NT.

The water levels were never below -60 cm in the wet year 2014, fluctuated at around -30 cm during most of time in the year, and were close to the fen surface from January to April and between November and December (Figure 28). Several significant drawdowns were observed in spring and summer 2014. However, large rainfall events resulted in several rapid increases in water table to near the surface. In 2015, the ground water levels started to decline in early April which was about 20 days earlier than the other two years, fluctuated around -50 cm and declined steadily again since May 2015, reaching the lowest level at -134 cm in early July (Figure 28). The water levels between May and July in 2015 were even about 20cm lower than the water level during the same period in 2013 (Figure 28). Rapid water level recovery occurred during the wet conditions in July, reaching -30 cm, before fluctuating at around -60 cm during the whole summer. The water levels raised steadily again in October 2015, but were not that close to the ground surface as during the other two years by the end of the year (Figure 28).

## 5.2. Temporal Dynamics of Carbon Fluxes at Baker's Fen

### 5.2.1. Wind Rose Plots

In Figure 29, the distribution of direction and source strength of NEE (left panels) and CH<sub>4</sub> (right panels) fluxes at BF in three different years during the measurement period (2013 to 2015) are presented. The figure illustrates the frequency of counts by wind direction, as well as the magnitudes of CO<sub>2</sub> and CH<sub>4</sub> fluxes (with non-gap-filled data) in separate years during the study period. The positive (toward red) values represent periods when the site was a source of CO<sub>2</sub>/ CH<sub>4</sub>; negative (toward blue) values denote periods when the site was a sink.

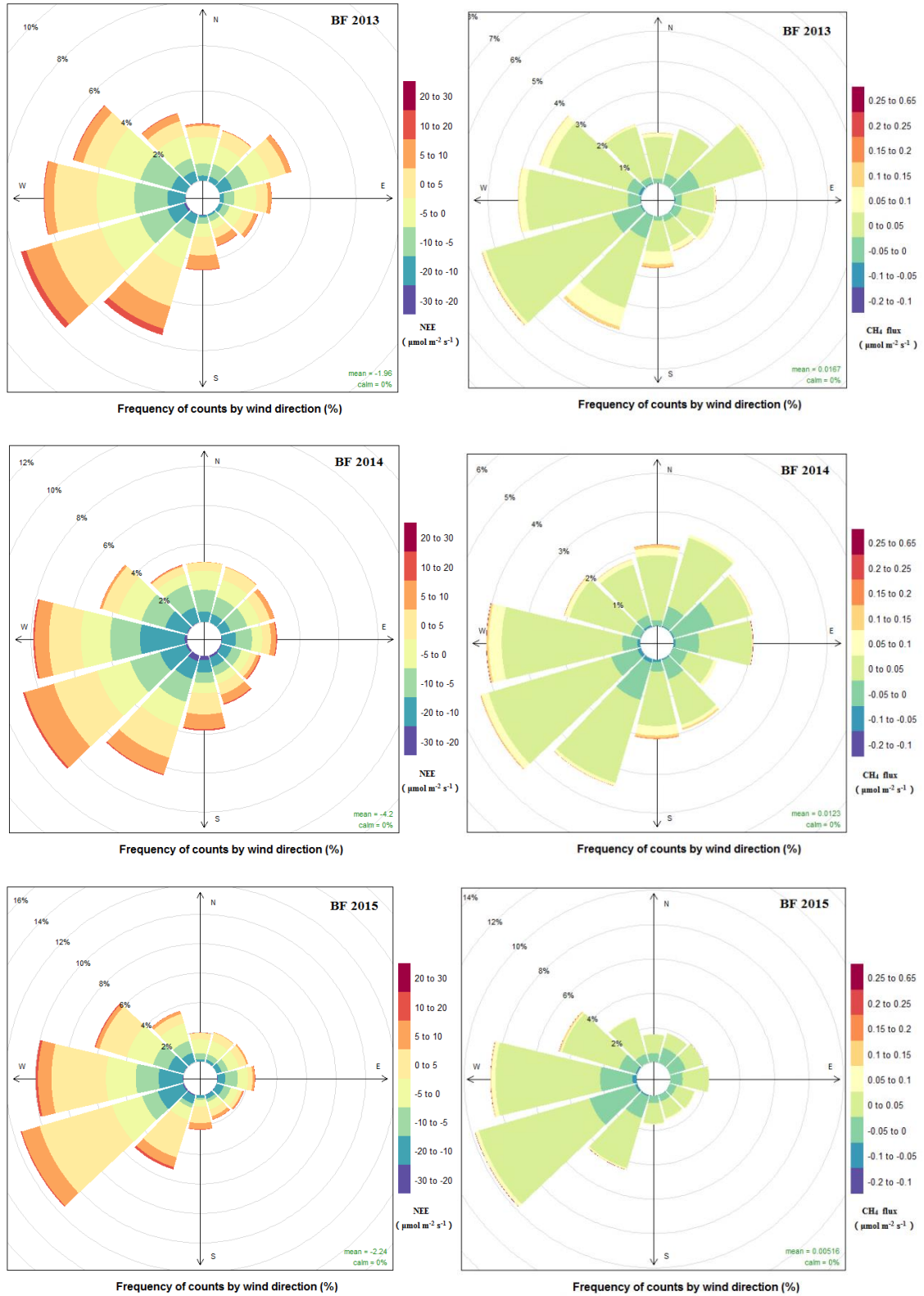


**Figure 29:** Distribution of direction and source strength of the measured (non-gap-filled) net ecosystem CO<sub>2</sub> exchange (NEE, left panels) and methane (CH<sub>4</sub>, right panels) fluxes in different years during the measurement period (2013 to 2015) at Baker's Fen in units of  $\mu\text{mol m}^{-2} \text{s}^{-1}$ . Positive values represent a source and negative a sink.

All three years' wind direction distribution data agree that the prevailing wind direction at the site is from southwest and west (Figure 29). This also indicated that the largest number of fluxes of both CO<sub>2</sub> and CH<sub>4</sub> originated from the prevailing wind directions. Both CO<sub>2</sub> and CH<sub>4</sub> flux magnitudes appear fairly evenly distributed in space, although with some indication of large fluxes coming preferentially from prevailing wind direction (Figure 29). The right panels of Figure 29 showed that large amount of CH<sub>4</sub> fluxes data are in the range of 0 - 0.05 μmol m<sup>-2</sup>s<sup>-1</sup> (in light green) in all three years. In 2013, the larger percentage of wind from the north-east was associated with an anomalously cold late winter and late spring. In 2015, the wind-flow came predominantly from the prevailing wind sectors between north-west and south-west, with very little wind arriving from the remaining wind sector, whereas during 2014 a relatively larger percentage of wind comes from the remaining sectors (Figure 29).

### 5.2.2. Fingerprint Plots

The “fingerprint” plots of NEE are presented in Figure 30 for the whole measurement period covering three full years from 2013 to 2015. Gap-filled (upper left plot) and measured (non-gap-filled; upper right plot) NEE data, as well as photosynthetic photon flux density (PPFD; lower right plot) and  $T_{air}$  (lower left plot) as the key meteorology variables are presented. The fingerprint plots show diurnal and seasonal changes in half-hourly CO<sub>2</sub> flux densities, as well as the temporal distribution of the data-gaps (upper right plot) and the performance of the method used to fill missing values (upper left plot) (Figure 30). The NEE data in the figures are presented in units of μmol CO<sub>2</sub> m<sup>-2</sup>s<sup>-1</sup>; PPFD and  $T_{air}$  are shown in μmol m<sup>-2</sup>s<sup>-1</sup> and °C, respectively. The fingerprint plots of NEE illustrate the “breathing” of the ecosystem over the measurement period. In the figure, colours toward the red end of the NEE scale denote periods when the site was losing CO<sub>2</sub> to the atmosphere (i.e. at night); whereas the colours toward the blue end indicate the periods when the site was removing CO<sub>2</sub> from the atmosphere (i.e. during summer daytime; Figure 30).

In general, data capture (after QC) was good throughout the whole measured period at the site (upper right plot Figure 30). Comparing measured (non-gap-filled) and gap-filled NEE data shows that most of the data gaps mainly occurred during winter or night-time due to insufficient power supply by the solar panels under winter / night-time conditions (longer periods of missing data) or the application of data QC procedures (short periods of data loss) (Figure 30). The only significant NEE data gap (total data loss for longer than one complete month) during the measurement period occurred in early January to mid-February 2014; this was due to the theft of batteries at the station. This large data gap occurred during the winter months when CO<sub>2</sub> fluxes were at a seasonal low, thus the filling of this data gap is less likely to introduce a large uncertainty in terms of the annual CO<sub>2</sub>-C budget compared with data losses during the main growing season. Generally speaking, the measured data (quality controlled) covered most of the growing season and daytime periods, again verifying the high quality of the measured data and improved the reliability of the gap-filling data (Figure 30). There was no data available for PPFD during 3<sup>rd</sup> January to 8<sup>th</sup> April due to instrument failure at the station following the theft of batteries (Figure 30).

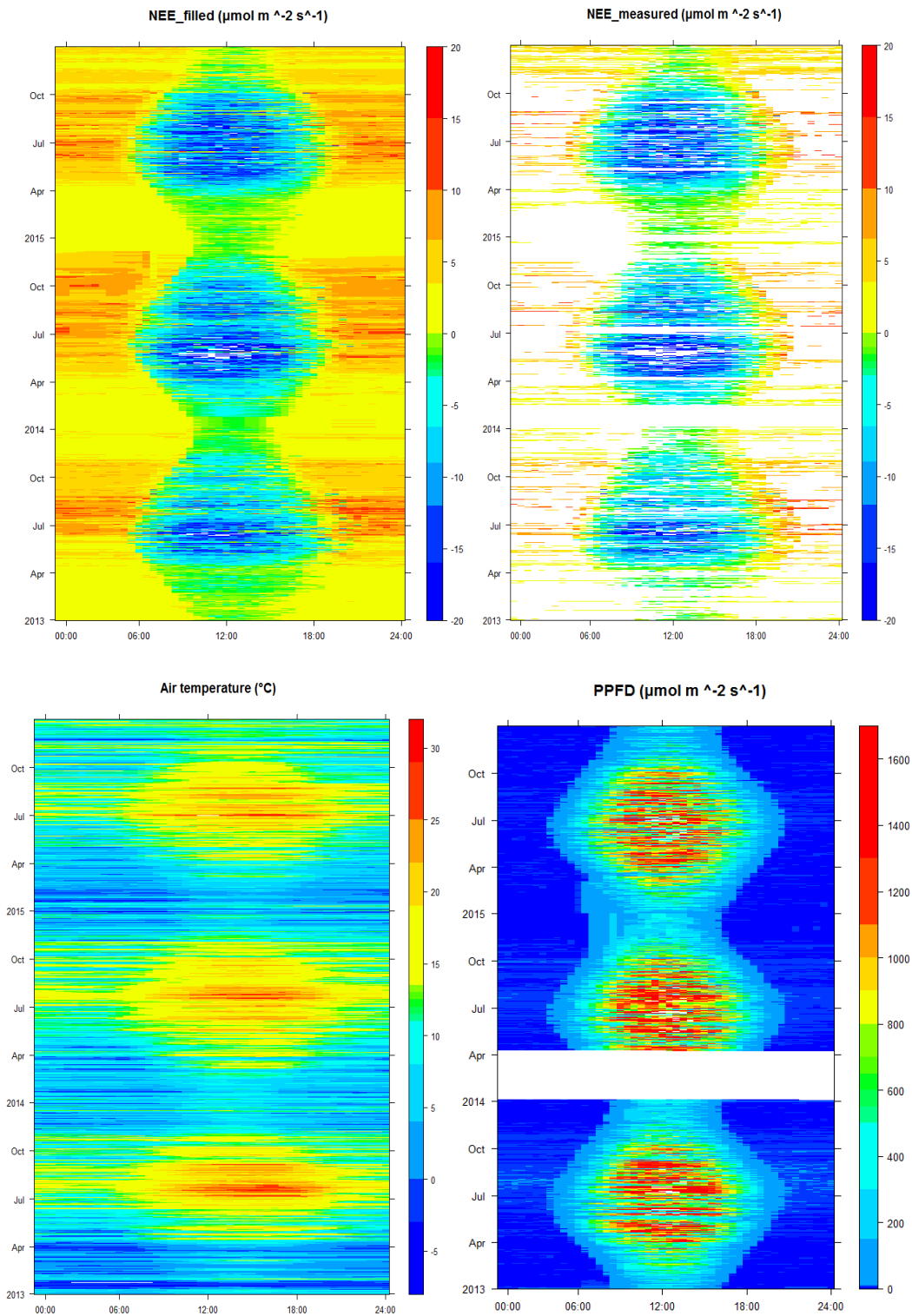


**Figure 30:** Net ecosystem  $\text{CO}_2$  exchange (NEE, top panels), air temperature ( $T_{\text{air}}$ , lower left), and photosynthetic photon flux density (PPFD, lower right) at Baker's Fen during the measurement period (2013 to 2015). Top left is gap-filled NEE data, top right is measured NEE data after quality control. NEE units are  $\mu\text{mol CO}_2 \text{ m}^{-2} \text{ s}^{-1}$ ; photosynthetic photon flux density (PPFD) and air temperature ( $T_{\text{air}}$ ) are shown in  $\mu\text{mol m}^{-2} \text{ s}^{-1}$  and  $^{\circ}\text{C}$ , respectively. Months are represented by increases along the ordinate; time of day is indicated along the abscissa. White space represents periods when no flux data were available.

The NEE seasonal pattern shows strong correspondence with the temperature and radiation regimes in all three years (Figure 30). The top panels show that the width of the daily uptake period was closely associated with changes in day length (radiation), whereas the magnitude of net daytime uptake closely corresponds with seasonal variations in temperature and radiation. The seasonal variations in the magnitude of night / winter CO<sub>2</sub> emission are associated with variations in  $T_{air}$  (Figure 30).

In the year 2013, the shorter growing season with delayed onset of spring and early arrival of cold winter is evident when comparing to the other two years, illustrated by a shorter period of CO<sub>2</sub> uptake during daytime and efflux during night-time in growing season (Figure 30 upper left plot). The year 2014 had a relatively long period with high magnitude of daytime net CO<sub>2</sub> uptake during the growing season (larger area with light blue colour); whereas 2015 had a slower increase in daytime net CO<sub>2</sub> uptake after spring when comparing to 2014. However, year 2015 had a relatively higher magnitude of nocturnal CO<sub>2</sub> losses and daytime CO<sub>2</sub> uptake during the growing season when compared to the other two years (with more areas of dark red and blue) (Figure 30 upper left plot).

### 5.2.3. Mean Diurnal Patterns

Monthly mean diurnal cycles (MDC) are a means of comparing seasonal and between-year differences in CO<sub>2</sub> and CH<sub>4</sub> fluxes on a side-by-side basis. The measurements included three complete annual cycles at BF (Figure 31). In this figure, each data point represents the mean of 30 minute values measured at the same time of day over the course of each month (e.g. for the 48 thirty minute intervals in each day). The MDCs of NEE, GPP (with negative values),  $R_{eco}$ , CH<sub>4</sub> flux as well as selected environmental variables PPF,  $T_{air}$ , VPD are represented in the figure. The water levels relative to the ground surface during the measurement period are shown as monthly means in the lowest panel (Figure 31). The NEE, GPP,  $R_{eco}$ , CH<sub>4</sub> flux and PPF data in the figures are presented in units of  $\mu\text{mol m}^{-2}\text{s}^{-1}$ ;  $T_{air}$ , VPD and water levels are shown in °C, hPa and cm, respectively. The figure shows the changes in the amplitude of the monthly diurnal cycles of NEE, assimilatory (GPP) and respiratory ( $R_{eco}$ ) activity and CH<sub>4</sub>

fluxes in response to phenological changes and illustrates seasonal, between-year differences during the measurement periods.

During the whole measurement period, the daily average NEE, GPP and  $R_{eco}$  showed a clear diurnal pattern in all months (Figure 31). The diurnal cycle was characterised by NEE becoming progressively more negative (positive) in response to increases (decreases) in irradiance and / or temperature. On the contrary, the GPP and  $R_{eco}$  showed similar diurnal patterns as irradiance and temperature. The maximum rates of GPP and  $R_{eco}$  (therefore the NEE) occurred as the irradiance peaked around solar noon (Figure 31).

The seasonal pattern of CO<sub>2</sub> fluxes at BF is characteristic of sites with permanent vegetation cover, with the lowest fluxes in winter (typically positive) and largest (positive and negative) values in the summer months as responses to weather conditions and ecosystem phenology. The daytime net CO<sub>2</sub> uptake (daytime GPP) during all months in all three years indicates that the photosynthesis was active at BF throughout the whole year during the measurement periods (Figure 31). The seasonal changes in the magnitude of the key meteorological variables (PPFD,  $T_{air}$  and VPD) which showed more suitable conditions from April to September for vegetation during the growing season co-determined the amplitude of the monthly diurnal patterns of GPP and  $R_{eco}$  therefore the NEE. Net CO<sub>2</sub> uptake rates were higher (more negative) between April and September than in the other months of the year in all three years. Whereas the lowest net uptake rates occurred in December in all years (Figure 31).

The monthly mean diurnal patterns reveal large between-year differences in the CO<sub>2</sub> fluxes among the three years at BF (Figure 31). The amplitude of CO<sub>2</sub> fluxes increases rapidly from spring to growing season, then declines steadily through late summer and autumn (Figure 31). The largest average net CO<sub>2</sub> uptake is observed in June for 2013, during May in 2014 and in June for 2015 (Figure 31). The warmer conditions in 2014 (compared to the other two years) are associated with larger nocturnal losses of CO<sub>2</sub> and more negative daytime NEE in most months, as well as the earlier start to the growing season in the year. The largest net difference in average NEE is observed in April (Figure 31).

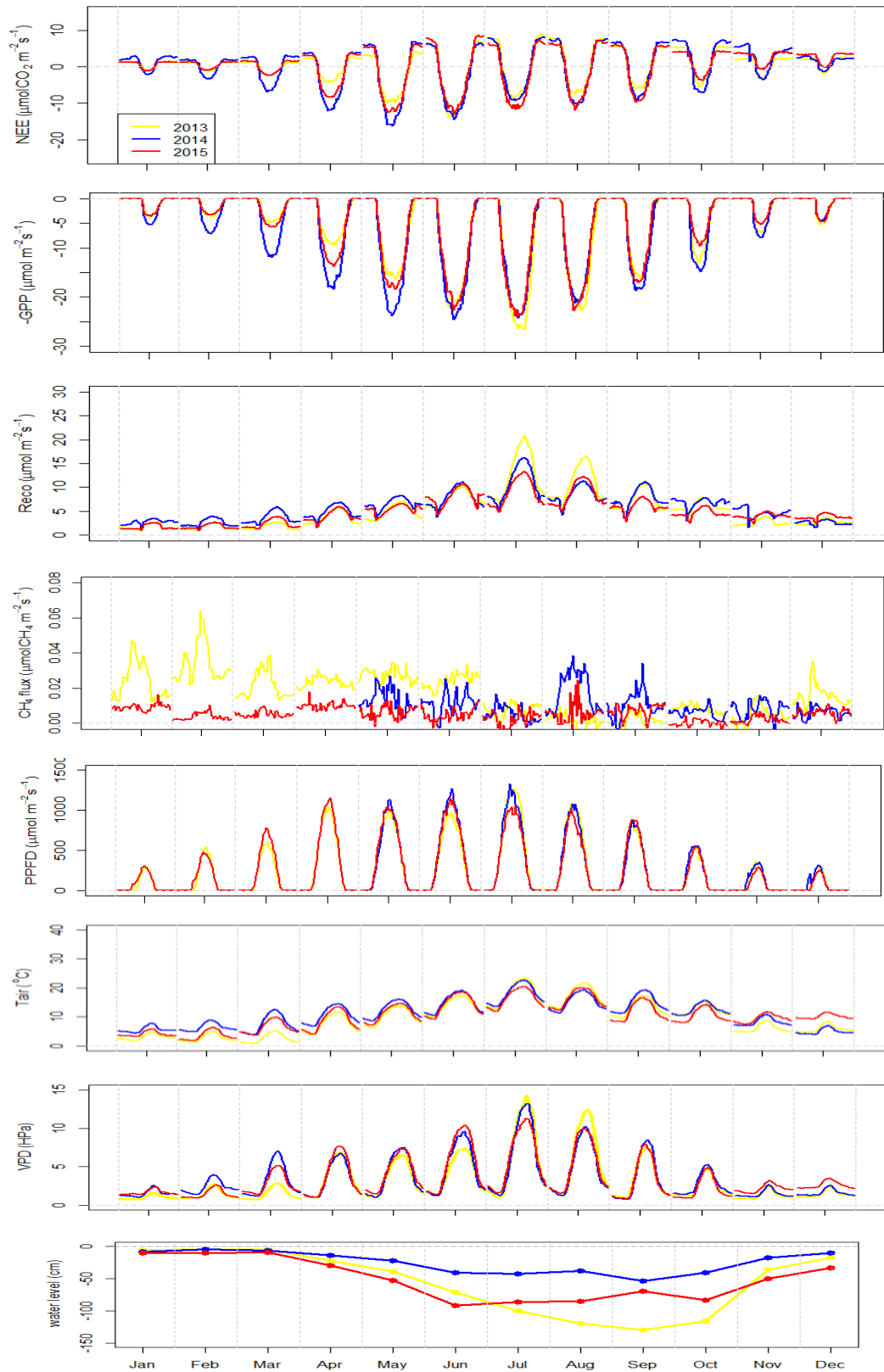


**Figure 31:** Comparison of monthly mean diurnal cycles of net ecosystem  $\text{CO}_2$  exchange (NEE) and  $\text{CH}_4$  fluxes at Baker's Fen during measurement period (2013 - 2015). Monthly diurnal averages were calculated using measured (not gap-filled) data. Average diurnal cycles of key meteorological variables are also provided. Estimates of daily GPP are shown in negative values to facilitate graphical reading. The lowest panel shows monthly mean water levels relative to the ground surface. Standard errors have been omitted to improve readability.

The maximum daily net CO<sub>2</sub> uptake ( $\pm 95\%$  confidence interval) range from  $-1.46 \pm 0.14$   $\mu\text{mol m}^{-2}\text{s}^{-1}$  to  $-14.7 \pm 0.67$   $\mu\text{mol m}^{-2}\text{s}^{-1}$ ,  $-3.12 \pm 0.17$  to  $-16.4 \pm 0.73$   $\mu\text{mol m}^{-2}\text{s}^{-1}$ ,  $-0.36 \pm 0.12$   $\mu\text{mol m}^{-2}\text{s}^{-1}$  to  $-13.8 \pm 0.64$   $\mu\text{mol m}^{-2}\text{s}^{-1}$  in all months in 2013, 2014 and 2015, respectively. These maximum monthly average daily net CO<sub>2</sub> uptake rates at BF were higher than the observations from studies at boreal peatlands (ranging from -4 to -11.5  $\mu\text{mol m}^{-2}\text{s}^{-1}$ ; Adkinson *et al.*, 2011; Humphreys *et al.*, 2006; Sagerfors *et al.*, 2009), but lower than an observation from a study in a Finnish grassland with an average of  $-18$   $\mu\text{mol m}^{-2}\text{s}^{-1}$  (Shurpali *et al.*, 2009).

Both the largest amplitude of the mean diurnal pattern of GPP and  $R_{eco}$  occurred in July in all three years when the average PPFD,  $T_{air}$  and VPD all reached their peaks in the year (Figure 31). In 2014, both the amplitude of GPP and  $R_{eco}$  were larger from January to June and from September to November comparing the same periods in the other two years (Figure 31). However, the amplitude of the mean diurnal pattern of GPP and  $R_{eco}$  were larger in July and August 2013 than in the same months in 2014 and 2015, associated with the warmer and wetter conditions (higher average PPFD,  $T_{air}$  and VPD; Figure 25) during the period in 2013 (Figure 31). The largest difference between years in average GPP was observed in April, whereas the largest difference in average  $R_{eco}$  was observed in July (Figure 31).

The CH<sub>4</sub> fluxes show virtually no diurnal cycle during the whole measurement period, though in some months (January, February and March in 2013, May, June, August and September in 2014, and August in 2015) there is an indication of larger CH<sub>4</sub> emission during the day (Figure 31). The magnitudes of average CH<sub>4</sub> fluxes from January to June, and December in 2013 were larger than in the same period in the other two years (no CH<sub>4</sub> data available in 2014 between January and April). Whereas, in 2014, the magnitudes of average CH<sub>4</sub> fluxes in August and September were larger than in 2013 and 2015 (Figure 31).

#### 5.2.4. Seasonal Trends in Daily Carbon Budgets

In Figure 32, time-courses of daily NEE (gap-filled) and the derived flux components GPP and  $R_{eco}$ , as well as CH<sub>4</sub> fluxes during the measurement period are presented. Estimates of daily GPP are shown using negative values to more effectively illustrate the opposing influences of the assimilatory (GPP) and respiratory ( $R_{eco}$ ) fluxes on the net CO<sub>2</sub> exchange. Daily values of important environmental variables (i.e. PPFD,  $T_{air}$  and water levels) are also provided (Figure 32). The three growing seasons were clearly characterised by the strong magnitude of the daily CO<sub>2</sub> exchange components. The winter periods (non-growing seasons) were characterised by low and constant assimilatory and respiratory fluxes (Figure 32). However, significant year-to-year differences in the magnitude were observed during the study period.

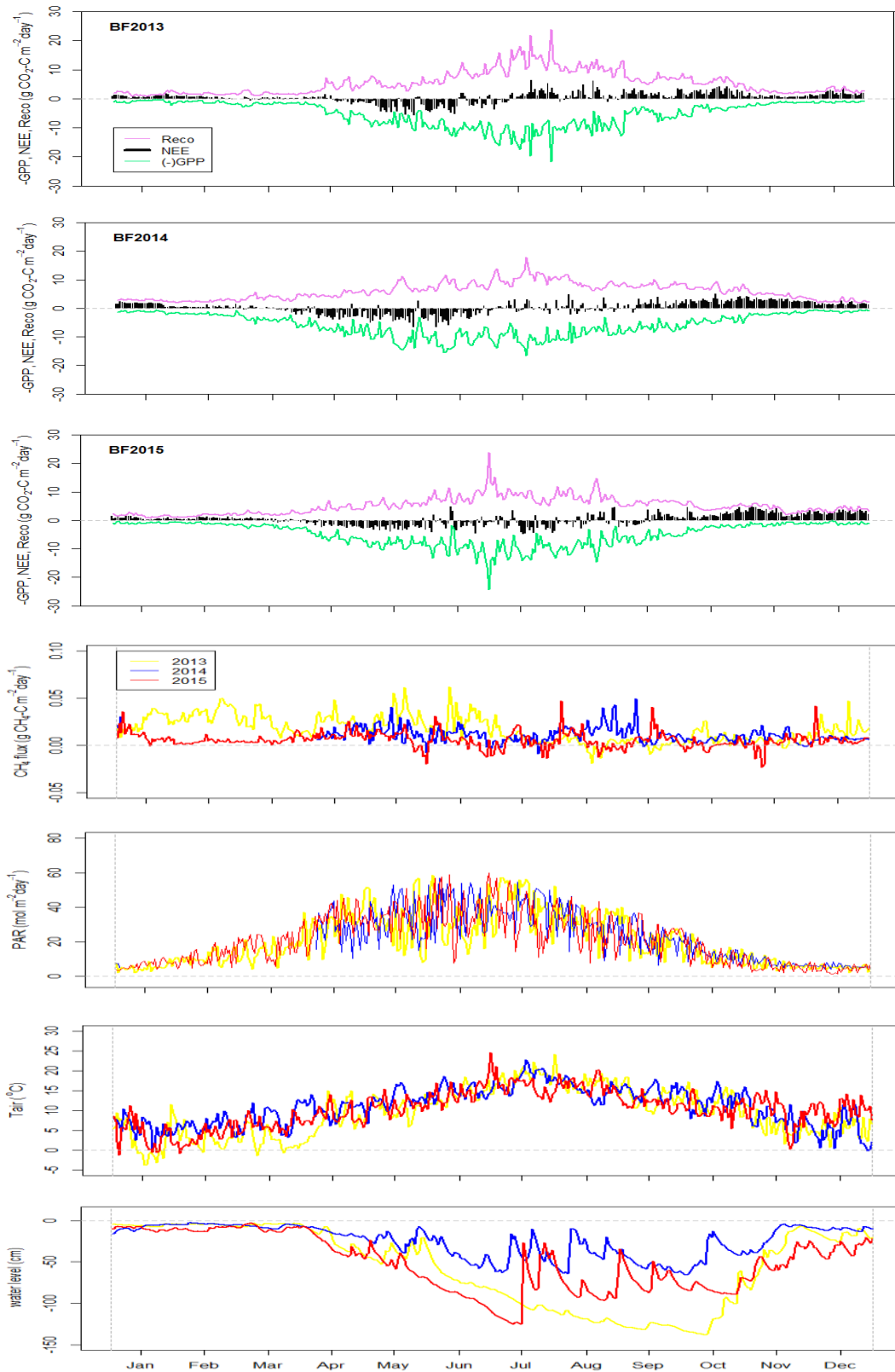


**Figure 32:** Seasonal change in daily  $\text{CO}_2$  and  $\text{CH}_4$  budget and environmental variables at Baker's Fen during the measurement period (2013 to 2015). Violet and Green bars show daily sums of ecosystem respiration ( $R_{\text{eco}}$ ) and gross primary production (GPP), respectively; black bars are total daily net ecosystem  $\text{CO}_2$  exchange (NEE).  $\text{CH}_4$  flux is total daily fluxes. All fluxes values are expressed as daily sums ( $\text{g C m}^{-2} \text{d}^{-1}$ ). PAR is total daily photosynthetically active radiation;  $T_{\text{air}}$  is daily average air temperature; and water level is the mean daily position of water levels relative to the ground surface.

The estimates of daily GPP and  $R_{eco}$  (green and violet lines) showed similar seasonal trends in all three years, starting from low daily values at the beginning of the year (non-growing season), increasing steadily throughout spring and summer, and reaching the peak in the middle of the growing season, then declining as the vegetation senesces with decreasing autumn day length (Figure 32). The estimates of daily NEE (black bar) also show similar seasonal trends in all three years, with the ecosystem starting to be a source of CO<sub>2</sub> at the beginning of the year (positive NEE), and turning to a sink when the vegetation starts to grow, and turning to a source again (after September, Figure 32). However, some differences in this general course occurred during the three year measurement period. The estimates of daily GPP and  $R_{eco}$  reached their peaks in the middle of July in 2013, early of July in 2014 and middle of June in 2015, indicating the intense CO<sub>2</sub> uptake occurred at different times in the three years (Figure 32). The cold spring in 2013 resulted in lower daily GPP and  $R_{eco}$  accordingly during the spring and early summer, therefore a delayed growing season, and started to become a sink of CO<sub>2</sub> (with negative NEE) from early April. However, the ecosystem turned to a source of CO<sub>2</sub> again earlier than in the other two years due to the rapid increases of temperature in 2013 summer. The ecosystem acted as a smaller source during November 2013 compared to the same period in 2014 and 2015, probably due to the colder November in 2013 (Figure 32). The warmer conditions in 2014 (compared to the other two years) resulted in an early start to the growing season in 2014, with the site acting as a sink of CO<sub>2</sub> from the beginning of March, following a balanced period between mid-June and September, and turned to a source again from early September (Figure 32). In 2015, the ecosystem acted as a sink of CO<sub>2</sub> during the most of the growing season from late March until August, and turned to a source from August throughout the whole winter. The larger positive daily NEE values in the winter of 2015 were associated with the warmer winter weather compared with the other two years (Figure 32; Table 6).

There is no clear seasonal pattern for mean daily CH<sub>4</sub> fluxes at BF. However, significant between-year differences in the magnitude of the CH<sub>4</sub> fluxes were observed (Figure 32). There is no CH<sub>4</sub> flux data between January and April in 2014 at BF. The CH<sub>4</sub> efflux was much larger from January until July in 2013 than in the same period in the other two years (Figure 32). August 2014 had larger effluxes than the other two

years in the same month, associated with the wetter but colder August in 2014. There is an indication that the ecosystem acted as a CH<sub>4</sub> sink during some periods in May, June and late October in 2015, associated with these dry periods in the year (Figure 25; 32).

The between-year differences of CO<sub>2</sub> fluxes can be more easily detected in the seasonal cumulative values of NEE, GPP and  $R_{eco}$ . Cumulative values computed on a monthly aggregation during the measurement period are presented in Table 6.

**Table 6:** Monthly total gross primary production, ecosystem respiration and net ecosystem CO<sub>2</sub> exchange estimated for Baker’s Fen during measurement period (2013 to 2015)

Month	GPP (g CO <sub>2</sub> -C m <sup>-2</sup> )			NEE (g CO <sub>2</sub> -C m <sup>-2</sup> )			$R_{eco}$ (g CO <sub>2</sub> -C m <sup>-2</sup> )		
	2013	2014	2015	2013	2014	2015	2013	2014	2015
January	26.31	37.61	27.07	26.98	47.34	23.59	53.29	84.95	50.66
February	37.15	64.61	32.22	14.10	14.08	22.01	51.25	78.69	54.23
March	52.16	126.29	64.38	2.42	-9.80	9.05	54.57	116.49	73.43
April	126.64	215.24	171.94	-6.90	-63.62	-47.19	119.74	151.62	124.75
May	228.66	302.01	242.74	-74.51	-92.26	-70.85	154.15	209.76	171.89
June	307.88	330.82	309.77	-69.23	-79.81	-38.53	238.65	251.01	271.24
July	381.17	331.07	315.64	29.22	7.20	-52.07	410.39	338.28	263.57
August	277.97	252.87	261.44	44.68	7.55	8.21	322.65	260.42	269.65
September	184.64	212.33	183.00	39.14	32.69	6.69	223.78	245.02	189.69
October	109.20	131.74	78.66	78.31	83.24	63.89	187.51	214.98	142.55
November	53.53	58.20	39.32	26.75	86.73	85.66	80.28	144.93	124.98
December	34.47	29.45	30.10	50.06	50.25	87.94	84.53	79.70	118.05

The maximum monthly total GPP values were observed in July in all three years, while 2013 had the largest monthly total GPP with 381.17 g CO<sub>2</sub>-C m<sup>-2</sup> month<sup>-1</sup> in the month of July (Table 6). The total GPP was higher during most months in 2014 than in 2013 and 2015, excluding July and August which were slightly lower than in 2013, and December which was slightly lower than the same month in 2015. These values were associated with the warmer conditions in July and August 2013 and the warmer December in 2015 (Table 6). The largest monthly total  $R_{eco}$  occurred in July of 2013

and 2014, but in June of 2015; while the 2013 July had the largest monthly  $R_{eco}$  (at  $410.39 \text{ g CO}_2\text{-C m}^{-2} \text{ month}^{-1}$ ) compared to all the months in the other two years (Table 6). The largest net  $\text{CO}_2$  uptake values were observed in May in all years, while there appeared the largest sink of  $\text{CO}_2$  at  $-92.26 \text{ g CO}_2\text{-C m}^{-2} \text{ month}^{-1}$  in May 2014 (Table 6). NEE changed to negative from March in 2014, which means the ecosystem acted as a sink of  $\text{CO}_2$  earlier in this year compared to the other two years. NEE in July 2015 delayed to become positive, which indicates the ecosystem was prolonged to be a sink of  $\text{CO}_2$  in the late end of the growing season in 2015. It is worth noting that the monthly total NEE in July 2015 was even higher than that in June 2015, which was associated with the abundant rainfall in July 2015 (Table 6).

**Table 7:** Monthly total methane flux at Baker's Fen during measurement period (2013 to 2015)

	CH <sub>4</sub> flux (g CH <sub>4</sub> -C m <sup>-2</sup> )		
	2013	2014	2015
January	0.756	--	0.296
February	1.050	--	0.121
March	0.658	--	0.174
April	0.750	--	0.319
May	0.868	0.407	0.194
June	0.753	0.348	0.128
July	0.235	0.185	0.109
August	0.029	0.573	0.175
September	0.058	0.329	0.225
October	0.254	0.199	0.008
November	0.148	0.256	0.068
December	0.507	0.195	0.193

Cumulative CH<sub>4</sub> fluxes computed on a monthly aggregation during the measurement period are presented in Table 7. In general, the monthly total CH<sub>4</sub> fluxes in most of the months of 2015 were lower than in the same period in 2013 and 2014; excluding August and September 2013 have the lowest CH<sub>4</sub> fluxes among the three years (Table 7). The largest CH<sub>4</sub> fluxes appeared in most months in 2013 compared to the other two years, excluding the months of August, September and November (Table 7). The

largest monthly total CH<sub>4</sub> flux occurred in February 2013 while the lowest value was observed in October 2015 (Table 7).

### 5.2.5. Annual Carbon Budgets

Annual cumulative NEE values at BF during the measurement period are presented in Figure 33. The random error calculated according to Finkelstein & Sims (2001) for measured NEE and the SD as reported by the gap-filling procedure for gap-filled NEE were used for computing the uncertainty ranges (see Section 4.3.6). The cumulative daily uncertainty range is presented as well in Figure 33. The uncertainties provide the maximum possible range of the accumulative NEE at BF during the measurement period. As previously described, all three years showed similar seasonal trends of CO<sub>2</sub> fluxes. However, the between-year differences of CO<sub>2</sub> fluxes can be more easily detected in accumulative trends. A positive slope of cumulative NEE is an indication of the ecosystem as a CO<sub>2</sub> source, while a negative slope indicates a CO<sub>2</sub> sink.

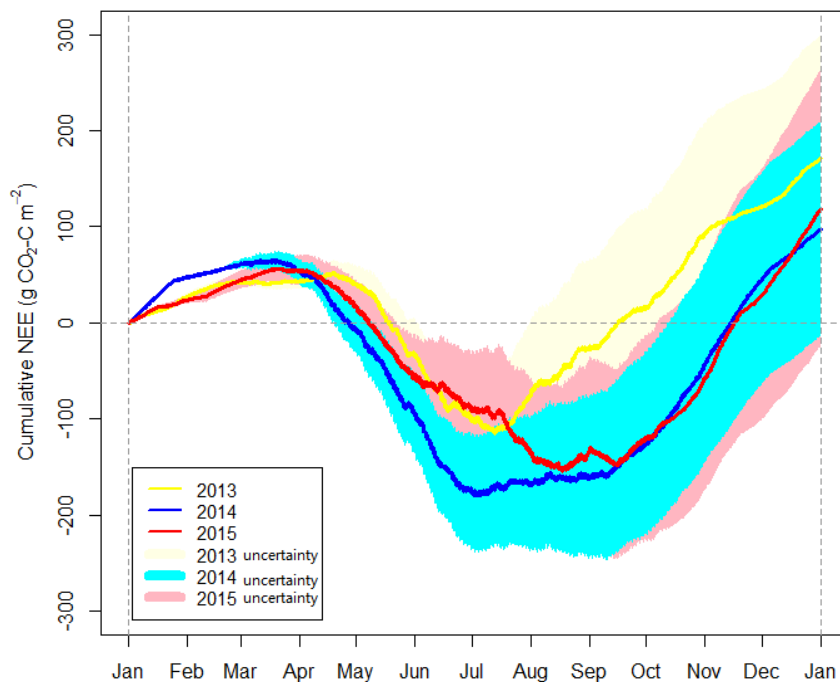


**Figure 33:** Annual cumulative net ecosystem CO<sub>2</sub> exchange (NEE) at Baker's Fen during measurement period (2013 to 2015), with cumulative daily range as uncertainties.

The 2013 data show the late increase in net CO<sub>2</sub> uptake in late spring (May) compared to the other two years, followed by a sharp but short-period of increasing net CO<sub>2</sub> uptake until mid-July, followed by a rapid increase of CO<sub>2</sub> emission throughout the rest of the year (Figure 33). The year 2014 experienced the earliest increase (in March) in net CO<sub>2</sub> uptake among the three years, with uptake increasing rapidly until July. A high increase of CO<sub>2</sub> emission in 2014 occurred in the middle of September, and then throughout the rest of winter (Figure 33). In comparison with 2014, 2015 experienced a more steady increase of net CO<sub>2</sub> uptake during the growing season, but with a slightly sharper increase in CO<sub>2</sub> emission after the growing season, thereby ending up with a slightly higher annual sum (positive) for NEE at the end of the year (Figure 33).

The annual cumulative NEE, GPP (negative) and  $R_{eco}$  during the measurement period are presented in Figure 34. Both the total accumulated GPP and  $R_{eco}$  in 2014 were higher than those in 2013 and 2015 during the generally warmer conditions (Figure 34). Both the estimates of total cumulative GPP and  $R_{eco}$  were lower at the beginning of the year in 2013 than in 2015. However, 2013 experienced a rapid increase of accumulative GPP and  $R_{eco}$  in July associated with the increasing average temperatures in July and August, and ended up with larger annual sums of GPP and  $R_{eco}$  when compared to 2015 (Figure 34; Table 8).

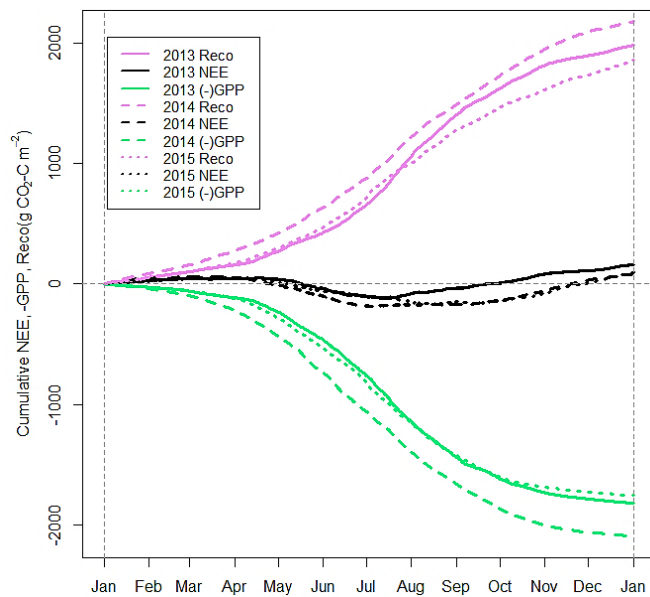


**Figure 34:** Annual cumulative net ecosystem CO<sub>2</sub> exchange (NEE), ecosystem respiration ( $R_{eco}$ ) and gross primary production (GPP) in black, violet and green respectively, during the measurement period (2013 to 2015) at Baker's Fen. The term -GPP is here the opposite of GPP and is introduced to facilitate graphical reading.

Annual accumulative CH<sub>4</sub> fluxes at BF during the measurement period are presented in Figure 35. There are no data available from 3<sup>rd</sup> January to 8<sup>th</sup> April, 2014. Here, the accumulative CH<sub>4</sub> data in 2014 is not used to compare with the other two years' data, but to show the cumulative trends using available data for the 2014 period only. The accumulative CH<sub>4</sub> at BF does not show evident decline during the whole measurement period (Figure 35). The cumulative CH<sub>4</sub> fluxes increase rapidly during the first half year of 2013 between January and July, following a much slower increase throughout the rest of year (Figure 35). The cumulative CH<sub>4</sub> fluxes in 2015 increase extremely slowly but steadily throughout the whole year, and ending up with a much lower annual sum of CH<sub>4</sub> fluxes at year end when compared to 2013 (Figure 35). In 2014, the slope of the accumulated fluxes was larger than the same period in 2013 and 2015 (Figure 35). Annual cumulative CH<sub>4</sub> was estimated at 6.07 g CH<sub>4</sub>-C m<sup>-2</sup>yr<sup>-1</sup> in 2013 and 2.01 g CH<sub>4</sub>-C m<sup>-2</sup>yr<sup>-1</sup> in 2015, corresponding to a net difference of around 4.06 g CH<sub>4</sub>-C m<sup>-2</sup> yr<sup>-1</sup> (Table 8).

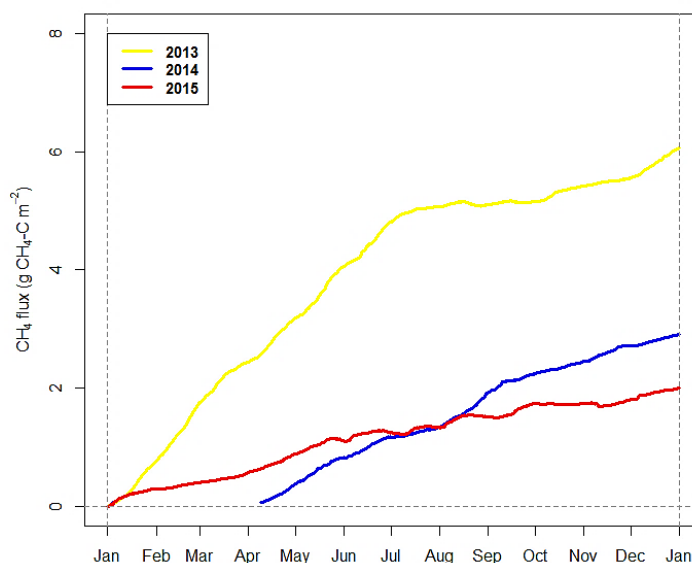


**Figure 35:** Annual cumulative CH<sub>4</sub> fluxes at Baker's Fen during measurement period (2013 to 2015). There is no data available from 3<sup>rd</sup> January to 8<sup>th</sup> April, 2014. The accumulative CH<sub>4</sub> data in 2014 doesn't use to compare with the other two years data.

The study site BF was a net source for CO<sub>2</sub> in all three years with annual gap-filled totals of 161.03±12.51 g CO<sub>2</sub>-C m<sup>-2</sup>yr<sup>-1</sup> in 2013, 83.61±11.53 g CO<sub>2</sub>-C m<sup>-2</sup>yr<sup>-1</sup> in 2014, and 98.39±13.31 g CO<sub>2</sub>-C m<sup>-2</sup>yr<sup>-1</sup> in 2015 (Table 8). The uncertainty in the annual

sums includes random measurement error and gap filling error estimates based on the Monte-Carlo simulation approach (see Section 4.3.6).

**Table 8:** CO<sub>2</sub>-equivalent comparison based on GWP for measurement period 2013 - 2015 at Baker's Fen

	Annual Budget	Carbon Balance (g C m <sup>-2</sup> )	GWP (100 years) (g CO <sub>2</sub> m <sup>-2</sup> )
2013 Carbon dioxide (CO <sub>2</sub> )	590.44 (±45.87) g CO <sub>2</sub> m <sup>-2</sup>	161.03 (±12.51)	590.44 (±45.87)
2013 Methane (CH <sub>4</sub> )	8.089 (±0.128) g CH <sub>4</sub> m <sup>-2</sup>	6.067 (±0.096)	202.23 (±3.2)
2013 gross primary production (GPP)	--	1819.79	--
2013 ecosystem respiration ( <i>R<sub>eco</sub></i> )	--	1980.81	--
2014 Carbon dioxide (CO <sub>2</sub> )	306.56 (±42.27) g CO <sub>2</sub> m <sup>-2</sup>	83.61 (±11.53)	306.56 (±42.27)
2014 Methane (CH <sub>4</sub> ) (Apr. – Dec.)	3.793 (±0.137) g CH <sub>4</sub> m <sup>-2</sup>	2.845 (±0.103)	94.825 (±3.425)
2014 gross primary production (GPP)	--	2092.26	--
2014 ecosystem respiration ( <i>R<sub>eco</sub></i> )	--	2175.86	--
2015 Carbon dioxide (CO <sub>2</sub> )	360.78 (±48.81) g CO <sub>2</sub> m <sup>-2</sup>	98.39 (±13.31)	360.78 (±48.81)
2015 Methane (CH <sub>4</sub> )	2.679 (±0.116) g CH <sub>4</sub> m <sup>-2</sup>	2.009 (±0.087)	66.975 (±2.9)
2015 gross primary production (GPP)	--	1756.28	--
2015 ecosystem respiration ( <i>R<sub>eco</sub></i> )	--	1854.67	--

The BF site was a source of CH<sub>4</sub> during each study year with annual gap-filled totals of 6.067 ± 0.096 g CH<sub>4</sub>-C m<sup>-2</sup>yr<sup>-1</sup> in 2013, and 2.009 ± 0.087 g CH<sub>4</sub>-C m<sup>-2</sup>yr<sup>-1</sup> in 2015 (Table 8). There is no CH<sub>4</sub> data available from January to April in 2014. The total CH<sub>4</sub> budgets between April and December in 2013 and 2015 are calculated for comparison with the available period total CH<sub>4</sub> budget in 2014. The ecosystem was still a source of

CH<sub>4</sub> during the comparison period (April to December), emitting  $3.504 \pm 0.079$  g CH<sub>4</sub>-C m<sup>-2</sup> in 2013,  $2.845 \pm 0.103$  g CH<sub>4</sub>-C m<sup>-2</sup> in 2014, and  $1.375 \pm 0.085$  g CH<sub>4</sub>-C m<sup>-2</sup> in 2015 (Table 8).

Ramaswamy *et al.* (2001) defined the GWP for each GHG based on the radiative forcing concept. Frolking *et al.* (2006) suggested that the global warming effects were enhanced by CH<sub>4</sub> emission during the first few decades, but later is diminished by the sequestration of CO<sub>2</sub>. The gap-filled CO<sub>2</sub> and CH<sub>4</sub> budgets were compared using a 100 year time horizon in this study during the study period, where CH<sub>4</sub> has a GWP of 25 (see Section 2.2.3; Table 8). The ecosystem was found to have a positive forcing (net warming) of 792.67, 401.38 and 427.75 g CO<sub>2</sub> m<sup>-2</sup>, in 2013, 2014 and 2015, respectively (the CH<sub>4</sub> budget in 2014 only accounted for the period April to December, and was not an annual budget; Table 8). The CH<sub>4</sub> flux contributed 16% - 26% of the total positive forcing (noting that the 2014 CH<sub>4</sub> budget was not an annual budget).

## 5.3. Response of Carbon Flux to Major Environmental Factors

### 5.3.1. Effects of Environmental Factors

The Pearson coefficients (*r*) of CO<sub>2</sub> and CH<sub>4</sub> fluxes to measured environmental factors (*T<sub>air</sub>*, RH, VPD, PAR and WT) at BF were tested by simple linear regression. The Pearson correlation coefficients (*r*), the square of the Pearson correlation coefficients (*R*<sup>2</sup>) and p-values for the correlation between fluxes and measured environmental factors have been reported in Table 9. The square of the Pearson correlation coefficient (*R*<sup>2</sup>) indicates the percentage of variance in *y* (i.e. flux) that can be explained by *x* (i.e. environmental factors). Stepwise multiple regressions were carried out to correlate fluxes with measured environmental factors. The best fit regression equations of fluxes against significantly related environmental factors and adjusted *R*<sup>2</sup> have been reported in Table 10.

**Table 9:** Pearson coefficients ( $r$ ) of fluxes (NEE, GPP,  $R_{eco}$ ,  $F_{CH4}$ ) on environmental factors at Baker's Fen. The square of the Pearson correlation coefficient ( $R^2$ ) have been presented in brackets. The p-values for the correlation have been presented as stars (\*).

	$T_{air}$	RH	VPD	PAR	WT
NEE	-0.290 (0.084)**	0.520 (0.270)**	-0.513 (0.263)**	-0.829 (0.687)**	-0.038 (0.001)*
$R_{eco}$	0.848 (0.719)**	-0.474 (0.225)**	0.771 (0.594)**	0.504 (0.254)**	-0.527 (0.278)**
GPP	0.718 (0.516)**	-0.509 (0.259)**	0.716 (0.513)**	0.795 (0.632)**	-0.348 (0.121)*
$F_{CH4}$	-0.100 (0.010)*	-0.034 (0.001)*	-0.014 (0.001)*	0.073 (0.005)*	0.187 (0.034)*

$T_{air}$ , air temperature; RH, relative humidity; VPD, vapour pressure deficit; PAR, photosynthetically active radiation; WT, water table; NEE, net ecosystem exchange;  $R_{eco}$ , ecosystem respiration; GPP, gross primary production;  $F_{CH4}$ , methane flux. \*,  $0.01 < p < 0.05$ ; \*\*,  $p < 0.01$ .

NEE was negatively correlated with  $T_{air}$ , VPD, PAR and WT, and positively correlated with RH (Table 9). While both  $R_{eco}$  and GPP were positively correlated with  $T_{air}$ , VPD and PAR, but negatively correlated with RH and WT. It should be noted that, compared to NEE and GPP,  $R_{eco}$  was more significantly correlated with WT at BF ( $p < 0.01$ ; Table 9).  $F_{CH4}$  displayed a negative correlation with  $T_{air}$ , RH and VPD, and positive correlation with PAR and WT. However, compared to the fluxes of  $CO_2$ ,  $F_{CH4}$  showed much less significant correlation with all these environmental factors ( $0.01 < p < 0.05$ , Table 9). Among these environmental factors, PAR accounted for the greatest proportion of variations for both of NEE and GPP (68.7% and 63.2%, respectively), while  $T_{air}$  and VPD significantly explained 71.9% and 59.4% of the variation for  $R_{eco}$  (it should be noted that,  $T_{air}$  have been used for computing the daytime  $R_{eco}$  during fluxes partitioning, see Section 4.1.4). WT only accounted for 3.4% of the variation in  $F_{CH4}$  (the greatest proportion of variation in  $F_{CH4}$  can be explained;  $0.01 < p < 0.05$ ; Table 9).

**Table 10:** Stepwise regression analysis of fluxes (NEE,  $R_{eco}$ , GPP and  $F_{CH4}$ ) against significantly related environmental factors at Baker's Fen

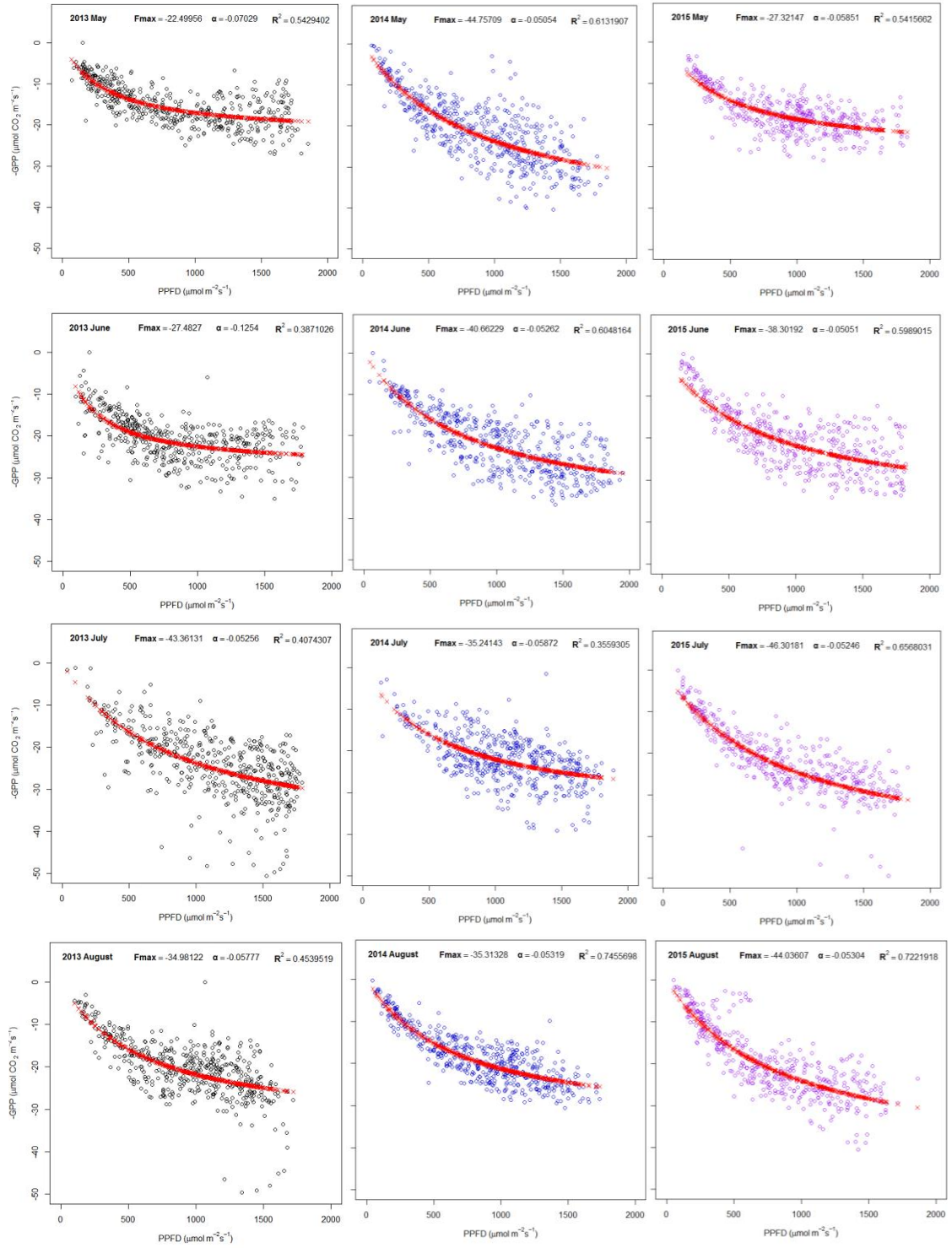
	Best fit regression equations	Adj-R <sup>2</sup>	p-values
NEE	$F = -0.13PAR - 0.026WT + 2.45$	0.712	**
$R_{eco}$	$F = 0.232T_{air} + 1.241VPD + 0.183RH - 0.01WT - 15.988$	0.865	**
GPP	$F = 0.011PAR + 0.655T_{air} - 3.666$	0.801	**
$F_{CH4}$	$F = 0.851 \times 10^{-4}WT + 0.686 \times 10^{-5}PAR + 0.1 \times 10^{-2}T_{air} + 0.016$	0.048	*

See Table 9 for abbreviations.

However, after combining all measured environmental factors in the stepwise multivariate regression analysis, PAR and WT together accounted for 71.2% of the variation in NEE (PAR accounted for 68.7%, WT accounted for 2.5%;  $p < 0.01$ ; Table 10). While  $T_{air}$ , VPD, RH, and WT can explain 86.5% of variation for  $R_{eco}$  ( $T_{air}$  accounted for 71.9%, the other three environmental factors together explained 14.6%;  $p < 0.01$ ; Table 10). As for GPP, PAR and  $T_{air}$  accounted for 80.1% of the variation in GPP (PAR accounted for 63.2%,  $T_{air}$  explained 16.9%;  $p < 0.01$ ; Table 10). However,  $F_{CH4}$  showed very weak relationship with these measured environmental factors (WT, PAR, and  $T_{air}$  together only can explain 4.8% of the variation in  $F_{CH4}$ ;  $0.01 < p < 0.05$ ; Table 10).

### 5.3.2. Light Response Curves

It is well acknowledged that light is an important environmental driver for variation in GPP during the daytime (Baldocchi *et al.*, 2001; Wagle & Kakani, 2014). The relation between GPP and PPFD can be described by a rectangular hyperbolic light response equation (see Section 4.3.8). The dependence of daytime GPP ( $R_g > 20 \text{ W m}^{-2}$ ) on light was simulated with the means of the rectangular hyperbolic light response function for different months during the growing season (May to October) in the measurement period (2013 to 2015) at BF (Figure 36). GPP are shown in negative values to facilitate graphical reading.



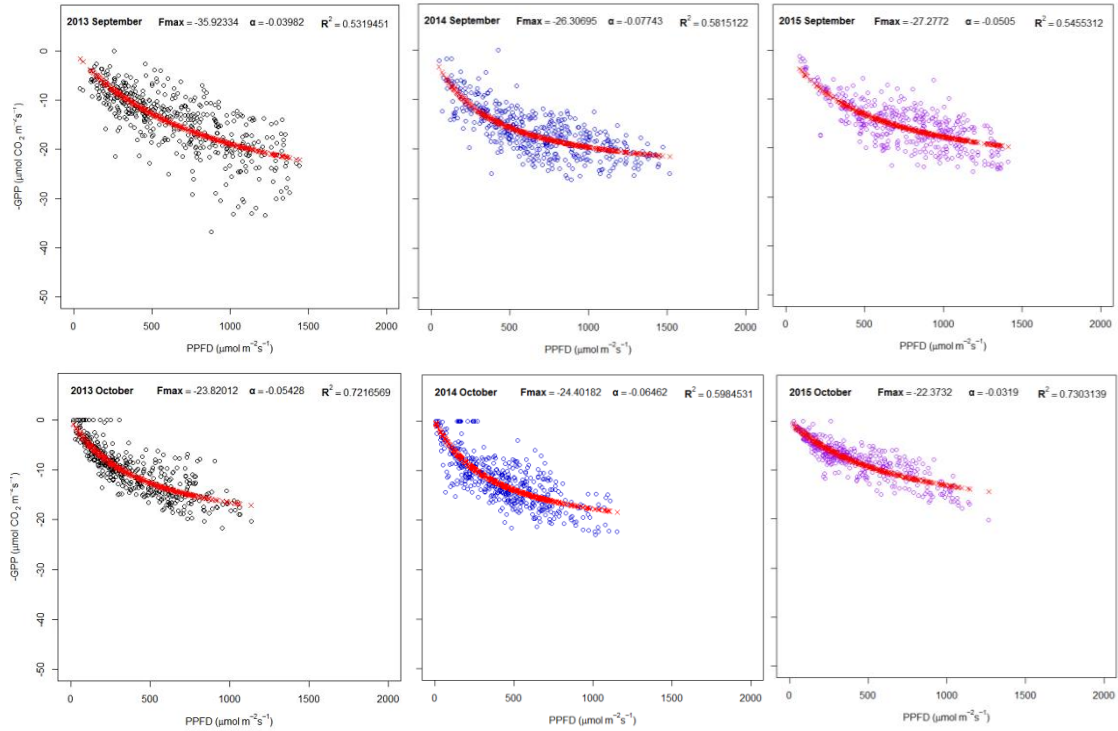


**Figure 36:** Light response curves of GPP plotted for different months during the growing season from 2013 to 2015 at Baker's Fen. Fitted curves represent the rectangular hyperbolic light response function (see Equation 14).  $F_{max}$  is the maximum  $\text{CO}_2$  flux at infinite light,  $\alpha$  is the ecosystem apparent quantum yield.

It is clear that seasonal changes in PPFD explained between about 35% and 75% of the variability in daytime GPP during the measurement periods covering the main growing seasons (Figure 36). Significant differences in the light response curves for GPP were observed among the three study years during the growing seasons. There was no light saturation of GPP apparent in any of the three study years. In general, the maximum rates of GPP ( $F_{max}$ , shown in negative values) in all months in 2014 were larger than in 2013 and 2015. The maximum rates of GPP in 2013 were observed in July with a calculated  $F_{max}$  value of  $-43.36 \mu\text{mol CO}_2 \text{ m}^{-2} \text{ s}^{-1}$ , from the rectangular hyperbola (Equation 14) fitted to the light response curve (Figure 36). In 2014, the maximum rates of GPP occurred in May which was much earlier than in either 2013 or 2015, with  $F_{max}$  value of  $-44.76 \mu\text{mol CO}_2 \text{ m}^{-2} \text{ s}^{-1}$  (Figure 36). In 2015, the peak  $F_{max}$  value was higher than in 2013 and 2014, at  $-46.30 \mu\text{mol CO}_2 \text{ m}^{-2} \text{ s}^{-1}$ , and occurred in July as well (Figure 36). The  $F_{max}$  decreased gradually after it reached the largest value in the year (the lowest values at  $-22.50$ ,  $-24.40$  and  $-22.37 \mu\text{mol CO}_2 \text{ m}^{-2} \text{ s}^{-1}$  for 2013, 2014 and 2015, respectively). During the senescence period (October), the maximum PPFD

values were much lower than for the other months at about  $1100 \mu\text{mol m}^{-2}\text{s}^{-1}$  in all three years (Figure 36).

The ecosystem apparent quantum yield ( $\alpha$ ) also differed among years during the growing season, with calculated values of 0.053, 0.051 and 0.052  $\text{mol mol}^{-1}$ , in July 2013, May 2014 and July 2015 (the month with the highest  $F_{max}$ ), respectively (Figure 36). The values of apparent quantum yield at BF were similar to those reported in other studies in temperate grasslands (Flanagan *et al.*, 2002; Wohlfahrt *et al.*, 2008).

### 5.3.3. Multi-scale Analysis of Environmental Controls on CO<sub>2</sub> Fluxes

The wavelet analysis allowed identification of correlations between environmental factors and ecosystem assimilatory (GPP) or respiratory ( $R_{eco}$ ) processes at multiple temporal scales, along the time domain (i.e. days of the year) during the measurement period at BF. Half-hourly gap-filled data were used and the temporal scales considered varied from daily to more than half annual (256 days). Only GPP and  $R_{eco}$  were analysed, because NEE is governed by factors that control both assimilatory (GPP) and respiratory ( $R_{eco}$ ) components. A wavelet coherence analysis was implemented between GPP and PPFD,  $T_{air}$ , VPD. The correlations between  $R_{eco}$  and VPD were also analysed by the wavelet coherence method. The  $R_{eco}$  was estimated base on the  $T_{air}$  during the flux partitioning procedure; therefore no correlation analysis was implemented between  $R_{eco}$  and  $T_{air}$  in this section.

In the wavelet coherence figures, the Y-axis represents the temporal scales in days, expressed with an exponential annotation, and the coloured areas represent regions of similar periodicities of two time series power spectra, from values of high coherence (towards to 1; red) to low coherence (towards to 0; blue). The black margin around coloured areas delimits the cone of influence (i.e. the region not influenced by edge effects; Vargas *et al.*, 2010).

In Figure 37, the large blue areas indicate the period with no PPFD data available from January to April 2014. The highest coherence between PPFD and GPP was at the daily scale during the whole period, indicative of a common diel cycle between PPFD and photosynthesis during all seasons due to the permanent vegetation cover at the study site. Some localised coherences at larger scales (4 - 16 days) can be identified during the growing seasons representing similar increasing patterns of PPFD and GPP during the period of plant activity (Figure 37). The localised coherences observed during the most of period in growing seasons and at even larger scales (16 - 64 days) indicating that the PPFD is not the limiting factor for photosynthesis during the growing seasons at BF (Figure 37).

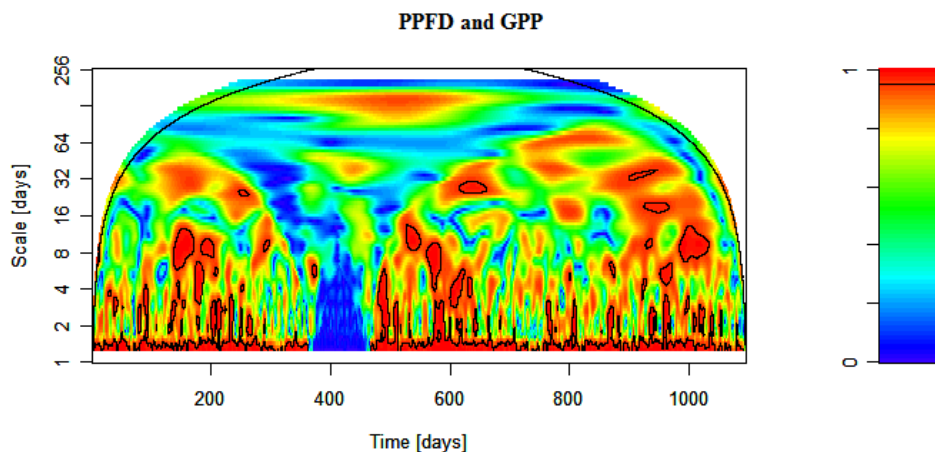


**Figure 37:** Wavelet coherence analysis between gross primary production (GPP) and photosynthetic photon flux density (PPFD) during the measurement period (2013 to 2015) at Baker's Fen. On the Y-axis the time-scale is reported. Low to high coherence values are represented in the colour palette from blue to red. There is no valid PPFD data during January to April 2014.

Regarding air temperature with GPP, the daily cycle coherence only was exhibited during the growing seasons (Figure 38). There are some localized coherences at the larger scale (8 - 64 days) can be identified during growing seasons as well (especially in warmer year 2014), underlying the photosynthesis activity was closely related to the increasing air temperature during the period of plant activity (Figure 38). Some localized coherences at half-month scale (7 - 16 days) during the senescence period indicate the similar decreasing patterns of air temperature and GPP during the non-growing seasons (Figure 38).

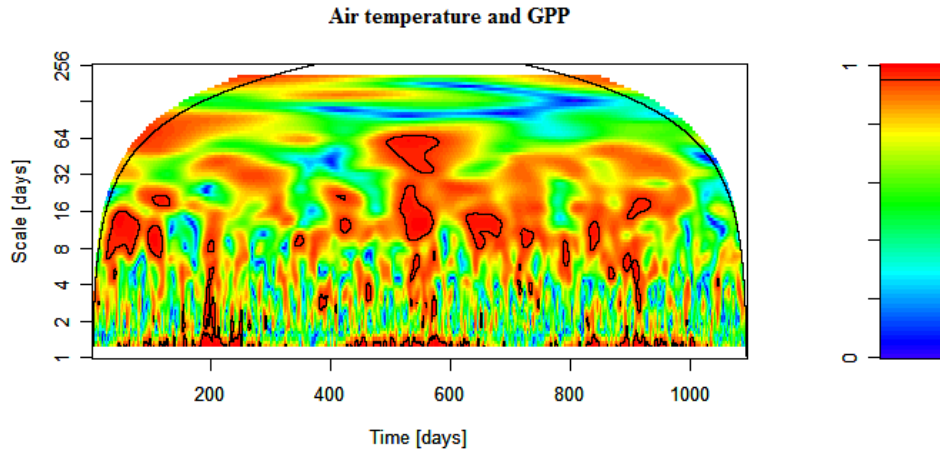


**Figure 38:** Wavelet coherence analysis between gross primary production (GPP) and air temperature ( $T_{air}$ ) during the measurement period (2013 to 2015) at Baker's Fen. On the Y-axis the time-scale is reported. Low to high coherence values are represented in the colour palette from blue to red.

Similar with  $T_{air}$ , VPD exhibited daily cycle coherence with photosynthesis only during the growing seasons, but with generally higher coherences with larger scales (7 - 64 days) (Figure 39). The high localized coherences identified at larger scale (7 - 64 days) during the growing seasons represented the great influence of increasing VPD on photosynthesis during the period of plant activity (Figure 39). There are only a few localized coherences found during the non-growing season at larger scales (16 - 32 days), probably associated with the similar decreasing patterns of VPD and photosynthesis in discontinuous non-stationary cooling events in late autumn and winter (Figure 39).

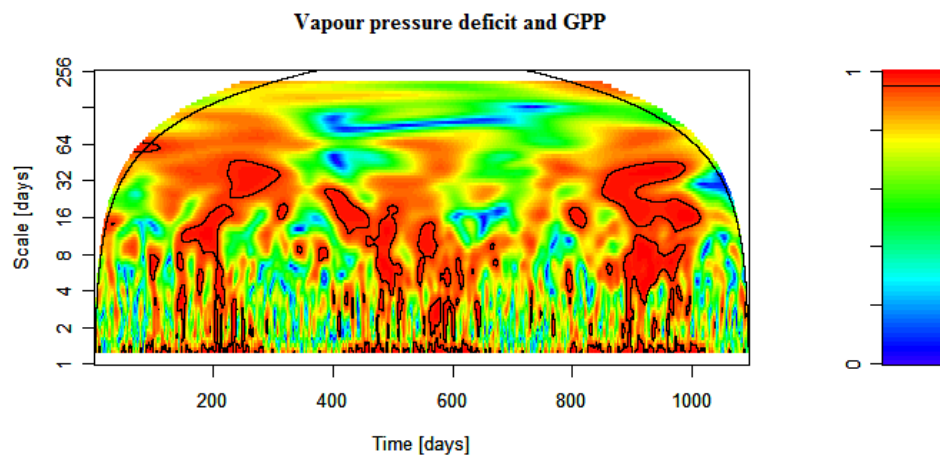


**Figure 39:** Wavelet coherence analysis between gross primary production (GPP) and vapour pressure deficit (VPD) during the measurement period (2013 to 2015) at Baker's Fen. On the Y-axis the time-scale is reported. Low to high coherence values are represented in the colour palette from blue to red.

Finally, wavelet coherence between  $R_{eco}$  and VPD is shown in Figure 40. Daily coherences can be found with VPD and respiration during the growing seasons in all three study years (Figure 40). The weekly localized coherences are evident for specific periods during the growing season, associated with rainfall / heat wave events producing effects on  $R_{eco}$  lasting some days (Figure 40). The high coherences can be found at seasonal / inter-seasonal scale (64 - 256 days) between VPD and  $R_{eco}$ , indicating VPD had a general influence on the respiration activity throughout the whole measurement period (Figure 40).

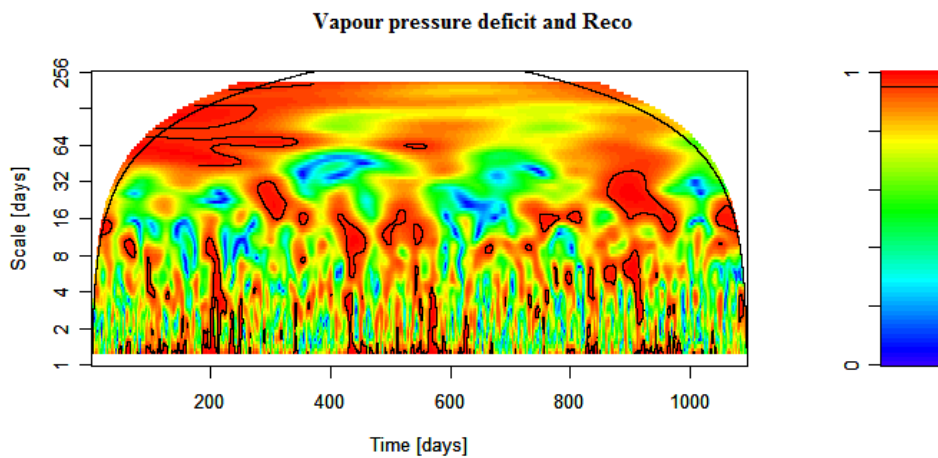


**Figure 40:** Wavelet coherence analysis between ecosystem respiration ( $R_{eco}$ ) and vapour pressure deficit (VPD) during the measurement period (2013 - 2015) at Baker's Fen. On the Y-axis the time-scale is reported. Low to high coherence values are represented in the colour palette from blue to red.

## 5.4. Discussion and Conclusion

### 5.4.1. EC Measurement Performance

The energy balance closure (EBC) is a means of assessing how well the EC system captures the different energy fluxes. In this way, the EBC is a limited check on the quality of the calculated fluxes by comparing the flux results from  $H_2O$  /  $CO_2$  IRGA (LE and H) after full data processing and QC with the direct measurements from the radiation sensor and soil heat flux plates ( $R_n$  and G) (Foken *et al.*, 2006).

The EBC with half-hour time scale data at BF (Figure 23) was towards the higher end of the 70 to 90% range reported from a range of FluxNet sites (regression slopes ranging from 0.53 to 0.99 with a mean of 0.79 and EBR ranging from 0.34 to 1.69 with a mean of 0.84) (Wilson *et al.*, 2002). The EBC was further improved by using the daily average in the analysis. This suggested a good overall system performance and high data reliability on the study site during the measurement period.

In reality, full EBC is rarely attained using the EC technique. The potential reasons for the lack of EBC measured by the EC technique were described in a previous section (4.3.7). The energy imbalance existing at BF could result from the poor performance of the heat flux plates in peat substrates (Laurila *et al.*, 2012). The neglected energy storage term (normally neglected at short vegetation sites with a relatively low measurement height) could be another explanation for the relative imbalance of EBC at BF (Harding & Lloyd, 2008; Jacobs *et al.*, 2008). Also, there are differences between the footprints of the eddy fluxes, the soil heat fluxes and the net radiation measurements, which remain an unresolved issue in the flux community (Balzarolo *et al.*, 2011). The CNR1 net radiometer at BF was set on another stand about 10 m away from the main EC tower (Figure 18) to avoid the disturbance from the main wind direction. However, that will increase the difference in the footprints of the EC fluxes measurements and the radiation measurements on this site.

The footprint estimates and the distribution of the wind field confirmed that the majority of the measured fluxes originated from the area of interest and that the contribution of the measured fluxes from the target ecosystem dominated by far the overall budget. Furthermore, the total flux data coverage was within the typical range of the coverage attained from the other EC sites (Falge *et al.*, 2001).

#### 5.4.2. Carbon Dioxide Fluxes

The regenerating site BF acted as a net source of CO<sub>2</sub> to the atmosphere during all three study years, with annual gap-filled totals of 161.03±12.51 g CO<sub>2</sub>-C m<sup>-2</sup>yr<sup>-1</sup> in 2013, 83.61±11.53 g CO<sub>2</sub>-C m<sup>-2</sup>yr<sup>-1</sup> in 2014 and 98.39±13.31 g CO<sub>2</sub>-C m<sup>-2</sup>yr<sup>-1</sup> in 2015 (Table 8). The annual CO<sub>2</sub> budget at BF is within the range of values reported for managed

and restored temperate and boreal grasslands (with peat soil) (Table 11). While a restored grassland peatland can act as a large atmospheric CO<sub>2</sub> sink with -232 to -446 g CO<sub>2</sub>-C m<sup>-2</sup>yr<sup>-1</sup> after 10 years of restoration (Hendriks *et al.*, 2007); several other restored grasslands under different management regimes also can act as a large source of CO<sub>2</sub> with 220±90 g CO<sub>2</sub>-C m<sup>-2</sup>yr<sup>-1</sup> noted at a site in the Netherlands (Jacobs *et al.*, 2007). Waddington *et al.* (2010) showed that a degraded peatland acted as a source of 245 g CO<sub>2</sub>-C m<sup>-2</sup> to the atmosphere during the growing season prior to restoration, but acted as a net sink of -20±5 g CO<sub>2</sub>-C m<sup>-2</sup> during the growing season only two years post-restoration. Waddington *et al.* (2010) proposed that the degraded peatland will likely return to a net C sink in 6 to 10 years post-restoration. BF showed a net CO<sub>2</sub> emissions reduction benefit of rewetting in 2014 and 2015 compared to drained and cultivated fens in the UK (with an emission of 108.94±17.11 g CO<sub>2</sub>-C m<sup>-2</sup>yr<sup>-1</sup> on average; Evans *et al.*, 2011). However, the study site BF showed no clear trends of turning to a net CO<sub>2</sub> sink during the study years, which might relate to the natural restoration regimes on the site.

The GPP and  $R_{eco}$  at BF during the study period were both higher than values reported in the literature (Table 11). The GPP at BF was even higher than the GPP range (i.e. 1393 to 1719 g CO<sub>2</sub>-C m<sup>-2</sup>yr<sup>-1</sup>) reported for extensively grazed temperate grasslands with peat soil (Jaksic *et al.*, 2006; Klumpp *et al.*, 2011). The higher GPP at BF likely reflects the large living plant biomass of BF relative to more northerly peatlands (Humphreys *et al.*, 2006) and the lack of biomass removal by mowing (although a certain amount of biomass at BF is removed due to grazing). The higher  $R_{eco}$  at BF compared to the other sites reported in the literature can be partly explained by greater contributions from autotrophic respiration and higher heterotrophic respiration rates related to warmer temperatures and large seasonal variations in water levels, which are also suggested by the results of a regression analysis (Lund *et al.*, 2010; Table 10). The warmer and drier conditions at BF could be another explanation for the higher rates of annual GPP and  $R_{eco}$ . The annual NEE at BF in the present study was similar to the values reported by Veenendaal *et al.* (2007), who undertook the measurements at an extensively grazed temperate grassland site, but significantly less positive than the range reported by Jacobs *et al.* (2007) on four temperate restored grassland sites and for a boreal drained site before restoration (Waddington *et al.*, 2010; Table 11).

**Table 11:** Comparison of annual carbon dioxide budgets for managed and restored temperate and boreal peatlands with permanent vegetation cover reported in literature (modified from Morrison, 2013).

Reference	Site description	NEE	GPP	$R_{eco}$
		(g CO <sub>2</sub> -C m <sup>-2</sup> yr <sup>-1</sup> )		
This study	Baker's Fen; grazed; rewetting	83.61±11.53 ~ 161.03±12.51	1756.28 ~ 2092.26	1854.67 ~ 2175.86
This study	Sedge Fen; semi-natural	-243.78±15.25 ~ -356.86±13.4	1437.15 ~ 1559.39	1193.37 ~ 1202.53
Hendriks <i>et al.</i> , (2007)	Restored semi-natural temperate grassland (peat depth: 2 m; WT: 0 to -40 cm; 10 years under restoration)	-232 ~ -446	1156 ~ 1314	866 ~ 924
Jacobs <i>et al.</i> , (2007)	Restored four temperate grasslands under different management regimes and different water table	220±90	1300±100	1520±30
Veenendaal <i>et al.</i> , (2007)	Temperate grassland in nature reserve (0.25 m peaty clay overlying 12 m eutrophic peat deposits; mown and grazed)	-5.7	1539	1542
Veenendaal <i>et al.</i> , (2007)	Temperate grassland peatland under intensively managed as daily farm (0.25 m peaty clay overlying 12 m eutrophic peat deposits; mown, grazed and fertilized)	133.9	1460	1596
Jin <i>et al.</i> , (2008)	Restored boreal freshwater marsh	390	--	--
Waddington <i>et al.</i> , (2010)	Drained boreal peatland (before restoration in 1999) growing season measurement (May to Oct.)	245	--	--
Waddington <i>et al.</i> , (2010)	Restored boreal peatland (two years post-restoration in 2002) growing season measurement (May to Oct.)	-20±5	--	--
Drewer <i>et al.</i> , (2010)	Low-lying acidic peat bog in Scotland	-324 ~ -500	--	--
Drewer <i>et al.</i> , (2010)	Open pristine nutrient-rich sedge fen in Finland	-15 ~ -145	--	--
Bernal & Mitsch, (2012)	Summarized temperate semi-natural freshwater wetlands in USA	-56 ~ -504	--	--
Herbst <i>et al.</i> , (2013)	Semi-natural boreal wet grassland (10 years under restoration)	-53 ~ -268	--	--
Aslan-Sungur <i>et al.</i> , (2016)	Disturbed temperate peatland (peat depth: 12 m; WT: 0 to -120 cm; grazed)	244 ~ 663	948 ~ 1090	1194 ~ 1726

Seasonal NEE variations and its component fluxes (i.e. GPP and  $R_{eco}$ ) were observed at BF during all three study years. Similar patterns were also found during the whole measurement period. Low magnitudes of CO<sub>2</sub> flux were observed during the early spring, photosynthesis was optimised through a fast increase of CO<sub>2</sub> uptake at the beginning of the growing season, then it reached a maximum peak when a seasonal peak of irradiance and temperature appeared, and finally declined as the vegetation senesced throughout autumn. The respiratory activities, in contrast, show a fairly constant increasing / decreasing trend during the growing season and senescence period. This seasonal trend is similar to that of most temperate and boreal peatland ecosystems (Bernal & Mitsch, 2012; Jacobs *et al.*, 2007). Despite this overall similarity in seasonal patterns, marked differences were observed in the seasonal magnitude of accumulated CO<sub>2</sub> exchanges at BF during the measurement period. Generally speaking, the higher rates of accumulated GPP and  $R_{eco}$  at this study site were associated with warmer and drier conditions. BF functioned as a net sink (monthly) of CO<sub>2</sub> between April and June in all three years, as well as in March 2014 and July 2015, indicating that the study site was likely to be a sink of CO<sub>2</sub> or a small net source during the growing seasons.

The regression analyses indicate that the short term responses of CO<sub>2</sub> fluxes to environmental factors fitted well with these considerations. The high adjusted R<sup>2</sup> value gained from the step-wise multivariate regression analysis between CO<sub>2</sub> fluxes and environmental factors also gives an indication that the environmental variables in these empirical models have the potential to be used to predict CO<sub>2</sub> fluxes at an ecosystem scale for similar ecosystems in future modelling studies (Table 10). In this study, GPP was found to be highly correlated with PAR and  $T_{air}$  (Table 9 and Table 10), which can be ascribed to their effects on the energy provider and photosynthetic activities, respectively. PAR is the energy source of photosynthesis and thus drives the variation of GPP, which has been highly highlighted by previous studies (Montieth, 1972; Ruimy *et al.*, 1995). The effect of  $T_{air}$  on GPP could relate to the influence of  $T_{air}$  on the activities of photosynthesis enzymes (Prince & Goward, 1995), or on the leaf area index (LAI) (Turner *et al.*, 2003). The other factors such as VPD, RH, and WT were also found to closely correlate with GPP but did not appear in the stepwise multivariate regression equations (Table 10). This may be the result of coarse correlations between

those factors and  $T_{air}$  or PAR.  $R_{eco}$  was found to be highly correlated with  $T_{air}$ , which can be attributed to the effect of temperature on metabolic rate (Enquist *et al.*, 2003). The effect of WT on  $R_{eco}$  has also been observed in previous studies (Hurkuck *et al.*, 2016; Sonntag *et al.*, 2010; Table 10). However, the effects of VPD and RH on  $R_{eco}$  were not conclusive, which may be explained by the influences of VPD or RH on stomatal closure and water / organic matter transportation rates within plants (Fessenden & Ehleringer, 2003; Xu *et al.*, 2004). Given NEE is the difference between GPP and  $R_{eco}$ , factors affecting the variations in GPP and  $R_{eco}$  will indirectly influence that of NEE, which could be explained by PAR and WT.

The contrasting environmental conditions during the three study years had a strong influence on the ecosystem processes at BF. In 2013, the lower rates of photosynthesis in spring and early summer (between January and June) were strongly associated with the low temperatures (one of the coldest winter-spring periods in the last few decades) and relatively low water levels during the period. The low rainfall since April to September (receiving 35% less precipitation than the average during the same period) is another factor strongly influencing the photosynthesis rate at BF during the period in 2013. Monson *et al.* (2002) proposed that the availability of liquid soil water at the beginning of the growing season together with warmer temperatures constitute the set of environmental controls causing full recovery of CO<sub>2</sub> uptake during the growing season in an ecosystem. The photosynthesis rates increased dramatically in July and August 2013 till the end of year and were closely related to the abrupt increase in temperatures in July and August 2013 (the warmest summer since 2006), and the abrupt shift away from a prolonged drought period in place since the beginning of 2013 during the last few months of the year. However, the warmer temperatures and low water table (very close to the historical minimum water levels) since July 2013 resulted in markedly high rates of  $R_{eco}$ , and therefore large net CO<sub>2</sub> losses for the second half of the year, as the total GPP was outweighed by an even higher accumulated  $R_{eco}$  during this period. This is consistent with the results of the multivariate regression analysis indicating that  $R_{eco}$  is more sensitive to WT variation than GPP (Table 10). This result also gives an indication of the importance of the timing of water availability and temperature increase to the full recovery of C uptake during the growing season (Monson *et al.*, 2005). Xu & Baldocchi (2004) suggested that the timing of rain events

had more impact than the total amount of precipitation on ecosystem processes (i.e. GPP and  $R_{eco}$ ). The prolonged drought period during the summer of 2013 had a strong influence on the ecosystem processes at the site; while the larger amount of rainfall in October came too late after the end of the growing season. As a result, the BF ecosystem in 2013 acted as a large source of CO<sub>2</sub> with an annual sum of  $161.03 \pm 12.51$  g CO<sub>2</sub>-C m<sup>-2</sup>yr<sup>-1</sup>, which is about twice the amounts for the other two study years. Surprisingly, the annual total GPP in 2013 (at  $1819.79$  g CO<sub>2</sub>-C m<sup>-2</sup>yr<sup>-1</sup>) was still higher than most of the values reported in the literature (Hendriks *et al.*, 2007; Jacobs *et al.*, 2007; Veenendaal *et al.*, 2007), which may be explained by the increase in  $R_{eco}$  which outweighed the GPP due to enhanced  $R_{eco}$  during the dry conditions over the growing season ( $R_{eco}$  is more significantly correlated with WT than GPP; Table 9).

In 2014, the study site experienced a quite unusual warm (one of the warmest years comparing to the long-term average) and wet year (the fourth wettest year in the UK records from 1910). The water levels at BF over the whole year of 2014 were close to or even above the historical maximum water level on the site, and were close to the peat surface for almost half of the year and never below 60 cm from the surface. As a result, the ecosystem had higher rates of photosynthesis in spring and early summer (January to July), and a relatively earlier start to the growing season (in March). However, the water levels declined to around 50 cm below the peat surface during the growing season, and this, combined with the warmer temperatures during this period, caused a higher  $R_{eco}$  during the growing season. From a C balance perspective, the increase in  $R_{eco}$  during the growing season offset the increase in GPP during the period to some extent. The marked decline in temperature in August 2014 caused an abrupt end to the increasing photosynthesis rates at BF during the 2014 growing season. But the larger amount of precipitation in August 2014 leads to an increasing water level and therefore lower rates of respiration in this month too. This is consistent with both  $R_{eco}$  and GPP showing a positive response to  $T_{air}$ ; however,  $R_{eco}$  shows a significantly negative response to WT (Table 9 & 10). During 2014, the BF ecosystem acted as a net source of CO<sub>2</sub> with annual gap-filled totals of  $83.61 \pm 11.53$  g CO<sub>2</sub>-C m<sup>-2</sup>yr<sup>-1</sup>.

2015 was quite a normal year in climatic aspects, with monthly mean temperatures quite close to the historical averages from January to October, but with a relatively

warm November and December. The cumulative precipitation in 2015 is similar to the historical records averages and the water levels at BF in 2015 were always in the range of historical records. Therefore, the year 2015 can be considered as a “control year” to reflect how the ecosystem processes behave in normal years at the study site. Surprisingly, BF acted as a relatively large net sink of CO<sub>2</sub> in July in 2015 (a net source in the other two years) due to the low total  $R_{eco}$  in this month. This could be explained by the larger amount of rainfall in July 2015 (receiving 87.7 mm in the month, 174% of the 1981 - 2010 average), which caused a low respiration rate and larger CO<sub>2</sub> uptake at the site. The site acted as a relatively larger net source of CO<sub>2</sub> at the end of year (November and December) compared to the other two years, at 85.66 g CO<sub>2</sub>-C m<sup>-2</sup> month<sup>-1</sup> in November (similar to November 2014 which was a quite warm year), and 87.94 g CO<sub>2</sub>-C m<sup>-2</sup> month<sup>-1</sup> in December. These values were strongly associated with the warmer condition in these two months which caused higher respiration rates at the site (Table 9). This larger CO<sub>2</sub> loss at the end of the year somehow offset the large CO<sub>2</sub> uptake in July. In summary, the BF site had an annual sum of 98.39±13.31 g CO<sub>2</sub>-C m<sup>-2</sup>yr<sup>-1</sup> for 2015, which is similar to the amount of CO<sub>2</sub> lost at the site in 2014. These results again prove the importance of timing of water availability and warm temperatures to ecosystem processes (Monson *et al.*, 2005). The right timing of the rain events during the growing season can increase the photosynthesis rates and therefore the CO<sub>2</sub> uptake rate (e.g. in July 2015). However, the unusual increase of temperature during the non-growing season might cause a larger  $R_{eco}$  and therefore a larger CO<sub>2</sub> loss from the ecosystem (e.g. during December 2015).

The ecosystem apparent quantum yield ( $\alpha$ ) calculated based on the rectangular hyperbolic light response function (Equation 14) during the growing season (May to October) at BF during the study period indicated that the ecosystem was able to utilize available light more effectively compared to treed peatlands (Flanagan *et al.*, 2002; Wohlfahrt *et al.*, 2008). Jacobs *et al.* (2007) proposed that the lower levels of self-shading under the open vegetation structure might be a good explanation for this.

### 5.4.3. Methane Fluxes

The annual mean CH<sub>4</sub> flux from the gap filled EC data at BF was 16 nmol CH<sub>4</sub> m<sup>-2</sup>s<sup>-1</sup> in 2013, 9.4 nmol CH<sub>4</sub> m<sup>-2</sup>s<sup>-1</sup> in 2014 (over the period between April and December), and 5.6 nmol CH<sub>4</sub> m<sup>-2</sup>s<sup>-1</sup> in 2015. All these values are towards the lower end of the wetland category as reported by Nicolini *et al.* (2013). The study site acted as a net source of CH<sub>4</sub> over all study years with annual cumulative CH<sub>4</sub> estimated at 6.067 ± 0.096 g CH<sub>4</sub>-C m<sup>-2</sup>yr<sup>-1</sup> in 2013 and 2.009 ± 0.087 g CH<sub>4</sub>-C m<sup>-2</sup>yr<sup>-1</sup> in 2015. The total cumulative CH<sub>4</sub> was estimated at 2.845 ± 0.103 during the period between April and December in 2014.

There are still only a few published longer-term CH<sub>4</sub> measurements using the EC technique from temperate fenlands. The annual sums of CH<sub>4</sub> flux reported in this study are towards the lower end of a reported range of CH<sub>4</sub> fluxes from global wetlands by Turetsky *et al.* (2014). The annual CH<sub>4</sub> budget at BF is lower than most of values reported from the other studies on temperate and boreal peatlands, however, surprisingly, it still acted as a net source of CH<sub>4</sub> under relatively dry conditions with low water levels. Shurpali & Verma (1998) observed an annual CH<sub>4</sub> emission of 13.9 to 15.3 g CH<sub>4</sub>-C m<sup>-2</sup>yr<sup>-1</sup> in a poor minerotrophic to oligotrophic peatland dominated by *Sphagnum papillosum* in Minnesota. In more northern locations, Rinne *et al.* (2007) reported an annual emission of 12.6 g CH<sub>4</sub>-C m<sup>-2</sup>yr<sup>-1</sup> in a boreal minerotrophic fen. Jackowicz-Korczynski *et al.* (2010) observed annual releases of between 19.54 and 22.7 g CH<sub>4</sub>-C m<sup>-2</sup>yr<sup>-1</sup> in a subarctic tall graminoid community, while Hargreaves *et al.* (2001) provided an estimate of annual CH<sub>4</sub> flux of 5.5 ± 0.4 g CH<sub>4</sub>-C m<sup>-2</sup>yr<sup>-1</sup> for Finnish mires which is similar to the observation in 2013 at BF.

The CH<sub>4</sub> flux with all measured environmental variables (i.e.  $T_{air}$ , WT, VPD, RH, and PAR) demonstrated very weak relationships in this study and this result is in common with some other EC studies on CH<sub>4</sub> fluxes (Table 9 & 10; e.g. Hargreaves *et al.*, 2001; Rinne *et al.*, 2007). The impacts of environmental changes on CH<sub>4</sub> flux are generally much more difficult to interpret due to the large number of controlling factors and potential for large spatial variability (Baldocchi *et al.*, 2012). It should be noted that, among all measured environmental variables, WT accounted for the greatest proportion of the variance of CH<sub>4</sub> flux in the multiple regression model (but only explained 3.5%;

Table 10). This gives an indication that WT may be one of the most important environmental drivers that is closely correlated to CH<sub>4</sub> flux; again, this conclusion is consistent with many other studies on peatland ecosystems (Cooper *et al.*, 2014; Lai *et al.*, 2014; Minke *et al.*, 2016; Juutinen *et al.*, 2016; Strack & Waddington, 2007). It is, however, hard to find a good explanation for the relatively higher CH<sub>4</sub> emissions during the first half year of 2013 compared to the other two years. This difficulty in identifying a strong functional relationship between CH<sub>4</sub> emission and environmental variables may be due to micro-topographical differences at the study site (Olson *et al.*, 2013), whilst the presence of drainage ditches and grazing animals could be another explanation since both can be additional sources of CH<sub>4</sub> to the atmosphere.

There are many studies suggesting that ruminating animals can contribute considerably to atmospheric CH<sub>4</sub> emissions at an ecosystem scale (Baldocchi *et al.*, 2012; Dengel *et al.*, 2011; Herbst *et al.*, 2011). However, the CH<sub>4</sub> emissions of ruminating animals have large spatial variability and are difficult to quantify only by EC measurements since the movements of the animals and the source area are not necessarily random and independent (Baldocchi *et al.*, 2012). A rough estimation made by Herbst *et al.* (2011) suggested that the CH<sub>4</sub> emitted through rumination amounted to about 11% of the total annual flux on their study site.

Grazing also has indirect effects on CH<sub>4</sub> fluxes in an ecosystem. Trampling by the animals may compact the soil and reduce its aeration, creating small hummocks and hollows within the study area (Herbst *et al.*, 2013). At BF, it became clear that there was an increase in perennially wet hollows over the study period. Bubier *et al.* (1993) proposed that there are large differences in CH<sub>4</sub> fluxes between hummocks and hollows, which are associated with vegetation, soil temperature and soil water content differences due to such changes in micro-topography. The changes in micro-topography also can cause changes in vegetation type. There were increasing amounts of common rush (*Juncus inflexus*) communities occurring in the perennially wet hollows at BF during the study period. Stands of *J. inflexus* are avoided by the cattle and this can be another reason for the increase in these communities over time (Herbst *et al.*, 2013). *Juncus* species can transport CH<sub>4</sub> through its aerenchymous tissues which let CH<sub>4</sub> by-pass the aerated zone in the soil without being oxidized (Ström *et al.*, 2005).

Schäfer *et al.* (2012) reported a chamber measurement study of CH<sub>4</sub> emissions from a *J. inflexus* covered meadow with a mean emission rate at 0.8 g m<sup>-2</sup>d<sup>-1</sup> which is much larger than the daily mean CH<sub>4</sub> flux at BF with 0.18 g m<sup>-2</sup>d<sup>-1</sup>. Brix *et al.* (2001) and Levy *et al.* (2012) also proposed that the presence of aerenchymous plants plays an important role in influencing the CH<sub>4</sub> fluxes in the ecosystem. However, the presence of aerenchymous plants is another indication of the restoration status on a rewetting site such as BF i.e. the appearance of typical wetland species such as *Juncus* species could be taken as an indication that restoration is moving in a desirable ecological direction. The gradual colonisation of the soil by methanogens due to the rewetting and vegetation changes can also increase the CH<sub>4</sub> emissions on the site (Liikanen *et al.*, 2006; Tuittila *et al.*, 2000; Waddington & Day, 2007).

Schrier-Uijl *et al.* (2011) proposed that ditches can contribute considerably to atmospheric CH<sub>4</sub> emissions at an ecosystem scale. The study also demonstrated that the ditch CH<sub>4</sub> emissions are extremely variable both spatially and temporally in a temperate lowland peatland (Schrier-Uijl *et al.*, 2011). Minkkinen & Laine (2006) also reported large CH<sub>4</sub> fluxes from ditches in a minerotrophic fen in Finland. This is consistent with the larger fluxes captured at the BF EC station which were mostly from a westerly direction where the ditch was located (Peacock *et al.*, 2016).

It seems plausible that the animals and ditches at BF may act as CH<sub>4</sub> hotspots, making the site act as a net source of CH<sub>4</sub> during the measurement period. Aerenchymous vegetation may also contribute to CH<sub>4</sub> flux.

## **Chapter 6**

# **Short-term Climate Response of Carbon Dioxide Fluxes in a Semi- natural Fen (Sedge Fen)**

## 6.1. Environmental Conditions

Study site two - SF is located within a short distance of study site one (BF). The meteorology i.e. air temperature, rainfall, humidity as well as the global radiation are therefore the same or very similar and were described in Chapter 5. However, the hydrology of the two sites is different and needs to be described separately.

### 6.1.1. Ground Water Levels at Sedge Fen

The monthly ground water levels at SF during the measurement period are presented and compared to the maxima and minima for the period 1994 - 2008 in Figure 41. The monthly mean water levels in almost all months during both 2014 and 2015 were higher than the historical maximum during 1994 - 2008, with the exception of July 2015 that had a slightly lower water level than the historical maximum July water level (Figure 41). The water levels in 2014 and 2015 were close to the fen surface (above 10 cm compared to the historical maximum in average) most of time during the year, and only 2015 experienced a dry June and July (Figure 41). In the year 2013, there was an extended period of surface inundation at the site from the start of the year until June. However, 2013 experienced a large and sustained period of water table drawdown during the summer, ultimately reaching approximately 80 cm below the fen surface as the lowest water level in the year, although this value still lies within the range of historical observations. From October 2013, the water level rapidly recharged to near the historical maximum level, but was still lower than the water levels in the other two years, ending the year at about 20 cm below the ground surface (Figure 41).

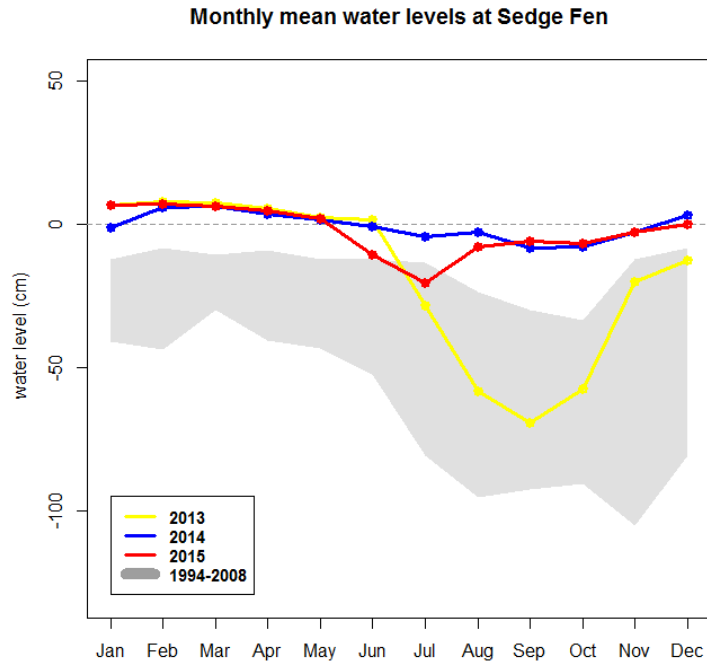


**Figure 41:** Monthly water level range 1994 - 2008 (grey) and 2013 (yellow), 2014 (blue), 2015 (red) monthly mean water levels relative to the fen surface measured at SF dipwell NW07. 2013 - 2015 data supplied by John Bragg @ the NT, historical data from Kelvin (2011).

The daily mean water levels at SF during the measurement period are presented in Figure 42. The water levels were close to the ground surface at the start of the year (January to May) in all years during the measurement period. In the year 2013, the water levels rapidly declined from mid-June to August before fluctuating around approximately 70 cm below ground level until October. This degree of drawdown was extreme and far greater than any observations at other intact fen sites recorded in the country (Evans *et al.*, 2015). The water level then increased steadily till the end of the year to about 10 cm below the fen surface, and continued to rise at the beginning of 2014 to above the ground (Figure 42).

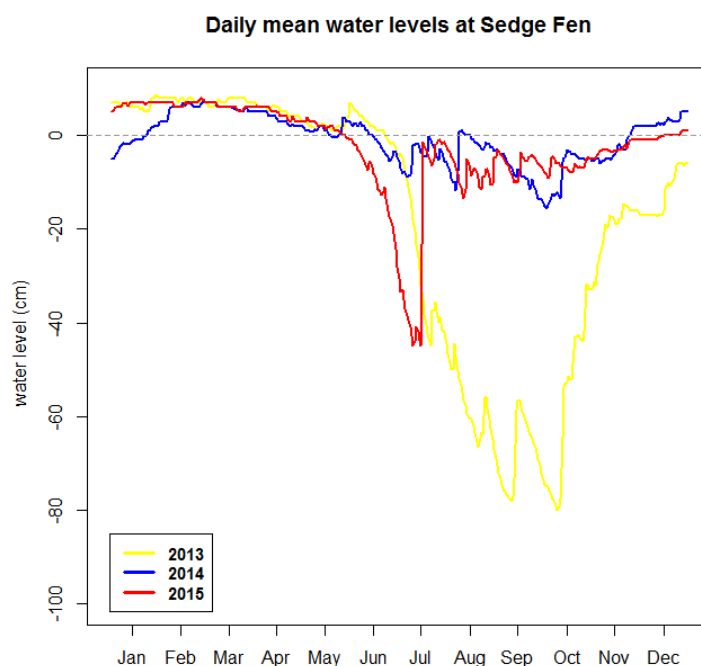


**Figure 42:** Mean daily position of water levels relative to the fen surface measured at SF dipwell NW07. Data supplied by John Bragg @ the NT.

During most of 2014 and 2015, the water levels remained significantly high, fluctuating around the ground surface (Figure 42). The only rapid drop occurred from May 2015 until the end of June, reaching the lowest water level in the year at -43 cm. However, the water level recovered dramatically in July and rapidly rose to near-surface levels in a week (Figure 42). In 2014, the hydrological variations were far less dramatic compared to the other two years, with far smaller water table drawdown through the growing season corresponding to higher precipitation during the summer (Figure 42).

## 6.2. Temporal Dynamics of Carbon Fluxes

### 6.2.1. Wind Rose Plots

In Figure 43, the distribution of direction and source strength of NEE at SF in separate years during the measurement period (2013 to 2015) is presented. The figure illustrates

the frequency of counts by wind direction, as well as the magnitudes of CO<sub>2</sub> flux (with non-gap-filled data) in separate years during the study period. The positive (toward red) values represent periods when the site was a source of CO<sub>2</sub>; negative (toward blue) values denote periods when the site was a sink.

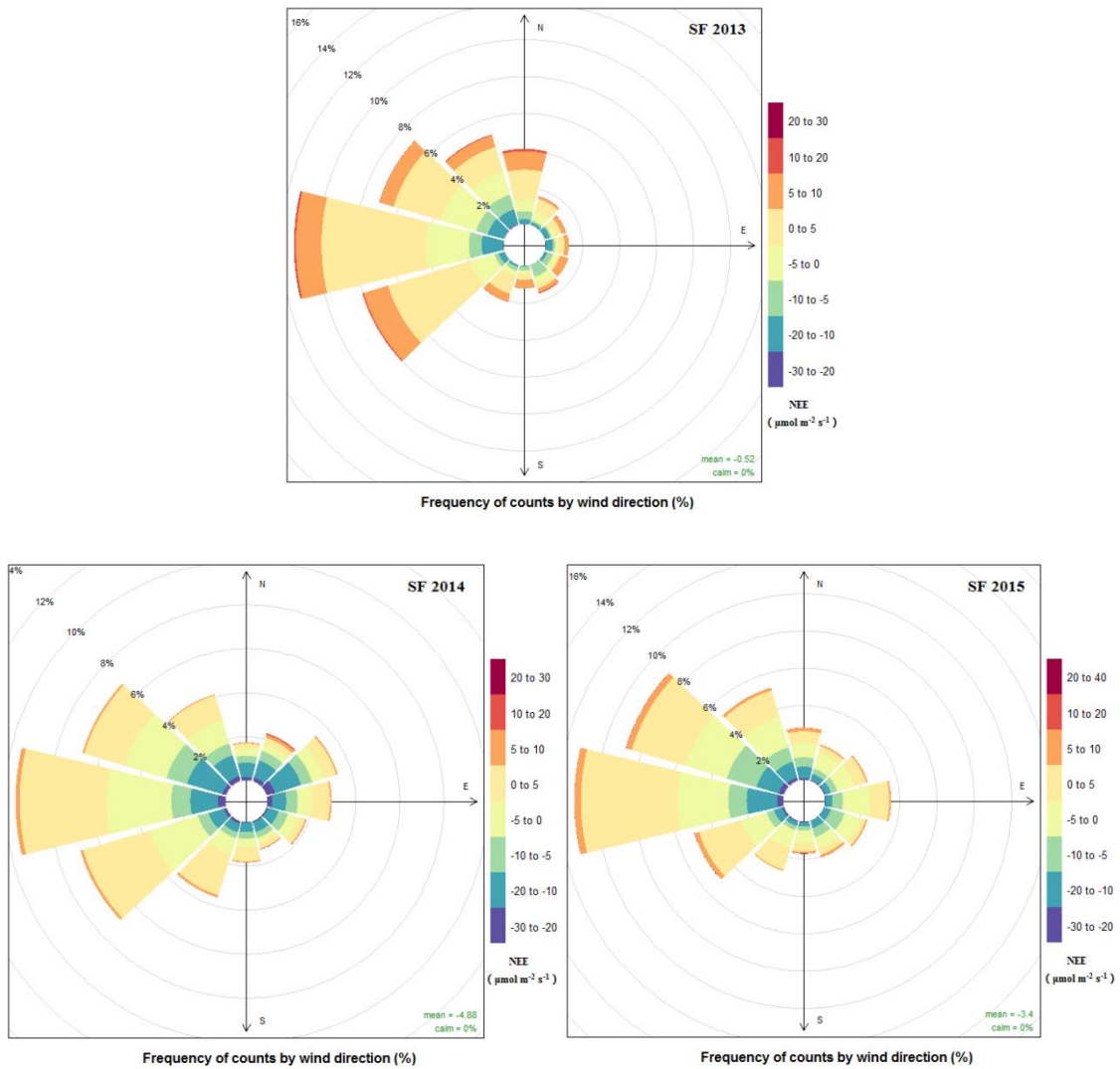


**Figure 43:** Distribution of direction and source strength of the measured (non-gap-filled) net ecosystem CO<sub>2</sub> exchange (NEE) in separate years during the measurement period (2013 to 2015) at Sedge Fen. Values are in the measured units of  $\mu\text{mol CO}_2 \text{m}^{-2} \text{s}^{-1}$ . Positive values represent a source and negative a sink.

The prevailing wind direction at SF is from the west in all three years (Figure 43). This figure also indicates that largest number of measured fluxes of CO<sub>2</sub> originated from the prevailing wind sectors between north-west and south-west (Figure 43). In 2013, a

larger percentage of wind from the north is comparable to a similar situation illustrated for the BF site. There was larger percentage of wind coming from the north-east and east in 2014 and 2015 compared to 2013. The year 2013 had higher magnitudes of CO<sub>2</sub> fluxes with positive values from all wind directions compared to the other two years; whereas 2014 had higher magnitudes of CO<sub>2</sub> fluxes with negative values from all wind directions (Figure 43).

### 6.2.2. Fingerprint Plots

The “fingerprint” plots of NEE at SF are presented in Figure 44 for the whole study period covering two and half years from August 2013 to December 2015. Gap-filled (upper left plot) and measured (non-gap-filled; upper right plot) NEE data, as well as global radiation ( $R_g$ ; lower right plot) and  $T_{air}$  (lower left plot) as the key meteorology variables are presented. The fingerprint plots show diurnal and seasonal changes in half-hourly CO<sub>2</sub> flux densities, as well as the temporal distribution of the data-gaps (upper right plot) and the performance of the method used to fill missing values (upper left plot) (Figure 44). The NEE data in the figures are presented in units of  $\mu\text{mol CO}_2 \text{ m}^{-2}\text{s}^{-1}$ ;  $R_g$  and  $T_{air}$  are shown in  $\text{Wm}^{-2}$  and  $^{\circ}\text{C}$ , respectively. The fingerprint plots of NEE illustrate the “breathing” of the ecosystem over the measurement period. In the figure, colours toward the red end of the NEE scale denote periods when the site was losing CO<sub>2</sub> to the atmosphere (e.g. at night); whereas the colours toward the blue end indicate the periods when the site was removing CO<sub>2</sub> from the atmosphere (i.e. during summer daytime; Figure 44).

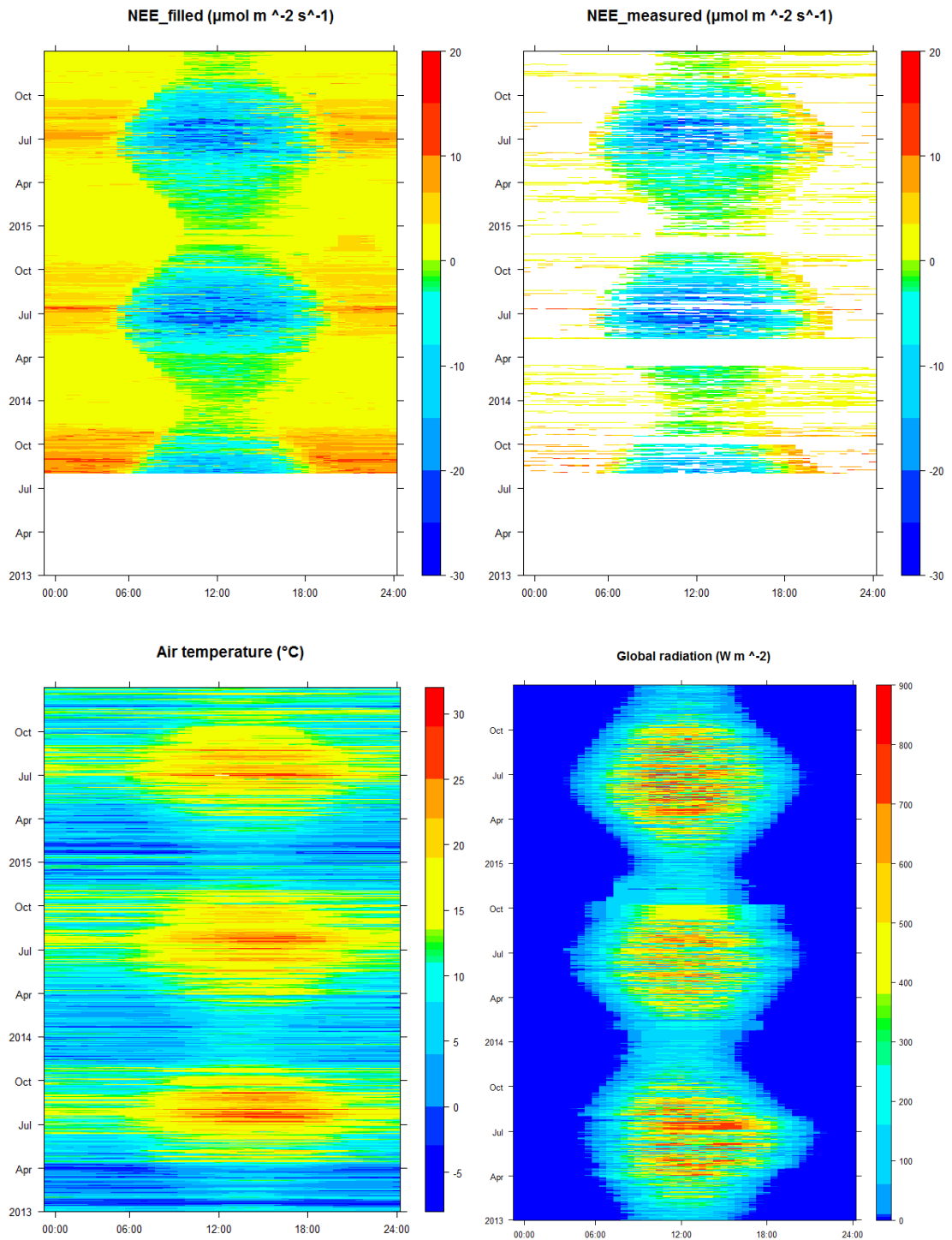


**Figure 44:** Fingerprint plots of net ecosystem  $\text{CO}_2$  exchange (top panels), air temperature (lower left), and global radiation ( $R_g$ , lower right) at Sedge Fen during the measurement period (August 2013 to 2015). Top left is gap-filled NEE data, top right is measured NEE data after quality control. NEE units are  $\mu\text{mol CO}_2 \text{ m}^{-2} \text{ s}^{-1}$ ; global radiation ( $R_g$ ) and air temperature ( $T_{\text{air}}$ ) are shown in  $\text{W m}^{-2}$  and  $^{\circ}\text{C}$ , respectively. Months are represented by increases along the ordinate; time of day is indicated along the abscissa. White space represents periods when no data were available.

Generally speaking, the data capture (after QC) was good during the whole measured period at SF (upper right plot Figure 44). Most of the data gaps occurred during the winter or at night-time due to insufficient power supply by the solar panels under winter / night-time conditions (longer periods of missing data) or the application of data QC procedures (short periods of data loss) (Figure 44). There are two significant NEE data gaps during the measurement period, one happened between 15<sup>th</sup> March and 8<sup>th</sup> May in 2014 due to data logging issues with a broken USB stick; another one happened during November and December 2014 caused by station power system upgrading. These two data gaps cover relatively short periods and occurred during the period when CO<sub>2</sub> fluxes were at a seasonal low. The filling of these two data gaps is, therefore, less likely to introduce a large uncertainty in terms of the annual CO<sub>2</sub>-C budget compared with data losses during the main growing season. For the most part, the measured data (quality controlled) covered most of the growing season and daytime periods, again verifying the high quality of the measured data and improving the reliability of the gap-filling data (Figure 44).

The seasonal pattern of NEE shows similar correspondence to the temperature and radiation as at BF (Figure 44).

In Figure 44, 2014 showed a similar ecosystem “breathing” pattern as in 2015, but had relatively smaller CO<sub>2</sub> night-time efflux (smaller area / lighter colour with orange-red colour) during the growing season compared to 2013 and 2015. During 2015 there was an earlier increase in daytime net CO<sub>2</sub> uptake after spring and relatively higher magnitude of daytime CO<sub>2</sub> uptake (with more areas of dark orange-red and blue) during the growing season compared to 2014 (Figure 44). However, 2013 had a longer period and higher magnitude of CO<sub>2</sub> efflux during night-time periods during August to November compared to the other two years (Figure 44).

### 6.2.3. Mean Diurnal Patterns

Monthly MDC plots are presented in Figure 45 to enable comparison of seasonal and between-year differences in CO<sub>2</sub> fluxes on a side-by-side basis at SF including two complete annual cycles and a half-year of data from August to December in 2013. In the MDC figure, each data point represents the mean of 30 minute values measured at the same time of the day over the course of each month (e.g. for the 48 thirty minute intervals in each day). The MDC of NEE, GPP (with negative values) and  $R_{eco}$ , as well as selected environmental variables PPFD,  $T_{air}$ , VPD are represented in the figure. There is no quantum sensor at SF station, therefore the PPFD data from BF have been used for SF since the two sites are sufficiently close (within 1 km of each other) therefore there is no difference in the incoming radiation between two stations. The water levels relative to the ground surface during the measurement period have been shown as monthly means in the lowest panel (Figure 45). The NEE, GPP,  $R_{eco}$  and PPFD data in the figures are presented in units of  $\mu\text{mol m}^{-2}\text{s}^{-1}$ ;  $T_{air}$ , VPD and water levels are shown in °C, hPa and cm, respectively. The figure shows the changes in the amplitude of the monthly diurnal cycles of NEE, assimilatory (GPP) and respiratory ( $R_{eco}$ ) activity in response to phenological changes and illustrates seasonal and between-year differences during the measurement periods.

During the whole measurement period, the daily average NEE, GPP and  $R_{eco}$ , as well as the  $T_{air}$ , PPFD and VPD showed a clear diurnal pattern in all months (Figure 45). The diurnal cycle was characterised by NEE becoming progressively more negative (positive) in response to increases (decreases) in irradiance and temperature. In contrast, the GPP and  $R_{eco}$  showed similar increasing / decreasing diurnal patterns as PPFD,  $T_{air}$  and VPD. The maximum rates of GPP and  $R_{eco}$  (and therefore the NEE) occurred as the irradiance peaked around solar noon (Figure 45).

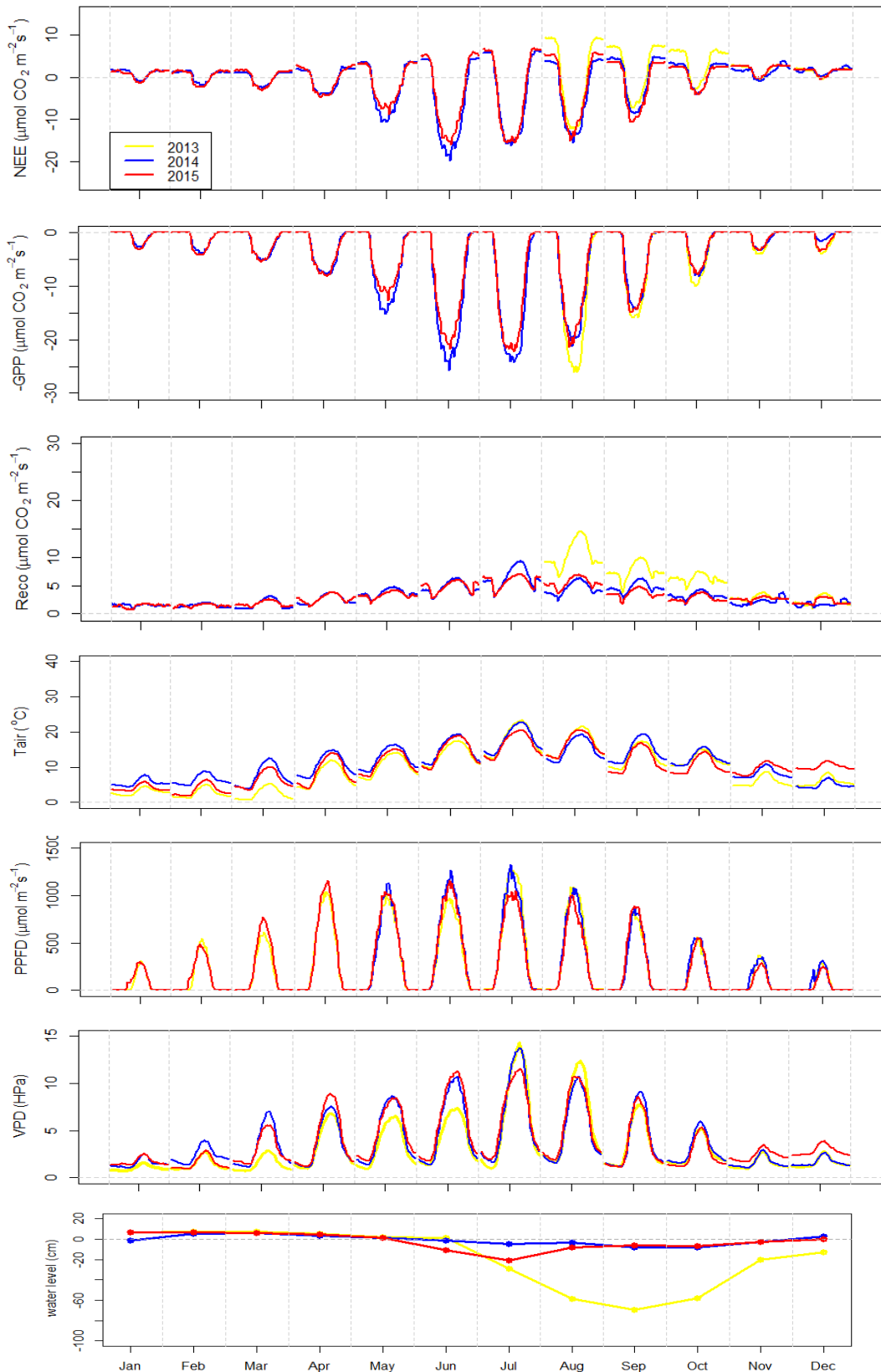


**Figure 45:** Comparison of monthly mean diurnal cycles of net ecosystem  $\text{CO}_2$  exchange at Sedge Fen during measurement period (August 2013 to 2015). Average diurnal cycles of key meteorological variables are also provided. Estimates of daily GPP are shown in negative values to facilitate graphical reading. The lowest panel shows monthly mean water levels relative to the ground surface. Standard errors have been omitted to improve readability.

The seasonal pattern of NEE at SF is characteristic of sites with a permanent vegetation cover, with the lowest fluxes in winter (typically positive) and largest (positive and negative) values in the summer months in response to the environment variables and ecosystem phenology. The daytime net CO<sub>2</sub> uptake (daytime GPP) during all months in all three years indicates that photosynthesis was active at SF throughout the whole year during the measurement periods even during the non-growing seasons (Figure 45). The seasonal changes in the magnitude of the key meteorological variables (PPFD,  $T_{air}$  and VPD) which showed more suitable conditions from May to September for vegetation during the growing season co-determined the amplitude of the monthly diurnal patterns of GPP and  $R_{eco}$  and therefore the NEE. As a result, the net CO<sub>2</sub> uptake rates were higher (more negative) between May and September than in the other months of year in 2014 and 2015. The months of August and September in 2013 had higher (more negative) NEE than the rest of year, and the NEE was the highest in August (Figure 45). The lowest net uptake rates of CO<sub>2</sub> occurred in December (positive mostly) in all years (Figure 45).

The MDC patterns during the study period reveal large between-year differences in the CO<sub>2</sub> fluxes at SF (Figure 45). In general, the amplitude of CO<sub>2</sub> fluxes increases rapidly from spring through the growing season then declines more steadily through late summer and autumn in all study years. The largest average net CO<sub>2</sub> uptake was observed in June for 2014, in July for 2015 and August for 2013 (no data before August 2013; Figure 45). The warmer conditions in 2014 (compared to the other two years) were associated with larger nocturnal losses (night  $R_{eco}$ ) of CO<sub>2</sub> and more negative daytime NEE (also see daytime GPP and  $R_{eco}$ ) in most of months, as well as the earlier start of the growing season in the year. The largest net difference in average NEE was observed in May over both years 2014 and 2015, i.e. at the beginning of the growing season (Figure 45).

The maximum daily net CO<sub>2</sub> uptake ( $\pm 95\%$  confidence interval) ranges from  $0.46 \pm 0.17 \mu\text{mol m}^{-2}\text{s}^{-1}$  to  $-12.3 \pm 4.47 \mu\text{mol m}^{-2}\text{s}^{-1}$ ,  $1.32 \pm 0.3$  to  $-20.7 \pm 4.73 \mu\text{mol m}^{-2}\text{s}^{-1}$ ,  $0.7 \pm 0.32 \mu\text{mol m}^{-2}\text{s}^{-1}$  to  $-14.7 \pm 3.68 \mu\text{mol m}^{-2}\text{s}^{-1}$  in 2013 (only between August to December), 2014 and 2015 (all months in the year), respectively. The maximum monthly average daily net CO<sub>2</sub> uptake rates at SF in 2013 and 2015 were similar to the observations

from studies of boreal peatlands (ranging from -4 to -11.5  $\mu\text{ mol m}^{-2}\text{s}^{-1}$ ; Adkinson *et al.*, 2011; Humphreys *et al.*, 2006; Sagerfors *et al.*, 2009), and lower than the observation from a study at a Finnish grassland with maximum average of -18  $\mu\text{ mol m}^{-2}\text{s}^{-1}$  (Shurpali *et al.*, 2009). Whereas the 2014 average daily NEE at SF was even higher than the observation at the Finnish grassland. However, the positive average daily NEE in December in all three study years were observed at SF.

The largest amplitude of the MDC pattern of GPP and  $R_{eco}$  (therefore the NEE) occurred during June to August in all three years when the average PPFD,  $T_{air}$  and VPD all reached their peaks in the year (Figure 45). In 2014, the amplitude of both GPP and NEE were larger between May and July (the main growing season) than in 2015 during the same period (no data for 2013). But the amplitude of  $R_{eco}$  in 2014 was similar as it in 2015 during the most of year, only with July and September being higher. However, the amplitude of the MDC pattern of GPP and  $R_{eco}$  was larger between August and October 2013 (no data earlier than August 2013) than in the same months in 2014 and 2015. This was associated with the rapid change to warmer and wetter conditions (higher average PPFD,  $T_{air}$  and VPD; Figure 25) in July 2013 (Figure 45). As a result, the nocturnal losses of  $\text{CO}_2$  were much higher in 2013 during the period than the other two years. The largest difference in both average GPP and  $R_{eco}$  was observed in August between 2013 and the other two years (Figure 45).

#### 6.2.4. Seasonal Trends in Daily Carbon Budgets

In Figure 46, time-courses of daily NEE (gap-filled) as well as the derived  $\text{CO}_2$  flux components GPP and  $R_{eco}$  during the measurement period (from August 2013 to 2015) are presented. Estimates of daily GPP are shown using negative values to more effectively illustrate the opposing influences of the assimilatory (GPP) and respiratory ( $R_{eco}$ ) fluxes on the net  $\text{CO}_2$  exchanges. Daily values of important environmental variables (i.e. PPFD,  $T_{air}$  and water levels) are also provided (Figure 46). The PPFD data from BF have been used for SF too (see Section 6.2.4). The growing seasons were clearly characterised by strong magnitude of the daily  $\text{CO}_2$  exchange components

(Figure 46). The non-growing seasons were characterised by low and constant assimilatory and respiratory fluxes (Figure 46). However, significant differences in the magnitude of the flux components were observed between year to year during the measurement period.

The estimates of daily GPP and  $R_{eco}$  (green and violet lines) showed similar seasonal trends, started from low daily values at the beginning of the year (non-growing season), increasing steadily throughout spring and summer, and reaching the peak in the middle of the growing season before declining as the vegetation senesced with decreasing autumn day length (Figure 46). The estimates of daily NEE (black bar) also show similar seasonal trends, with the ecosystem starting to be a source of CO<sub>2</sub> at the beginning of the year (positive NEE), and turning to a sink when the vegetation starts to grow, and the ultimately turning to a source again (Figure 46). However, significant differences in this general course occurred over the measurement period.

The estimates of daily GPP and  $R_{eco}$  reached their peaks between June and July in 2014 and 2015, indicating the intense assimilatory and respiratory activities by plants that occurred in the middle of the growing season. The second half year of 2013 had relatively larger daily CO<sub>2</sub> emissions from the ecosystem to atmosphere (with larger positive NEE) from August till December compared to the same period in the other two years (Figure 46). The warmer and wetter conditions in 2014 (compared to the other two years) resulted in the early start of the growing season in 2014, with SF acting as a relatively larger sink of CO<sub>2</sub> from April until mid-September, and then gradually turning to a small source until the end of the year (Figure 46). Whereas, in 2015, the ecosystem acted as a relatively smaller sink of CO<sub>2</sub> during a relatively shorter period in the growing season between May and mid-August compared to 2014 (Figure 46).

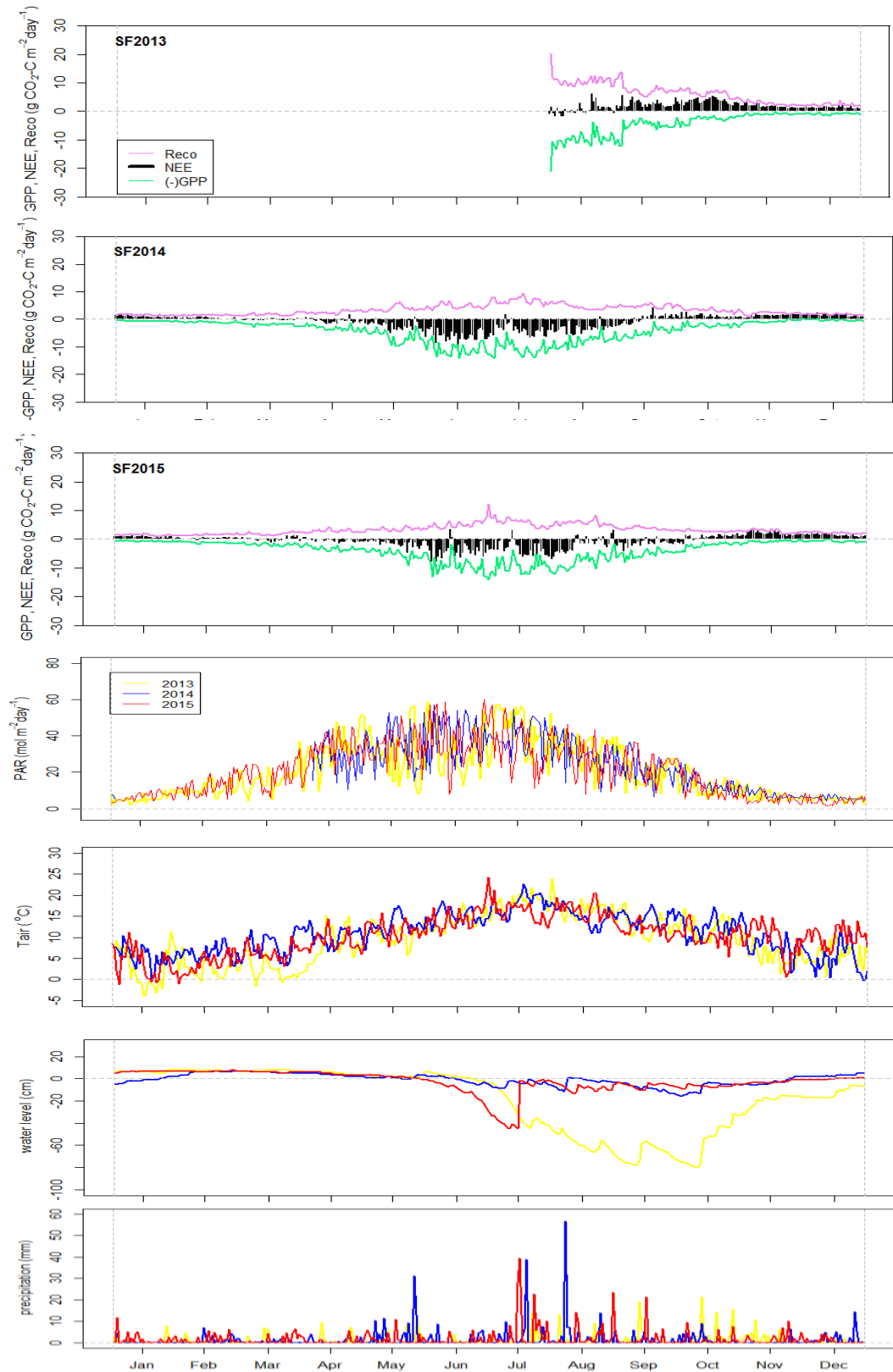


**Figure 46:** Seasonal change in daily CO<sub>2</sub> budget and environmental variables at Sedge Fen during the measurement period (August 2013 to 2015). Violet and Green bars show daily sums of ecosystem respiration ( $R_{eco}$ ) and gross primary production (GPP), respectively; black bars are total daily net ecosystem CO<sub>2</sub> exchange (NEE). PAR is total daily photosynthetically active radiation;  $T_{air}$  is daily average air temperature; and water level is the mean daily position of water levels relative to the ground surface.

The between-year differences in CO<sub>2</sub> fluxes can be more easily detected in the seasonal cumulative values of NEE, GPP and  $R_{eco}$ . Cumulative values computed on a monthly aggregation basis during the measurement period are presented in Table 12.

**Table 12:** Monthly total gross primary production, ecosystem respiration and net ecosystem CO<sub>2</sub> exchange estimated for Sedge Fen during measurement period (August 2013 to 2015)

	GPP (g CO <sub>2</sub> -C m <sup>-2</sup> )			NEE (g CO <sub>2</sub> -C m <sup>-2</sup> )			$R_{eco}$ (g CO <sub>2</sub> -C m <sup>-2</sup> )		
	2013	2014	2015	2013	2014	2015	2013	2014	2015
Jan.	--	18.52	20.89	--	28.94	23.18	--	47.46	44.07
Feb.	--	33.43	37.25	--	11.58	8.76	--	45.01	46.02
Mar.	--	57.71	55.81	--	-3.58	0.78	--	54.13	56.60
Apr.	--	97.96	99.59	--	-18.83	-15.85	--	79.14	83.74
May	--	195.41	153.22	--	-78.31	-46.88	--	117.10	106.34
Jun.	--	333.95	286.60	--	-187.75	-124.56	--	146.20	162.04
Jul.	--	327.07	288.46	--	-122.62	-113.39	--	204.46	175.07
Aug.	296.34	240.96	227.70	22.30	-102.90	-54.43	318.64	138.06	173.26
Sep.	170.65	150.05	157.49	66.73	-3.03	-44.87	237.38	147.02	112.62
Oct.	84.08	69.18	63.42	111.05	33.65	21.51	195.13	102.84	84.94
Nov.	30.34	25.25	23.97	56.86	41.27	59.38	87.20	66.52	83.36
Dec.	27.43	9.89	22.74	42.37	44.70	42.57	69.80	54.60	65.32

The maximum monthly total GPP values were observed in June and July (no significant difference between these two months) in 2014 and 2015, while 2014 had the largest monthly total GPP with 333.95 g CO<sub>2</sub>-C m<sup>-2</sup> month<sup>-1</sup> in June (Table 12). The largest monthly total GPP in 2013 occurred in August at 296.34 g CO<sub>2</sub>-C m<sup>-2</sup> month<sup>-1</sup> (Table 12). The monthly total GPP values were quite similar in 2014 and 2015 during most of the months in the year, with the exception of December 2014 which had a significantly lower monthly GPP at 9.89 g CO<sub>2</sub>-C m<sup>-2</sup> month<sup>-1</sup> (the lowest monthly GPP of all months during the study period). The monthly total GPP values were higher during the second half-year in 2013 than in 2014 and 2015, which was associated with the warmer conditions in July and August 2013 (Table 12). The largest monthly total

$R_{eco}$  occurred in July in 2014 and 2015, but August in 2013 (no data available before August 2013), while the 2013 August had the largest monthly  $R_{eco}$  (at 318.64 g CO<sub>2</sub>-C m<sup>-2</sup> month<sup>-1</sup>) compared to all the months in the other two years (Table 12). Similar to the GPP values, the monthly total  $R_{eco}$  values were larger in all months during the second half-year in 2013 than in the same periods of 2014 and 2015 (Table 12). The monthly total  $R_{eco}$  were quite similar in the years 2014 and 2015.

The largest net CO<sub>2</sub> uptake was observed in June in 2014 and 2015, while June 2014 acted as the largest sink month at -187.75 g CO<sub>2</sub>-C m<sup>-2</sup> month<sup>-1</sup> (Table 12). The ecosystem acted as a sink of CO<sub>2</sub> between March and September (more than half of the year) in 2014 and 2015, while 2014 acted as a larger sink of CO<sub>2</sub> than in 2015 during most months, excepting September (Table 12). Surprisingly, the ecosystem acted as a source of CO<sub>2</sub> from August 2013 throughout the rest of the year, with a significantly large CO<sub>2</sub> emission in October of 111.05 g CO<sub>2</sub>-C m<sup>-2</sup> month<sup>-1</sup>, which may be associated with the warmer and drier (lower water table) August and October in 2013 (Figure 25; Table 12).

### 6.2.5. Annual Carbon Dioxide Budget

Annual cumulative NEE values for SF during the measurement period are presented in Figure 47. The random error calculated according to Finkelstein & Sims (2001) for measured NEE and the SD as reported by the gap-filling procedure for gap-filled NEE were used for computing the uncertainty ranges (see Section 4.3.6). The cumulative daily uncertainty range is presented in Figure 47. The uncertainties provide the maximum possible range of the accumulative NEE at SF during the measurement period. As previously described, all study years showed similar seasonal trends of CO<sub>2</sub> fluxes. However, the between-year differences of CO<sub>2</sub> fluxes can be more easily detected in accumulative trends. A positive slope of cumulative NEE indicates that the ecosystem is behaving as a CO<sub>2</sub> source, while a negative slope indicates a CO<sub>2</sub> sink.

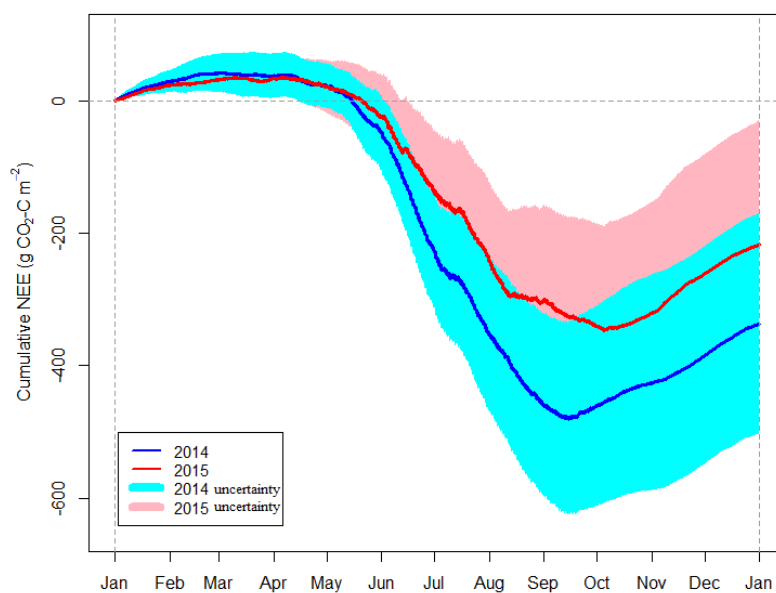


**Figure 47:** Annual cumulative net ecosystem  $CO_2$  exchange (NEE) at Sedge Fen in 2014 and 2015, with cumulative daily range as uncertainties. Year 2013 doesn't include in the plot since lack of full year data.

The ecosystem acted as a source of  $CO_2$  during the period from January to mid-June in both 2014 and 2015 (Figure 47). Year 2014 experienced an earlier increase in net  $CO_2$  uptake than occurred in 2015, and the site acted as a larger sink of  $CO_2$  in 2014 than in 2015 during the rest of year (Figure 47). The increase in  $CO_2$  emission after the growing season occurred earlier in 2014 than in 2015, and both years had similar increasing slope of  $CO_2$  emission until the end of the year (Figure 47). Therefore, 2014 still ends up with a higher annual sum (negative) of NEE and as a larger sink of  $CO_2$  than in 2015 (Figure 47).

The annual cumulative NEE, GPP (negative) and  $R_{eco}$  during the study period are presented in Figure 48. The estimates of total accumulated  $R_{eco}$  were very similar in year 2014 and 2015. The estimates of total accumulated GPP were quite similar in the first several months (January to May) in both years, but were higher in 2014 from mid-June until the end of the year when compared to 2015. Therefore, the accumulative NEE shows very similar patterns to GPP for the two years.

Annual cumulated GPP was estimated at 1559.39 and 1437.15  $g\ CO_2-C\ m^{-2}yr^{-1}$ , in 2014 and 2015, respectively. Annual cumulative  $R_{eco}$  was estimated at 1202.53 and 1193.37  $g\ CO_2-C\ m^{-2}yr^{-1}$ , in 2014 and 2015, respectively (Table 13).

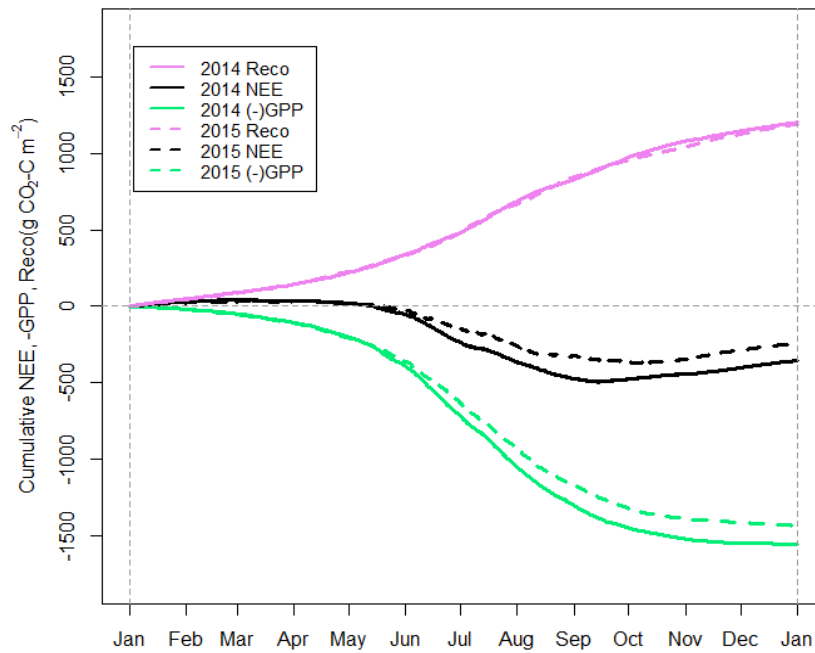


**Figure 48:** Annual cumulative net ecosystem CO<sub>2</sub> exchange (NEE), ecosystem respiration ( $R_{eco}$ ) and gross primary production (GPP) in black, violet and green respectively, in 2014 and 2015 at Sedge Fen. Year 2013 doesn't include in the plot since lack of full year data. The term -GPP is here the opposite of GPP and is introduced to facilitate graphical reading.

Site SF was a net sink for CO<sub>2</sub> in 2014 and 2015 with annual gap-filled totals of  $-356.86 \pm 13.4$  g CO<sub>2</sub>-C m<sup>-2</sup>yr<sup>-1</sup> in 2014, and  $-243.78 \pm 15.25$  g CO<sub>2</sub>-C m<sup>-2</sup>yr<sup>-1</sup> in 2015 (Table 13). The uncertainty of the annual sums is based on the Monte-Carlo simulation procedure (see Section 4.3.6).

The ecosystem was a larger sink of CO<sub>2</sub> in 2014 compared to 2015. However, the two years had no significant difference in annual  $R_{eco}$  at  $1202.53$  g CO<sub>2</sub>-C m<sup>-2</sup>yr<sup>-1</sup> and  $1193.37$  g CO<sub>2</sub>-C m<sup>-2</sup>yr<sup>-1</sup> in 2014 and 2015, respectively (Table 13). Therefore, the large differences in the annual CO<sub>2</sub> budget between the two years were due to the significant difference in the annual GPP at  $1559.39$  g CO<sub>2</sub>-C m<sup>-2</sup>yr<sup>-1</sup> and  $1437.15$  g CO<sub>2</sub>-C m<sup>-2</sup>yr<sup>-1</sup> in 2014 and 2015, respectively (Table 13).

**Table 13:** The comparison of carbon balance at Sedge Fen during the measurement period. No flux data available before August 2013, the total carbon balance between the period August and December for 2013, 2014 and 2015 are compared.

	Annual Budget (g CO <sub>2</sub> m <sup>-2</sup> )	Carbon Balance (g C m <sup>-2</sup> )	GWP (100 years) (g CO <sub>2</sub> m <sup>-2</sup> )
2014 Carbon dioxide (CO <sub>2</sub> )	-1308.5 (±49.13)	-356.86 (±13.4)	-1308.5 (±49.13)
2014 gross primary production (GPP)	--	1559.39	--
2014 ecosystem respiration ( <i>R<sub>eco</sub></i> )	--	1202.53	--
2015 Carbon dioxide (CO <sub>2</sub> )	-893.86 (±55.92)	-243.78 (±15.25)	-893.86 (±55.92)
2015 gross primary production (GPP)	--	1437.15	--
2015 ecosystem respiration ( <i>R<sub>eco</sub></i> )	--	1193.37	--
2013 Carbon dioxide (CO <sub>2</sub> ) (Aug. - Dec.)	1091.16 (±33.59)	297.59 (±9.16)	1091.16 (±33.59)
2013 gross primary production (GPP) (Aug. - Dec.)	--	629.96	--
2013 ecosystem respiration ( <i>R<sub>eco</sub></i> ) (Aug. - Dec.)	--	927.55	--
2014 Carbon dioxide (CO <sub>2</sub> ) (Aug. - Dec.)	33.99 (±22.15)	9.27 (±6.04)	33.99 (±22.15)
2014 gross primary production (GPP) (Aug. - Dec.)	--	505.92	--
2014 ecosystem respiration ( <i>R<sub>eco</sub></i> ) (Aug. - Dec.)	--	515.19	--
2015 Carbon dioxide (CO <sub>2</sub> ) (Aug. - Dec.)	61.93 (±37.55)	16.89 (±10.24)	61.93 (±37.55)
2015 gross primary production (GPP) (Aug. - Dec.)	--	506.92	--
2015 ecosystem respiration ( <i>R<sub>eco</sub></i> ) (Aug. - Dec.)	--	523.81	--

During the period between August and December when there is available data in 2013, SF acted as a net source for CO<sub>2</sub> in all three years with  $297.59 \pm 9.16$  g CO<sub>2</sub>-C m<sup>-2</sup> period<sup>-1</sup> in 2013,  $9.27 \pm 6.04$  g CO<sub>2</sub>-C m<sup>-2</sup> period<sup>-1</sup> in 2014 and  $16.89 \pm 10.24$  g CO<sub>2</sub>-C m<sup>-2</sup> period<sup>-1</sup> in 2015 (Table 13). There is no significant difference between the total NEE, GPP and  $R_{eco}$  during these periods in 2014 and 2015. The total GPP during this period in 2013 was larger than in 2014 and 2015 (with a net difference about 123 g C m<sup>-2</sup>), whereas the total  $R_{eco}$  during the period in 2013 was almost two times that of the total  $R_{eco}$  during the period in 2014 or 2015 (with a net difference about 412 g C m<sup>-2</sup>).

The SF had a negative GWP (net cooling) over the investigated time period, at  $-1308.5 \pm 49.13$  g CO<sub>2</sub> m<sup>-2</sup> in 2014 and  $-893.86 \pm 55.92$  g CO<sub>2</sub> m<sup>-2</sup> in 2015 over a 100-year time horizon.

## 6.3. Response of Carbon Flux to Environmental Factors

### 6.3.1. Effects of Environmental Factors

The Pearson coefficients ( $r$ ) of CO<sub>2</sub> fluxes to measured environmental factors ( $T_{air}$ , RH, VPD, PAR and WT) at SF were tested by simple linear regression. The Pearson correlation coefficients ( $r$ ), the square of the Pearson correlation coefficients ( $R^2$ ) and p-values for the correlation between fluxes and measured environmental factors are reported in Table 14. Stepwise multiple regressions were carried out to correlate fluxes with measured environmental factors. The best fit regression equations of fluxes against significantly related environmental factors and adjusted  $R^2$  are reported in Table 15.

**Table 14:** Pearson coefficients ( $r$ ) of fluxes (NEE, GPP and  $R_{eco}$ ) on environmental factors at Sedge Fen. The square of the Pearson correlation coefficient ( $R^2$ ) have been presented in brackets. The p-values for the correlation have been presented as stars (\*).

	$T_{air}$	RH	VPD	PAR	WT
NEE	-0.437 (0.191)**	0.557 (0.310)**	-0.615 (0.378)**	-0.838 (0.702)**	-0.136 (0.018)*
$R_{eco}$	0.705 (0.497)**	-0.365 (0.133)**	0.599 (0.359)**	0.387 (0.149)**	-0.619 (0.383)**
GPP	0.697 (0.486)**	-0.471 (0.222)**	0.666 (0.444)**	0.772 (0.596)**	-0.215 (0.046)*

$T_{air}$ , air temperature; RH, relative humidity; VPD, vapour pressure deficit; PAR, photosynthetically active radiation; WT, water table; NEE, net ecosystem exchange;  $R_{eco}$ , ecosystem respiration; GPP, gross primary production. \*,  $0.01 < p < 0.05$ ; \*\*,  $p < 0.01$ .

The correlation between  $CO_2$  fluxes and measured environmental factors at SF showed exactly the same patterns as at the BF site. NEE was negatively correlated with  $T_{air}$ , VPD, PAR and WT, and positively correlated with RH (Table 14). While both  $R_{eco}$  and GPP were positively correlated with  $T_{air}$ , VPD and PAR, they were negatively correlated with RH and WT (Table 14). It should be noted that, compared to NEE and GPP,  $R_{eco}$  was more significantly correlated with WT at SF ( $p < 0.01$ ; Table 14). Same as at BF, PAR accounted for the largest percentage of variation for both NEE and GPP (70.2% and 59.6%, respectively). However, besides  $T_{air}$ , both WT and VPD significantly explained the variation for  $R_{eco}$  at SF (38.3% and 35.9%, respectively;  $p < 0.01$ ; Table 14).

**Table 15:** Stepwise regression analysis of fluxes (NEE,  $R_{eco}$  and GPP) against significantly related environmental factors at Sedge Fen.

	Best fit regression equations	Adj-R <sup>2</sup>	p-values
NEE	$F = -0.014PAR - 0.047WT + 2.518$	0.727	**
$R_{eco}$	$F = 0.102T_{air} - 0.061WT + 0.668VPD + 0.102RH - 8.225$	0.777	**
GPP	$F = 0.011PAR + 0.642T_{air} - 5.137$	0.731	**

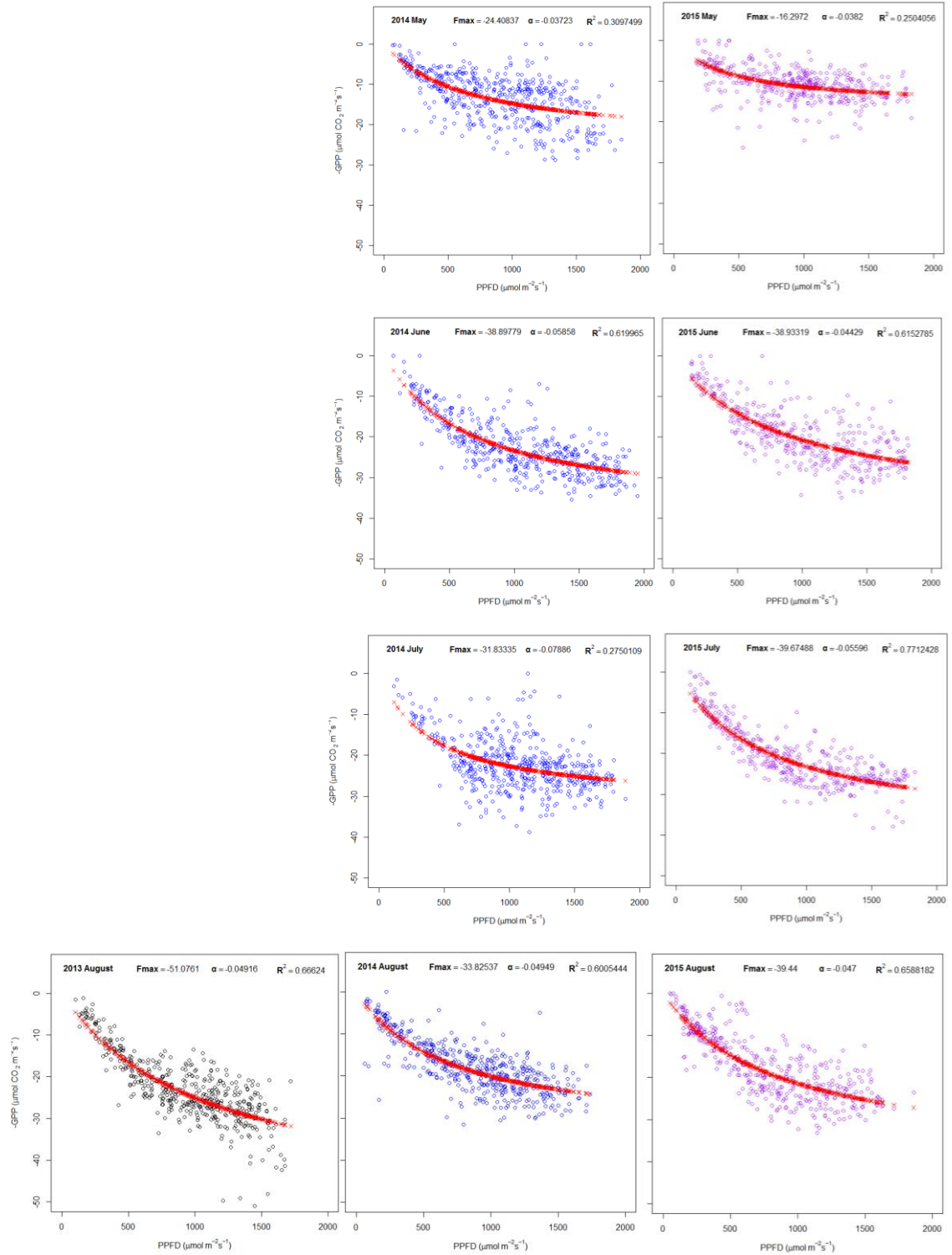
See Table 14 for abbreviation.

After combining all measured environmental factors at SF in the stepwise multiple regression analysis, PAR and WT together accounted for 72.7% of the variation in NEE (PAR accounted for 70.3%, WT explained the rest 2.4%;  $p < 0.01$ ; Table 15).

While  $T_{air}$ , WT, VPD, and RH together can explain 77.7% of the variation for  $R_{eco}$  ( $T_{air}$  accounted for 49.7%, the other three factors together explained 28%;  $p < 0.01$ ; Table 15). As for GPP, PAR and  $T_{air}$  together accounted for 73.1% of the variation in GPP (PAR explained 59.6%,  $T_{air}$  accounted for the remaining 13.5%;  $p < 0.01$ ; Table 15). It should be noted that  $R_{eco}$  at SF was more significantly correlated to WT compared to at BF (WT accounted for the second greatest proportion of the variance of  $R_{eco}$  at SF; Table 10 & 15).

### 6.3.2. Light Response Curves

The relation between GPP and PPFD can be described by a rectangular hyperbolic light response function (see Section 4.3.8). The dependence of daytime GPP ( $R_g > 20 \text{ W m}^{-2}$ ) on light was simulated with the means of the rectangular hyperbolic light response function (Equation 14) for different months during the growing season (May to October) over the study period (August 2013 to 2015) at SF (Figure 49). GPP are shown as negative values to facilitate graphical reading.



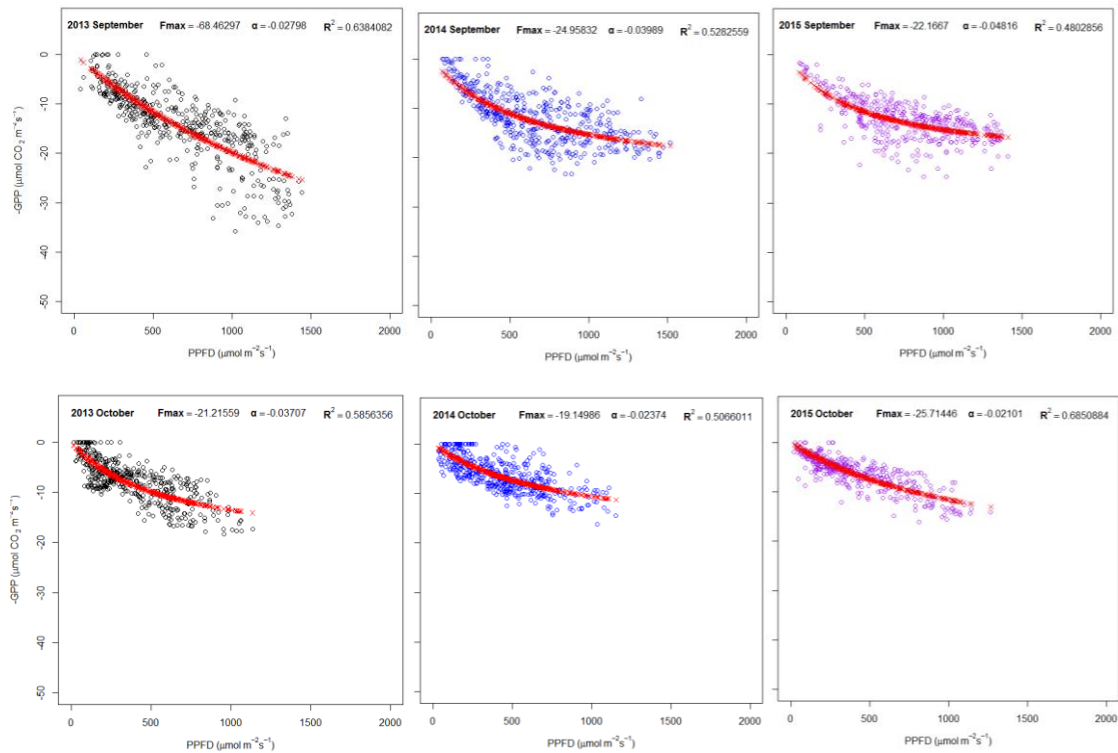


**Figure 49:** light response curves of GPP plotted for different months during the growing season from August 2013 to 2015 at Sedge Fen. Fitted curves represent the rectangular hyperbolic light response function (see Equation 14).  $F_{max}$  is the maximum  $\text{CO}_2$  flux at infinite light,  $\alpha$  is the ecosystem apparent quantum yield.

Based on the rectangular hyperbolic light response function, the seasonal changes in PPFD explained between about 25% and 77% of the variability in daytime GPP during the measurement period in the main growing seasons (Figure 49). There were significant differences in the light response curves for GPP in the main growing seasons during the study years. There was no light saturation of GPP evidenced on the study site during the measurement period.

No significant differences were observed between the maximum rates of GPP ( $F_{max}$ , showed in negative values) in all months of the growing seasons in 2014 and 2015. Whereas, the maximum rates of GPP in August and September 2013 were much higher than in the same months of 2014 and 2015. The maximum rates of GPP in 2013 were observed in September with a calculated  $F_{max}$  value of  $-68.46 \mu\text{mol CO}_2 \text{m}^{-2}\text{s}^{-1}$ , from the rectangular hyperbola (Equation 14) fitted to the light response curves (Figure 49). In 2014, the maximum rates of GPP occurred in June with  $F_{max}$  value of  $-38.90 \mu\text{mol CO}_2 \text{m}^{-2}\text{s}^{-1}$  (Figure 49). In 2015, the peak  $F_{max}$  value was similar to that in 2014 but occurred

one month later in July with  $F_{max}$  value of  $-39.67 \mu\text{mol CO}_2 \text{ m}^{-2}\text{s}^{-1}$  (Figure 49). The  $F_{max}$  decreased gradually when vegetation recession started in the year (the lowest values at  $-21.22$ ,  $-19.15$  and  $-16.30 \mu\text{mol CO}_2 \text{ m}^{-2}\text{s}^{-1}$  for 2013, 2014 and 2015, respectively, at beginning or end of growing seasons). During the senescence period (October, the start of winter), the maximum PPFD values were much lower than during the main growing season months at about  $1100 \mu\text{mol m}^{-2}\text{s}^{-1}$  in all years (Figure 49).

The ecosystem apparent quantum yield ( $\alpha$ ) also differed among years during the main growing seasons, with calculated values of  $0.028$ ,  $0.059$  and  $0.056 \text{ mol mol}^{-1}$ , in September 2013, June 2014 and July 2015 (the month with the highest  $F_{max}$ ), respectively (Figure 49). The range of apparent quantum yield ( $\alpha$ ) values for SF are similar to those reported in other studies of temperate grasslands (Flanagan *et al.*, 2002; Wohlfahrt *et al.*, 2008).

### 6.3.3. Multi-scale Analysis of Environmental Controls

As at BF, the half-hourly gap-filled data were used and the time scales considered varied from daily to more than half annual (256 days). The wavelet coherence analysis has been implemented between GPP and PPFD,  $T_{air}$ , VPD in this study. The correlations between  $R_{eco}$  and VPD also have been analysed by the wavelet coherence method. The  $R_{eco}$  was estimated base on the  $T_{air}$  during the flux partitioning procedure; therefore no correlation analysis was implemented between  $R_{eco}$  and  $T_{air}$  in this section.

In Figure 50, the large blue areas indicate the period with no valid  $\text{CO}_2$  flux data before August 2013, and no PPFD data available during January to April 2014 at SF. The PPFD data at BF have been used on SF since there was no valid PPFD measurement at SF. The highest coherence between PPFD and GPP was at the daily scale during whole years, indicative of a common diel cycle between PPFD and photosynthesis during all seasons on the permanent vegetation cover site (Figure 50). Remarkable localised coherences at monthly scales ( $< 32$  days) occur in all growing seasons representing

similar increasing patterns of PPFD and GPP during the period of plant activity (Figure 50). There is no evidence of coherences at larger scales during the non-growing season (Figure 50).

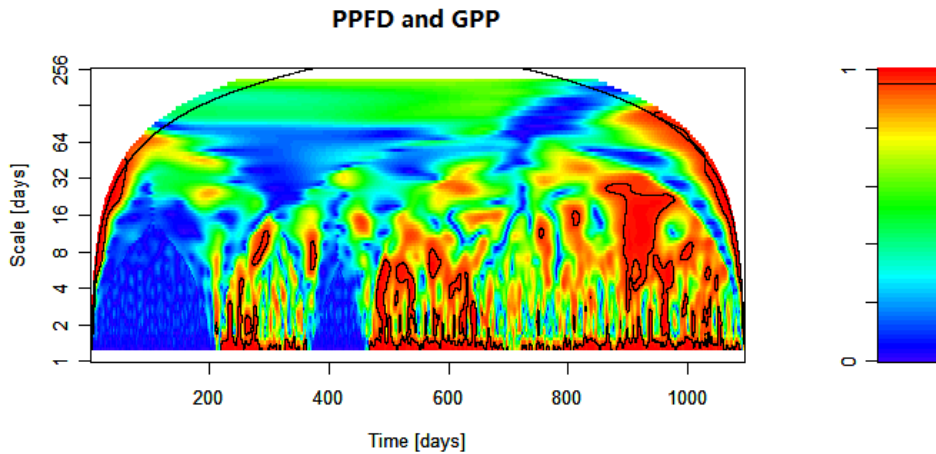


**Figure 50:** Wavelet coherence analysis between gross primary production (GPP) and photosynthetic photon flux density (PPFD) during the measurement period (August 2013 to 2015) at Sedge Fen. On the Y-axis the time-scale is reported. Low to high coherence values are represented in the colour palette from blue to red. The PPFD data was measured at BF. There is no valid PPFD data during January to April 2014, no valid CO<sub>2</sub> flux data before August 2013.

In Figure 51, the large blue areas indicate the period with no valid CO<sub>2</sub> flux data before August 2013 (as well as in the following Figures 52 & 53). Regarding GPP with air temperature, the daily cycle coherence is only exhibited during the growing seasons (Figure 51). There are some localized coherences at larger scale (8 - 64 days) that can be identified during the growing seasons as well (especially in the warmer year of 2014), indicating that the underlying photosynthesis activity was closely related to the increasing air temperature during the period of plant activity (Figure 51). Some localized coherences at half-month scale (7 - 16 days) during the senescence period indicate the similar decreasing patterns of air temperature and GPP in the non-growing season during rain or cooling events (Figure 51).

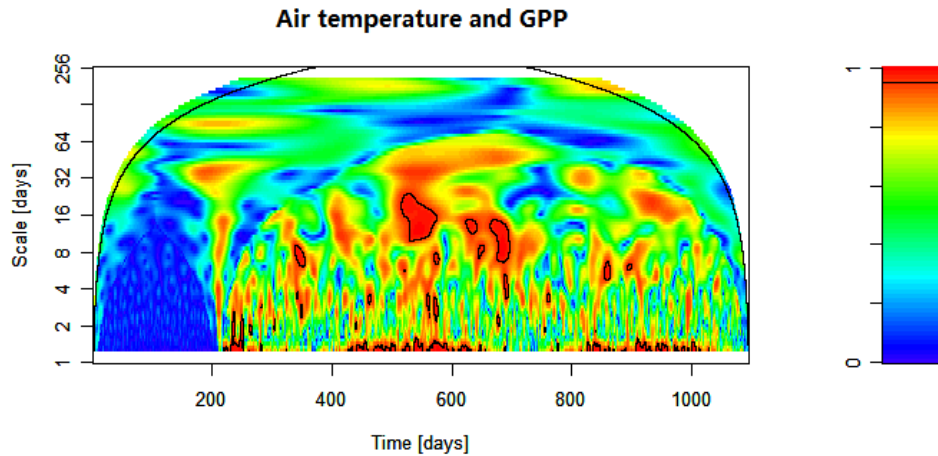


**Figure 51:** Wavelet coherence analysis between gross primary production (GPP) and air temperature ( $T_{air}$ ) during the measurement period (August 2013 to 2015) at Sedge Fen. On the Y-axis the time-scale is reported. Low to high coherence values are represented in the colour palette from blue to red. There is no valid  $CO_2$  flux data before August 2013.

In Figure 52, similar with  $T_{air}$ , the VPD exhibits daily cycle coherence with photosynthesis only during the growing seasons, but with generally higher coherences with larger scales (7 - 32 days) than  $T_{air}$  with GPP. The high localized coherences identified at larger scale (7 - 32 days) during the growing seasons indicate the great influence of increasing of VPD on photosynthesis during the period of plant activity (Figure 52). There are only few localized coherences found in the non-growing season at larger scales that may be associated with the similar decreasing patterns of VPD and photosynthesis in discontinuous non-stationary cooling events in the late autumn and winter (Figure 52).

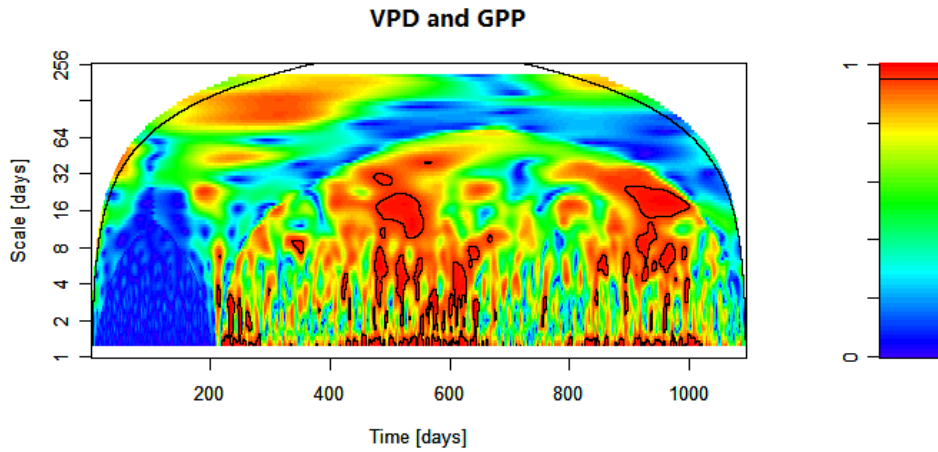


**Figure 52:** Wavelet coherence analysis between gross primary production (GPP) and vapour pressure deficit (VPD) during the measurement period (August 2013 to 2015) at Sedge Fen. On the Y-axis the time-scale is reported. Low to high coherence values are represented in the colour palette from blue to red. There is no valid CO<sub>2</sub> flux data before August 2013.

The wavelet coherence between  $R_{eco}$  and VPD is shown in Figure 53. Weak daily coherences can be found with VPD and respiration during the growing seasons (Figure 53). The weekly (2 - 8 days) and monthly (16 - 32 days) localized coherences are evident for specific periods during the growing season, and area associated with rainfall / heat wave events producing effects on  $R_{eco}$  lasting some days (Figure 53).

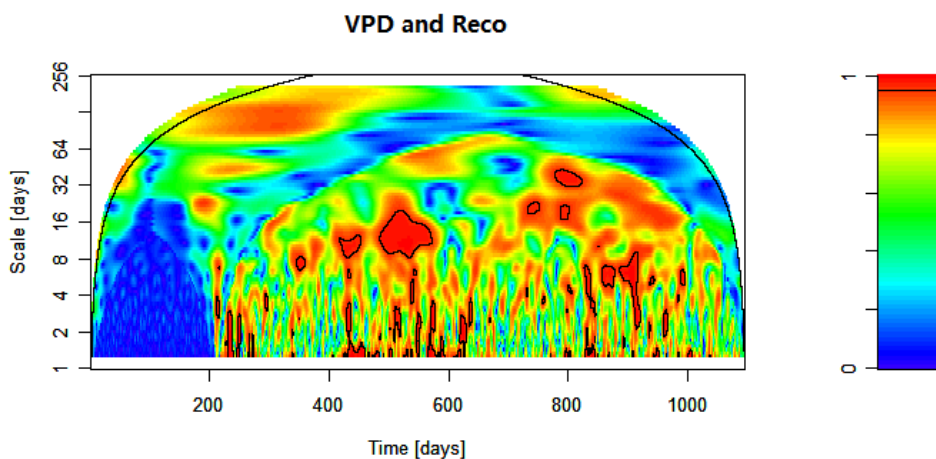


**Figure 53:** Wavelet coherence analysis between ecosystem respiration ( $R_{eco}$ ) and vapour pressure deficit (VPD) during the measurement period (August 2013 to 2015) at Sedge Fen. On the Y-axis the time-scale is reported. Low to high coherence values are represented in the colour palette from blue to red. There is no valid CO<sub>2</sub> flux data before August 2013.

## 6.4. Discussion and Conclusion

### 6.4.1. EC Measurement Performance

The energy balance closure (EBC) with half-hour time scale data at SF (Figure 24) is similar to the values reported from the other sites (see Section 5.4.1) (Wilson *et al.*, 2002). The EBC was further improved by using the daily average in the analysis. This suggested a good overall system performance and high data reliability on the study site during the measurement period.

The energy imbalance existing at SF could result from the poor performance of the heat flux plates in peat substrates (Laurila *et al.*, 2012), in particular, in high water level conditions. The neglected energy storage term and the neglected water heat storage could be another explanation for the relative imbalance in EBC at SF (Harding & Lloyd, 2008; Jacobs *et al.*, 2008). The EC tower at SF is taller than the tower at BF; however, the storage term under the instruments is still neglected on this site as the measurement height is still much lower than the measurements at forested sites (Leuning *et al.*, 2012). Furthermore, the differences between the footprints of the eddy fluxes, the soil heat fluxes and the net radiation measurements are still an unresolved issue relevant to the imbalance of the EBC in the community (Balzarolo *et al.*, 2011).

The footprint estimates and the distribution of the wind field confirm that the majority of the measured fluxes originate from the area of interest at SF and that the contribution of the measured fluxes from the target ecosystem dominates the overall budget. Furthermore, the total flux data coverage during the measurement period at SF is within the typical range of the coverage attained from other EC sites (Falge *et al.*, 2001).

## 6.4.2. Carbon Dioxide Fluxes

The semi-natural site SF acted as a net sink of atmospheric CO<sub>2</sub> in 2014 and 2015 (the two study years with complete annual cycles), with an annual sum of  $-356.86 \pm 49.13$  g CO<sub>2</sub>-C m<sup>-2</sup>yr<sup>-1</sup> in 2014 and  $-243.78 \pm 15.25$  g CO<sub>2</sub>-C m<sup>-2</sup>yr<sup>-1</sup> in 2015. The annual CO<sub>2</sub> budget at SF is within the range of values reported from a series of studies on different temperate semi-natural freshwater wetlands in the USA (Bernal & Mitsch, 2012), and a semi-natural boreal wet grassland in Denmark (Herbst *et al.*, 2013), while Drewer *et al.* (2010) reported a lower annual CO<sub>2</sub> uptake at  $-15$  to  $-145$  g CO<sub>2</sub>-C m<sup>-2</sup>yr<sup>-1</sup> from a minerotrophic sedge fen in Finland. The total CO<sub>2</sub> budget during the period between August and December in 2013 shows that the site was a net source of CO<sub>2</sub> to the atmosphere with  $297.59 \pm 9.16$  g CO<sub>2</sub>-C m<sup>-2</sup> period<sup>-1</sup>, which is much higher than the total amounts in 2014 and 2015 during the same period (with  $9.27 \pm 6.04$  and  $16.89 \pm 10.24$  g CO<sub>2</sub>-C m<sup>-2</sup> period<sup>-1</sup> in 2014 and 2015, respectively). The ecosystem was likely acting as even a small source of atmospheric CO<sub>2</sub> during the drier year of 2013. The ecosystem had a negative GWP (net cooling) over the investigated time period, at  $-1308.5 \pm 49.13$  g CO<sub>2</sub> m<sup>-2</sup> in 2014 and  $-893.86 \pm 55.92$  g CO<sub>2</sub> m<sup>-2</sup> in 2015 over a 100-year time horizon (CO<sub>2</sub> only).

Large seasonal variation in the CO<sub>2</sub> exchange process was observed at SF over the investigated time period. The study years showed broadly similar overall seasonal patterns in NEE and its component fluxes (i.e. GPP and  $R_{eco}$ ) at SF, which is similar to the patterns shown in BF (described in Section 5.4.2). Despite this overall similarity in seasonal patterns, significant differences were observed in the seasonal magnitude of accumulated CO<sub>2</sub> exchanges at SF over the investigated time period. The ecosystem functioned as a net sink (monthly) of CO<sub>2</sub> between April and September in 2014 and 2015, as well as in March 2014, indicating that the study site acted as a large sink of CO<sub>2</sub> during the growing season.

As at BF, the short term responses of CO<sub>2</sub> fluxes to environmental factors fitted well to the theory speculations in regression analyses for SF. The high adjusted R<sup>2</sup> value gained from the step-wise multivariate regression analysis between CO<sub>2</sub> fluxes and environmental factors also gives an indication that the environmental variables in these

empirical models have the potential to be used to predict CO<sub>2</sub> fluxes at an ecosystem scale for similar ecosystems in future modelling studies (Table 15). As at BF, GPP was found to be highly correlated with PAR and  $T_{air}$ , and  $T_{air}$  accounted for the greatest proportion of the variation in  $R_{eco}$  at SF (Table 14 & 15). It should be noted that,  $R_{eco}$  was highly correlated to  $T_{air}$  partly because of the  $T_{air}$  having been used for computing the daytime  $R_{eco}$  during flux partitioning (see Section 4.1.4). However,  $R_{eco}$  was more significantly correlated to WT at SF compared to BF (besides of  $T_{air}$ , WT accounted for the greatest proportion of the variance of  $R_{eco}$  at SF, Table 15). This is consistent with many other studies suggesting that the  $R_{eco}$  on waterlogged peatland ecosystems is more sensitive to WT fluctuation than in relatively drier conditions (Juszczak *et al.*, 2013; Moore & Dalva, 1993; Updegraff *et al.*, 2001). As at BF, NEE, as the difference between GPP and  $R_{eco}$ , was indirectly affected by the factors influencing GPP or  $R_{eco}$ , which, as at SF, was found to be explained by PAR and WT.

The contrasting environmental conditions over the investigated time period had a strong influence on the ecosystem processes at the site. The period between August and December in 2013 (the period with available data in 2013) was a warm period (the warmest summer since 2006, warmer October and December than the historical averages) with extremely dry August and September (prolonged drought period in 2013) and relatively wet October to December. The water levels at SF in 2013 were quite low between August and October (at around 55 cm below the peat surface), and increased to around 10 cm below the peat surface at the end of the year (November and December). The total GPP between August and December 2013 at 629.96 g CO<sub>2</sub>-C m<sup>-2</sup> was higher than the total GPP during the same period in the other two study years (with 505.92 and 506.92 g CO<sub>2</sub>-C m<sup>-2</sup> in 2014 and 2015, respectively), which was closely associated with the warm conditions during the period. Moreover, the higher rate of photosynthesis that occurred in August and September 2013 during the prolonged drought period indicates that the warm temperature and adequate light availability outweighed the influences of dry conditions during the growing season. This is consistent with the results of the regression analysis which showed that GPP was more significantly correlated with  $T_{air}$  and VPD compared to WT at SF (Table 14). Lindroth *et al.* (2007) suggested a similar explanation, with temperature being the strongest driver of GPP in a study of boreal mires. However, the total  $R_{eco}$  was much higher

during the period in 2013 at  $927.55 \text{ g CO}_2\text{-C m}^{-2}$  in comparison to the other two years (with  $515.19$  and  $523.81 \text{ g CO}_2\text{-C m}^{-2}$  in 2014 and 2015, respectively). As a result, the ecosystem acted as a net source of  $\text{CO}_2$  during this period, which can be explained by the increase in  $R_{eco}$  outweighing the GPP due to enhanced  $R_{eco}$  in dry conditions in August and September. This result is consistent with the respiratory activities ( $R_{eco}$ ) being more sensitive to WT compared to photosynthesis (GPP) do (Table 14), and also further supports the importance of the timing of water availability and adequate temperature on ecosystem processes (Monson *et al.*, 2005).

2014 was unusually warm (one of the warmest years compared to the long-term average) and wet (the fourth wettest year in the UK since records began in 1910) compared to the other two study years. The water levels at SF in 2014 were quite close to or even above the peat surface for the whole year, and never below 10 cm from the surface. The warmer and wetter conditions resulted in higher rates of photosynthesis during most of growing season months (May to July; Table 15). However, the lower temperature in August (the coldest August over the last few decades) and much less rainfall in September (the driest September for the whole country average since 1910) resulted in relatively lower GPP and  $R_{eco}$  in August, and relatively low GPP but high  $R_{eco}$  in September. The period when high respiratory activities occurred in September and October on the site was the warm period but the only period that the water table was its lowest level (at around 10 cm below the peat surface) in the year. The ecosystem acted as a large sink of  $\text{CO}_2$  in 2014 under warm and wet conditions with an annual sum of  $-356.86 \pm 49.13 \text{ g CO}_2\text{-C m}^{-2}\text{yr}^{-1}$ .

The year 2015 had close to average temperatures in most of months, but a much warmer November and December (the mildest December in the records since 1659). In general, 2015 was much colder than 2014 (at  $0.7 \text{ }^\circ\text{C}$  below annual mean temperature). The water levels at SF were close to the peat surface for most of the year, but with a dramatic decrease in June and July (reaching about 40 cm below the surface) due to the driest month in the year occurring in June. June, November and December in 2015 were the only months when the monthly total  $R_{eco}$  values were larger than in the same months in 2014 due to the dry period in June and the warmer conditions at the end of year in 2015. The annual total  $R_{eco}$  of 2015 ( $1193.37 \text{ g CO}_2\text{-C m}^{-2}\text{yr}^{-1}$ ) was quite close

to the annual total  $R_{eco}$  in 2014 (1202.53 g CO<sub>2</sub>-C m<sup>-2</sup>yr<sup>-1</sup>), while the annual total GPP in 2014 (1559.39 g CO<sub>2</sub>-C m<sup>-2</sup>yr<sup>-1</sup>) was much higher than in 2015 (1437.15 g CO<sub>2</sub>-C m<sup>-2</sup>yr<sup>-1</sup>). These results suggest that temperature is the strongest driver of GPP, while the water level combined with temperature are the most important factors influencing the  $R_{eco}$  (including autotrophic and heterotrophic respiration) which is consistent with the results of the multiple regression analysis (Lindroth *et al.*, 2007; Table 15).

The ecosystem apparent quantum yield ( $\alpha$ ) calculated based on the rectangular hyperbolic light response function (Equation 14) during the growing season (May to October) at SF over the measurement period indicates that the SF vegetation attained higher maximum assimilation rates compared to BF. This difference in light use characteristics can be most likely explained by the larger peak season biomass at SF than at BF during the growing season (Humphreys *et al.*, 2010; Lund *et al.*, 2010).

## **Chapter 7**

# **Comparison of Carbon Dioxide Fluxes between Two Temperate Lowland Fens with Different Land-use Types**

## 7.1. Environmental Conditions

### 7.1.1. Ground Water Levels

In general, site BF was drier than SF during all three study years (i.e. the ground water levels were lower) (Figure 54). The differences in the ground water levels at the two sites were generally larger during the growing seasons but relatively smaller in spring, early summer and winter (Figure 54). The amplitudes of variation of ground water levels were larger at BF than at SF in all years (Figure 54).

Both sites experienced the lowest water levels in 2013 during the growing season months (June to October) over the measurement period (Figure 54). In 2013, the water levels at both sites were close to the peat surface at the beginning of the year (January to April), while water levels at SF were slightly above the surface and at BF were slightly below ground surface during the period (Figure 54). An early decline of water levels appeared in mid-April at BF in 2013, which was about three months earlier than the water level decline at SF during that year (Figure 54). The largest difference in water levels at the two sites in 2013 occurred in late June; with the BF level about 80 cm lower than at SF. A similar large difference persisted through until mid-October in 2013 when the rainfall amount increased dramatically (October was the wettest month in the year) (Figure 54). The water levels at both sites started to increase in mid-October following the abundant rainfall, while the BF water level increased more dramatically with addition of ground water onto the site from the adjacent lode. Both sites water level then remained close to the ground surface until the end of the year (Figure 54).

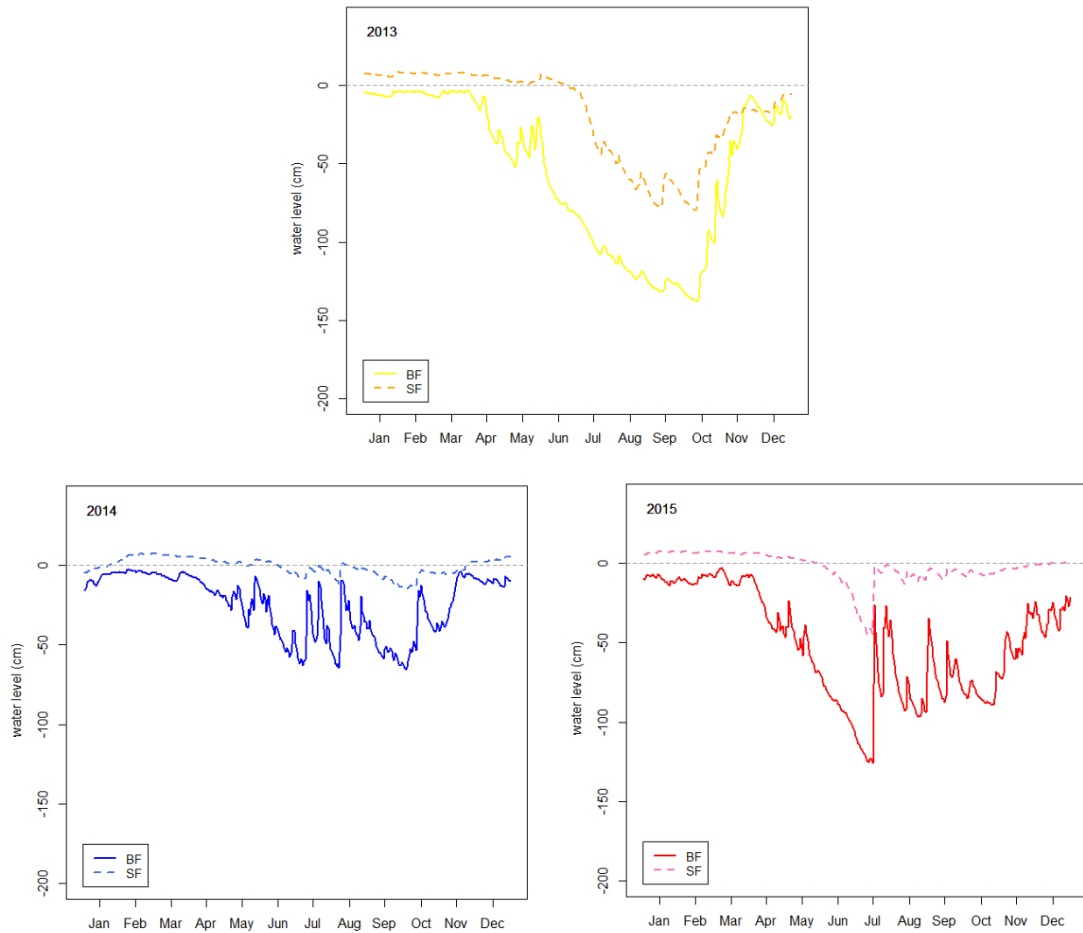


**Figure 54:** Ground water levels at Baker's Fen and Sedge Fen during measurement period. Data show the mean daily position of water levels relative to the peat surface measured at BF dipwell 107-1 and SF dipwell NW07. Data supplied by John Bragg @ the NT.

The water levels at both sites were close to the ground surface for most of time in 2014 compared to the conditions in the other two years (Figure 54). Several significant drawdowns were observed during the growing season in 2014 at BF; however large rainfall events resulted in several rapid increases in water table to near the surface (Figure 54). The largest difference between the two sites water levels was about 50 cm (lower at BF) and this only occurred during a short period when a significant drawdown appeared at BF (Figure 54).

The water levels at both sites were close to the ground surface at the beginning of the year (from January until early April). A continuous decline in water level occurred from early April through to mid-July at BF, while the water level decreased much later

at SF (in late May), followed by a dramatic increase in mid-July at both sites due to the plentiful rainfall of that month (Figure 54). The water levels at SF remained close to the ground surface after July, while several rapid drawdowns followed by rapid recoveries were observed at BF between July and November (Figure 54). At the end of 2015, the water levels at BF increased to about 30 cm below surface (Figure 54). The largest difference between water levels at the two sites was about 80 cm, with this situation occurring for most of time from early June until November 2015 (Figure 54).

Owing to the differences in the water levels between the two sites, the soil temperature, soil water content and vegetation types are quite different. However, as there is no reliable soil temperature and soil water content data from the study sites due to instrument failures during the measurement period. Currently, continuous measurements of soil temperature and soil water content are being conducted at both sites, with the aim of providing more detailed environmental measurements data for future studies.

## 7.2. Seasonal Patterns of Carbon Dioxide Fluxes

Figure 55 compares the monthly total of  $R_{eco}$ , GPP and NEE at BF and SF over the measurement period (SF data are only available since August 2013).

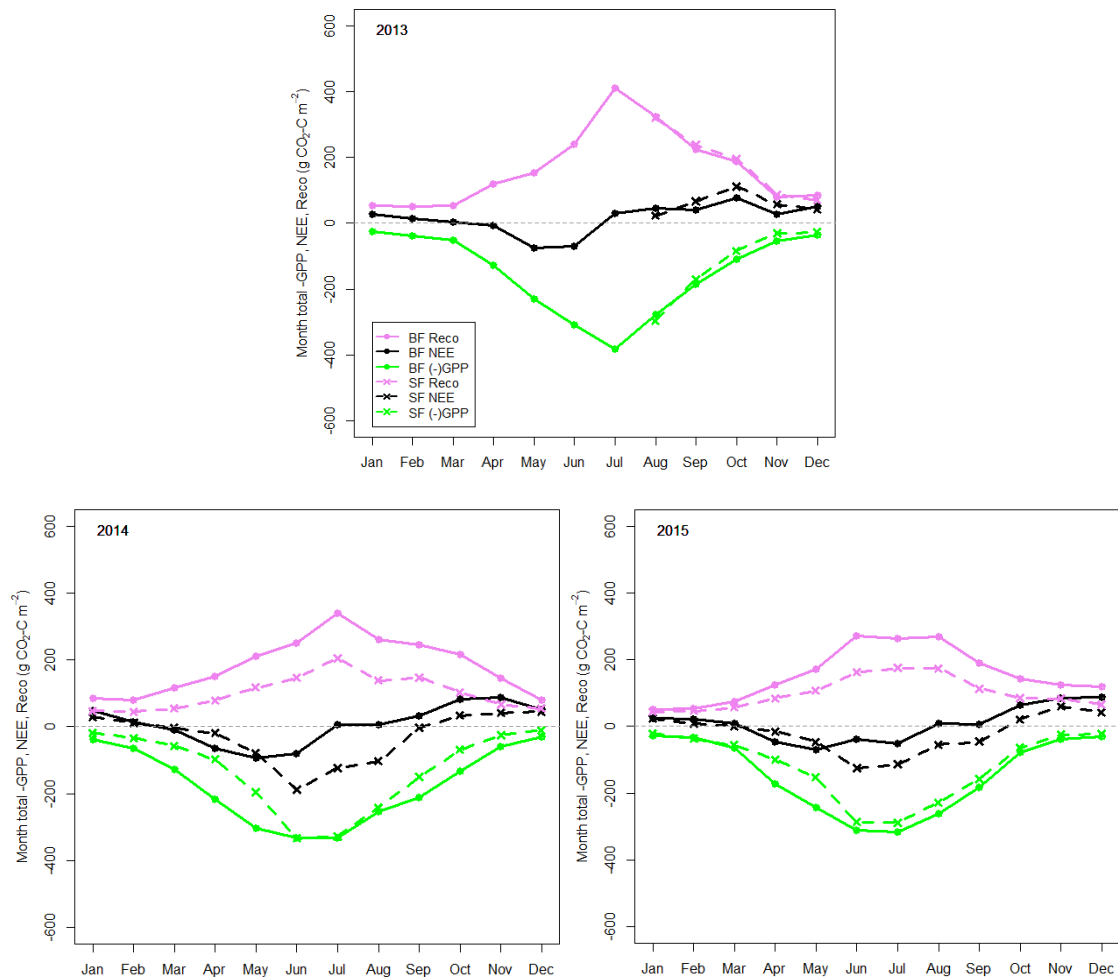


**Figure 55:** Comparison of monthly total net ecosystem  $\text{CO}_2$  exchange (NEE), ecosystem respiration ( $R_{eco}$ ) and gross primary production (GPP) in black, violet and green respectively, at two study sites (Baker's Fen and Sedge Fen) during the measurement period. Data is only available since August 2013 at Sedge Fen. The term  $-GPP$  is here the opposite of GPP and is introduced to facilitate graphical reading.

In general, the monthly total GPP and  $R_{eco}$  at SF were quite close to monthly total GPP and  $R_{eco}$  at BF respectively in 2013. The monthly total GPP,  $R_{eco}$  and NEE showed similar patterns in 2014 and 2015 at the two sites (Figure 55). The monthly total GPP and  $R_{eco}$  at BF were larger than the values at SF in most months of 2014 and 2015 (Figure 55; Table 16). The between-site differences in total monthly  $R_{eco}$  were generally larger than the between-site differences in monthly total GPP (Figure 55). The largest between-site differences in monthly total  $R_{eco}$  occurred in July of 2014 and in June of 2015, while the largest between-site differences in monthly total GPP occurred in April of 2014 and in May of 2015 (Figure 55).

**Table 16:** Comparison of monthly total gross primary production (GPP), ecosystem respiration ( $R_{eco}$ ) and net ecosystem CO<sub>2</sub> exchange (NEE) between Baker's Fen (BF) and Sedge Fen (SF) during measurement period.

Year	Month	GPP (g CO <sub>2</sub> -C m <sup>-2</sup> )		NEE (g CO <sub>2</sub> -C m <sup>-2</sup> )		$R_{eco}$ (g CO <sub>2</sub> -C m <sup>-2</sup> )	
		BF	SF	BF	SF	BF	SF
2013	Jan.	26.31	--	26.98	--	53.29	--
	Feb.	37.15	--	14.10	--	51.25	--
	Mar.	52.16	--	2.42	--	54.57	--
	Apr.	126.64	--	-6.90	--	119.74	--
	May	228.66	--	-74.51	--	154.15	--
	Jun.	307.88	--	-69.23	--	238.65	--
	Jul.	381.17	--	29.22	--	410.39	--
	Aug.	277.97	296.34	44.68	22.30	322.65	318.64
	Sep.	184.64	170.65	39.14	66.73	223.78	237.38
	Oct.	109.20	84.08	78.31	111.05	187.51	195.13
	Nov.	53.53	30.34	26.75	56.86	80.28	87.20
	Dec.	34.47	27.43	50.06	42.37	84.53	69.80
2014	Jan.	37.61	18.52	47.34	28.94	84.95	47.46
	Feb.	64.61	33.43	14.08	11.58	78.69	45.01
	Mar.	126.29	57.71	-9.80	-3.58	116.49	54.13
	Apr.	215.24	97.96	-63.62	-18.83	151.62	79.14
	May	302.01	195.41	-92.26	-78.31	209.76	117.10
	Jun.	330.82	333.95	-79.81	-187.75	251.01	146.20
	Jul.	331.07	327.07	7.20	-122.62	338.28	204.46
	Aug.	252.87	240.96	7.55	-102.90	260.42	138.06
	Sep.	212.33	150.05	32.69	-3.03	245.02	147.02
	Oct.	131.74	69.18	83.24	33.65	214.98	102.84
	Nov.	58.20	25.25	86.73	41.27	144.93	66.52
	Dec.	29.45	9.89	50.25	44.70	79.70	54.60
2015	Jan.	27.07	20.89	23.59	23.18	50.66	44.07
	Feb.	32.22	37.25	22.01	8.76	54.23	46.02
	Mar.	64.38	55.81	9.05	0.78	73.43	56.60
	Apr.	171.94	99.59	-47.19	-15.85	124.75	83.74
	May	242.74	153.22	-70.85	-46.88	171.89	106.34
	Jun.	309.77	286.60	-38.53	-124.56	271.24	162.04
	Jul.	315.64	288.46	-52.07	-113.39	263.57	175.07
	Aug.	261.44	227.70	8.21	-54.43	269.65	173.26
	Sep.	183.00	157.49	6.69	-44.87	189.69	112.62
	Oct.	78.66	63.42	63.89	21.51	142.55	84.94
	Nov.	39.32	23.97	85.66	59.38	124.98	83.36
	Dec.	30.10	22.74	87.94	42.57	118.05	65.32

The monthly total GPP and  $R_{eco}$  at SF were quite close to monthly total GPP and  $R_{eco}$  at BF in 2013 during the period with available data between August and December, with slightly lower monthly total GPP at SF and therefore relatively larger net CO<sub>2</sub> losses at SF than at BF in September, October and November in 2013 (Figure 55; Table 16).

In 2014, the monthly total GPP at BF showed an earlier but more gradual increase in spring and early summer and reached a peak in June and July, while SF showed a much later but more rapid increase and reached a similar maximum monthly total during June and July (Figure 55; Table 16). While the monthly total  $R_{eco}$  at both study sites showed similar seasonal patterns, there was a higher magnitude at BF (Figure 55). As a result, the total net CO<sub>2</sub> uptake was higher at BF during April and May but lower than at SF in June, July and August in 2014 (Figure 55; Table 16). In 2014, the largest difference in monthly NEE occurred in July with the largest between-site differences in monthly total  $R_{eco}$  during this month (Figure 55). Monthly net CO<sub>2</sub> losses were higher at BF than at SF from August until the end of the year, while SF still acted as a CO<sub>2</sub> sink in August 2014 (Figure 55; Table 16).

The monthly total GPP,  $R_{eco}$  and NEE show similar patterns in 2015 as in 2014 at the two sites (Figure 55). The monthly total GPP at BF shows an earlier but more gradual increase since March and then reaches a peak in June and July, while at SF it shows a later but more rapid increase and reaches a similar maximum monthly total in the year during the same period (Figure 55; Table 16). The monthly total  $R_{eco}$  shows similar seasonal patterns at the two sites, but with higher magnitude at BF from March until the end of year (Figure 55). Therefore the total net CO<sub>2</sub> uptake was slightly higher at BF only in April and May but lower than at SF in June, July and August (Figure 55; Table 16). SF still acted (monthly) as a sink of CO<sub>2</sub> in August and September in 2015, while BF was already a source of CO<sub>2</sub> during the same months (Figure 55; Table 16). Monthly net CO<sub>2</sub> losses were higher at BF than at SF from October to December in 2015 (Figure 55; Table 16).

Figure 56 displays the comparisons of accumulated GPP,  $R_{eco}$  and NEE between the two study sites during the measurement period. It should be noted that in the year 2013,

data were only available since August 2013 at SF. Therefore the accumulated GPP,  $R_{eco}$  and NEE were only compared during August and December in 2013 between the two sites, while the lower two plots show comparisons of full annual accumulative GPP,  $R_{eco}$  and NEE between the two sites (Figure 56).

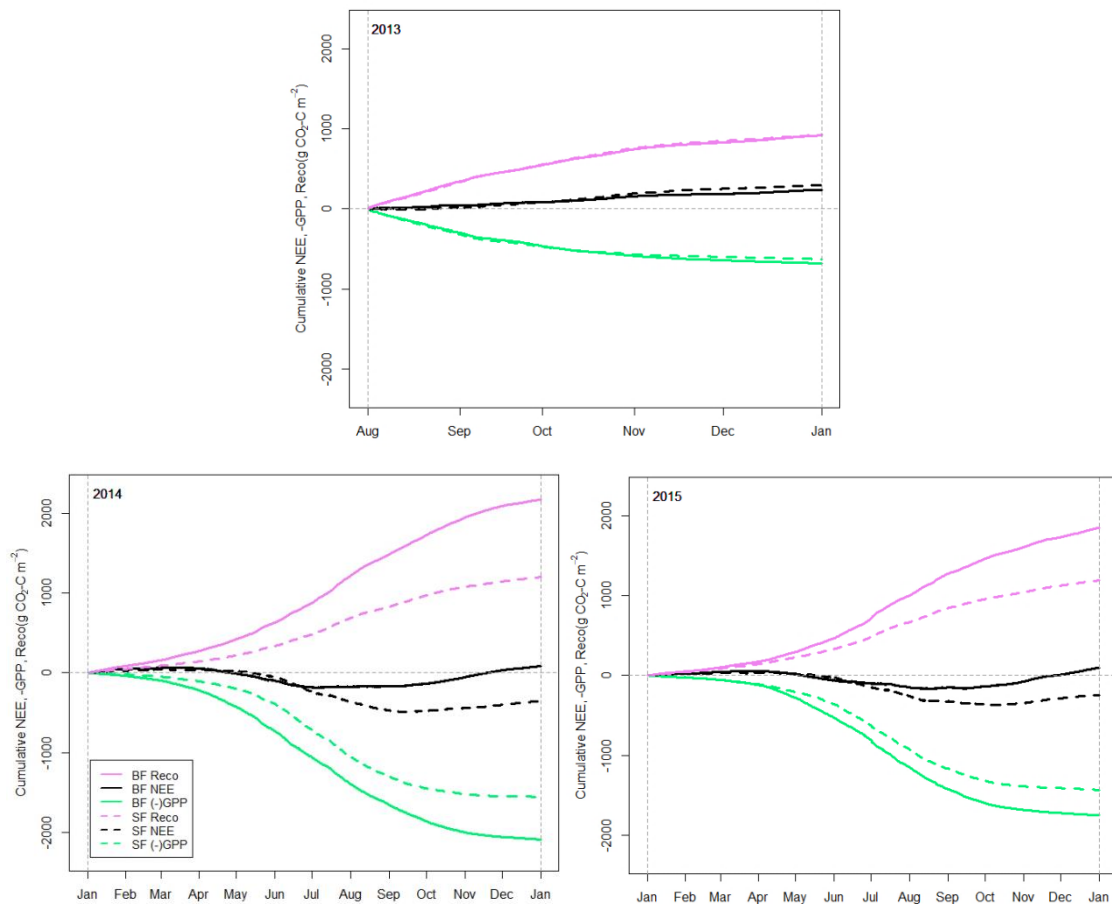


**Figure 56:** Comparison of accumulative net ecosystem  $\text{CO}_2$  exchange (NEE), ecosystem respiration ( $R_{eco}$ ) and gross primary production (GPP) in black, violet and green respectively, at two study sites (Baker's Fen and Sedge Fen) during the measurement period. The year 2013 only showed accumulative comparison between August and December since no data available before August 2013 at SF. The term  $-GPP$  is here the opposite of GPP and is introduced to facilitate graphical reading.

The accumulative comparisons show more clearly that the estimated GPP and  $R_{eco}$  at BF were larger than the estimated GPP and  $R_{eco}$  at SF during the whole year in 2014 and 2015 (Figure 56). The larger between-site differences in cumulated  $R_{eco}$  than the between-site differences in cumulated GPP result from differences in the annual  $\text{CO}_2$  budgets at the two study sites. The BF acted as a net source of  $\text{CO}_2$  in both years 2014 and 2015; while SF acted as a net atmospheric  $\text{CO}_2$  sink (Table 17). The net differences

in annual total GPP between two sites were 532.87 g CO<sub>2</sub>-C m<sup>-2</sup>yr<sup>-1</sup> in 2014 and 319.13 g CO<sub>2</sub>-C m<sup>-2</sup>yr<sup>-1</sup> in 2015 (Table 17). The net differences in annual total  $R_{eco}$  between two sites were larger than for GPP, with 973.33 g CO<sub>2</sub>-C m<sup>-2</sup>yr<sup>-1</sup> and 661.3 g CO<sub>2</sub>-C m<sup>-2</sup>yr<sup>-1</sup>, in 2014 and 2015, respectively (Table 17). Therefore the net differences in annual NEE between two sites are 440.47 ± 24.93 g CO<sub>2</sub>-C m<sup>-2</sup>yr<sup>-1</sup> in 2014 and 342.17 ± 28.56 g CO<sub>2</sub>-C m<sup>-2</sup>yr<sup>-1</sup> in 2015 (Table 17).

**Table 17:** The comparison of carbon balance between Baker’s Fen and Sedge Fen during the measurement period. No available data before August 2013 at SF, the total carbon balance between the period August and December for 2013, 2014 and 2015 are compared too.

	Carbon Balance (g C m <sup>-2</sup> )	
	BF	SF
2013 net ecosystem CO <sub>2</sub> exchange (NEE)	161.03 (±12.51)	--
2013 gross primary production (GPP)	1819.79	--
2013 ecosystem respiration ( $R_{eco}$ )	1980.81	--
2014 net ecosystem CO <sub>2</sub> exchange (NEE)	83.61 (±11.53)	-356.86 (±13.4)
2014 gross primary production (GPP)	2092.26	1559.39
2014 ecosystem respiration ( $R_{eco}$ )	2175.86	1202.53
2015 net ecosystem CO <sub>2</sub> exchange (NEE)	98.39 (±13.31)	-243.78(±15.25)
2015 gross primary production (GPP)	1756.28	1437.15
2015 ecosystem respiration ( $R_{eco}$ )	1854.67	1193.37
2013 net ecosystem CO <sub>2</sub> exchange (NEE) (Aug. - Dec.)	240.07 (±8.04)	297.59 (±9.16)
2013 gross primary production (GPP) (Aug. - Dec.)	681.52	629.96
2013 ecosystem respiration ( $R_{eco}$ ) (Aug. - Dec.)	921.59	927.55
2014 net ecosystem CO <sub>2</sub> exchange (NEE) (Aug. - Dec.)	259.72 (±7.47)	9.27 (±6.04)
2014 gross primary production (GPP) (Aug. - Dec.)	695.97	505.92
2014 ecosystem respiration ( $R_{eco}$ ) (Aug. - Dec.)	955.68	515.19
2015 net ecosystem CO <sub>2</sub> exchange (NEE) (Aug. - Dec.)	247.46 (±8.87)	16.89 (±10.24)
2015 gross primary production (GPP) (Aug. - Dec.)	604.40	506.92
2015 ecosystem respiration ( $R_{eco}$ ) (Aug. - Dec.)	851.86	523.81

The total GPP,  $R_{eco}$  and NEE during the period from August to December in 2013 are quite similar between the two sites (Figure 56). There are no significant differences between the total GPP,  $R_{eco}$  and NEE at BF during the period (August to December) over the three study years (Table 17). However, the total GPP during 2013 at SF was larger than in 2014 and 2015 (with a net difference of about  $123 \text{ g C m}^{-2}$ ), whereas the total  $R_{eco}$  during the period in 2013 was almost two times that of the total  $R_{eco}$  during the same periods in 2014 or 2015 (with a net difference about  $412 \text{ g C m}^{-2}$ ) (Table 17). Such large differences in total  $R_{eco}$  between August and December in 2013 at SF were associated with the warm and dry (low water levels) conditions at the site during that period.

### 7.3. Annual Carbon Dioxide Budget

BF acted as a net source of  $\text{CO}_2$  to the atmosphere in all three study years, emitting  $161.03 \pm 12.51$ ,  $83.61 \pm 11.53$  and  $98.39 \pm 13.31 \text{ g CO}_2\text{-C m}^{-2}\text{yr}^{-1}$  in 2013, 2014 and 2015, respectively (Table 17). SF acted as a net atmospheric  $\text{CO}_2$  sink in 2014 and 2015, at  $-356.86 \pm 13.4$  and  $-243.78 \pm 15.25 \text{ g CO}_2\text{-C m}^{-2}\text{yr}^{-1}$ , respectively (Table 17). Total  $\text{CO}_2$  loss at SF for the period August to December 2013 was estimated at  $297.59 \pm 9.16 \text{ g CO}_2\text{-C m}^{-2}\text{yr}^{-1}$  (Table 17). Based on the NEE estimates at SF during the last five months in 2013, it is likely that the SF was either close to  $\text{CO}_2$  neutral or a small net  $\text{CO}_2$  source in 2013. Although such a deduction cannot simply be assumed, the two study sites do show similar variations in their annual  $\text{CO}_2$  budgets over all three study years.

## 7.4. Discussion and Conclusion

Theoretically, peatland ecosystems are expected to function as CO<sub>2</sub> sinks as they accumulate a major part of the carbon fixed through photosynthesis into peat (Rydin & Jeglum, 2013). However, the exact CO<sub>2</sub> budget of the ecosystem will depend on the climate conditions, vegetation types and land management of the site, and it is difficult to predict if the ecosystem is in equilibrium (e.g. following restoration) (Dröslér *et al.*, 2008).

In addition to climatic conditions (described in Chapter 5 & 6), site management plays an important role in influencing the environmental conditions and vegetation types, and therefore the ecosystem C budget (Herbst *et al.*, 2013). Hendriks *et al.* (2007) reported a consistent CO<sub>2</sub> uptake between -232 and -446 g C m<sup>-2</sup>yr<sup>-1</sup> from a restored (rewetting) grassland peatland. In contrast, Jacobs *et al.* (2007) observed an unexpected large CO<sub>2</sub> emission of 220±90 g C m<sup>-2</sup>yr<sup>-1</sup> on average for four grassland peatlands with relatively high water levels with / without management. However, Hatala *et al.* (2012) reported that a grazed degraded (former drained but not yet restored) peatland in California emitted up to 300 g C m<sup>-2</sup>yr<sup>-1</sup> as CO<sub>2</sub> and 3 g C m<sup>-2</sup>yr<sup>-1</sup> as CH<sub>4</sub> to the atmosphere. This is consistent with reports of European drained grasslands on peat soils that always act as net CO<sub>2</sub> sources due to peat decomposition (Elsgaard *et al.*, 2012; Maljanen *et al.*, 2010). The rewetting (restoration) of such sites can be considered as an improvement with respect to the CO<sub>2</sub> balance in such ecosystems as it will likely reduce CO<sub>2</sub> emission to the atmosphere.

The two sites in this study, one being a rewetting (regenerating) grassland on peat soils (BF), and the other a nearly undisturbed sedge peatland (SF), are in the same area of Wicken Fen NNR. Therefore, they experience similar climatic conditions (see Section 5.1). The different land status and land management and, therefore, different vegetation types, soil temperature and soil water content *etc.* on the two sites are the main factors influencing the C balance between ecosystem and atmosphere. The most notable environmental difference between the two sites is the contrasting hydrological conditions, with SF experiencing year-round higher water levels (see Section 7.1). The

similar regression equations for CO<sub>2</sub> flux components explained by measured environmental factors between the two study sites indicated that the two ecosystems were comparable in terms of underlying environmental controls. However, the different coefficients of the regression equations for the different sites gives an indication that the relative importance of the environmental factors in defining CO<sub>2</sub> flux seems to be site specific (Juszczak *et al.*, 2013).

The impacts of ground water levels on the CO<sub>2</sub> fluxes in peatland ecosystems remain under discussion in the literature. Lloyd (2006) determined a linear reduction in R<sub>10</sub> (respiration rate at 10 °C; Lloyd & Taylor, 1994) with raising water levels which is consistent with theory and expectations (Drösler *et al.*, 2008). In contrast, some other research has reported no influence of water levels on *R<sub>eco</sub>* (Elsgaard *et al.*, 2012; Parmentier *et al.*, 2009). However, in this study, water levels (and therefore the different soil temperatures and soil water contents due to the different water levels) showed a strong influence on the *R<sub>eco</sub>* at both sites (Table 9 & 14), and therefore influenced the CO<sub>2</sub> balance of both ecosystems. This was particularly clearly shown at the SF site during the prolonged drought conditions of 2013 when the total *R<sub>eco</sub>* was much larger (at 927.55 g C m<sup>-2</sup>) during August and December in 2013 than the total *R<sub>eco</sub>* in 2014 and 2015 for the same period (at 515.19 and 523.81 g C m<sup>-2</sup>, respectively). These differences were closely associated with the much lower water table during the same measurement period in 2013. Notably, there were no significant differences in annual total *R<sub>eco</sub>* at BF between any of the three study years. However, the position of the water table had a strong influence on the seasonal course of *R<sub>eco</sub>*, and therefore the NEE, at both sites. For example, the *R<sub>eco</sub>* values for July and August 2013 at BF were much higher than for the same period during 2014 and 2015. Under similar climatic conditions, water levels are therefore one of the main factors influencing the *R<sub>eco</sub>* at the two study sites, i.e. the BF with a much lower water table compared to SF during all years had a relatively lower *R<sub>eco</sub>* over the whole measurement period. This is also consistent with the results of the regression analysis that *R<sub>eco</sub>* was significantly correlated with WT followed by *T<sub>air</sub>* and VPD on both sites (Table 9 & 14).

The different vegetation types at the two study sites play an important role in influencing photosynthesis and, therefore, the GPP and NEE of the ecosystems, as is

evident from Figure 55. Under the same climatic conditions and even with similar water tables from the beginning of the year in both 2014 and 2015, the monthly total GPP showed an earlier increase and a later decrease before / after the growing season at BF than at SF. This is consistent with the characteristics of an evergreen grassland, since the small grass buds will start to grow as soon as the temperature reaches their requirements, while the grass only stops growing when the temperature reaches their lower limits for growth in winter (Alward *et al.*, 1999; Tilman *et al.*, 2006). In contrast, the sedge-dominated vegetation at SF showed a much shorter growing period, but nevertheless resulted in a higher total GPP at SF compared to BF. Vegetation cutting could be another major influencing factor on the C budget of the sedge-dominated SF ecosystem, although there were no cutting events at this site during the measurement period. Nevertheless, the site management regime implemented by the NT means that the SF will have sedge cutting taking place every 3 to 5 years and the influence of this activity (i.e. biomass removal, with potentially a different vegetation growth rate after cutting) would be an interesting issue to address in future studies at this site.

Grazing can be another factor influencing the CO<sub>2</sub> fluxes from a land management perspective. However, it remains unclear to what extent the animals that graze at the BF study site contributed to the reduction in net CO<sub>2</sub> uptake compared to the more undisturbed SF site. Some research has suggested that some unexpected CO<sub>2</sub> fluxes (emissions) may well have a relationship with grazing animals according to flux footprint analysis (Baldocchi *et al.*, 2012; Herbst *et al.*, 2011). In their study, Herbst *et al.* (2013) suggested that the respiration of grazing animals may well have had a relationship with the reduction in daytime maximum NEE (less negative).

Herbst *et al.* (2013) also proposed that, at their study sites, the inter-annual CO<sub>2</sub> flux variability is determined by the growing season length (vegetation type), cutting frequency and grazing intensity, but not the changes in water table and temperature.

In conclusion, these results suggest that land management such as water level control and grazing have a strong influence on the CO<sub>2</sub> fluxes (on CH<sub>4</sub> fluxes too, see Chapter 5) between the ecosystem and atmosphere, although there are several other land management regimes (i.e. mowing) that also may well have an influence on the C

balance of the fen ecosystem (Herbst *et al.*, 2013; Veenendaal *et al.*, 2007). It is important to maintain an appropriate height of water level to prevent carbon losses from peatland ecosystems to the atmosphere as CO<sub>2</sub>. However, the enhanced CH<sub>4</sub> emissions from the ecosystem to the atmosphere due to the high water levels also needs to be considered carefully before setting the restoration regime. A compromise may be to bring the water table close to the fen peat surface, thus reducing CO<sub>2</sub> emissions while simultaneously providing a shallow near-surface aerobic zone to limit CH<sub>4</sub> emissions.

Evidence from field observation studies, long-term experiments and modeling research consistently suggests that land management and land use change significantly affect soil C stocks (Ostle *et al.*, 2009). Data from Dawson & Smith (2007) indicated that the loss of soil C occurred when peatland, grasslands and forestry had been converted to arable lands; in contrast, the conversion of croplands into native ecosystems resulted in soil carbon gains (Table 18).

**Table 18:** Potential changes in soil carbon storage resulting from land use change. Positive value indicates soil carbon losses; negative value indicates soil carbon gains (Data from Dawson & Smith, 2007).

Land use change	Annual carbon budget (g C m <sup>-2</sup> yr <sup>-1</sup> )
Arable to grassland (50 years)	-30 ~ -80
Arable to grassland (35 years)	-60
Arable to grassland (15-25 years)	-30 ~ -190 ( $\pm 60$ )
Arable to permanent pasture	-30
Arable to forestry (115 years)	-50
Arable to forestry (25 years)	-30 ~ -60
Grassland ~ afforestation (90 years)	-10 $\pm$ 2
Grassland ~ arable	100 ~ 170
Forestry ~ arable	60
Forestry ~ grassland	10 $\pm$ 10
Peatland ~ cultivation	220 ~ 540
Wetland ~ arable	100 ~ 1900
Re-vegetation on abandoned arable	-30 ~ -60
Re-vegetation on wetlands from arable	-220 ~ -460
Re-vegetation on wetlands from grassland	-80 ~ -390

As a former arable regenerating fen, BF showed a net CO<sub>2</sub> emission reduction in 2014 and 2015 compared to drained and continuously cultivated fens in the UK (a reduction of 25.33 ± 5.58 and 10.55 ± 3.8 g CO<sub>2</sub>-C m<sup>-2</sup>yr<sup>-1</sup> in 2014 and 2015 respectively, compared with an average annual emission of 108.94 ± 17.11 g CO<sub>2</sub>-C m<sup>-2</sup>yr<sup>-1</sup>; Evans *et al.*, 2011), demonstrating the benefits of changing land use from arable to native ecosystems from a C store perspective. However, as a regenerating fen peatland, the BF site did not show a clear trend of converting to a net CO<sub>2</sub> sink, with no clear evidence of an increasing presence of peat forming vegetation species during the study years. While the appearance of aerenchymous wetland plants, i.e. *Juncus* species (a typical wetland species), on BF could be taken as an indication that restoration was moving in a desirable ecological direction on the site, the majority of the site remained dominated by agricultural grasses rather than characteristic wetland species. It is also worth noting that the carbon losses that result from land use changes can happen rapidly, within years, but are extremely difficult to reverse in the short term. Therefore, restoration activities in peatlands, that are expected to re-establish the C sink function of the disturbed ecosystem, require much longer periods before they become fully effective (Page *et al.*, 2009; Schumann & Joosten, 2008). Hendricks *et al.* (2007) indicated that a restored temperate peat soil grassland functioned as a net C sink storing -232 ~ -446 g CO<sub>2</sub>-C m<sup>-2</sup>yr<sup>-1</sup> after more than 10 years restoration, which is in the same range of CO<sub>2</sub> annual budget as the SF site (i.e. a comparably nearly undisturbed temperate fen). Successful restoration of peatland ecosystems as presented by Hendricks *et al.* (2007) indicates the possibility that the C sink function of a disturbed peatland ecosystem (e.g. BF site) can be re-established, with gradual transformation to an analogue native ecosystem (e.g. SF site) although the time scale may be quite long. Therefore, such successful restoration can potentially increase and protect existing soil C stocks and future sequestration.

Land management and land use change are two of the most important short-term determinants of C stocks and sequestration of an ecosystem (Ostle *et al.*, 2009). Land management policy needs to include strategies to prevent or reduce soil C losses as a result of land use changes. In peatland ecosystems, particularly, soil C stocks can be

maintained and increased by halting drainage for agriculture (Haigh, 2006), maintaining an appropriate height of water level (Waddington & Price, 2000), reducing grazing intensity (Ward *et al.*, 2007), and species management for enhanced C stocks (Fisher *et al.*, 1994).

## **Chapter 8**

# **Conclusions, Research Limitations and Outlook**

## 8.1. Thesis Conclusions

This thesis presents the first long-term direct C flux measurements for a temperate lowland fen peatland in East Anglia. The dynamics and magnitude of CO<sub>2</sub>, H<sub>2</sub>O, CH<sub>4</sub> and energy fluxes were quantified by measurements using the EC technique at two monitoring sites at a regenerating and a semi-natural fen at Wicken Fen NNR, Cambridgeshire. This Ph.D. project presented an opportunity to investigate ecosystem responses to climate variability and the impact of wetland restoration measures by comparing two different land-use types in a fen peatland. The research results will lead to a better quantitative understanding of the relationships between fen peatlands and global change, and the opportunities for GHG emissions mitigation arising from restoration rewetting of fen peatlands formerly under arable agriculture.

**Chapter 5** presented long-term measurements of CO<sub>2</sub> and CH<sub>4</sub> fluxes at a lowland temperate fen that had been restored after a long history of agricultural use. These are believed to be the first measurements of their kind in both the UK and temperate Europe. Several conclusions were drawn in response to, and extending beyond the defined research objectives of this chapter:

- ✓ The regenerating site (BF) functioned as a net source of CO<sub>2</sub> in all three measurement years, emitting  $161.03 \pm 12.51$  g CO<sub>2</sub>-C m<sup>-2</sup>yr<sup>-1</sup> in 2013,  $83.61 \pm 11.53$  g CO<sub>2</sub>-C m<sup>-2</sup>yr<sup>-1</sup> in 2014, and  $98.39 \pm 13.31$  g CO<sub>2</sub>-C m<sup>-2</sup>yr<sup>-1</sup> in 2015 to the atmosphere.
- ✓ The regenerating site (BF) functioned as a net source of CH<sub>4</sub> over the measurement period, emitting  $6.067 \pm 0.096$  g CH<sub>4</sub>-C m<sup>-2</sup>yr<sup>-1</sup> in 2013,  $2.009 \pm 0.087$  g CH<sub>4</sub>-C m<sup>-2</sup>yr<sup>-1</sup> in 2015 and  $2.845 \pm 0.103$  g CH<sub>4</sub>-C m<sup>-2</sup> between 8<sup>th</sup> April and 31<sup>st</sup> December in 2014 to the atmosphere.
- ✓ The regenerating site (BF) exerted a positive forcing (net warming) on the global climate of  $792.67$  g CO<sub>2</sub> m<sup>-2</sup> in 2013,  $401.38$  g CO<sub>2</sub> m<sup>-2</sup> in 2014 and

427.75 g CO<sub>2</sub> m<sup>-2</sup> in 2015, over a 100 year time horizon (the CH<sub>4</sub> budget in 2014 only accounted for the period between 8<sup>th</sup> April to 31<sup>st</sup> December). CH<sub>4</sub> contributed 16% - 26% of the total positive forcing.

- ✓ The regenerating site (BF) showed a net CO<sub>2</sub> emissions reduction in 2014 and 2015 compared to drained and continuously cultivated fens in the UK, demonstrating the benefits of rewetting.
- ✓ The results give an indication that the timing of water availability and adequate temperature potentially have a major role compared to total seasonal precipitation and seasonal temperature in influencing land / atmosphere CO<sub>2</sub> exchanges in the fen ecosystem, especially during the growing season.
- ✓ Grazing ruminating animals and waterlogged ditches may act as methane hotspots, and play an important role in enhancing CH<sub>4</sub> emissions from the fen ecosystem to the atmosphere.
- ✓ The vegetation community of species with well-developed aerenchymous tissues (*Juncus* spp.) may play an important role as a 'shunt' for CH<sub>4</sub> emissions from the soil to the atmosphere.

**Chapter 6** presents long-term direct flux measurements of land / atmosphere CO<sub>2</sub> exchange at a nearly undisturbed lowland temperate fen peatland. The following conclusions were drawn:

- ✓ The semi-natural site (SF) functioned as a net sink of atmospheric CO<sub>2</sub> in 2014 and 2015, with annual sums of -356.86±49.13 g CO<sub>2</sub>-C m<sup>-2</sup>yr<sup>-1</sup> in 2014 and -243.78±15.25 g CO<sub>2</sub>-C m<sup>-2</sup>yr<sup>-1</sup> in 2015.
- ✓ The semi-natural site (SF) functioned as a net source of atmospheric CO<sub>2</sub> during the period between 1<sup>st</sup> August and 31<sup>st</sup> December in 2013 with a total CO<sub>2</sub> budget of 297.59±9.16 g CO<sub>2</sub>-C m<sup>-2</sup> period<sup>-1</sup>. The ecosystem likely acted as even a small source of atmospheric CO<sub>2</sub> in the drier year of 2013.

- ✓ The semi-natural site (SF) had a negative GWP (net cooling) over the investigated time period, at  $-1308.5 \pm 49.13 \text{ g CO}_2 \text{ m}^{-2}$  in 2014 and  $-893.86 \pm 55.92 \text{ g CO}_2 \text{ m}^{-2}$  in 2015 over 100-year time horizons (CO<sub>2</sub> only).
- ✓ The large inter-annual variability in CO<sub>2</sub> exchange on the site indicates the sensitivity of the nearly undisturbed site to annual and seasonal changes in climatic conditions.
- ✓ The large CO<sub>2</sub> losses during warm and dry conditions (low water level) in 2013 highlight the importance of maintaining an appropriate water level height to prevent carbon losses from this relatively undisturbed peatland to the atmosphere as CO<sub>2</sub>.

In **Chapter 7**, the long-term direct flux measurements of land / atmosphere CO<sub>2</sub> exchange at two lowland temperate fens in the same nature reserve provide a good basis for comparing the CO<sub>2</sub> fluxes from lowland temperate fens with different land-use types under similar climate conditions. This results in the following conclusions:

- ✓ The position of the water table showed a strong influence on the  $R_{eco}$  at both sites, therefore influencing the land / atmosphere CO<sub>2</sub> exchange at both ecosystems.
- ✓ The differences in dominant vegetation species resulting in different photosynthesis processes play an important role in influencing the GPP and therefore the land / atmosphere CO<sub>2</sub> exchange of the two sites.
- ✓ The other land management regimes (i.e. grazing, mowing) may well play an important role in influencing the C balance on the ecosystems and should be investigated further in subsequent studies.

In general, the BF site still is a source of GHGs to the atmosphere after more than twenty years of conservation management. Conservation management of the SF site is, in most years, ensuring that it operates as a C sink. But water supply, particularly during dry summer periods, is a key concern that can reduce the C sink function or convert the fen to a small source. The dominant environmental controls on C balance at both sites are temperature and water table height; both the timing of water availability and adequate temperatures during the main growing season potentially have major roles. This is a key finding and one that is supported by other studies (e.g. Couwenberg, 2011; Jauhiainen *et al.*, 2016; Wilson *et al.*, 2016). Methane emissions increase with increasing WT; ditches are also hotspots for methane emissions (e.g. Peacock *et al.*, 2016) as are ruminating livestock (e.g. Baldocchi *et al.*, 2012; Dengel *et al.*, 2011; Herbst *et al.*, 2011) and aerenchymous plants (e.g. Brix *et al.*, 2001; Levy *et al.*, 2012). And ideal management scenario for both BF and SF might be to maintain the WT as close to the peat surface as possible without causing waterlogging and to reduce the area of open ditches. Producing complete C balance for these sites would require additional study of fluvial C losses that were outwith this study. But even without this, it is possible to conclude that rewetting of BF is moving in the right direction, since it is reducing GHG emissions compared to intensively farmed peat soils. A critical management issue is maintaining high water levels throughout the year.

The restoration status of BF following rewetting could have been / still be influenced by pre-rewetting climate and hydrological boundary conditions, nutrient status, previous land use history, restoration time period, and vegetation status (Jauhiainen *et al.*, 2016). For example, CH<sub>4</sub> emissions of former agricultural land after rewetting can be much higher than from other previous land use types (Harpenslager *et al.*, 2015; Hendricks *et al.*, 2007). However, the BF site did not show particularly high CH<sub>4</sub> emissions during the measurement period. This could be explained by rewetting seeming to result in high initial CH<sub>4</sub> emissions that decline over time on nutrient rich sites as the plant litter inundated during rewetting activities is decomposed (Augustin *et al.*, 2012; Limpens *et al.*, 2008). Although CO<sub>2</sub> emissions will have reduced immediately upon rewetting, the recovery period for reactivation of the sink function typical of an un-drained organic soil may vary from several years to many decades (Bonn *et al.*, 2016; Samaritani *et al.*, 2011; Tuittila *et al.*, 1999; Wilson *et al.*, 2013).

Re-establishment of the peat-forming vegetation and a high vegetation biomass on rewetting sites are necessary to restore the pre-reclamation peat function that ultimately leads to long-term C sequestration in the soil (Jauhiainen *et al.*, 2016). Therefore, the best prognosis for peatland restoration is likely to maintain a sufficiently high WT to minimize CO<sub>2</sub> emissions from aerobic decomposition while also establishing high-biomass peat-forming vegetation cover. As a result, although a site such as BF can remain a CO<sub>2</sub> source during the first years after rewetting, over longer time frames (a few decades), this type of site could be expected to eventually approach a steady state C sequestration rate typical of un-drained sites (Petrone *et al.*, 2003; Waddington *et al.*, 2010; Wilson *et al.*, 2016). Given the importance of these findings for global climate policy, this study supports the view that rewetting and restoration of drained organic soils should be included in greenhouse gas emission mitigation strategies (IPCC, 2014b; Joosten *et al.*, 2012).

## 8.2. Research Limitations and Future Research Outlook

It is important to recognise the limitations in the current research, and equally important to address those issues in future research in order to ensure methodological and practical improvements.

### 8.2.1. Ancillary Measurements

During the measurement period, not all supporting environmental measurements were available at the study sites. To build a complete EC measurement station, more ancillary environmental measurements (e.g. of soil temperature, soil water content) should be obtained at the sites in support of on-going research.

No ecosystem phenological data were included in this study. Future research would be improved by acquisition of phenological data such as MODIS, EVI, LAI, aboveground biomass *etc.* at a site scale to enable more effective interpretation of the flux results.

### 8.2.2. Other Carbon and GHG Fluxes

At an ecosystem scale, the net ecosystem carbon budget (NECB) represents the total rate of organic C flux in the ecosystem. The net flux of several forms of C contributing to NECB are the flux of CO<sub>2</sub>, CO, CH<sub>4</sub> and other fluvial gains / losses of C (i.e. DOC, DIC, VOC and PC) (Billett *et al.*, 2010; Dinsmore *et al.*, 2010). As another important GHG, the land / atmosphere exchange of N<sub>2</sub>O is also as important as the other GHGs (i.e. CO<sub>2</sub> and CH<sub>4</sub>) from a climate change perspective.

This study only included measurements of CO<sub>2</sub> fluxes at SF, and CO<sub>2</sub> and CH<sub>4</sub> fluxes at BF. Theoretically, the SF site may act as a net source of CH<sub>4</sub> during warm periods with high water levels. It is likely that SF can also maintain CH<sub>4</sub> emissions during dry periods due to the presence of deep-rooted “shunt” species (i.e. *Phragmites australis*). The emission of CH<sub>4</sub> to the atmosphere could nullify the cooling influence of the CO<sub>2</sub> emissions at SF during the measurement period. Emissions of N<sub>2</sub>O could be locally high at BF because of the presence of grazing animals (Couwenberg *et al.*, 2011; Couwenberg, 2011). Therefore, to obtain a full understanding of the GHG budget of both sites, it would be necessary to include measurements of CH<sub>4</sub> and N<sub>2</sub>O.

To gain a better understanding of full C and GHG balance of the ecosystem, future research should aim to capture the full C and GHG exchange between ecosystem and atmosphere.

### 8.2.3. Station Maintenance

It was not possible to calibrate all the instruments at a desired frequency during the study period. The lack of calibration could directly influence the quality of the flux measurements as well as other ancillary measurements. A yearly or 6-monthly factory calibration is strongly recommended for future studies. However, a factory calibration may take several weeks, in which case replacement instruments are required for backup. Regular *in situ* calibrations for some instruments (i.e. *in situ* calibrations of LI-7500A H<sub>2</sub>O channels by dew point generator) and cross-calibrations of instruments from two sites are also recommended for future study.

The low data coverage during the winter time, and especially during winter nights, occurred at both sites due to insufficient power supply. This issue could be improved by upgrading of the power systems at both sites. To ensure sufficient power supply during winter, changing the angle of the solar panels according to the solar altitude angle and regular battery maintenance are recommended for future study.

### 8.2.4. Spatial Heterogeneity and Representativeness

The EC measurements only provide measurements at the ecosystem scale, but the flux dynamics at scales below that of the EC footprint have not been included in this study. There are many chamber studies that suggest that measurements of gaseous C exchanges can show large temporal and spatial variability (e.g. Becker *et al.*, 2009; Bubier *et al.*, 2003; Teh *et al.*, 2011); and the heterogeneity of the study site can strongly influence the gaseous C exchange at the ecosystem scale (Cai *et al.*, 2010; Laine *et al.*, 2006; Riutta *et al.*, 2007). Small scale chamber measurements combined with comprehensive footprint modelling are strongly recommended for future studies in order to gain a better understanding of the source and contribution of the gaseous C fluxes in the fen ecosystem. Chamber measurements also can improve the data gap-filling and partitioning of EC flux results, and provide data on which to separate

autotrophic and heterotrophic respiration (Jauhiainen *et al.*, 2011; Reichstein *et al.*, 2005).

The GHG (e.g. CO<sub>2</sub>, CH<sub>4</sub>) fluxes can be quite different in similar ecosystems due to different land management activities (i.e. mowing, grazing and regulation of water table); therefore the representativeness of the study sites and the opportunity to transfer knowledge to other similar ecosystems is still uncertain (Schrier-Uijl *et al.*, 2009). To assess the transferability of our results to other similar ecosystems, further study would require additional EC flux measurements in similar, i.e. fenland, ecosystems and under similar climate conditions.

#### 8.2.5. Up-scaling of Observation Results

A spatial modelling based on the observation of GHG fluxes can be a potential research direction for future study (e.g. Papale & Valentini, 2003; Xiao *et al.*, 2012). Such analysis requires longer term and spatially-comprehensive measurements crossing a range of soil conditions, vegetation types and land management regimes in the region with land cover remote sensing information and land surface models (Reichstein *et al.*, 2007; Smith *et al.*, 2012). A predictive model can be used for calculating GHG fluxes under certain climatic and environmental conditions (Smith *et al.*, 2012).

# Reference

- Acreman, M.C., Harding, R.J., Lloyd, C.R. and McNeil, D.D. (2003). Evaporation characteristics of wetlands: Experience from a wet grassland and a reedbed using eddy correlation measurements. *Hydrology and Earth System Sciences*, **7**: 11-21.
- Acreman, M.C., Fisher, J., Stratford, C.J., Mould, D.J. and Mountford, M.O. (2007). Hydrological science and wetland restoration: some case studies from Europe. *Hydrology and Earth System Sciences*, **11**:158-169.
- Acreman, M. C. & Jos é P. (2000). Wetlands. In: Acreman, M. (Eds.). *The Hydrology of the UK: A Study of Change*. Routledge.
- Adkinson, A.C., Syed, K.H. and Flanagan, L. (2011). Contrasting responses of growing season ecosystem CO<sub>2</sub> exchange to variation in temperate and water table depth in two peatlands in northern Alberta, Canada. *Journal of Geophysical Research*, **116**: 1-17.
- Alward, R.D., Detling, J.K. and Milchunas, D.G. (1999). Grassland vegetation changes and nocturnal global warming. *Science*, **283**(5399): 229-231.
- Anglian Water Services Limited. (2007). *Strategic Direction Statement 2010 - 2035*.
- Aslan-Sungur, G., Lee, X.H., Evrendilek, F. and Karakaya, N. (2016). Large inter-annual variability in net ecosystem carbon dioxide exchange of a disturbed temperate peatland. *Science of the Total Environment*, **554**: 192-202.
- Aubinet, M., Grelle, A., Ibrom, A., Rannik, U. and Moncrieff, J. (2000). Estimates of the annual net carbon and water exchange of forests: the EUROFLUX methodology. *Advances in Ecological Research*, **30**: 113-175.
- Aubinet, M., Vesala, T. and Papale, D. (Eds.). (2012). *Eddy Covariance: A Practical Guide to Measurement and Data Analysis*. Springer, Dordrecht.
- Augustin, J., Merbach, W., Schmidt, W. and Reining, E. (1996). Effect of changing temperature and water table on trace gas emission from minerotrophic mires. *Angewandte Botanik*, **70**: 45-51.
- Augustin, J., Couwenberg, J. and Minke, M. (2012). Peatlands and greenhouse gases. In: Tanneberger, F. & Wichtmann, W. (Eds.) *Carbon Credits From Peatlands Rewetting. Climate – Biodiversity – Land Use*. Schweizerbart, Stuttgart, 13-19.
- Aurela, M., Laurila, T. and Tuovinen, J-P. (2002). Annual CO<sub>2</sub> balance of a subarctic fen in northern Europe: Importance of the wintertime efflux. *Journal of Geophysical Research*, **107**(D21): 4607.
- Aurela, M., Lohila, A., Tuovinen, J.P., Hatakka, J., Riutta, T. and Laurila, T. (2009). Carbon dioxide exchange on a northern boreal fen. *Boreal Environment Research*, **14**: 699-710.
- Badiou, P., McDougal, R., Pennock, D. and Clark, B. (2011). Greenhouse gas emissions and carbon sequestration potential in restored wetlands of the Canadian prairie pothole region. *Wetlands Ecology and Management*, **19**: 237-256.

- Baird, A.J., Holden, J. and Chapman, P. (2009). A Literature Review of Evidence on Emissions of Methane in Peatlands. DEFRA Project: SPO574.
- Baird, A.J., Belyea, L.R., Comas, X., Reeve, A.S. and Slater, L.D. (Eds.). (2009). *Carbon Cycling in Northern Peatlands*. American Geophysical Union, Washington, DC, USA.
- Baldocchi, D.D. (2003). Assessing the eddy covariance technique for evaluating carbon dioxide exchange rates of ecosystems: past, present and future. *Global Change Biology*, **9**: 479-492.
- Baldocchi, D.D. (2008). Breathing of the terrestrial biosphere: lessons learned from a global network of carbon dioxide flux measurement system. *Australian Journal of Botany*, **56**(1): 1.
- Baldocchi, D.D., Hincks, B.B. and Meyers, T.P. (1988). Measuring Biosphere-Atmosphere Exchanges of Biologically Related Gases with Micrometeorological Methods. *Ecology*, **69**: 1331-1340.
- Baldocchi, D.D., Valentini, R., Running, S., Oechel, W. and Dahlman, R. (1996). Strategies for measuring and modelling carbon dioxide and water vapour fluxes over terrestrial ecosystems. *Global Change Biology*, **2**: 159-168.
- Baldocchi, D.D., Falge, E., Gu, L., Olson, R., Hollinger, D., Running, S., Anthoni, P., Bernhofer, C., Davis, K. and Evans, R. (2001a). FluxNet: A new tool to study the temporal and spatial variability of ecosystem-scale carbon dioxide, water vapour, and energy flux densities. *Bulletin of the American Meteorological Society*, **82**(11): 2415-2434.
- Baldocchi, D.D., Falge, E. and Wilson, K. (2001b). A spectral analysis of biosphere-atmosphere trace gas flux densities and meteorological variables across hour to multi-year time scales. *Agricultural and Forest Meteorology*, **107**(1): 1-27.
- Baldocchi, D.D., Detto, M., Sonnentag, O., Verfaillie, J., Teh, Y. A., Silver, W. and Kelly, N.M. (2012). The challenges of measuring methane fluxes and concentrations over a peatland pasture. *Agricultural Forest Meteorology*, **153**: 177-187.
- Balzarolo, M., Anderson, K., Nichol, C., Rossini, M., Vescovo, L., Arriga, N., Wohlfahrt, G., Calvet, J.C., Carrara, A., Cerasoli, S., Cogliati, S., Daumard, F., Eklundh, L., Elbers, J.A., Evrendilek, F., Handcock, R.N., Kaduk, J., Klumpp, K., Longdoz, B., Matteucci, G., Meroni, M., Montagnani, L., Ourcival, J.M., Sanchez-Canete, E.P., Pontauiller, J.Y., Juszczak, R., Scholes, B. and Martin, M.P. (2011). Ground-based optical measurements at European flux sites: a review of methods, instruments and current controversies. *Sensors*, **11**(8): 7954-7981.
- Becker, T., Kutzbach, L., Forbrich, I., Schneider, J., Jager, D., Thees, B. and Wilmking, M. (2009). Do we miss the hot spots? The use of very high resolution aerial photographs to quantify carbon fluxes in peatlands. *Biogeosciences*, **5**: 1387-1393.
- Bengtson, P. & Bengtsson, G. (2007). Rapid turnover of DOC in temperate forests accounts for increased CO<sub>2</sub> production at elevated temperatures. *Ecology Letter*, **10**: 783-790.
- Bernal, B. & Mitsch, W.J. (2012). Comparing carbon sequestration in temperate freshwater wetland communities. *Global Change Biology*, **18**: 1636-1647.
- Bernal, B. & Mitsch, W.J. (2013). Carbon sequestration in two created riverine wetlands in the Midwestern United States. *Journal of Environmental Quality*, **42**: 1236-1244.
- Billett, M.F., Charman, D.J., Clark, J.M., Evans, C.D., Ostle, N.J., Worrall, F., Burden, A., Dinsmore, K.J., Jones, T., McNamara, N.P., Parry, L., Rowson, J.G. and Rose, R. (2010). Carbon balance of UK peatlands: current state of knowledge and future research challenges. *Climate Research*, **45**: 13-29.

- Blackman, F.F. (1905). Optima and limiting factors. *Annals of Botany*, **19**: 281-295.
- Blodau, C. (2002). Carbon cycling in peatlands – a review of processes and controls. *Environmental Review*, **10**: 111-134.
- Blodau, C. & Moore, T.R. (2003). Experimental response of peatland carbon dynamics to a water table fluctuation. *Aquatic Sciences*, **65**: 47-62.
- Bonan, G.B. (2008). Forests and climate change: forcing, feedbacks, and the climate benefits of forests. *Science*, **320**: 1444-1449.
- Bonn, A., Allott, T., Evans, M., Joosten, H., Stoneman, R. and Marton-Lefevre, J. (2016). *Peatland Restoration and Ecosystem Services: Science, Policy and Practice*. Cambridge University Press, U.K.
- Bradley, R.I. (1997). Carbon loss from drained lowland fens. In: Canell, M.G.R. (Eds.). *Carbon Sequestration in Vegetation and Soils*. London, Department of Environment.
- Brix, H., Sorrell, B.K. and Schierup, H.H. (1996). Gas fluxes achieved by in situ convective flow in *Phragmites australis*. *Aquatic Botany*, **54**(2-3): 151-163.
- Brix, H., Sorrel, B.K. and Lorenzen, B. (2001). Are Phragmites-dominated wetlands a net source or net sink of greenhouse gases? *Aquatic Botany*, **69**: 313-324.
- Brooks, K.N. (1992). Surface hydrology. In: Wright Jr., H.E., Coffin, B.A. and Asseng, N.E.P. (Eds.), *The patterned peatlands of Minnesota*, University of Minnesota Press, St. Paul.
- Bubier, J.L., Moore, T.R. and Roulet, N.T. (1993). Methane emissions from wetlands in the mid-boreal region of northern Ontario Canada. *Ecology*, **74**: 2240-2254.
- Bubier, J.L., Moore, T.R., Bellisario, L., Comer, N.T. and Crill, P.M. (1995). Ecological controls on methane emissions from a northern peatland complex in the zone of discontinuous permafrost, Manitoba, Canada. *Global Biogeochemical Cycles*, **9**: 455-470.
- Bubier, J.L., Bhatia, G., Moore, T.R., Roulet, N.T. and Lafleur, P.M. (2003). Spatial and temporal variability in growing-season net ecosystem carbon dioxide exchange at a large peatland in Ontario, Canada. *Ecosystems*, **6**: 353-367.
- Bullock, A. & Acreman, M. (2003). The role of wetlands in the hydrological cycle. *Hydrology and Earth System Sciences*, **7**: 358-389.
- Burba, G. (2013). *Eddy Covariance Method: for Scientific, Industrial, Agricultural, and Regulatory Applications*. LI-COR Biosciences, Lincoln, USA.
- Burba, G. & Anderson, D. (2010). *A Brief Practical Guide to Eddy Covariance Flux Measurements: Principles and Workflow Examples for Scientific and Industrial Applications*. LI-COR Biosciences, Lincoln, USA.
- Byrne, K.A., Chojnicki, B., Christensen, T.R., Drösler, M., Freibauer, A., Friborg, T., Froelking, S., Lindroth, A., Mailhammer, J., Malmer, N., Selin, P., Turunen, J., Valentini, R. and Zetterberg, L. (2004). EU peatlands: Current carbon stocks and trace gas fluxes. *CarbonEurope-GHG Concerted Action-Synthesis of the European Greenhouse Gas Budget, Report 4/2004*, CarboEurope.
- Cai, T., Flanagan, L.B. and Syed, K.H. (2010). Warmer and drier conditions stimulate respiration more than photosynthesis in a boreal peatland ecosystem: Analysis of automatic chambers and eddy covariance measurements. *Plant, Cell and Environment*, **33**: 394-407.

- Campbell Scientific. (1996). *SKP215 Quantum Sensor User Guide*. Campbell Scientific Inc., Shepshed, UK.
- Campbell Scientific. (2006). *TCAV Averaging Soil Thermocouple Probe Instruction Manual*. Campbell Scientific Inc., Shepshed, UK.
- Campbell Scientific. (2009). *Model HMP45C Temperature and Relative Humidity Probe Instruction Manual*. Campbell Scientific Inc., Shepshed, UK.
- Campbell Scientific. (2010). *ARG100 Tipping Bucket Raingauge User Guide*. Campbell Scientific Inc., Shepshed, UK.
- Campbell Scientific. (2011). *CNR1 Net Radiometer Instruction Manual*. Campbell Scientific Inc., Shepshed, UK.
- Campbell Scientific. (2012). *Model HFP01 Soil Heat Flux Plate Instruction Manual*. Campbell Scientific Inc., Shepshed, UK.
- Campbell Scientific. (2013). *CRI1000 Measurement and Control System, Operators Manual*. Campbell Scientific Inc., Shepshed, UK.
- Campbell Scientific. (2015a). *CSAT3 Three Dimensional Sonic Anemometer Instruction Manual*. Campbell Scientific Inc., Shepshed, UK.
- Campbell Scientific. (2015b). *CS616 and CS625 Water Content Reflectometer Instruction Manual*. Campbell Scientific Inc., Shepshed, UK.
- Canadell, J.G., Ciais, P., Dhakal, S., Dolman, H., Friedlingstein, P., Gurney, K.R., Held, A., Jackson, R.B., Le Quéré, C., Malone, E.L., Ojima, D.S., Patwardhan, A., Peters, G.P. and Raupach, M.R. (2010). Interactions of the carbon cycle, human activity, and the climate system: a research portfolio. *Current Opinion in Environmental Sustainability*, **2**: 301-311.
- Carter, V. (1986). An overview of the hydrologic concerns related to wetlands in the U.S. *Canadian Journal of Botany*, **64**: 364-374.
- Cazelles, B., Chavez, M., Berteaux, D., Menard, F., Vik, J.O., Jenouvrier, S. and Stenseth, N.C. (2008). Wavelet analysis of ecological time series. *Oecologia*, **156**: 287-304.
- Chanton, J.P., Whiting, G.J., Happell, J.D. and Gerard, G. (1993). Contrasting rates and diurnal patterns of methane emission from emergent aquatic macrophytes. *Aquatic Botany*, **46**(2): 111-128.
- Chanton, J.P. & Whiting, G.J. (1995). Trace gas exchange in freshwater and coastal marine environments: ebullition and transports by plant. In: Matson, P.A. and Harriss, R.C. (Eds.), *Biogenic Trace Gases: Measuring Emissions from Soil and Water*, Wiley-Blackwell.
- Chanton, J.P. & Whiting, G.J. (1996). Methane stable isotopic distributions as indicators of gas transport mechanisms in emergent aquatic plants. *Aquatic Botany*, **54**: 227-236.
- Chapin III, F.S., Matson, P.A. and Mooney, H.A. (2002). *Principles of Terrestrial Ecosystem Ecology*, Springer.
- Chapin III, F.S., Woodwell, G.M., Randerson, J.T., Rastetter, E.B., Lovett, G.M., Baldocchi, D.D., Clark, D.A., Harmon, M.E., Schimel, D.S., Valentini, R., Wirth, C., Aber, J.D., Cole, J.J., Goulden, M.L., Harden, J.W., Heimann, M., Howarth, R.W., Matson, P.A., McGuire, A.D., Melillo, J.M., Mooney, H.A., Neff, J.C., Houghton, R.A., Pace, M.L., Ryan, M.G., Running, S.W., Sala, O.E., Schlesinger, W.H. and

- Schulze, E.D. (2006). Reconciling carbon-cycle concepts, terminology, and methods. *Ecosystems*, **9**: 1041-1050.
- Charman, D. (2002). *Peatlands and Environmental Change*. John Wiley & Sons Ltd., Chichester, United Kingdom.
- Chimner, R.A. & Cooper, D.J. (2003). Influence of water table levels on CO<sub>2</sub> emissions in a Colorado subalpine fen: an in site microcosm study. *Soil Biology and Biochemistry*, **35**: 245-351.
- Ciais, P., Reichstein, M., Viovy, N., Granier, A., Oge <sup>é</sup> J., Allard, V., Buchmann, N., Aubinet, M., Bernhofer, C., Carrara, A., Chevallier, F., Noblet, N.D., Friend, A., Friedlingstein, P., Grünwald, T., Heinesch, B., Keronen, P., Knohl, A., Krinner, G., Loustau, D., Manca, G., Matteucci, G., Miglietta, F., Ourcival, J.M., Papale, D., Pilegaard, K., Rambal, S., Seufert, G., Soussana, J.F., Sanz, M.J., Schulze, E.D., Vesala, T. and Valentini, R. (2005). Europe-wide reduction in primary productivity caused by the heat and drought in 2003. *Nature*, **437**: 529-533.
- Conway, V.M. (1936). Studies in the autecology of *Cladium mariscus* R. Br. I. Structure and development. *New Phytologist*, **35**: 177-204.
- Conway, V.M. (1938). Studies in the autecology of *Cladium mariscus* R. Br. V. The distribution of the species. *New Phytologist*, **37**: 312-328.
- Cooper, M.D.A., Evans, C.D., Zielinski, P., Levy, P.E., Gray, A., Peacock, M., Norris, D., Fenner, N. and Freeman, C. (2014). In-filled ditches are hotspots of landscape methane flux following peatland rewetting. *Ecosystems*, **17**(7): 1227-1241.
- Couwenberg, J. (2011). Greenhouse gas emissions from managed peat soils: is the IPCC reporting guidance realistic? *Mires and Peat*, **8**: 1-10.
- Couwenberg, J., Thiele, A., Tanneberger, F., Augustin, J., B ärisch, S., Dubovik, D., Liashchynskaya, N., Michaelis, D., Minke, M., Skuratoitch, A. and Joosten, H. (2011). Assessing greenhouse gas emissions from peatlands using vegetation as a proxy. *Hydrobiologia*, **674**: 67-89.
- Czepiel, P.M, Crill, P.M. and Harriss, R.C. (1995). Environmental factors influencing the variability of methane oxidation in temperate zone soils. *Journal of Geophysical Research*, **100**: 9359-9364.
- Darby, H.C. (1956). *The Draining of the Fens (second edition)*. Cambridge University Press, Cambridge, United Kingdom.
- Darby, H.C. (1983). *The Changing Fenland*. Cambridge University Press, Cambridge, United Kingdom.
- Dawson, J.C. & Smith, P. (2007). Carbon losses from soil and its consequences for land-use management. *Science of the Total Environment*, **382**: 165-190.
- Dengel, S., Levy, P.E., Grace, J., Jones, S.K. and Skiba, U.M. (2011). Methane emissions from sheep pasture, measured with an open-path eddy covariance system. *Global Change Biology*, **17**: 3524-3533.
- Denman, K.L., Brasseur, G.P., Chidthaisong, A., Ciais, P., Cox, P.M., Dickinson, R.E., Hauglustaine, D.A., Heinze, C., Holland, E.A., Jacob, D.J., Lohmann, U., Ramachandran, S., Leite da Silva Dia, P., Wofsy, S.C., Zhang, X.Y. and Steffen, W. (2007). *Couplings Between Changes in the Climate System and Biogeochemistry. Climate Change 2007: The Physical Science Basis*. Cambridge University Press.
- Desai, A. R., Bolstad, P.V., Cook, B.D., Davis, K.J. and Carey, E.V. (2005). Comparing net ecosystem exchange of carbon dioxide between and old-growth and mature forest in the upper Midwest, USA. *Agricultural and Forest Meteorology*, **128**: 33-55.

- Detto, M., Verfaillie, J., Anderson, F., Xu, L. and Baldocchi, D. (2011). Comparing laser-based open- and closed-path gas analyzers to measure methane fluxes using the eddy covariance method. *Agricultural and Forest Meteorology*, **151**(10): 1312-1324.
- Dinsmore, K.J., Billett, M.F., Skiba, U.M., Rees, R.M., Drewer, J. and Helfter, C. (2010). Role of the aquatic pathway in the carbon and greenhouse gas budgets of a peatland catchment. *Global Change Biology*, **16**: 2750-2762.
- Drewer, J., Lohila, A., Aurela, M., Laurila, T., Minkinen, K., Penttila, T., Dinsmore, K.J., McKenzie, R.M., Helfter, C., Flechard, C., Sutton, M.A. and Skiba, U.M. (2010). Comparison of greenhouse gas fluxes and nitrogen budgets from an ombrotrophic bog in Scotland and a minerotrophic sedge fen in Finland. *European Journal of Soil Science*, **61**: 640-650.
- Drösler, M., Freibauer, A., Christensen, T.R. and Friborg, T. (2008). Observations and status of peatland greenhouse gas emissions in Europe. In: Dolman, A.J., Valentini, R. and Freibauer, A. (Eds.). *Springer Ecological Series*, **203**: 243-262.
- Dunfield, P., Knowles, R., Dumont, R. and Moore, T.R. (1993). Methane production and consumption in temperate and sub-arctic peat soils – response to temperature and pH. *Soil Biology and Biochemistry*, **25**: 321-326.
- Dörr, H., Katruff, L. and Levin, I. (1992). Soil texture parameterization of the methane uptake in aerated soils. *Chemosphere*, **26**: 697-713.
- Elbers, J.A., Jacobs, C.M.J., Kruijt, B., Jans, W.W.P. and Moors, E.J. (2011). Assessing the uncertainty of estimated annual totals of net ecosystem productivity: A practical approach applies to a mid-latitude temperate pine forest. *Agricultural and Forest Meteorology*. **151**: 1823-1830.
- Elsgaard, L., Görres, C.M., Hoffmann, C.C., Blicher-Mathiesen, G., Schelde, K. and Petersen, S.O. (2012). Net ecosystem exchange of CO<sub>2</sub> and carbon balance for eight temperate organic soils under agricultural management. *Agricultural Ecosystem Environment*, **162**: 52-67.
- Enquist, B.J., Economo, E.P., Huxman, T.E., Allen, A.P., Ignace, D.D. and Gillooly, J.F. (2003). Scaling metabolism from organisms to ecosystems. *Nature*, **423**(6940): 639-642.
- Evans, C.D., Chapman, P.J., Clark, J.M., Monteith, D.T. and Cresser, M.S. (2006). Alternative explanations for rising dissolved organic carbon export from organic soils. *Global Change Biology*, **12**: 2044-2053.
- Evans, C.D., Worrall, F., Holden, J., Chapman, P., Smith, P. and Artz, R. (2011). A programme to address evidence gaps in greenhouse gas and carbon fluxes from UK peatlands. *JNCC Report, No.443*, JNCC, Peterborough, United Kingdom.
- Evans, C.D., Burden, A., Morrison, R., Baird, A., Callaghan, N., Chapman, P., Cumming, A., Dixon, S., Evans, J., Gauci, V., Haddaway, N., Heppell, K., Healey, J., Holden, J., Hughes, S., Kaduk, J., Jones, D., Matthews, R., Menichino, N., Misselbrook, Y., Page, S., Pan, G., Peacock, M., Pullin, A., Rayment, M., Ridley, L., Robinson, I., Stanley, K., Ward, H., Archer, E. and Worrall, F. (2014). *First Annual Data Report to DEFRA Under Project SP1210: Lowland Peatland Systems in England and Wales – Evaluating Greenhouse Gas Fluxes and Carbon Balances*.
- Evans, C.D., Morrison, R., Williamson, J., Burden, A., Baird, A., Brown, E., Callaghan, N., Chapman, P., Cumming, A., Dean, H., Dixon, S., Dooling, G., Evans, J., Gauci, V., Grayson, R., He, Y.F., Heppell, K., Holden, J., Hughes, S., Kaduk, J., Jones, D., Matthews, R., Menichino, N., Misselbrook, Y., Page, S., **Pan, G.**, Parry, L., Peacock, M., Rayment, M., Ridley, L., Robinson, I., Matthew, S. and Worrall, F.

- (2015). *Second Annual Data Report to DEFRA Under Project SP1210: Lowland Peatland Systems in England and Wales – Evaluating Greenhouse Gas Fluxes and Carbon Balances*.
- Falge, E., Baldocchi, D., Olson, R., Anthoni, P., Aubinet, M., Bernhofer, C., Burba, G., Culemans, R., Clement, R., Dolman, H., Granier, A., Ta Lai, C., Law, B.E., Meyers, T., Moncrieff, J., Moors, E., Munger, J.W., Pilegaard, K., Rannik, U., Rebmann, C., Suyker, A., Tenhunen, J., Tu, K., Verma, S., Vesala, T., Wilson, K. and Wofsy, S. (2001). Gap filling strategies for defensible annual sums of net ecosystem exchange. *Agricultural and Forest Meteorology*, **107**(1): 43-69.
- Fessenden, J.E. & Ehleringer, J.R. (2003). Temporal variation in  $\delta^{13}\text{C}$  of ecosystem respiration in the Pacific Northwest: links to moisture stress. *Oecologia*, **136**(1): 129-136.
- Finkelstein, P.L. & Sims, P.F. (2001). Sampling error in eddy correlation flux measurements. *Journal of Geophysical Research: Atmospheres*, **106**(D4): 3503-3509.
- Fisher, M.J., Rao, I.M., Ayarza, M.A., Lascano, C.E., Sanz, J.I., Thomas, R.J. and Vera, R.R. (1994). Carbon storage by introduced deep-rooted grasses in the South American savanna. *Nature*, **371**: 236-238.
- Flanagan, L.B., Wever, L.A. and Carlson, P.J. (2002). Seasonal and inter-annual variation in carbon dioxide exchange and carbon balance in a northern temperate grassland. *Global Change Biology*, **8**(7): 599-615.
- Foken, T. (2008). *Micrometeorology*. Springer-Verlag, Berlin Heidelberg.
- Foken, T. & Wichura, B. (1996). Tools for quality assessment of surface-based flux measurements. *Agricultural and Forest Meteorology*, **78**: 83-105.
- Foken, T., Aubinet, M., Finnigan, J.J., Leclerc, M.Y., Mauder, M. and Paw U.K.T. (2011). Results of a panel discussion about the energy balance closure correction for trace gases, *Bulletin of the American Meteorological Society*, **92**:ES13-ES18.
- Foken, T., Aubinet, M. and Leuning, R. (2012). The eddy covariance method, In: Aubinet, M., Vesala, T. and Papale, D. (Eds.). *Eddy Covariance: A Practical Guide to Measurement and Data Analysis*. Springer, Dordrecht.
- Foken, T., Göckede, M., Mauder, M., Mahrt, L., Amiro, B. and Munger, W. (2004). Post field data quality control. In: Lee, X., Massman, W. and Law, B. (Eds.). *Handbook of Micrometeorology: A Guide for Surface Flux Measurement and Analysis*. Kluwer Academic Press, Dordrecht.
- Foken, T., Wimmer, F., Mauder, M., Thomas, C. and Liebethal, C. (2006). Some aspects of the energy balance closure problem. *Atmospheric Chemistry and Physics*, **6**: 4395-4402.
- Fowler, D., Hargreaves, K.J., Macdonald, J.A. and Gardiner, B. (1995a). Methane and CO<sub>2</sub> exchange over peatland and the effects of afforestation. *Forestry*, **68**: 327-334.
- Fowler, D., Hargreaves, K.J., Skiba, U., Milne, R., Zahniser M.S., Moncrieff, J.B., Beverland, I.J., Gallagher, M.W., Ineson, P., Garland, J. and Johnson, C. (1995b). Measurements of CH<sub>4</sub> and N<sub>2</sub>O fluxes at the landscape scale using micrometeorological methods. *Philosophical Transactions of the Royal Society*, **351**: 339-356.
- Freeman, C., Evans, C.D. and Monteith, D.T. (2001). Export of organic carbon from peat soils. *Nature*, **412**: 785.

- Freeman, C., Fenner, N. and Ostle, N.J. (2004). Export of dissolved organic carbon from peatlands under elevated carbon dioxide levels. *Nature*, **430**: 195-198.
- Frey, K.E. & Smith, L.C. (2005). Amplified carbon release from vast Western Siberian peatlands by 2100. *Geophysical Research Letters*, **32**.
- Friday, L.E. (Eds.) (1997). *Wicken Fen: The Making of a Wetland Nature Reserve*. Harley Brooks, Colchester, United Kingdom.
- Friday, L.E. & Colston, A. (1999). Wicken Fen: The restoration of a Wetland Nature Reserve. *British Wildlife. October edition*.
- Friend, A.D., Arneeth, A., Kiang, N.Y., Lomas, M., Ogee, J., Rodenbeck, C., Running, S., Santaren, J., Sitch, S., Viovy, N., Woodward, F.I. and Zaehle, S. (2007). FluxNet and modelling the global carbon cycle. *Global Change Biology*, **13**: 610-633.
- Frolking, S., Bubier, J.L., Moore, T.R., Ball, T., Bellisario, L.M., Bhardwaj, A., Carroll, P., Crill, P.M., Lafleur, P.M., McCaughey, J.H., Roulet, N.T., Suyker, A.E., Verma, S.B., Waddington, J.M. and Whiting, G.J. (1998). Relationship between ecosystem productivity and photosynthetically active radiation from northern peatlands. *Global Biogeochemical Cycles*, **12**: 115-126.
- Frolking, S., Roulet, N.T. and Fuglestedt, J. (2006). How northern peatlands influence the Earth's radiative budget: Sustained methane emission versus sustained carbon sequestration. *Journal of Geophysical Research*, **111**: 177.
- Frolking, S. & Roulet, N.T. (2007). Holocene radiative forcing impact of northern peatland carbon accumulation and methane emissions. *Global Change Biology*, **13**: 1079-1088.
- Galvagno, M. (2011). Carbon dioxide exchange of an alpine grassland: integration of eddy covariance, proximal sensing and models. PhD dissertation, University of Milano-Bicocca.
- Gardiner, J.S. & Tansley, A.G. (Eds.). (1923). *The Natural History of Wicken Fen*. Bowes & Bowes.
- Gasca-Tucker, D.L. & Acreman, M.C. (2000). Modelling ditch water levels on the Pevensey Levels wetland, a lowland wet grassland wetland in East Sussex, UK. *Physical Chemistry of the Earth (B)*, **25**: 593-597.
- Gasca-Tucker, D.L., Acreman, M.C., Agnew, C.T. and Thompson, J.R. (2007). Estimating evaporation from a wet grassland. *Hydrology and Earth System Sciences*, **11**: 270-282.
- Gash, J.H.C & Dolman, A.J. (2003). Sonic anemometer cosine response and flux measurement. I Theoretical aspects and the effect of flux-angle distribution. *Agricultural and Forest Meteorology*, **119**: 195-207.
- Gausi, V. (2008). *Great Fen Project: Carbon Balance and Offset Potential of the Great Fen Project*. The Open University and Gauci Land Carbon Consulting.
- Gill Instruments. (2007). *Wind Master Ultrasonic Anemometer User Manual*. Gill Instruments Ltd., Lymington, UK.
- Gilman, K. (1988). *The Hydrology of Wicken Fen*. Institute of Hydrology.
- Glaser, P.H., Chanton, J.P., Morin, P., Resenberry, D.O., Siegel, D.I., Ruud, O., Chasar, L.I. and Reeve, A.S. (2004). Surface deformations as indicators of deep ebullition fluxes in a large northern peatland, *Global Biogeochemistry*, **18**(1).

- Glenn, A.J., Flanagan, L.B., Syed, K.H. and Carlson, P.J. (2006). Comparison of net ecosystem CO<sub>2</sub> exchange in two peatlands in western Canada with contrasting dominant vegetation, *Sphagnum* and *Carex*. *Agricultural and Forest Meteorology*, **140**: 115-135.
- Godwin, H. (1931). Studies in the ecology of Wicken Fen: I. The ground water level of the fen. *Journal of Ecology*, **19**: 440-473.
- Godwin, H. & Bharucha, F.R. (1932). Studies in the ecology of Wicken Fen: II. The fen water table and its control of plant communities. *The Journal of Ecology*, **20**: 157-191.
- Gowing, J.W. (1977). *The Hydrology of Wicken Fen and its Influence on the Acidity of the Soil*. MSc Thesis. Cranfield Institute of Technology.
- Gorham, E. (1991). Northern peatlands: role in the carbon cycle and probable responses to climatic warming. *Ecological Applications*, **1**: 182-195.
- Goulden, M.L., Munger, J.W., Fan, S., Daube, B.C. and Wofsy, S.C. (1996). Measurements of carbon sequestration by long-term eddy covariance: methods and a critical evaluation of accuracy. *Global Change Biology*, **2**: 169-182.
- Granath, G., Strengbom, J. and Rydin, H. (2010). Rapid ecosystem shifts in peatlands: linking plant physiology and succession. *Ecology*, **91**: 3047-3056.
- Griffis, T.J., Rouse, W.R. and Waddington, J.M. (2000). Inter-annual variability of net ecosystem CO<sub>2</sub> exchange at a subarctic fen. *Global Biogeochemical Cycles*, **14**: 1109-1121.
- Grinsted, A., Moore, J. and Jevrejeva, S. (2004). Application of the cross wavelet transform and wavelet coherence to geophysical time series. *Nonlinear Processes in Geophysics*, **11**(5/6): 561-566.
- Gu, L.H., Falge, E.M., Boden, T., Baldocchi, D.D., Black, T.A., Saleska, S.R., Suni, T., Verma, S., Vesala, T., Wofsy, S. and Xu, L.K. (2005). Objective threshold determination for night-time eddy flux filtering. *Agricultural and Forest Meteorology*, **128**(3): 179-197.
- Gunnarsson, U., Malmer, N. and Rydin, H. (2002). Dynamics or constancy in *Sphagnum* dominated mire ecosystems? A 40-year study. *Ecography*, **25**(6): 685-704.
- Göckede, M., Rebmann, C. and Foken, T. (2004). A combination of quality assessment tools for eddy covariance measurements with footprint modelling for the characterisation of complex sites. *Agricultural and Forest Meteorology*, **127**(3), 175-188.
- Hahn-Schöfl, M., Zak, D., Minke, M., Gelbrecht, J., Augustin, J. and Freibauer, A. (2011). Organic sediment formed during inundation of a degraded fen grassland emits large fluxes of CH<sub>4</sub> and CO<sub>2</sub>. *Biogeosciences*, **8**: 1539-1550.
- Haigh, M. (2006). Environmental change in headwater peat wetlands, UK. In: Krecek, K.J. & Haigh, M. (Eds.), *Environmental Role of Wetlands in Headwaters*. Springer, Netherlands.
- Harding, R.J. & Lloyd, C.R. (2008). Evaporation and energy balance of a wet grassland at Tadham Moor on the Somerset Levels. *Hydrological Processes*, **22**: 2346-2357.
- Hargreaves, K.J. & Fowler, D. (1998). Quantifying the effects of water table and soil temperature on the emission of methane from peat wetland at the field scale. *Atmospheric Environmental*, **32**: 3275-3282.

- Hargreaves, K.J., Fowler, D., Pitcairn, C.E.R. and Aurela, M. (2001). Annual methane emission from Finnish mires estimated from eddy covariance campaign measurements. *Theory Applied Climatology*, **70**(1-4): 203-213.
- Hargreaves, K.J., Milne, R. and Cannell, M.G.R. (2003). Carbon balance of afforested peatland in Scotland. *Forestry*, **76**: 299-317.
- Harpenslager, S.F., van den Elzen, E., Kox, M.A.R., Smolders, A.J.P., Ettwig, K.F. and Lamers, L.P.M. (2015). Rewetting former agricultural peatlands: Topsoil removal as a prerequisite to avoid strong nutrient and greenhouse gas emissions. *Ecological Engineering*, **84**: 159-168.
- Harris, L.E. (1953). *Vermuyden and the Fens: A Study of Sir Cornelius Vermuyden*. Cleaver-Hulme Press.
- Harriss, R.C., Sebacher, D.I. and Day, F.P. (1982). Methane flux in the Great Dismal Swamp. *Nature*, **297**: 673-674.
- Hatala, J.A., Detto, M., Sonnentag, O., Deverel, S.J., Verfaillie, J. and Baldocchi, D.D. (2012). Greenhouse gas (CO<sub>2</sub>, CH<sub>4</sub>, H<sub>2</sub>O) fluxes from drained and flooded agricultural peatlands in the Sacramento-San Joaquin Delta. *Agriculture, Ecosystems and Environment*, **150**: 1-18.
- Heikkinen, J.E.P., Maljanen, M., Aurela, M., Hargreaves, K.J. and Martikainen, P.J. (2002). Carbon dioxide and methane dynamics in a sub-Arctic peatland in northern Finland. *Polar Research*, **21**: 49-62.
- Heimann, M. (2011). Atmospheric Science: Enigma of the recent methane budget. *Nature*, **476**(7359): 157-158.
- Heimann, M. & Reichstein, M. (2008). Terrestrial ecosystem carbon dynamics and climate feedbacks. *Nature*, **451**(7176): 289-292.
- Heinsch, F., Zhao, M., Running, S., Kimball, J., Nemani, R., Davis, K., Bolstad, P., Cook, B., Desai, A. and Ricciuto, D. (2006). Evaluation of remote sensing based terrestrial productivity from MODIS using regional tower eddy flux network observations. *Geoscience and Remote Sensing, IEEE Transactions on*, **44**(7): 1908-1925.
- Hendriks, D.M.D., van Huissteden, J., Dolman, A.J. and van der Molen, M.K. (2007). The full greenhouse gas balance of an abandoned peat meadow. *Biogeosciences*, **4**: 411-424.
- Herbst, M., Friborg, T., Ringgaard, R. and Soegaard, H. (2011). Interpreting the variations in atmospheric methane fluxes observed above a restored wetland. *Agricultural and Forest Meteorology*, **151**(7): 841-853.
- Herbst, M., Friborg, T., Schelde, K., Jensen, R., Ringgaard, R., Vasquez, V., Thomsen, A.G. and Soegaard, H. (2013). Climate and site management as driving factors for the atmospheric greenhouse gas exchange of a restored wetland. *Biogeosciences*, **10**: 39-52.
- Hirano, T., Segah, H., Harada, T., Limin, S., June, T., Hirata, R. and Osaki, M. (2007). Carbon dioxide balance of a tropical peat swamp forest in Kalimantan, Indonesia. *Global Change Biology*, **13**: 412-425.
- Holden, J., Chapman, P.J. and Labadz, J.C. (2004). Artificial drainage of peatlands: hydrological and hydro-chemical process and wetland restoration. *Progress in Physical Geography*, **28**: 95-123.
- Holden, J., Walker, J., Evans, M.G., Worrall, F. and Bonn, A. (2008). *A Compendium of Peat Restoration and Management Projects*. DEFRA Report, SP0556.

- Hooijer, A., Page, S., Canadell, J.G., Silvius, M., Kwadijk, J., Hosten, H. and Jauhianinen, J. (2010). Current and future CO<sub>2</sub> emissions from drained peatlands in Southeast Asia. *Biogeosciences*, **7**(5): 1505-1514.
- Hornibrook, E.R.C., Bowes, H.L., Culbert, A. and Gallego-sala, A.V. (2009). Methanotrophy potential versus methane supply by pore water diffusion in peatlands. *Biogeosciences*, **6**(8): 1490-1504.
- Horst, T.W. & Weil, J.C. (1994). How far is far enough? The fetch requirements for micrometeorological measurement of surface fluxes. *Journal of Atmospheric and Oceanic Technology*, **11**: 1018-1025.
- Hsieh, C. I., Katul, G. and Chi, T. W. (2000). An approximate analytical model for footprint estimation of scalar fluxes in thermally stratified atmospheric flows. *Advances in Water Resources*, **23**(7): 765-772.
- Hughes, F.M.R., Stroh, P.A., Adams, W.M., Kirby, K.J., Mountford, J.O. and Warrington, S. (2011). Monitoring and evaluating large-scale, 'open-ended' habitat creation projects: A journey rather than a destination. *Journal for Nature Conservation*, **19**: 245-253.
- Hughes, P.D.M. & Barber, K.E. (2004) Contrasting pathways to ombrotrophy in three raised bogs from Ireland and Cumbria, England. *Holocene*, **14**:65-77.
- Humphreys, E.R., Lafleur, P.M., Flanagan, L.B., Hedstrom, N., Syed, K.H., Glenn, A.J. and Granger, R. (2006). Summer carbon dioxide and water vapour fluxes across a range of northern peatlands. *Journal of Geophysical Research*, **111**.
- Hurkuck, M., Brümmer, C. and Kutsch, W.L. (2016). Near-neutral carbon dioxide balance at a semi-natural, temperate bog ecosystem. *Journal of Geophysical Research: Biogeosciences*, **121**(2): 370-384.
- IPCC (2001). *Climate change 2001: The scientific basis*. Cambridge University Press, Cambridge, United Kingdom.
- IPCC (2008). *IPCC AR4 Synthesis Report Appendix Glossary*. Cambridge University Press, Cambridge, United Kingdom.
- IPCC (2014a). *Climate Change 2014: Synthesis Report. Contribution of Working Groups I, II and III to the Fourth Assessment Report of the Intergovernmental Panel on Climate Change*, 104 pp., IPCC, Geneva, Switzerland.
- IPCC (2014b). *2013 Supplement to the 2006 Inter-Governmental Panel on Climate Change Guidelines for National Greenhouse Gas Inventories: Wetlands*. Hiraishi, T., Krug, T., Tanabe, K., Srivastava, N., Baasansuren, J., Fukuda, M. and Troxler, T.G. (Eds.). IPCC, Switzerland.
- Jackowicz-Korczynski, M., Christensen, T.R., Backstrand, K., Crill, P., Friborg, T., Mastepanov, M. and Strom, L. (2010). Annual cycle of methane emission from a subarctic peatland. *Journal of Geophysical Research: Biogeosciences*, **115**.
- Jacobs, S.F.J., Heasinkveld, B.G. and Hostag, A.A.M. (2008). Towards closing the surface energy budget at a mid-latitude grassland. *Boundary-Layer Meteorology*, **126**: 125-136.
- Jaksic, V., Kiely, G., Albertson, J., Oren, R., Katul, G., Leahy, P. and Byrne, K. (2006). Net ecosystem exchange of grassland in contrasting wet and dry years. *Agricultural and Forest Meteorology*, **139**: 323-334.
- Jauhianinen, J., Hooijer, A. and Page, S.E. (2012). Carbon dioxide emissions from an *Acacia* plantation on peatland in Sumatra, Indonesia. *Biogeosciences*, **9**: 617-630.

- Jauhiainen, J., Page, S.E. and Vasander, H. (2016). Greenhouse gas dynamics in degraded and restored tropical peatlands. *Mires and Peat*, **17**(6): 1-12.
- Jenkins, G.J. (2009). *UK Climate Projections: Briefing Report*. Met Office Hadley Centre.
- Joosten, H. (2009). *The Global Peatland CO<sub>2</sub> Picture: Peatlands Status and Emissions in All Countries of the World*. Wetland International, Ede.
- Joosten, H. & Clarke, D. (2002). *Wise Use of Mires and Peatlands – Background and Principles Including a Framework for Decision-making*. International Mire Conservation Group/ International Peat Society.
- Joosten, H., Tapio-Bistrom, M.-L., and Tol, S. (Eds.). (2012). *Peatlands – Guidance for Climate Change Mitigation through Conservation, Rehabilitation and Sustainable Use*. Mitigation of Climate Change in Agriculture (MICCA) Programme, FAO/Wetlands International Rome, 100pp.
- Juszczak, R., Humphreys, E., Acosta, M., Michalak-Galczevska, M., Kayzer, D. and Olejnik, J. (2013). Ecosystem respiration in a heterogeneous temperate peatland and its sensitivity to peat temperature and water table depth. *Plant and Soil*, **366**(1): 505-520.
- Juutinen, S., Bubier, J., Larmola, T., Humphreys, E., Arnkil, S., Roy, C. and Moore, T. (2016). Nutrient load can lead to enhanced CH<sub>4</sub> fluxes through changes in vegetation, peat surface elevation and water table depth in ombrotrophic bog. *EGU General Assembly 2016*, 17-22 April, Vienna Austria, P.12050.
- Kaduk, J., Pan, G., Cumming, A., Evans, J.G., Kelvin, J., Hughes, J., Peacock, M., Gauci, V., Page, S. and Balzter, H. (2015). Water table depth regulates evapotranspiration and methane flux of a near-pristine temperate lowland fen measured by eddy covariance and static chambers (Manuscript).
- Kai, F.M., Tyler, S.C., Randerson, J.T. and Blake, D.R. (2011). Reduced methane growth rate explained by decreased Northern Hemisphere microbial sources. *Nature*, **476**(7359): 194-197.
- Kasimir-Klemedtsson, A., Klemedtssopm, L., Berglund, K., Martikainen, P., Silvola, J. and Oenema, O. (1997). Greenhouse gas emissions from farmed organic soils: a review. *Soil Use and Management*, **13**: 245-250.
- Kellner, E., Baird, A.J., Osterwoud, M., Harrison, K. and Waddington, J.M. (2006). Effect of temperature and atmospheric pressure on methane ebullition from near-surface peats. *Geophysical Research Letters*, **33**(18).
- Kelvin, J. (2011). *Evaporation in Fen Wetlands*. PhD. thesis, University of Cranfield.
- Kendon, M., Marsh, T. and Parry, S. (2013). The 2010 - 2012 droughts in England and Wales. *Weather*, **68**: 88-95.
- Kendon, M., McCarthy, M. and Jevrejeva, S. (2015). *State of the UK Climate 2014*. Met Office, Exeter, UK.
- Kirschke, S., Bousquet, P., Ciais, P., Saunois, M., Canadell, J. G., Dlugokencky, E. J., Cameron-Smith, P., *et al.* (2013). Three decades of global methane sources and sinks. *Nature Geoscience*, **6**(10): 813-823.
- Kljun, N., Calanca, P., Rotach, M.W., and Schmid, H.P. (2004). A simple parameterisation for flux footprint predictions. *Boundary-Layer Meteorology*, **112**(3): 503-523.

- Klumpp, K., Tallec, T., Guix, N. and Soussanna, J.F. (2011). Long-term impacts of agricultural practices and climatic variability on carbon storage in a permanent pasture. *Global Change Biology*, **17**: 3534-3545.
- Koehler, A.K., Sottocornola, M. and Kiely, G. (2011). How strong is the current carbon sequestration of an Atlantic blanket bog? *Global Change Biology*, **17**: 309-319.
- Kormann, R., & Meixner, F.X. (2001). An analytical footprint model for non-neutral stratification. *Boundary-Layer Meteorology*, **99**(2): 207-224.
- Kroon, P.S. (2010). *Eddy Covariance Observations of Methane and Nitrous Oxide Emissions: Towards More Accurate Estimates from Ecosystems*. PhD. Thesis. Technical University Delft.
- Kroon, P.S., Schrier-Uijl, A.P., Hensen, A., Veenendaal, E.M. and Jonker, H.J.J. (2010). Annual balances of CH<sub>4</sub> and N<sub>2</sub>O from a managed fen meadow using eddy covariance flux measurements. Special Issue: Nitrogen and greenhouse gas exchange. *European Journal of Soil Science*, **61**(5): 773-784.
- Kruse, C.W., Moldrop, P. and Iversen, N. (1996). Modelling diffusion and reaction in soil II. Atmospheric methane diffusion and consumption in a forest soil. *Soil Science*, **161**: 355-365.
- Lafleur, P.M., Hember, R.A., Admiral, S.W. and T.R., Roulet. (2005a). Annual and seasonal variability in evapotranspiration and water table at a shrub-covered bog in southern Ontario, Canada. *Hydrological Processes*, **19**: 3533-3550.
- Lafleur, P.M., Moore, T.R., Roulet, N.T. and Frohking, S. (2005b). Ecosystem respiration in a cool temperate bog depends on peat temperature but not water table. *Ecosystems*, **8**: 619-629.
- Lafleur, P.M., Roulet, N.T. and Admiral, S.W. (2001). Annual cycle of CO<sub>2</sub> exchange at a bog peatland. *Journal of Geophysical Research*, **106**: 3071-3081.
- Lafleur, P.M., Roulet, N.T., Bubier, J.L., Frohking, S. and Moore, T.R. (2003). Inter-annual variability in the peatland-atmosphere carbon dioxide exchange at an ombrotrophic bog. *Global Biogeochemical Cycles*, **17**(2): 1036.
- Lai, D.Y.F. (2009). Methane dynamics in northern peatlands: a review. *Pedosphere*, **19**(4): 409-421.
- Lai, D.Y.F., Moore, T.R. and Roulet, N.T. (2014). Spatial and temporal variations of methane flux measured by auto-chambers in a temperate ombrotrophic peatland. *Journal of Geophysical Research: Biogeosciences*, **119**(5): 864-880.
- Laidlaw, C. (2011). The Wicken Fen Vision: grazing an evolving landscape. *Conservation Land Management*.
- Laine, J., Silvola, J. and Tolonen, K. (1996). Effect of water-level drawdown on global climate warming: Northern peatlands. *Ambio*, **25**: 179-184.
- Laine, A., Sottocornola, M., Kiely, G., Byrne, K.E., Wilson, D. and Tuittila, E.S. (2006). Estimating net ecosystem exchange in a patterned ecosystem: Example from blanket bog. *Agricultural and Forest Meteorology*, **138**: 231-243.
- Lamers, L.P.M., Smolders, A.J.P and Roelofs, J.G.M. (2002). The restoration of fens in the Netherlands. *Hydrobiologia*, **478**: 107-130.

- Lasslop, G., Reichstein, M., Papale, D., Richardson, A.D., Arneth, A., Barr, A., Stoy, P. and Wohlfahrt, G. (2010). Separation of net ecosystem exchange into assimilation and respiration using a light response curve approach: critical issues and global evaluation. *Global Change Biology*, **16**: 187-208.
- Laurila, T., Aurela, M. and Tuovinen, J.P. (2012). Eddy covariance measurements over wetlands. In: Aubinet, M., Vesala, T. and Papale, D. (Eds.). *Eddy Covariance: A Practical Guide to Measurement and Data Analysis*. Springer, Dordrecht.
- Le Quéré C., Raupach, M.R., Canadell, J.G., Marland, G., Bopp, L., Ciais, P., Conway, T.J., Doney, S.C., Feely, R.A., Foster, P., Friedlingstein, P., Gurney, K., Houghton, R.A., House, J.I., Huntingford, C., Levy, P., Lomas, M.R., Majkut, J., Metzl, N., Ometto, J.P., Peters, G.P., Prentice, C.I., Randerson, J.T., Running, S.W., Sarmiento, J.L., Schuster, U., Sitch, S., Takahashi, T., Viovy, N., van de Werf, G.R. and Woodward, F.I. (2009). Trends in the sources and sinks of carbon dioxide. *Nature Geosciences*, **2**: 831-836.
- Lee, X., Massman, W. and Law, B. (2004). *Handbook of Micrometeorology: A Guide for Surface Flux Measurement and Analysis*. Kluwer Academic Press, Dordrecht.
- Lenschow, D.H. (1995). Micrometeorological techniques for measuring biosphere-atmosphere trace gas exchange. In: Matson, P.A. and Harriss, R.C. (Eds.). *Biogenic Trace Gases: Measuring Emissions from Soil and Water*. Blackwell Science Ltd., Oxford, United Kingdom.
- Leppä M., Laine, A.M., Sevakivi, M.L. and Tuittila, E.S. (2011). Differences in CO<sub>2</sub> dynamics between successional mire plant communities between wet and dry summers. *Journal of Vegetation Science*, **22**: 357-366.
- Leuning, R. (2004). Measurements of Trace Gas Fluxes in the Atmosphere Using Eddy Covariance: WPL Corrections Revisited. In: *Handbook of Micrometeorology: A Guide for Surface Flux Measurement and Analysis*, Eds. Lee, X., Massman, W. and Law, B. Kluwer Academic Press, Dordrecht, pp. 119-132.
- Leuning, R., van Gorsel, E., Massman, W.J. and Isaac, P.R. (2012). Reflections on the surface energy imbalance problem. *Agricultural and Forest Meteorology*, **156**: 65-74.
- Levy, P.E., Burden, A., Cooper, M.D.A., Dinsmore, K.J., Drewer, J., Evans, C., Fowler, D., Gaiawyn, J., Gray, A., Jones, S.K., Jones, T., McNamara, N.P., Mills, R., Ostle, N., Sheppard, L.J., Skiba, U., Sowerby, A., Ward, S.E. and Zielinko, P. (2012). Methane emissions from soils: synthesis and analysis of a large UK data set. *Global Change Biology*, **18**: 1657-1669.
- LI-COR, Inc. (2015a). *LI-7500A Open-Path CO<sub>2</sub> / H<sub>2</sub>O Gas Analyzer Instruction Manual*. LI-COR Biosciences, Lincoln, Nebraska, USA.
- LI-COR, Inc. (2015b). *LI-7700 Open-Path CH<sub>4</sub> Analyzer Instruction Manual*. LI-COR Biosciences, Lincoln, Nebraska, USA.
- LI-COR, Inc. (2015c). *EddyPro<sup>®</sup> Software Instruction Manual 11<sup>th</sup> edition*. LI-COR Biosciences, Lincoln, Nebraska, USA.
- Liikanen, A., Huttunen, J.T., Karjalainen, S.M., Heikkinen, K., Väisänen, T.S., Nykänen, H. and Martikainen, P.J. (2006). Temporal and seasonal changes in greenhouse gas emissions from a constructed wetland purifying peat mining runoff waters. *Ecological Engineering*, **26**(3): 241-251.

- Limpens, J., Berendse, F., Blodua, C., Canadell, J.G., Freeman, C., Holden, J., Roulet, N., Rydin, H. and Schaeppmen-Strub, G. (2008). Peatlands and the carbon cycle: from local processes to global implications – a synthesis. *Biogeosciences*, **5**: 1475-1491.
- Lindroth, A., Lund, M., Nilsson, M., Aurela, M., Christensen, T.R., Laurila, T., Rinne, J., Riutta, T., Sagerfors, J., Strom, L. and Tuovinen, J. (2007). Environmental controls on the CO<sub>2</sub> exchange in north European mires. *Tellus*, **59B**: 812-825.
- Livingston, G.P. & Hutchinson, G.L. (1995). Enclosure-based measurement of trace gas exchange: applications and sources of error. In: Matson, P.A. & Harriss, R.C. (Eds.), *Biogenic Trace Gases: Measuring Emissions from Soil and Water*. Blackwell Science, Cambridge.
- Lloyd, C.R. (2006). Annual carbon balance of a managed wetland meadow in the Somerset Levels, UK. *Agricultural and Forest Meteorology*, **138**: 168-179.
- Lloyd, J. & Taylor, J.A. (1994). On the temperature dependence of soil respiration. *Functional Ecology*, **8**: 315-323.
- Lock, J.M., Friday, L.E. and Bennett, T.J. (1997). The management of the fen. In: Friday, L.E. (Eds.). *Wicken Fen: The Making of a Wetland Nature Reserve*. Harley.
- Lohoar, G., & Ballard, S. (1990). *Turf digging at Wicken Fen*. Cambridgeshire Collection.
- Lohila, A., Aurela, M., Tuovinen, J.-P. and Laurila, T. (2004). Annual CO<sub>2</sub> exchange of a peat field growing spring barley or perennial forage grass. *Journal of Geophysical Research*, **109**: 1-13.
- Lohila, A., Minkkinen, K., Aurela, M., Tuovinen, J.-P., Penttila, T., Ojanen, P. and Laurila, T. (2011). Greenhouse gas flux measurements in a forestry-drained peatland indicate a large carbon sink. *Biogeosciences*, **8**: 3202-3218.
- Magyari, E., Sumegi, P., Braun, M., Jakab, G. and Molnar, M. (2001). Retarded wetland succession: anthropogenic and climatic signals in a Holocene peat bog profile from north-east Hungary. *Journal of Ecology*, **89**:1019-1032.
- Malhi, Y., McNaughton, K. and Von Randow, C. (2004). Low frequency atmospheric transport and surface flux measurements. In: Lee, X., Massman, W. and Law, B. (Eds.). *Handbook of Micrometeorology: A Guide for Surface Flux Measurement and Analysis*, Kluwer Academic Publishers, Dordrecht.
- Malmer, N. (1986). Vegetation gradients in relation to environmental conditions in north-western European mires. *Canadian Journal of Botany*, **64**: 375-383.
- Maljanen, M., Sigurdsson, B.D., Gutmundsson, J., Oskarsson, H., Huttunen, J.T. and Markitainen, P.J. (2010). Greenhouse gas balances of managed peatlands in the Nordic countries – present knowledge and gaps. *Biogeosciences*, **7**: 2711-2738.
- Mann, J. & Lenschow, D.H. (1994). Errors in airborne flux measurements. *Journal of Geophysical Research: Atmospheres*, **99**(D7), 14519-14526.
- Maraun, D., Kurths, J. and Holschneider, M. (2007). Non-stationary Gaussian processes in wavelet domain: synthesis, estimation and significance testing. *Physical Review E*, **75**: 016707.

- Martikainen, P.J., Nykänen, H., Crill, P. and Silvola, J. (1993). Effect of a lowered water table on carbon dioxide, methane and nitrous oxide due to forest drainage or mire sites of different trophic. *Plant and Soil*, **168**: 571-577.
- Massman, W. & Clement, R. (2004). Uncertainty in eddy covariance flux estimates resulting from spectral attenuation. In: *Handbook of Micrometeorology*, Springer Netherlands.
- Mauder, M., & Foken, T. (2011). *Documentation and instruction manual of the eddy covariance software package TK3*. Univ., Abt. Mikrometeorologie.
- Mauder, M., Foken, T., Clement, R., Elbers, J., Eugster, W., Grünwald, T., Heusinkveld, B. and Kolbe, O. (2008). Quality control of Carbon-Europe flux data - part 2: Inter-comparison of eddy covariance software. *Biogeosciences*, **5**: 451-462.
- Megonigal, J.P., Hines, M.E. and Visscher, P.T. (2004). Anaerobic metabolism: Linkages to trace gases and aerobic processes. In: Schlesinger, W.H. (Eds.). *Biogeochemistry*, Elsevier-Pergamon, Oxford, United Kingdom.
- Merbold, L., Kutsch, W.L., Corradi, C., Kolbe, O., Reibmann, C., Stoy, P.C., Zimov, Z.A. and Schulze, E.-D. (2009). Artificial drainage and associated carbon fluxes (CO<sub>2</sub>/ CH<sub>4</sub>) in a tundra ecosystem. *Global Change Biology*, **15**: 2599-2612.
- Met office (2013a). *2010 Weather Summaries Annual Assessments*. Met Office, Exeter, UK.
- Met office (2013b). *2011 Weather Summaries Annual Assessments*. Met Office, Exeter, UK.
- Met office (2013c). *2012 Weather Summaries Annual Assessments*. Met Office, Exeter, UK.
- Met office (2014). *2013 Weather Summaries Annual Assessments*. Met Office, Exeter, UK.
- Met office (2015). *2014 Weather Summaries Annual Assessments*. Met Office, Exeter, UK.
- Met office (2016). *2015 Weather Summaries Annual Assessments*. Met Office, Exeter, UK.
- McCartney, M.P., de la Hera, A., Acreman, M.C. and Mountford, O. (2001). *An Investigation of the Water Budget of Wicken Fen*. Centre for Ecology and Hydrology, Wallingford, United Kingdom.
- McCartney, M.P. & de la Hera, A. (2004). Hydrological assessment for wetland conservation at Wicken Fen. *Wetland Ecological Management*, **12**: 189-204.
- Minke, M., Augustin, J., Burlo, A., Yarmashuk, T., Chuvashova, H., Thiele, A., Freibauer, A., Tikhonov, V. and Hoffmann, M. (2016). Water level, vegetation composition, and plant productivity explain greenhouse gas fluxes in temperate cutover fens after inundation. *Biogeosciences*, **13**(13): 3945-3970.
- Minkinen, K. & Laine, J. (2006). Vegetation heterogeneity and ditches create spatial variability in methane fluxes from peatlands drained for forestry. *Plant and Soil*, **285**(1-2): 289-304.
- Mitsch, W.J. & Gosselink, J.G. (2000). *Wetlands* (3<sup>rd</sup> Edition). John Wiley & Sons, New York, USA.
- Moffat, A.M., Papale, D., Reichstein, M., Hollinger, D.Y., Richardson, A.D., Barr, A.G., Beckstein, C., Braswell, B.H., Churkina, G., Falge, E., Gove, J.H., Heimann, M., Hui, D., Jarvis, A.J., Kattge, J., Noormets, A. and Stauch, V.J. (2007). Comprehensive comparison of gap-filling techniques for eddy covariance net carbon fluxes. *Agricultural and Forest Meteorology*, **147**: 209-232.

- Moncrieff, J., Valentini, R., Greco, S., Seufert, G. and Ciccioli, P. (1997). Trace gas exchange over terrestrial ecosystems: methods and perspectives in micrometeorology. *Journal of Experimental Botany*, **48**: 1133-1142.
- Moncrieff, J., Clement, R., Finnigan, J. and Meyers, T. (2004). Averaging, de-trending, and filtering of eddy covariance time series. In: Lee, X., Massman, W. and Law, W. (Eds.). *Handbook of Micrometeorology*, Kluwer Academic Press, Dordrecht.
- Monson, R., Sparks, J., Resenstiel, T., Scott-Denton, L., Huxman, T., Harley, P., Turnipseed, A., Burns, S., Backlund, B. and Hu, J. (2005). Climatic influences on net ecosystem CO<sub>2</sub> exchange during the transition from wintertime carbon source to springtime carbon sink in a high-elevation, subalpine forest, *Oecologia*, **146** (1): 130-147.
- Monson, R. & Baldocchi, D.D. (2014). *Terrestrial Biosphere-Atmosphere Fluxes*. Cambridge University Press, Cambridge, United Kingdom.
- Monteith, J.L. (1972). Solar Radiation and Productivity in Tropical Ecosystems. *Journal of Applied Ecology*, **9**(3): 747-766.
- Monteith, D.T., Stoddard, J.L. and Evans, C.D. (2007). Dissolved organic carbon trends resulting from changes in atmospheric deposition chemistry. *Nature*, **450**: 537-540.
- Montzka, S.A., Dlugokencky, E.J. and Butler, J.H. (2011). Non-CO<sub>2</sub> greenhouse gases and climate change. *Nature*, **476**(7358): 43-50.
- Moore, C.J. (1986). Frequency response corrections for eddy correlation systems. *Boundary-Layer Meteorology*, **37**: 17-35.
- Moore, N.W. (1997). The Fenland Reserves. In: Friday, L.E. (Eds.), *Wicken Fen: The Making of a Wetland Nature Reserve*, Harley Brooks, Colchester, United Kingdom.
- Moore, T.R. & Basiliko, N. (2006). Decomposition. In: Wieder, R.K. & Vitt, D.H. (Eds.), *Boreal Peatland Ecosystems*, Ecological Studies Vol. 188, Springer-Verlag, Berlin.
- Moore, T.R. & Dalva, M. (1993). The influence of temperature and water table position on carbon dioxide and methane emissions from laboratory columns of peatland soils. *Journal of Soil Science*, **44**: 651-661.
- Moore, T.R., Roulet, N.T. and Waddington, J.M. (1998). Uncertainty in predicting the effect of climatic change on the carbon cycling of Canadian peatlands. *Climatic Change*, **40**: 229-245.
- Morgan, A. (2005). *Investigation of Farming Methods on Changes in Vegetation and Soil Properties of Restored Fenlands Over Time*. MSc Thesis. Cranfield University, Bedford.
- Morris, J., Gowing, D.J.G., Mills, J. and Dunderdale, J.A.L. (2000). Reconciling economic and environmental objectives: the case of recreating wetlands in the fenland area of Eastern England. *Agriculture, Ecosystems and Environment*, **79**: 245-257.
- Morris, J., Graves, A., Angus, A., Hess, T., Lawson, C., Camino, M., Truckell, I. and Holman, I. (2010). *Restoration of Lowland Peatland in England and Impacts on Food Production and Security*. Report to Natural England. Cranfield University. Bedford.
- Morrison, R., Page, S., Kaduk, J., Acreman, M., Harding, R. and Baltzer, H. (2013). Annual CO<sub>2</sub> budget of a regenerating ex-arable peatland in the East Anglian Fens. In: *Emissions of Greenhouse Gases from UK Managed Lowland Peatlands: Report to DEFRA under Project SPI210: Lowland Peatland Systems in England and Wales – Evaluating Greenhouse Gas Fluxes and Carbon Balances*.

- Mosier, A., Schimer, D. and Valentine, D. (1991). Methane and nitrous oxide fluxes in native fertilized and cultivated grasslands. *Nature*, **350**: 330-332.
- MPI Biogeochemistry. (2014). *REddyProc: A R Package for EC Flux Gap-Filling and Flux Partitioning*, edited, Max Planck Institute for Biogeochemistry, Jena, Germany.
- Munger, J.W., Loescher, H.W. and Luo, Q. (2012). Measurement, tower and site design considerations. In: Aubinet, M., Vesala, T. and Papale, D. (Eds.). *Eddy Covariance: A Practical Guide to Measurement and Data Analysis*, Springer, Dordrecht.
- Murphy, J.M., Sexton, D.M.H., Jenkins, G.J., Booth, B.B.B., Brown, C.C., Clark, R.T., Collins, M., Harris, G.R., Kendon, E.J., Betts, R.A., Brown, S.J., Humphrey, K.A., McCarthy, M.P., McDonald, R.E., Stephens, A., Wallace, C., Warren, R., Wilby, R. and Wood, R.A. (2009). *UK Climate Projections Science Report: Climate Change Projections*. Met Office Hadley Centre.
- Nakai, T., Van der Molen, M. K., Gash, J. H. C. and Kodama, Y. (2006). Correction of sonic anemometer angle of attack errors. *Agricultural and Forest Meteorology*, **136**(1), 19-30.
- Nakai, T. & Shimoyama, K. (2012). Ultrasonic anemometer angle of attack errors under turbulent conditions. *Agricultural and Forest Meteorology*, **162**:14-26.
- National Trust. (2007). *The Wicken Fen Vision: Our Strategy to Create a Large New Nature Reserve for Wildlife and People in Cambridgeshire*. The National Trust, Bury St. Edmonds.
- National Trust. (2009). *Wicken Fen Vision: A National Trust Strategy to Create a 53 square kilometre Nature Reserve for Wildlife and People in Cambridgeshire*. The National Trust, Bury St. Edmonds.
- National Trust. (2011). *Wicken Fen Vision: The Grazing Programme Explained*. The National Trust, Bury St. Edmonds.
- Natural England (2010). *England's Peatlands: Carbon Storage and Greenhouse Gases (NE257)*.
- Ness, L. & Procter-Nicholls, L. (2008). *Hydrology of the Wicken Fen Vision and Detailed Analysis of the Hydrology and Carbon of Area D*. Haycock Associates, Pershore.
- Nicolini, G., Castaldi, S., Fratini, G. and Valentini, R. (2013). A literature overview of micrometeorological CH<sub>4</sub> and N<sub>2</sub>O flux measurements in terrestrial ecosystems. *Atmospheric Environment*, **81**: 311-319.
- Nieveen, J.P., Campbell, D.I., Schipper, L.A. and Blair, I.J. (2005). Carbon exchange of grazed pasture on a drained peat soil. *Global Change Biology*, **11**: 607-618.
- Nilsson, M., Sagerfors, J., Buffam, I., Laudon, H., Eriksson, T., Grelle, A., Klemetsson, L., Weslein, P. and Lindroth, A. (2008). Contemporary carbon accumulation in a boreal oligotrophic minerogenic mire – a significant sink after accounting for all C fluxes. *Global Change Biology*, **14**: 2317-2332.
- NOAA. (2010). *Annual Greenhouse Gas Index (AGGI)*. URL: <http://www.esrl.noaa.gov/gmd/aggi>
- Oechel, W.C., Vourlitis, G.L., Hastings, S.J., Zulueta, R.C., Hinzman, L. and Kane, D. (2000). Acclimation of ecosystem CO<sub>2</sub> exchange in the Alaskan Arctic in response to decadal climate warming. *Nature*, **406**: 978-981.
- Oke, T.R. 1987. *Boundary Layer Climates*, 2<sup>nd</sup> Ed. Routledge.

- Olivier, J.G.J., van Aardenne, J.A., Dentener, F., Pagliari, V., Ganzeveld, L.N. and Peters, J.A.H.W. (2005). Recent trends in global greenhouse gas emissions: regional trends 1970-2000 and spatial distribution of key sources in 2000. *Environmental Science*, **2**: 81-99.
- Olson, D.M., Griffis, T.J., Noormets, A., Kolka, R. and Chen, J. (2013). Inter-annual, seasonal, and retrospective analysis of the methane and carbon dioxide budgets of a temperate peatland. *Journal of Geophysical Research: Biogeosciences*, **118**: 226-238.
- Ostle, N.J., Levy, P.E., Evans, C.D. and Smith, P. (2009). UK land use and soil carbon sequestration. *Land Use Policy*, **26**: S274-S283.
- Page, S.E., Siegert, F., Rieley, J.O., Boehm, H.D.V., Jaya, A. and Limin, S. (2002). The amount of carbon released from peat and forest fires in Indonesia during 1997. *Nature*, **420**(6911): 61-65.
- Page, S.E., Hoscilo, A., Wosten, H., Jauhiainen, J., Silvius, M., Rieley, J., Ritzema, H., Tansey, K., Graham, L., Vasander, H. and Limin, S. (2009). Restoration ecology of lowland tropical peatlands in Southeast Asia: current knowledge and future research directions. *Ecosystems*, **12**: 888-905.
- Page, S.E., Rieley, J.O. and Banks, C.J. (2011). Global and regional importance of the tropical peatland carbon pool. *Global Change Biology*, **17**(2): 798-818.
- Page, S.E., Morrison, R., Malins, C., Hooijer, A., Rieley, J.O. and Jauhiainen, J. (2011). *Review of peat surface greenhouse gas emissions from oil palm plantations in Southeast Asia* (ICCT White Paper 15). Washington: International Council on Clean Transportation.
- Pan, G. (2010). *Effects of Water Table and Nitrogen Supply on Performance of Sphagnum Species in Calcareous Rich Fens*. Master thesis Supervised by Prof. Rydin, H., Department of Plant Ecology, EBC, Uppsala University, Sweden. [http://www.ibg.uu.se/upload/2010-09-22\\_124022\\_898/Gong%20Pan%20E.pdf](http://www.ibg.uu.se/upload/2010-09-22_124022_898/Gong%20Pan%20E.pdf)
- Pan, G., Kaduk, J., Balzter, H., Page, S.E., Morrison, R., Acreman, M. and Harding R.J. (2012). *FENFLUX: The Short-term Climate Response of Carbon Dioxide and Methane Fluxes from a Regenerating Fen in East Anglia, UK*. Proc. 14<sup>th</sup> International Peat Congress, Stockholm, Sweden. June 3-8, 2012.
- Papale, D. (2012). Data gap-filling. In: Aubinet, M., Vesala, T. and Papale, D. (Eds.). *Eddy Covariance: A Practical Guide to Measurement and Data Analysis*, Springer, Dordrecht.
- Papale, D. & Valentini, R. (2003). A new assessment of European forests carbon exchanges by eddy fluxes and artificial neural network specialization. *Global Change Biology*, **9**: 525-535.
- Papale, D., Reichstein, M., Aubinet, M., Canfora, E., Bernhofer, C., Kutsch, W., Longdoz, B., Rambal, S., Valentini, R., Vesala, T. and Yakir, D. (2006). Towards a standardized processing of net ecosystem exchange measured with the eddy covariance technique: algorithms and uncertainty estimation. *Biogeosciences*, **3**: 571-583.
- Parish, F., Sirin, A., Charman, D., Joosten, H., Minaeva, T. and Silvius, M. (Eds.) (2008). *Assessment on Peatlands, Biodiversity and Climate Change*. Global Environment Centre, Kuala Lumpur and Wetlands International, Wageningen, Netherlands.
- Parmentier, F.J.W., van der Molen, M.K., de Jeu, R.A.M., Hendriks, D.M.D and Dolman, A.J. (2007). CO<sub>2</sub> fluxes and evaporation on a peatland in the Netherlands appear not affected by water table fluctuations. *Agriculture and Forest Meteorology*, **149**: 1201-1208.
- Parry, S., Marsh, T. and Kendon, M. (2013). 2012: from drought to floods in England and Wales. *Weather*, **68**: 268-274.

- Pastor, J., Peckham, B., Bridgham, S.D., Weltzin, J. and Chen, J. (2002). Plant community dynamics, nutrient cycling, and alternative stable equilibria in peatlands. *American Naturalist*, **160**: 553-568.
- Peacock, M., Ridley, L.M., Evans, C.D. and Guaci, V. (2016). Management effects on greenhouse gas dynamics in fen ditches. *Science of the Total Environment*, **11**:1-12.
- Pedrotti, E., Rydin, H., Ingmar, T., Hytteborn, H., Turunen, P. and Granath, G. (2014). Fine-scale dynamics and community stability in boreal peatlands: revisiting a fen and a bog in Sweden after 50 years. *Ecosphere*, **5**(10): 1-24.
- Petrone, R.M., Waddington, J.M. and Price, J.S. (2003). Ecosystem-scale flux of CO<sub>2</sub> from a restored vacuum harvested peatland. *Wetlands Ecology and Management*, **11**(6): 419-432.
- Prince, S.D. & Goward, S.N. (1995). Global primary production: A remote sensing approach. *Journal of Biogeography*, **22**(4-5): 815-835.
- Quinty, F. & Rochefort, L. (2003). *Peatland Restoration Guide (2<sup>nd</sup> Edition)*. Canadian Sphagnum Moss Association and New Brunswick Department of Natural Resources and Energy, Québec, Canada.
- R Core Team. (2014). *R: A Language and Environment for Statistical Computing*, R Foundation for Statistical Computing, Vienna, Austria.
- Rabinowitch, E.I. (1951). *Photosynthesis and Related Processes*, vol. 2, part 1. Wiley-Interscience, New York.
- Ramaswamy, V., Boucher, O., Haigh, J., Hauglustaine, D., Haywood, J., Myhre, G., Nakajima, T., Shi, G.Y. and Solomon, S. (2001). Radiative forcing of climate change, In: Houghton, J.T. *et al.* (Eds.), *Climate Change 2001, Contribution of Working Group I to the Third Assessment Report of the Intergovernmental Panel on Climate Change*, Cambridge University Press, New York, USA.
- RAMSAR. (2014). *The List of Wetlands of International Importance*.
- Raupach, M.R. & Canadel, J.G. (2010). Carbon and the Anthropogenic. *Current Opinions in Environmental Sustainability*, **2**: 210-218.
- Rebmann, C., Kolle, O., Heinesch, B., Quech, R., Ibrom, A. and Aubinet, M. (2012). Data Acquisition and Flux Calculations. In: Aubinet, M., Vesala, T. and Papale, D. (Eds.). *Eddy Covariance: A Practical Guide to Measurement and Data Analysis*, Springer, Dordrecht.
- Reddy, K.R. & Delaune, R.D. (2008). *Biogeochemistry of Wetlands*. CRC Press, Boca Raton, USA.
- Reichstein, M., Falge, E., Baldocchi, D., Papale, D., Aubinet, M., Berbigier, P., Bernhofer, C., Buchmann, N., Gilmanov, T., Granier, A., Grünwald, T., Havrůnková K., Ilvesniemi, H., Janous, D., Knohl, A., Laurila, T., Lohila, A., Loustau, D., Matteucci, G., Meyers, T., Miglietta, F., Ourcival, J.-M., Pumpanen, J., Rambal, S., Rotenberg, E., Sanz, M., Tenhunen, J., Seufert, G., Vaccari, F., Vesala, T., Yakir, D. and Valentini, R. (2005). On the Separation of Net Ecosystem Exchange into Assimilation and Ecosystem Respiration: review and improved algorithm. *Global Change Biology*, **11**(9): 1424-1439.
- Reichstein, M., Ciais, P., Papale, D., Valentini, R., Running, S., Viovy, N., Cramer, W., Granier, A., Oge J., Allard, V., Aubinet, M., Bernhofer, C., Buchmann, N., Carrara, A., Grünwald, T., Heimann, M., Heinesch, B., Knohl, A., Kutsch, W., Loustau, D., Manca, G., Matteucci, G., Miglietta, F., Ourcival, J.M., Pilegaard, K., Pumpanen, J., Rambal, S., Schaphoff, S., Seufert, G., Soussana, J.F., Sanz, M.J., Vesala, T. and Zhao, M. (2007). Reduction of ecosystem productivity and respiration during the European summer 2003 climate anomaly: a joint flux tower, remote sensing and modelling analysis.

*Global Change Biology*, **13**: 634-651.

Reichstein, M., Stoy, P.C., Desai, A.R., Lasslop, G. and Richardson, A.D. (2012). Partitioning of net fluxes. In: Aubinet, M., Vesala, T. and Papale, D. (Eds.). *Eddy Covariance: A Practical Guide to Measurement and Data Analysis*, Springer, Dordrecht.

Renger, M., Wessolek, G., Schwärzel, K., Sauerbrey, R. and Siewert, C. (2002). Aspects of peat conservation and water management, *Journal of Plant Nutrition and Soil Science*, **165**: 487-493.

Richardson, A.D. & Hollinger, D.Y. (2007). A method to estimate the additional uncertainty in gap-filled NEE resulting from long gaps in the CO<sub>2</sub> flux record. *Agricultural & Forest Meteorology*, **147**(3): 199-208.

Richardson, A.D., Mahecha, M.D., Falge, E., Kattge, J., Moffat, A.M., Papale, D., Reichstein, M., Stauch, V.J., Braswell, B.H., Churkina, G., Kruijt, B. and Hollinger, D.Y. (2008). Statistical properties of random CO<sub>2</sub> flux measurement uncertainty inferred from model residuals. *Agricultural and Forest Meteorology*, **148**(1): 38-50.

Rinne, J., Riutta, T., Pihlatie, M., Aurela, M., Haapanala, S., Tuovinen, J.P., Tuittila, E.S. and Vesala, T. (2007). Annual cycle of methane emission from a boreal fen measured by the eddy covariance technique. *Tellus Series B - Chemical and Physical Meteorology*, **59**(3): 449-457.

Riutta, T., Laine, J., Aurela, M., Rinne, J., Vesala, T., Laurila, T., Haapanala, S., Pihlatie, M. and Tuittila, E.S. (2007). Spatial variation in plant community functions regulates carbon gas dynamics in a boreal fen ecosystem. *Tellus Series B - Chemical and Physical Meteorology*, **59**: 838-852.

Rodhe, H. & Svensson, B. (1995). Impact on the greenhouse effect of peat mining and combustion. *Ambio*, **24**: 221-225.

Rogiers, N., Conen, F., Furger, M., Stockli, R. and Eugster, W. (2009). Impact of past and present land management on the C-balance of a grassland in the Swiss Alps. *Global Change Biology*, **14**: 2613-2625.

Roobroeck, D., Butterbach-Bahl, K., Bruggemann, N. and Boeckx, P. (2010). Di-nitrogen and nitrous oxide exchanges from an un-drained monolith fen: short term responses following nitrate addition. *European Journal of Soil Science*, **61**: 662-670.

Rotherham, I.D. (2013). *The Lost Fens: England's Greatest Ecological Disaster*. Stroud: History, United Kingdom.

Roulet, N.T. (2000). Peatlands, carbon storage, greenhouse gases, and the Kyoto protocol: prospects and significance for Canada. *Wetlands*, **20**(4): 605-615.

Roulet, N. & Moore, T.R. (2006). Browning the waters. *Nature*, **444**: 283-284.

Roulet, N., Moore, T.R., Bubier, J. and Lafleur, P. (1992). Northern fens - methane flux and climate change, *Tellus B.*, **44**: 100-105.

Roulet, N., Lafleur, P.M., Richard, P.J.H, Moore T.R., Humphreys, E.R. and Bubier, J. (2007). Contemporary carbon balance and late Holocene carbon accumulation in a northern peatland. *Global Change Biology*, **13**: 397-411.

Rowell, T.A. & Harvey, H.J. (1988). The recent history of Wicken Fen, Cambridgeshire, England: A guide to ecological development. *Journal of Ecology*, **76**: 73-90.

Rowell, T.A. (1997). The History of the Fen. In: Friday, L.E. (Eds.). *Wicken Fen: The Making of a*

Wetland Nature Reserve, Harley Brooks, Colchester, United Kingdom.

Ruimy, A., Jarvis, P.G., Baldocchi, D.D. and Saugier, B. (1995). CO<sub>2</sub> Fluxes over Plant Canopies and Solar Radiation: A Review. In: Begon, M. & Fitter, A.H. (Eds.). *Advances in Ecological Research*. Academic Press.

Ruppert, J., Mauder, M., Thomas, C. and Lüers, J. (2006). Innovative gap-filling strategy for annual sums of CO<sub>2</sub> net ecosystem exchange. *Agricultural and Forest Meteorology*, **138**: 5-18.

Rydin, H. (1985). Effect of water level on desiccation of *Sphagnum* in relation to surrounding Sphagna. *Oikos*, 374-379.

Rydin, H., Sjörs, H. and Löffroth M. (1999). Mires. In: Rydin, H., Snoeijs, P. and Diekmann, M. (Eds.). *Swedish Plant Geography*, pp. 91-112. Svenska V äxtgeografiska S ällskapet, Uppsala, Sweden.

Rydin, H. & Jeglum, J.K. (2013). *The Biology of Peatlands 2<sup>nd</sup> Eds.* Oxford University Press, Oxford, United Kingdom.

Saarnio, S., Morero, M., Shurpali, N., Tuittila, E.-S., Makila, E.-S. and Alm, J. (2007). Annual CO<sub>2</sub> and CH<sub>4</sub> fluxes of pristine boreal mires as a background for the lifecycle analysis of peat energy. *Boreal Environmental Research*, **12**: 101-113.

Sagerfors, J., Lindroth, A., Grelle, A., Klemmedtsson, L., Weslien, P. and Nilsson, M. (2009). Annual CO<sub>2</sub> and CH<sub>4</sub> fluxes of pristine boreal mires as a background for the lifecycle analyses of peat energy. *Boreal Environment Research*, **12**: 101-113.

Samaritani, E., Siegenthaler, A., Yli-Petays, M., Buttler, A., Christin, P.-A. and Mitchell, E.A.D. (2011). Seasonal net ecosystem carbon exchange of a regenerating cutaway bog: How long does it take to restore the C-sequestration function? *Restoration Ecology*, **19**(4): 480-489.

Scheupp, P.H., Leclerc, M.Y., Macpherson, J.I. and Desjardins, R.L. (1990). Footprint prediction of scalar fluxes from analytical solutions of the diffusion equation. *Boundary-Layer Meteorology*, **50**: 355-373.

Schotanus, P., Nieuwstadt, F.T.M. and Bruin, H.A.R. (1983). Temperature measurement with a sonic anemometer and its application to heat and moisture fluxes. *Boundary-Layer Meteorology*, **26**: 81-93.

Schrier-Uijl, A.P., Kroon, P.S., Hensen, A., Leffelaar, P.A., Berendse, F. and Veenendaal, E.M. (2009). Comparison of chamber and eddy covariance - based CO<sub>2</sub> and CH<sub>4</sub> emission estimates in a heterogeneous grass ecosystem on peat. *Agricultural and Forest Meteorology*, **150**: 825-831.

Schrier-Uijl, A.P., Veraart, A.J., Leffelaar, P.A., Berendse, F. and Veenendaal, E.M. (2011). Release of CO<sub>2</sub> and CH<sub>4</sub> from lakes and drainage ditches in temperate wetlands. *Biogeochemistry*, **102**(1-3): 265-279.

Schumann, M. & Joosten, H. (2008). *Global Peatland Restoration Manual*. International Mire Conservation Group.

Schäfer, C.K., Elsgaard, L., Hoffmann, C.C. and Petersen, S.O. (2012). Seasonal methane dynamics in three temperate grasslands on peat. *Plant Soil*, **357**: 339-353.

Seiler, W., Conrad, R. and Scharffe, D. (1984). Field studies of methane emission from termite nests into the atmosphere and measurements of methane uptake by tropical soils. *Journal of Atmospheric Chemistry*, **1**: 171-186.

- Shurpali, N.J. & Verma, S.B. (1998). Micrometeorological measurements of methane flux in a Minnesota peatland during two growing seasons. *Biogeochemistry*, **40**(1): 1-15.
- Shurpali, N.J., Hyvonen, N.P., Huttunen, J.T., Clement, R.J., Reichstein, M., Nykanen, H., Biasi, C. and Martikainen, P.J. (2009). Cultivation of perennial grass for bioenergy on a boreal organic soil – carbon sink or source? *Bioenergy*, **1**:35-50.
- Silvola, J., Alm, J. Ahlholm, U., Nykänen, H. and Martikainen, P.J. (1996). CO<sub>2</sub> fluxes from peat in boreal mires under varying temperature and moisture conditions. *Journal of Ecology*, **84**: 219-228.
- Sirin, A., Charman, D., Joosten, H., Minaeva, T. and Silvius, M. (2008). Assessment on peatlands, biodiversity and climate change. *Wetlands International*.
- Smith, P. (2004). Soil as carbon sinks: the global context. *Soil Use and Management*, **20**: 212-218.
- Smith, P., Smith, J., Flynn, H., Killham, K., Rangel-Castro, I., Foereid, B., Aitkenhead, M., Chapman, S., Towers, W., Bell, J., Lumsdon, D., Milne, R., Thomson, A., Simmons, I., Skiba, U., Reynolds, B., Evans, C., Frogbrook, Z., Bradley, I., Whitmore, A. and Falloon, P. (2007). *ECOSSE: Estimating Carbon in Organic Soils Sequestration and Emission*. Environment and Rural Affairs Department. Scottish Executive. Edinburgh.
- Smith, P., Lanigan, G., Kutsch, W.L., Buchmann, N., Eugster, W., Aubinet, M., Ceschia, E., Beziat, Yeluripati, J.B., Osborne, B., Moors, E.J., Brut, A., Wattenberg, M., Saunders, M. and Jones, M. (2010). Measurements necessary for assessing the net ecosystem carbon budget of croplands. *Agriculture, Ecosystems and Environment*, **139**:302-315.
- Smith, P., Davues, C.A., Ogle, S. Zanchi, G., Bellarby, J., Bird, N., Boddey, R.M., McNamara, N.P., Powlson, D., Cowie, A., van Noordwijk, M., Davis, S.C., Richter, D.D.B., Kryzanowski, L., van Wijk, M.T., Stuart, J., Kirton, A., Eggar, D., NewtonCross, G., Adhya, T.K. and Braimoh, A.K. (2012). Towards an integrated global framework to assess the impacts of land use and management change on soil carbon: current capability and future vision. *Global Change Biology*, **18**: 2089-2101.
- Snäll, T., Ribeiro, P.J. and Rydin, H. (2003). Spatial occurrence and colonisations in patch – tracking meta-populations: local conditions versus dispersal. *Oikos*, **103**(3): 566-578.
- Solomon, S., Qin, D., Manning, M., Alley, R.B., Berntsen, T., Bindoff, N.L., Chen, Z., Chidthaisong, A., Gregory, J.M., Hegerl, G.C., Heimann, M., Hewitson, B., Hoskins, B.J., Joos, F., Jouzel, J., Kattsov, V., Lohmann, U., Matsuno, T., Molina, M., Nicholls, N., Overpeck, J., Raga, G., Ramaswamy, V., Ren, J., Rusticucci, M., Somerville, R.F., Stocker, T.F., Whetton, P., Wood, R.A. and Wratt, D. (2007). Technical Summary. In: Solomon, S., Qin, D. and Manning, M. *et al.* (Eds.), *Climate Change 2007: The Physical Science Basis. Contribution of Working Group I to the Fourth Assessment Report of the Intergovernmental Panel on Climate Change*, Cambridge University Press, Cambridge, United Kingdom and New York.
- Sonnentag, O., van der Kamp, G., Barr, A.G. and Chen, J.M. (2010). On the relationship between water table depth and water vapour and carbon dioxide fluxes in a minerotrophic fen. *Global Change Biology*, **16**: 1762-1776.
- Sottocornola, M. & Kiely, G. (2010). Hydro-meteorological controls on the CO<sub>2</sub> exchange variation in an Irish blanket bog. *Agricultural and Forest Meteorology*, **150**: 287-297.
- Stamp, I., Baird, A.J. and Heppell, C.M. (2013). The importance of ebullition as a mechanism of methane loss to the atmosphere in a northern peatland. *Geophysical Research Letters*, **40**(10): 2087-2090.

- Stenseth, N.C., Myrnes, A., Ottersen, G., Hurrell, J.W., Chan, K.S. and Lima, M. (2002). Ecological effects of climate fluctuations. *Science*, **297**: 1292-1296.
- Stoy, P., Richardson, A., Baldocchi, D.D., Katul, G., Stanovick, J., Mahecha, M., Reichstein, R., Detto, M., Law, B. and Wohlfahrt, G. (2009). Biosphere-atmosphere exchange of CO<sub>2</sub> in relation to climate: a cross-biome analysis across multiple time scales. *Biogeosciences*, **6**(10): 2297-2312.
- Strack, M. (Eds.) (2008). *Peatlands and Climate Changes*. International Peat Society, Jyväskylä Finland.
- Strack, M. & Waddington, J.M. (2007). Response of peatland carbon dioxide and methane fluxes to a water table drawdown experiment. *Global Biogeochemical Cycles*, **21**(1).
- Stroh, P.A., Hughes, F.M.R., Sparks, T.H. and Mountford, O. (2012). The influence of time on the soil seed bank and vegetation across a landscape-scale wetland restoration project. *Restoration Ecology*, **20**: 103-112.
- Stull, R.B. (1988). *An Introduction to Boundary Layer Meteorology*, Kluwer Academic Press, Dordrecht.
- Ström, L., Mastepanov, M. and Christensen, T.R. (2005). Species-specific effects of vascular plants on carbon turnover and methane emissions from wetlands. *Biogeochemistry*, **75**(1): 65-82.
- Taiz, L. & Zeiger, E. (2010). *Plant Physiology*, Sinauer Associates, Sunderland, M.A., USA.
- Tamiya, H. (1951). Some theoretical notes on the kinetics of algal growth. *Botanical Magazine*, **6**: 167-173.
- Taneva, L. & Gonzalez-Meler, M. (2011). Distinct patterns in the diurnal and seasonal variability in four components of soil respiration in a temperate forest under free-air CO<sub>2</sub> enrichment. *Biogeosciences*, **8**: 3077-3092.
- Tanneberger, F. & Wichtmann, W. (Eds.). (2011). *Carbon Credits from Peatland Rewetting*. Schweizerbart Science Publishers, Stuttgart, Germany.
- Teh, Y.A., Silver, W.L. and Conrad, M. (2005). Oxygen effects on methane production and oxidation in humid tropical forest soils. *Global Change Biology*, **11**(8): 1283-1297.
- Teh, Y.A., Silver, W.L., Sonnentag, O., Detto, M., Kelly, M. and Baldocchi, D.D. (2011). Large Greenhouse Gas Emissions from a Temperate Peatland Pasture. *Ecosystems*, **14**: 311-325.
- Thompson, D. (2008). Carbon management by land and marine managers. *Natural England Research Report NERR026*. Natural England, Sheffield, United Kingdom.
- Tilman, D., Reich, P.B. and Knops, J.M. (2006). Biodiversity and ecosystem stability in a decade-long grassland experiment. *Nature*, **441**(7093): 629-632.
- Torrence, C. & Compo, G. (1998). A practical guide to wavelet analysis. *Bulletin of the American Meteorological Society*, **79**(1): 61-78.
- Trenberth, K.E., Jones, P.D., Ambenje, P., Bojariu, R., Easterling, D., Klein, A., Parker, D. and Rahimzadeh, F. (2007). Observation: Surface and atmospheric climate change. In: *Climate Change 2007: The Physical Science Basis. Contribution of Working Group I to the Fourth Assessment Report of the Intergovernmental Panel on Climate Change*. Cambridge University Press, Cambridge, United Kingdom.
- Tuittila, E.-S., Komulainen, V.-M., Vasander, H. and Laine, J. (1999). Restored cut-away peatland as a sink for atmospheric CO<sub>2</sub>. *Oecologia*, **120**: 563-574.

- Tuittila, E.-S., Komulainen, V.-M., Vasander, H., Nykänen, H., Martikainen, P.J. and Laine, J. (2000). Methane dynamics of a restored cut-away peatland. *Global Change Biology*, **6**: 569-581.
- Turetsky, M.R., Wieder, K., Halsey, L. and Vitt, D. (2002). Current disturbance and the diminishing peatland carbon sink. *Geophysical Research Letters*, **29**(11).
- Turetsky, M.R., Kotowska, A., Bubier, J., Dise, N.B., Crill, P., Hornibrook, E.R., Minkinen, K., Moore, T.R., Myers-Smith, I.H., Nykänen, H., Olefeldt, D., Rinne, J., Saarnio, S., Shurpali, N., Tuittila, E.-S., Waddington, J.M., White, J.R., Wickland, K.P. and Wilmking, M. (2014). A synthesis of methane emissions from 71 northern, temperate, and subtropical wetlands. *Global Change Biology*, **20**(7): 2183-2197.
- Turner, D.P., Urbanski, S., Bremer, D., Wofsy, S.C., Meyers, T., Gower, S.T. and Gregory, M. (2003). A cross-biome comparison of daily light use efficiency for gross primary production. *Global Change Biology*, **9**(3): 383-395.
- Turunen, J., Tomppo, E., Tolonen, K. and Reinikainen, A. (2002). Estimating carbon accumulation rates of un-drained mires in Finland – application to boreal and subarctic regions. *The Holocene*, **12**: 69-80.
- Twine, T.E., Kustas, W.P., Norman, J.M., Cool, D.R., Houser, P.R., Meyers, T.P., Prueger, J.H., Starks, P.J. and Wesely, M.L. (2000). Correcting eddy covariance flux underestimates over grassland. *Agricultural and Forest Meteorology*, **103**: 279-300.
- UNFCCC, 1997. *Kyoto Protocol to the United Nations Framework Convention on Climate Change*.
- Updegraff, K., Bridgman, S.D., Pastor, J., Weishampel, P. and Harth, C. (2001). Response of CO<sub>2</sub> and CH<sub>4</sub> emissions from peatland to warming and water table manipulation. *Ecological Applications*, **11**: 311-326.
- Urban, N.R., Bayley, S.E. and Eisenreich, S.J. (1989). Export of dissolved organic carbon and acidity from peatlands. *Water Resources Research*, **25**: 1619-1628.
- van Diggelen, R., Middleton, B., Bakker, J., Grootjans, A. and Wassen, M. (2006). Fens and floodplains of the temperate zone: Present status, threats, conservation and restoration. *Applied Vegetation Science*, **9**: 157-162.
- Valentini, R., Matteucci, G., Dolman, A., Schulze, E., Rebmann, C., Moors, E., Granier, A., Gross, P., Jensen, N. and Pilegaard, K. (2000). Respiration as the main determinant of carbon balance in European forests. *Nature*, **404**(6780), 861-865.
- Vargas, R., Detto, M., Baldocchi, D. and Allen, M. (2010). Multi-scale analysis of temporal variability of soil CO<sub>2</sub> production as influenced by weather and vegetation. *Global Change Biology*, **16**(5): 1589-1605.
- Vargas, R., Carbone, M., Reichstein, M. and Baldocchi, D. (2011). Frontiers and challenges in soil respiration research: from measurements to model-data integration. *Biogeochemistry*, 1-13.
- Vasander, H. & Kettunen, A. (2006). Carbon in peatlands. In: Wieder, K. & Vitt, D.H. (Eds.), *Boreal peatlands ecosystems*, Springer-Verlag, Berlin, Germany.
- Veenendaal, E.M., Kolle, O., Leffelaar, P.A., Schrier-Uijl, A.P., Van Huissteden, J., Van Walsem, J., Mödler, F. and Berendse, F. (2007). CO<sub>2</sub> exchange and Carbon balance in two grassland sites on eutrophic drained peat soils. *Biogeosciences Discussions*, **4**: 1633-1671.

- ven Breemen, N. (1995). How *Sphagnum* bogs down other plants. *Trends in Ecology and Evolution*, **10**: 270-275.
- Vickers, D. & Mahrt, L. (1997). Quality control and flux sampling problems for tower and aircraft data. *Journal of Atmospheric and Oceanic Technology*, **14**: 512-526.
- Vitt, D.H. (2006). Function characteristics and indicators of boreal peatlands. In: Wieder, R.K. and Vitt, D.H. (Eds.). *Boreal Peatland Ecosystems*. Springer, New York.
- Waddington, J.M. & Day, S.M. (2007). Methane emissions from a peatland following restoration. *Journal of Geophysical Research: Biogeosciences*, **112**(G3).
- Waddington, J.M., Griffis, T.J. and Rouse, W.R. (1998). Northern Canadian wetlands: Net ecosystem CO<sub>2</sub> exchange and climatic change. *Climatic Change*, **40**: 267-275.
- Waddington, J.M. & Price, J.S. (2000). Effect of peatland drainage, harvesting, and restoration on atmospheric water and carbon exchange. *Physical Geography*, **21**: 433-451.
- Waddington, J.M. & Roulet, N.T. (2000). Carbon balance of a boreal patterned peatland. *Global Change Biology*, **6**: 87-97.
- Waddington, J.M., Strack, M. and Greenwood, M.J. (2010). Toward restoring the net carbon sink function of degraded peatlands: short-term response in CO<sub>2</sub> exchange to ecosystem-scale restoration. *Journal of Geophysical Research: Biogeosciences*, **115**: G01008.
- Wagle, P. & Kakani, V.G. (2014). Environmental controls of daytime net ecosystem exchange of carbon dioxide in switch-grass. *Agriculture, Ecosystems and Environment*, **186**: 170-177.
- Walter, B.P., Heimann, M. and Matthews, E. (2001). Modelling modern methane emissions from natural wetlands, Model description and results. *Journal of Geophysical Research*, **106**: 34189-34206.
- Walther, G., Post, E., Convey, P., Menzel, A., Parmesan, C., Beebee, T.J.C., Fromentin, J., Hoegh-Guldberg, O. and Bairlein, F. (2002). Ecological response to recent climate change. *Nature*, **416**: 389-395.
- Wang, C.R., Huang, G.H., Liang, Z.B., Wu, J., Xu, G.Q., Yue, J. and Shi, Y. (2002). Advances in the research on sources and sinks of CH<sub>4</sub> and CH<sub>4</sub> oxidation (uptake) in soil. *Chinese Journal of Applied Ecology*, **13**: 1707-1712. (In Chinese).
- Warburton, J. (2003). Wind-splash erosion of bare peat on UK peatland moorland. *Catena*, **52**: 191-207.
- Ward, S.E., Bardgett, R.D., McNamara, N.P., Adamson, J.K. and Ostle, N.J. (2007). Long-term consequences of grazing and burning on northern peatland carbon dynamics. *Ecosystems*, **10**: 1069-1083.
- Warrington, S., Soans, C. and Cooper, H. (2009). The Wicken Fen vision: the first 10 years. *Ecos (Norwich)*, **30**: 58-65.
- Webb, E.K., Pearman, G.I. and Leuning, R. (1980). Correction of flux measurements for density effects due to heat and water vapour transfer. *Royal Meteorological Society Quarterly Journal*, **106**: 85-100.
- Whalen, S.C. (2005). Biogeochemistry of methane exchange between natural wetlands and the atmosphere. *Environmental Engineering Science*, **22**(1): 73-94.
- Whalen, S.C. & Reeburgh, W.S. (1990). Consumption of atmospheric methane by tundra soil. *Nature*, **346**: 160-162.

- Wheeler, B.D., Shaw, S.C., Fojt, W.J. and Robertson, R.A. (Eds.). (1995). *Restoration of Temperate Wetlands*. John Wiley & Sons, Chichester, United Kingdom.
- Whiting, G.J. & Chanton, J.P. (2001). Greenhouse carbon balance of wetlands: methane emission versus carbon sequestration. *Telma*, **53B**: 521-528.
- Wilczak, J.M., Oncley, S.P. and Stage, S.A. (2001). Sonic anemometer tilts correction algorithms. *Boundary-Layer Meteorology*, **99**: 127-150.
- Wilson, M.A. & Carpenter, S.R. (1999). Economic valuation of freshwater ecosystem services in the United States: 1971 - 1997. *Ecological Applications*, **9**(3): 772-783.
- Wilson, D., Farrell, C.A., Muller, C., Hepp, S. and Renou-Wilson, F. (2013). Rewetted industrial cutaway peatlands in western Ireland: prime location for climate change mitigation? *Mires and Peat*, **11**(1): 1-22.
- Wilson, D., Blain, D., Couwenberg, J., Evans, C.D., Murdiyarto, D., Page, S.E., Renou-Wilson, F., Rieley, J.O., Sirin, A., Strack, M. and Tuittila, E.-S. (2016). *Mires and Peat*, **17**(4): 1-28.
- Winergardner, D.L. (1995). *An Introduction to Soils for Environmental Professionals*. Lewis publishers, Florida, USA.
- Wohlfahrt, G., Hammerle, A., Haslwanter, A., Bahn, M., Tappeiner, U. and Cernusca, A. (2008). Seasonal and inter-annual variability of the net ecosystem CO<sub>2</sub> exchange of temperate grassland: effects of weather and management. *Journal of Geophysical Research*, **113**(8):110.
- Worrall, F., Chapman, P., Holden, J., Evans, C., Artz, R., Smith, P. and Grayson, R. (2011). *A Review of Current Evidence on Carbon Fluxes and Greenhouse Gas Emissions from UK Peatland*. JNCC Report, No. 442.
- Xiao, J., Chen, J., Davis, K.J. and Reichstein, M. (2012). Advances in up-scaling of eddy covariance measurements of carbon and water fluxes. *Journal of Geophysical Research*, **117**.
- Xu, L.K., Baldocchi, D.D. and Tang, J.W. (2004). How soil moisture, rain pulses, and growth alter the response of ecosystem respiration to temperature. *Global Biogeochemical Cycles*, **18**(4).
- Xu, L.K. & Baldocchi, D.D. (2004). Seasonal variation in carbon dioxide exchange over a Mediterranean annual grassland in California. *Agricultural and Forest Meteorology*, **123**(1-2): 79-96.
- Zeeman, M., Hiller, R., Gilgen, A., Michuna, P., Pluss, P., Buchmann, N. and Eugster, W. (2010). Management and climate impacts on net CO<sub>2</sub> fluxes and carbon budgets of three grasslands along an elevation gradient in Switzerland. *Agricultural and Forest Meteorology*, **150** (4): 519-538.

# Appendix A: Instrument Calibration Certificates

Sedge Fen

## LI-7500 CO<sub>2</sub>/H<sub>2</sub>O Analyzer

Calibration Certificate

Serial Number 75H-0190

Date: 24.09.2012

Technician MT

### CO<sub>2</sub> Calibration Values

A = 1.55436E2

B = 1.62431E4

C = 3.92991E7

D = -1.20690E10

E = 1.68224E12

XS = 0.0097

Z = 4.50000E-3

### H<sub>2</sub>O Calibration Values

A = 5.32317E3

B = 3.47061E6

C = 6.31208E7

XS = -0.0028

Z = 5.80000E-3

### Pressure Calibration\*

A0 =

A1 =

\* Ver 3.0.1 and above

### Zero/Span set on 25.09.2012

CO<sub>2</sub> Zero = 0.8930

CO<sub>2</sub> Span = 0.9978 (at 750 ppm)

CO<sub>2</sub> Span2 = 0

H<sub>2</sub>O Zero = 0.9597

H<sub>2</sub>O Span = 1.0026 (at 15 C)

H<sub>2</sub>O Span2 = 0

**Figure A1:** LI-7500 CO<sub>2</sub>/ H<sub>2</sub>O analyzer at Sedge Fen was calibrated in 2012.

S

**LI-7500 CO<sub>2</sub>/H<sub>2</sub>O Analyzer**

**Calibration Certificate**

**Serial Number 75H-0190**

**Date:** 24.11.2014

**Technician** M.P.

**CO<sub>2</sub> Calibration Values**

**A** = 1.81286E2  
**B** = 2.00267E4  
**C** = 4.41623E7  
**D** = -1.59775E10  
**E** = 2.47579E12  
**XS** = 0.0086  
**Z** = 5.50000E-3

**Signal Strength\***

**B** = 1.6  
**C** = 3.2  
\* Ver 6.5 and above

**H<sub>2</sub>O Calibration Values**

**A** = 5.21431E3  
**B** = 3.58640E6  
**C** = 9.68756E5  
**XS** = -0.0025  
**Z** = 7.90000E-3

**Pressure Calibration**

**A0** = 57.160  
**A1** = 15.250  
<serial number>

**Zero/Span set on 25.11.2014**

CO<sub>2</sub> Zero = 0.9140  
CO<sub>2</sub> Span = 1.0016 (at 601 ppm)  
CO<sub>2</sub> Span2 = 0.0000  
H<sub>2</sub>O Zero = 0.9570  
H<sub>2</sub>O Span = 0.9928 (at 14 C)  
H<sub>2</sub>O Span2 = 0.0000  
CX = 35266.7

**Figure A2:** LI-7500 CO<sub>2</sub>/H<sub>2</sub>O analyzer at Sedge Fen was calibrated in 2014.

---

**LI-7500 CO<sub>2</sub>/H<sub>2</sub>O Analyzer**

**Calibration Certificate**

**Serial Number 75H-1368**

**Date:** 20.09.2012

**Technician** M.R.

**CO<sub>2</sub> Calibration Values**

A = 1.309831E2

B = 6.480051E3

C = 3.071771E7

D = -8.16117E9

E = 9.848901E11

XS = 0.0079

Z = 6.80000E-3

**H<sub>2</sub>O Calibration Values**

A = 4.635841E3

B = 2.907561E6

C = 1.414921E7

XS = -0.0013

Z = 4.05000E-2

**Pressure Calibration\***

A0 =

A1 =

\* Ver 3.0.1 and above

**Zero/Span set on 21.09.2012**

CO<sub>2</sub> Zero = 0.8372

CO<sub>2</sub> Span = 1.0000 (at 750 ppm)

CO<sub>2</sub> Span2 = 0

H<sub>2</sub>O Zero = 1.0232

H<sub>2</sub>O Span = 1.0042 (at 15 C)

H<sub>2</sub>O Span2 = 0

---

**Figure A3:** LI-7500 CO<sub>2</sub>/H<sub>2</sub>O analyzer at Baker's Fen was calibrated in 2012.

**LI-7500A CO<sub>2</sub>/H<sub>2</sub>O Analyzer**

**Calibration Certificate**

Serial Number 75H-2568

Date: 25 Aug 2014  
Code:29899

Technician JW  
Jan W.

**CO<sub>2</sub> Calibration Values**

A = 1.51997E2  
B = -4.53462E3  
C = 5.68002E7  
D = -1.99113E10  
E = 2.72666E12  
XS = 0.0010  
Z = 4.00000E-4

**Signal Strength<sup>1</sup>**

B = 0.583  
C = 3.044  
\* Ver 6.5 and above

**H<sub>2</sub>O Calibration Values**

A = 5.46995E3  
B = 4.26450E6  
C = -2.51696E8  
XS = 0.0000  
Z = 2.34000E-2

**Zero/Span set on 26 Aug 2014**

CO<sub>2</sub> Zero = 0.9400  
CO<sub>2</sub> Span = 1.0014 (at 753 ppm)  
CO<sub>2</sub> Span2 = 0.0000  
H<sub>2</sub>O Zero = 0.8411  
H<sub>2</sub>O Span = 1.0048 (at 12 C)  
H<sub>2</sub>O Span2 = 0.0000  
CX = 41820.9

The data and analyses associated with this gas analyzer calibration are available from [www.licor.com/env/support](http://www.licor.com/env/support).



LI-COR, inc.  
P.O. Box 4425  
Lincoln, NE 68504 USA

Phone: 402-467-3576  
FAX: 402-467-2819  
Toll-free: 1-800-447-3576 (U.S. & Canada)

*Figure A4: LI-7500 CO<sub>2</sub>/H<sub>2</sub>O analyzer at Baker's Fen was calibrated in 2014.*

**LI-7500A CO<sub>2</sub>/H<sub>2</sub>O Analyzer**

**Calibration Certificate**

**Serial Number 7511-1368**

**Date:** 25.02.2015

**Technician** \_\_\_\_\_

**CO<sub>2</sub> Calibration Values      Signal Strength\***

**A =** 1.26621E2

**B =**

**B =** 1.63928E4

**C =**

**C =** 2.34175E7

\* Ver 6.5 and above

**D =** -5.35870E9

**E =** 6.39218E11

**XS =** 0.0146

**Z =** 6.50000E-3

**H<sub>2</sub>O Calibration Values**

**A =** 4.55777E3

**B =** 3.22667E6

**C =** -1.19506E8

**XS =** 0.0001

**Z =** 4.86000E-2

**Zero/Span set on 27.02.2015**

CO<sub>2</sub> Zero = 0.8684

CO<sub>2</sub> Span = 0.9924 (at 750 ppm)

CO<sub>2</sub> Span2 = 0.0000

H<sub>2</sub>O Zero = 0.8799

H<sub>2</sub>O Span = 0.9919 (at 14 C)

H<sub>2</sub>O Span2 = 0.0000

CX = 46974.4

**Figure A5:** LI-7500 CO<sub>2</sub>/H<sub>2</sub>O analyzer at Baker's Fen was calibrated in 2015.

**LI-7550 Analyzer Interface Box**

**Calibration Certificate**

**Serial Number AIU-1179**

**Date:** 01 Oct 2013

**Technician** MA

**Pressure Sensor**

A0 = 58.62

A1 = 15.48

s/n = PX-3603



LI-COR, Inc.  
P.O. Box 4425  
Lincoln, NE 68504 USA

Phone: 402-467-3576  
FAX: 402-467-2819  
Toll-free: 1-800-447-3576 (U.S. & Canada)

*Figure A6: LI-7550 analyzer interface box at Baker's Fen was calibrated in 2013.*

**LI-7700 CH<sub>4</sub> Analyzer**  
**Performance Verification**  
**Serial Number TG1-0253**

**Date:** 13 Jun 2012      **Technician** JLF

**Settings**  
Zero = -12.6811 set on 2012-06-13 22:38:31  
Span = 0.000100845 set on 2012-06-13 23:08:55

serialnumber = TG1-0253  
lasermoddepth = 10900  
laserstarttemp = 9  
blockstarttemp = 30  
blockstarttemplovrange = 5  
rssidroptresh = 0  
pzero = 57.6  
pspan = 15.13  
samplgain = 0  
refgain = 0  
mirrorpos = 0  
offset1 = 32768  
delta1 = 67  
offset2 = 0  
delta2 = 0  
dither = 30000  
sampledcoffset = 314  
sampleacoffset = -965  
sampleopticaloffset = 0

**LI-COR** | LI-COR, inc. | Phone: 402-467-3576  
SINCE 1987 | P.O. Box 4425 | FAX: 402-467-2819  
Lincoln, NE 68504 USA | Toll-free: 1-800-447-3576 (U.S. & Canada)

**Figure A7:** LI-7700 methane analyzer at Baker's Fen was calibrated in 2012.



SKYE INSTRUMENTS LTD.  
21, DDOLE ENTERPRISE PARK,  
LLANDRINDOD WELLS,  
POWYS. LD1 6DF. U.K.  
TEL: +44 (0) 1597 824811 FAX: +44 (0) 1597 824812  
email: skyemail@skyeinstruments.com  
website: www.skyeinstruments.com

**CALIBRATION CERTIFICATE No : QUA/3016/0312**

UNIT TYPE :- PAR QUANTUM SENSOR  
.....  
SERIAL NUMBER :- SKP 215 41088  
.....  
OUTPUTS :- 0.01509  $\mu\text{A} / \mu\text{mol m}^{-2} \text{s}^{-1}$   
.....  
10.00  $\mu\text{V} / \mu\text{mol m}^{-2} \text{s}^{-1}$   
.....  
DATE OF CALIBRATION :- 02/02/2012  
.....  
LAMP REFERENCE :- SK4  
.....  
A/D UNIT :- 039353, F5204  
.....

Calibrated against a National Physical Laboratory UK reference standard lamp.  
Uncertainty 5% (typically  $< \pm 3\%$ ) based on an estimated confidence of not less than 95%

Calibrated By :- G. Sims  
.....  
Checked By :- *A. M. Jones*  
.....  
Issue Date :- 05/03/2012  
.....

THIS UNIT IS DUE FOR RECALIBRATION WITHIN 2 YEARS OF THE ABOVE  
CALIBRATION DATE

Date of Last Calibration :- N/A  
.....  
% Change Since Last Calibration :- N/A  
.....

Figure A8: PAR quantum sensor at Baker's Fen was calibrated in 2012.

8



CALIBRATION CERTIFICATE OF UPPER AND LOWER PYRANOMETERS

CERTIFICATE NUMBER : 011079071 S65
FOUR-COMPONENT RADIOMETER : CNR1
SERIAL NUMBER : 071565
SENSITIVITY : 8.73 µV/W/m²
IMPEDANCE UPPER SENSOR : 26.6 Ohm
LOWER SENSOR : 35.6 Ohm
TEMPERATURE : 22 ±2 °C
REFERENCE PYRANOMETER : Kipp & Zonen CMP 3 sn071176 active from January 1, 2014
CALIBRATION DATE : 13 October 2014 (recalibration is recommended every two years)
IN CHARGE OF TEST : V.Tromp

Calibration procedure
The upper calibration procedure is based on a solar simulator (reference pyranometer) in direct artificial sunlight (1000 W/m²) and a solar simulator at incidence angle 15° W Metrol Heliode high pressure gas discharge lamp. Around the lamp is a reflector with a diameter of 10 cm. The reflector is made of pyranometers with a constant diameter. The reflector and test pyranometer are mounted on a table which can rotate. The distance of the pyranometer is approximately 100 cm. A diagram of the calibration procedure is shown in figure 1. The pyranometer is mounted on a table which can rotate with a speed of 10 rpm.

History of traceability
The reference pyranometer was calibrated and recalibrated by the calibration laboratory of the National Institute of Standards and Technology (NIST) in Gaithersburg, Maryland, USA. The measurements were performed in 1998, 2001, 2004, 2007, 2010, 2013 and 2016. The measurements were performed in 1998, 2001, 2004, 2007, 2010, 2013 and 2016. The measurements were performed in 1998, 2001, 2004, 2007, 2010, 2013 and 2016. The measurements were performed in 1998, 2001, 2004, 2007, 2010, 2013 and 2016.

The calibration of the upper sensor was done by the solar simulator with a solar constant of 1000 W/m². The calibration of the lower sensor was done by the solar simulator with a solar constant of 1000 W/m². The calibration of the upper sensor was done by the solar simulator with a solar constant of 1000 W/m². The calibration of the lower sensor was done by the solar simulator with a solar constant of 1000 W/m².

Calibration of the upper sensor was done by the solar simulator with a solar constant of 1000 W/m². The calibration of the lower sensor was done by the solar simulator with a solar constant of 1000 W/m².

Justification of total instrument calibration uncertainty
The combined uncertainty of the calibration of the upper sensor is 0.5% and of the lower sensor is 0.5%.

Notice
The calibration certificate applies to the instrument only. The data of the instrument is not valid if the instrument is damaged or if the instrument is not used according to the instructions for use.

Table with 4 columns: Page, Kipp & Zonen NV, Date, and other details.

Figure A9: CNR1 radiometer at Baker's Fen was calibrated in 2014.

R

April 2015  
\* Copy \*

## CALIBRATION CERTIFICATE OF UPPER AND LOWER PYRGEOMETERS

**CERTIFICATE NUMBER** : 011764071515  
**FOUR-COMPONENT RADIOMETER** : CNR1  
**SERIAL NUMBER** : 071515  
**SENSITIVITY** : 9.28  $\mu\text{V}/\text{W}/\text{m}^2$   
**IMPEDANCE UPPER SENSOR** : 102.1 Ohm  
**LOWER SENSOR** : 85.8 Ohm  
**REFERENCE PYRGEOMETER** : Kipp & Zonen CGR 3 sn Delft1 active from 01 October 2013  
**CALIBRATION DATE** : 17 February 2015 (recalibration is recommended every two years)  
**IN CHARGE OF TEST** : V.Tromp

### Calibration procedure

The reference and test pyrgeometer are mounted horizontally on a table under an extended warm plate (67°C). The table can rotate to exchange the positions of both instruments. The net irradiance at the pyrgeometers is approximately 150  $\text{W}/\text{m}^2$ . The indoor procedure is based on a sequence of simultaneous readings. After 60 s exposure to the warm plate, the output voltages of both pyrgeometer are integrated 30 s. Next both pyrgeometers are covered by a blackened "shutter" with stable "room temperature". After 60 s both signals are integrated again during 30 s. The resulting two "zero" signals are subtracted from the former signals to get comparable responses. In this way is compensated for temperature differences between both pyrgeometers. Next the pyrgeometer positions are interchanged by rotation of the table and the procedure is repeated. The mean of former and later responses is compared to derive the sensitivity figure of the test pyrgeometer. In this way asymmetry in the warm plate configuration and IR environment is cancelled out. The obtained sensitivity is valid for similar conditions as during the outdoors calibration of the reference CGR 3.

### Hierarchy of traceability

The reference CGR 3 has been compared against a reference pyrgeometer CGR 4 under mainly clear sky conditions during night time at Kipp & Zonen, Delft Holland. (On his turn the CGR 4 was calibrated outdoors 7 July to 2 December 2012 at the IR-centre of the World Radiation Center Davos against their pyrgeometer reference group during 80 measurement days.) The reference CGR 3 and CGR 4 were placed horizontally side by side. During the calibration period on 1 October 2013 the (outgoing) radiation signal ( $U/S$ ) ranged from -72 to -66  $\text{W}/\text{m}^2$ . The instrument temperatures ranged from -6.4 to +10.1 °C with a mean of +8.1 °C. The pyrgeometer thermopile outputs ( $U_{CGR3}$ ,  $U_{CGR4}$ ) and body temperatures ( $T_{CGR3}$ ,  $T_{CGR4}$ ) were measured every second by a COMBLOG 1020 data logger and averages of 60 measurements have been logged as 1 min. values. Later on the downward radiation ( $L_d$ ) can be determined with the formula:

$$L_d = \frac{U_{CGR4}}{S} + 5.67 \cdot 10^{-8} \cdot T_{CGR4}^4$$

For the CGR 4 sn F00280 a sensitivity  $S$  of  $11.32 \pm 0.4 \mu\text{V}/\text{W}/\text{m}^2$  has been applied and with its voltage  $U_{CGR4}$  and temperature  $T_{CGR4}$  data the reference  $L_d$  is calculated ranging, from +238 to +308  $\text{W}/\text{m}^2$ . For the reference CGR 3 a one minute average sensitivity  $S_{CGR3}$  is calculated with the formula:

$$S_{CGR3} = U_{CGR3} \cdot (L_d - 5.67 \cdot 10^{-8} \cdot T_{CGR3}^4)^{-1}$$

The final  $S_{CGR3}$  is the average of one minute  $S_{CGR3}$ 's determined in periods with a net IR signal  $< -46 \text{ W}/\text{m}^2$  (Clear sky). The sum of all periods must be at least 4 hours. The CGR 3 sn Delft1 sensitivity and its calculated expanded uncertainty are:  $10.02 \pm 0.46 \mu\text{V}/\text{W}/\text{m}^2$ .

### Justification of total instrument calibration uncertainty

The expanded (95% probability) calibration uncertainty is the "root sum square" of two uncertainties:

1. The expanded uncertainty due to random effects during the comparison outdoors at Kipp & Zonen, Delft partly due to different instrumental properties of the reference CGR 3 and the reference CGR 4 and partly due to the datalogger voltage and temperature (resistance) measurement uncertainties is:  $\pm 0.46/10.02 = \pm 4.6\%$ . This includes the uncertainty in the calibration of the reference CGR 4 as given by the World Radiation Center in Davos.
2. The expanded uncertainty of the transfer procedure (calibration by comparison) is estimated to be 1.4%. This is mainly due to deviations between the spectral transmittance of the window of the reference and the window of the test pyrgeometer and due to their different TC.

The estimated combined expanded (95%) uncertainty is  $\sqrt{4.6^2 + 1.4^2} = 4.8\%$ .

### Notice

The calibration certificate supplied with the instrument is at the date of first use. Even though the calibration certificate is dated relative to manufacture, or recalibration, the instrument does not undergo any sensitivity changes when kept in the original packing. From the moment the instrument is taken from its packaging and exposed to irradiance the sensitivity may deviate with time. See the "non-stability" value (% change in sensitivity per year) given in the radiometer specifications.

Page	Kipp & Zonen B.V.	T: +31 (0) 15 2755 210	VAT no.: NL0055.74.857.B.01
1/1	Delftechpark 36, 2628 XH Delft	F: +31 (0) 15 2620 351	Trade Register no.: 27239004
	P.O. Box 507, 2600 AM Delft	info@kippzonen.com	Member of IME1
	The Netherlands	www.kippzonen.com	

**Figure A10:** CNR1 radiometer at Sedge Fen was calibrated in 2015.

## Appendix B: Data Post-processing and Analysis R Code

```
#####  
#### Data post-processing & analysis  
#### author<<  
#### GP & JK based on REddyProc from AMM  
#####  
  
##### source("EPDataProc_BF.R")  
library(REddyProc)  
library(base)  
library(ggplot2)  
library(lazyeval)  
library(maps)  
library(grid)  
library(lattice)  
library(dplyr)  
library(openair)  
library(splines)  
library(survival)  
library(Formula)  
library(lmodel2)  
library(Hmisc)  
library(graphics)  
library(Rcpp)  
library(minpack.lm)  
library(RColorBrewer)  
  
##### Change dir  
setwd("E:\\Working Post Process\\BF_2013")  
  
##### Set year, site, start/end dates  
Year<- 2013  
Site<-'Bakers'  
StartDate<-"2013-01-01"  
EndDate<-"2013-12-31"  
  
##### latitude of site in degrees  
latdeg<-52  
ID1<-'BF'  
SL<-substr(Site,start=1,stop=1)  
  
##### list of time stamps for the full output  
FD=c('20130112', '2016-01-01T000001', '2016-01-01T000002')  
  
##### Format of files  
nf<-length(FD)/3 # number of files  
dim(FD)<-c(3,nf)  
FileData<-as.data.frame(t(FD))  
names(FileData)<-c('ID2list','T1list','T2list')  
ID2list<-FileData$ID2list  
T1list <-FileData$T1list  
T2list <-FileData$T2list  
  
##### list of full output file names  
FList=paste('eddypro_',ID1,'_',ID2list[1],'_full_output_',T1list[1],  
'_.csv',sep="", collapse="")
```

```

for (i in 2:nf) {FList=c(FList, paste('eddypro_',ID1,'_',ID2list[i],
'_full_output_',T1list[i],'.csv',sep="", collapse=""))
}
zMAD <- 5.5 # following Papale et al. (2006):
# multiplier to set spike size in spike detection using
# the median of absolute deviation about the median
(MAD)
# that is a robust outlier estimator (Sachs, 1996).

##### functions used
# date setup
source("datesetup.R")

# day night indicator
source("dayni.R") #set up function dayni to calculate a day night
indicator

# function for loading Eddy Pro (EP) data
source("fLoadEPIntoDataframe.R")

# function for selecting data clumms from the loaded EddyPro data from
'BF'
source("dataselB2.R")

# data rejection due to absolute limits
source("limitsrej.R")
# set up function for rejection of data due to
outrange values
# takes whole data frame as argument

# data rejection due to absolute limits
source("lowdataqualrej.R")
# set up function for rejection of data due to low
quality
# takes whole data frame as argument

# run mean outlier
source("runmeanoutlier.R")

# spike detection
source("spikes.R") # set up function spikes for spike
detection
# spikes <- function(VARo, DAYNI, zMAD) {

# stuff for plotting
source("plotstuff.R")

# reading ogives
source('readogives.R')

# determination of u* threshold
source("uStarThr.R")

```

```

# reading dipwell data
source('getdipwelldata.R')

# Plotting & data analysis
source('plotting.R')

##### Very important - set up a date range
dt.F<-datesetup(StartDate,EndDate)

##### Checking start date and end date, no. of files and all files
StartDate
EndDate
nf
FileData

##### Read input files and put data together
lbmd<-(-1)
for (i in 1:nf) { #length(FList)
  EPFOfile<-FList[i]
  print(paste("reading full output file ",EPFOfile))

# load eddypro formatted data full output
  EPD.F <- fLoadEPIntoDataframe(EPFOfile,Typ='FO')

# load eddypro formatted biomet data
  print(paste("reading biomet file ",EPFOfile))
  BMD.F <- fLoadEPIntoDataframe(EPFOfile,Typ='BM',T2=T2list[i],
lastBMDOY=lbmd)
  message("Data read")
  lbmd=BMD.F$DOY[nrow(BMD.F)]

# reading ogives
  print(paste("reading ogives ",EPFOfile))
  O.F <- readogives(ID2list[i],Typ='OG')
  message('Data read')
  if( i==1) {
    EPDA.F <- EPD.F; BMDA.F <- BMD.F
    OGIVE.F <-O.F
  } else {
    print("Joining EddyDataFile")
    EPDA.F <- rbind(EPDA.F,EPD.F)
    print("Joining BioMetDataFile")
    BMDA.F <- rbind(BMDA.F,BMD.F)
    print("Joining ogives")
    OGIVE.F <- rbind(OGIVE.F,O.F)
  }
}
  message("read and put data together done") #end of for (i in
1:length(FList))

##### Merging data with date and timestamps
ED.F<-merge(dt.F,EPDA.F,by=c("date","time"),all.x=TRUE)
ED.F[["date.y"]]<-NULL;ED.F[["time.y"]]<-NULL;ED.F[["fDoY.y"]]<-NULL;

```

```

names(ED.F)[names(ED.F)=="date.x"] <- "date"
names(ED.F)[names(ED.F)=="time.x"] <- "time"
names(ED.F)[names(ED.F)=="fDoY.x"] <- "fDoY"
BD.F<-merge(dt.F,BMDA.F,by=c("date","time"),all.x=TRUE)
BD.F[["date.y"]]<-NULL; BD.F[["time.y"]]<-NULL; BD.F[["fDoY.y"]]<-
NULL;
names(BD.F)[names(BD.F)=="date.x"] <- "date"
names(BD.F)[names(BD.F)=="time.x"] <- "time"
names(BD.F)[names(BD.F)=="fDoY.x"] <- "fDoY"

##### Convert gap flags to NA
OG.F <- fConvertGapsToNA(OGIVE.F)
Ogive.F<-merge(dt.F,OG.F,by=c("date","time"),all.x=TRUE)
Ogive.F[["date.y"]]<-NULL;Ogive.F[["time.y"]]<-
NULL;Ogive.F[["fDoY.y"]]<-NULL;
names(Ogive.F)[names(Ogive.F)=="date.x"] <- "date"
names(Ogive.F)[names(Ogive.F)=="time.x"] <- "time"
names(Ogive.F)[names(Ogive.F)=="fDoY.x"] <- "fDoY"
Ogive.F$Hog=as.numeric(as.character(Ogive.F$Hog))
Ogive.F$H2Oog=as.numeric(as.character(Ogive.F$H2Oog))
Ogive.F$CO2og=as.numeric(as.character(Ogive.F$CO2og))
Ogive.F$CH4og=as.numeric(as.character(Ogive.F$CH4og))

##### Data selection into EddyData.F
EddyData.F=dataselB2(ED.F,BD.F,Year)
nEdDat=nrow(EddyData.F)

##### available data checking 1
message(c('NO. of CO2 after data selection: ',
sum(!is.na(EddyData.F$NEE))))
message(c('NO. of LE after data selection: ',
sum(!is.na(EddyData.F$LE))))
message(c('NO. of H after data selection: ',
sum(!is.na(EddyData.F$H))))
message(c('NO. of CH4 after data selection: ',
sum(!is.na(EddyData.F$CH4))))
message(c('NO. of H2O after data selection: ',
sum(!is.na(EddyData.F$H2O))))
message(c('NO.of Tair after selection: ',
sum(!is.na(EddyData.F$Tair1))))
message(c('NO. of RH after data selection: ',
sum(!is.na(EddyData.F$RH1))))
message(c('NO. of PAR after data selection: ',
sum(!is.na(EddyData.F$PAR1))))
message(c('NO. of SWin after selection: ',
sum(!is.na(EddyData.F$SWin))))
message(c('NO. of SWout after selection: ',
sum(!is.na(EddyData.F$SWout))))
message(c('NO. of LWin after data selection: ',
sum(!is.na(EddyData.F$LWin))))
message(c('NO. of LWout after selection: ',
sum(!is.na(EddyData.F$LWout))))
xl=length(EddyData.F$NEE)

##### read dipwell data

```

```

ED.F<-EddyData.F
EddyData.F<-getdipwelldata(ED.F,Site,2013)

##### throw out junk put in by eddypro
#### take as first indication is that Rn=0
xi=which(EddyData.F$Rn==0)
EddyData.F$Rn[xi] <- NA; EddyData.F$Rg[xi] <- NA
EddyData.F$SWin[xi] <- NA; EddyData.F$SWout[xi] <- NA
EddyData.F$LWin[xi] <- NA; EddyData.F$LWout[xi] <- NA
EddyData.F$rain[xi] <- NA
EddyData.F$shf1[xi] <- NA; EddyData.F$shf2[xi] <- NA
EddyData.F$shf3[xi] <- NA;
EddyData.F$shf4[xi] <- NA

##### then throw out duplicates occurring in a row in Rn
xi=which(EddyData.F$Rn[2:nEdDat]==EddyData.F$Rn[1:nEdDat-1])+1
EddyData.F$Rn[xi] <- NA; EddyData.F$Rg[xi] <- NA
EddyData.F$SWin[xi] <- NA; EddyData.F$SWout[xi] <- NA
EddyData.F$LWin[xi] <- NA; EddyData.F$LWout[xi] <- NA
EddyData.F$rain[xi] <- NA
EddyData.F$shf1[xi] <- NA; EddyData.F$shf2[xi] <- NA
EddyData.F$shf3[xi] <- NA;
EddyData.F$shf4[xi] <- NA

message("EddyData Data frame set up")

#### Some date checking
sum(EddyData.F$DoY>0,na.rm=TRUE)
for ( i in 1:366) { nd<-sum(EddyData.F$DoY==i,na.rm=TRUE)
  if(nd!=48 & nd!=96) {
    print(c(i,nd))
    print(EddyData.F$fDoY[which(EddyData.F$DoY==i)])
    print(EddyData.F$fDoY[which(EddyData.F$DoY==i+1)])
  } else {
    print(c(i,nd))
  }
} # End of for

xx<-EddyData.F$fDoY[2:nEdDat]-EddyData.F$fDoY[1:nEdDat-1]
print(c(which(xx<0.019),xx[xx<0.019],
EddyData.F$fDoY[which(xx<0.019)]))
print(c(which(xx>0.022),xx[xx>0.022],
EddyData.F$fDoY[which(xx>0.022)]))

##### Add day/night indicator Day=1, Night=0
# last/first night before/after day = 0.333
# last/first day before/after night = 0.666
ED.F<-EddyData.F
EddyData.F<-dayni(ED.F,latdeg)

message('Added day night indicator')
message('De-spiking start QC')

##### Despiking
#### Put in columns for spikes and despiked data and save original data

```

```

EddyData.F <- cbind(EddyData.F,NEEo=EddyData.F$NEE,NEEsp=0,
LEo=EddyData.F$LE,LEsp=0)
EddyData.F <- cbind(EddyData.F,Ho=EddyData.F$H,Hsp=0,
fCH4o=EddyData.F$fCH4,fCH4sp=0)

##### detect spikes in chunks of 13 days of data
for (i in 1:trunc(nEdDat/48/13)) {
  zz=c(((i-1)*13*48+1):(i*13*48))      # 13 day chunks
                                      # day/night indicator:
dayni[zz]
  ##### determine spike locations
  EddyData.F$NEEsp[zz] <- spikes(EddyData.F$NEEo[zz],
EddyData.F$dayni[zz],zMAD)
  EddyData.F$LEsp[zz] <- spikes(EddyData.F$LEo[zz],
EddyData.F$dayni[zz],zMAD)
  EddyData.F$Hsp[zz] <- spikes(EddyData.F$Ho[zz],EddyData.F$dayni[zz],
zMAD)
  EddyData.F$fCH4sp[zz]<- spikes(EddyData.F$fCH4o[zz],
EddyData.F$dayni[zz],zMAD)
  } # End of for

##### put in missing values when there are spikes
xD <- (EddyData.F$NEEsp==1) ; EddyData.F$NEE[which(xD)] <- NA
message(c('Despiking: Number of NEE data removed: ', sum(xD,
na.rm=T) ))
xD <- (EddyData.F$LEsp==1) ; EddyData.F$LE[which(xD)] <- NA
message(c('Despiking: Number of LE data removed: ', sum(xD,na.rm=T)
))
xD <- (EddyData.F$Hsp==1) ; EddyData.F$H[which(xD)] <- NA
message(c('Despiking: Number of H data removed: ', sum(xD,na.rm=T)
))
xD <- (EddyData.F$fCH4sp==1); EddyData.F$fCH4[which(xD)] <- NA
message(c('Despiking: Number of fCH4 data removed: ', sum(xD,
na.rm=T) ))

message('De-spiking done')
##### "Remove" despiking
EddyData.F$NEE<-EddyData.F$NEEo
EddyData.F$LE<-EddyData.F$LEo
EddyData.F$H<-EddyData.F$Ho
EddyData.F$fCH4<-EddyData.F$fCH4o

##### Remove data due to fixed limitations (variable ranges)
EDX.F <- EddyData.F
EddyData.F <-limitsrej(EDX.F)
message('Data removed due to fixed ranges')
uStarThr(EddyData.F$Tair,EddyData.F$Ustar,EddyData.F$NEE,
EddyData.F$dayni)

##### Remove data due to inappropriate quality
EDX.F <- EddyData.F
EddyData.F <- lowdataqualrej(EDX.F)
EddyData.F <- lowdataqualrej(EDX.F, Ogive.F)

message('Low quality data removed')

```

```

    message(c('Number of CO2 data after QC: ',
sum(!is.na(EddyData.F$NEE))))
    message(c('Number of LE data after QC: ', sum(!is.na(EddyData.F$LE))))
    message(c('Number of H data after QC: ', sum(!is.na(EddyData.F$H))))
    message(c('Number of CH4 data after QC: ',
sum(!is.na(EddyData.F$CH4))))
    message(c('Number of H2O data after QC: ',
sum(!is.na(EddyData.F$H2O))))
    message(c('Number of Tair data after QC: ',
sum(!is.na(EddyData.F$Tair1))))
    message(c('Number of RH data after QC: ',
sum(!is.na(EddyData.F$RH1))))
    message(c('Number of PAR data after QC: ',
sum(!is.na(EddyData.F$PAR1))))
    message(c('Number of SWin data after QC: ',
sum(!is.na(EddyData.F$SWin))))
    message(c('Number of SWout data after QC: ',
sum(!is.na(EddyData.F$SWout))))
    message(c('Number of LWin data after QC: ',
sum(!is.na(EddyData.F$LWin))))
    message(c('Number of LWout data after QC: ',
sum(!is.na(EddyData.F$LWout))))

##### calculations using screened data
##### Global radiation (Rg)
EddyData.F <- cbind(EddyData.F, Rg=EddyData.F$Rg2)
EddyData.F$Rg[EddyData.F$Rg<0] <-0

##### Net radiation (Rn)
EddyData.F$Rn=EddyData.F$LWin-EddyData.F$LWout+EddyData.F$SWin-
EddyData.F$SWout

##### Average soil heat flux (shf)
EddyData.F<-cbind(EddyData.F,shf=rowMeans(cbind(EddyData.F$shf1,
EddyData.F$shf2,EddyData.F$shf3,EddyData.F$shf4),na.rm=TRUE))

##### Average soil water cotent (swc)
EddyData.F<-cbind(EddyData.F,swc=rowMeans(cbind(EddyData.F$swc1,
EddyData.F$swc2,EddyData.F$swc3,EddyData.F$swc4),na.rm=TRUE))
message(c('Number of Rg data after QC: ', sum(!is.na(EddyData.F$Rg))))
message(c('Number of Rn data after QC: ', sum(!is.na(EddyData.F$Rn))))
message(c('Number of shf data after QC: ',
sum(!is.na(EddyData.F$shf))))
message(c('Number of swc data after QC: ',
sum(!is.na(EddyData.F$swc))))

##### decide on which met data to use
##### weather station Tair and RH
EddyData.F <- cbind(EddyData.F, Tair=EddyData.F$Tair1)
EddyData.F <- cbind(EddyData.F, RH=EddyData.F$RH1)
message(c('Number of Tair data after QC: ',
sum(!is.na(EddyData.F$Tair))))
message(c('Number of RH data after QC: ',
sum(!is.na(EddyData.F$RH))))

```

```

##### Calculate VPD from Tair and rH
EddyData.F<-cbind(EddyData.F,
  VPD=fCalcVPDfromRHandTair(EddyData.F$RH,EddyData.F$Tair))
message(c('Number of VPD data after QC: ',
sum(!is.na(EddyData.F$VPD))))

##### Water table flag

EddyData.F <- cbind(EddyData.F,wtstep=as.numeric(EddyData.F$WT>(-15)))
EddyData.F <- cbind(EddyData.F,wtstep=as.numeric(BD.F$WT>(-0.15)))

##### Energy balance
##### change the NA gaps in shf to 0
xx=EddyData.F$shf
xx[is.na(xx)]<-0
EddyData.F <- cbind(EddyData.F, shf0=xx)
vf=EddyData.F$Ein
vf[is.na(vf)]<-0
EddyData.F <- cbind(EddyData.F, Ein=vf)

##### calculate Ein, Eout, Enet
EddyData.F <- cbind(EddyData.F, Ein=EddyData.F$Rn-EddyData.F$shf0)
EddyData.F <- cbind(EddyData.F, Eout=EddyData.F$H+EddyData.F$LE)
EddyData.F <- cbind(EddyData.F, Enet=EddyData.F$Ein-EddyData.F$Eout)
message(c('Number of shf0 data for EBC: ',
sum(!is.na(EddyData.F$shf0))))
message(c('Number of Ein data for EBC: ',
sum(!is.na(EddyData.F$Ein))))
message(c('Number of Eout data for EBC: ',
sum(!is.na(EddyData.F$Eout))))

##### Add time stamps in POSIX time format
EDWPX.F<-fConvertTimeToPosix(EddyData.F,'YDH',Year.s='Year',
  Day.s='DoY',Hour.s='Hour')
EddyDataWithPosix.F <- data.frame(DateTime=EDWPX.F$DateTime,
  NEE=EDWPX.F$NEE, H=EDWPX.F$H, LE=EDWPX.F$LE,Rn=EDWPX.F$Rn,
  Ein=EDWPX.F$Ein,
  Eout=EDWPX.F$Eout, Enet=EDWPX.F$Enet,Rg=EDWPX.F$Rg, Tair=EDWPX.F$Tair,

  shf=EDWPX.F$shf,VPD=EDWPX.F$VPD, RH=EDWPX.F$RH, fCH4=EDWPX.F$fCH4,
  ET=EDWPX.F$fH2O,wt=EDWPX.F$WT, Ustar=EDWPX.F$Ustar, rain=EDWPX.F$rain,

  PAR=EDWPX.F$PAR1,swc=EDWPX.F$swc, wtstep=EDWPX.F$wtstep)
colnames(EDWPX.F)

##### Initialize R5 reference class sEddyProc for processing of eddy
data
##### with all variables needed for processing later
EddyProc.C <- sEddyProc$new(Site, EddyDataWithPosix.F,
  c('NEE','Rg','Tair','VPD','RH','shf','H','LE',
  'Rn','Eout','Ein','Enet','fCH4','wt','ET','Ustar',
  'rain','PAR','swc','wtstep'))

```

```

####xxxx!! PLOT of all data in directory \plots (of current R working
dir)
for (var in c('NEE', 'H', 'LE', 'shf', 'Rn', 'Tair', 'VPD', 'Rg', 'fCH4', 'ET',
'PAR')) {
  EddyProc.C$sPlotFingerprint(var)
  EddyProc.C$sPlotDiurnalCycle(var)
  EddyProc.C$sPlotHHHFluxes(var)
}

####xxxx!! PLOT individual years to screen (of current R graphics
device)
for ( iy in 2013 ) {
  EddyProc.C$sPlotHHHFluxesY('NEE', Year.i=iy)
  EddyProc.C$sPlotFingerprintY('H', Year.i=iy)
  EddyProc.C$sPlotFingerprintY('LE', Year.i=iy)
  EddyProc.C$sPlotFingerprintY('shf', Year.i=iy)
  EddyProc.C$sPlotFingerprintY('Rg', Year.i=iy)
}

##### Fill gaps in variables with MDS gap filling algorithm
EddyProc.C$sMDSGapFill('NEE', FillAll.b=TRUE)
EddyProc.C$sMDSGapFillAfterUstar('NEE', UstarThres.V.n=0.3,
UstarSuffix.s='Th')
colnames(EddyProc.C$sExportResults())

##### Partition NEE into GPP and respiration (GPP<0?)
##### Gap-filled Tair (and NEE) needed for partitioning
EddyProc.C$sMDSGapFill('Tair', FillAll.b=FALSE)
EddyProc.C$sMRFluxPartition(FluxVar.s = 'NEE_f', QFFluxVar.s
='NEE_fqc',
  QFFluxValue.n = 0, TempVar.s = 'Tair_f', QFTempVar.s = 'Tair_fqc',
  QFTempValue.n = 0, RadVar.s = 'Rg', Lat_deg.n=52.3, Long_deg.n=0.3,
  TimeZone_h.n=0, debug.l = list(useLocalTime.b = FALSE))

##### Gap fill variable with (non-default) variables and limits
EddyProc.C$sMDSGapFill('LE', V1.s='Rn', T1.n=30, V2.s='VPD', T2.n=5,
V3.s='Tair', T3.n=2.5, FillAll.b=TRUE)
EddyProc.C$sMDSGapFill('H', V1.s='Rn', T1.n=30, V2.s='VPD', T2.n=5,
V3.s='Tair', T3.n=2.5, FillAll.b=TRUE)
EddyProc.C$sMDSGapFill('ET', V1.s='Rn', T1.n=30, V2.s='VPD', T2.n=5,
V3.s='Tair', T3.n=2.5, FillAll.b=TRUE)
EddyProc.C$sMDSGapFill('Rn', V1.s='Rn', T1.n=30, FillAll.b=TRUE)
EddyProc.C$sMDSGapFill('shf', V1.s='shf', T1.n=2, FillAll.b=TRU
EddyProc.C$sMDSGapFill('Rg', V1.s='Rg', T1.n=50, FillAll.b=TRUE)
EddyProc.C$sMDSGapFill('PAR', V1.s='PAR', T1.n=10, FillAll.b=TRUE)
EddyProc.C$sMDSGapFill('swc', V1.s='swc', T1.n=2, FillAll.b=TRUE)
EddyProc.C$sMDSGapFill('fCH4', V1.s='Rn', T1.n=30, V2.s='wt', T2.n=2,
V3.s='Tair', T3.n=2.5, FillAll.b=TRUE ) # R2=0.6313
EddyProc.C$sMDSGapFill('fCH4', V1.s='wt', T1.n=2, V2.s='Tair', T2.n=2.5,
V3.s='Rn', T3.n=30, FillAll.b=TRUE ) # R2=0.5154
EddyProc.C$sMDSGapFill('fCH4', V1.s='Rn', T1.n=30, V2.s='Tair',
T2.n=2.5,

```

```

V3.s='wt',T3.n=2, FillAll.b=TRUE ) # R2=0.5666

##### Export gap filled data to standard data frame
FilledEddyData.F <- EddyProc.C$ExportResults()
colnames(FilledEddyData.F)
FilledEddyData.F <- cbind(DateTime=EddyDataWithPosix.F$DateTime,
FilledEddyData.F)
colnames(FilledEddyData.F)
FilledEddyData.F$NEE_f
colnames(EddyDataWithPosix.F)
write.csv(FilledEddyData.F,'test')

#####xxxx calculate daily sums
daysum <- function(xts) { xts[is.na(xts)]=0; xl=length(xts);
zz=cumsum(xts)
xx=seq(48,xl, by=48); yy=zz[xx]
return(yy-c(0,yy[1:(xl/48-1)])) }

monthsum <- function(xts) { xts[is.na(xts)]=0; xl=length(xts);
zz=cumsum(xts)
xx=seq(xl/12,xl, by=xl/12); yy=zz[xx]
return(yy-c(0,yy[1:11])) }

##### Generate plots of filled data in directory \plots
for ( var in c('NEE','H','LE','shf','Rn','fCH4','ET') ) {
varf=paste(var,"_f",sep=''); varfsd=paste(var,"_fsd",sep='')
EddyProc.C$PlotHHFluxes(varf)
EddyProc.C$PlotFingerprint(varf)
EddyProc.C$PlotDiurnalCycle(varf)
EddyProc.C$PlotDailySums(varf,varfsd)
}
EddyProc.C$PlotDailySumsY('GPP_f',Year.i=Year)
EddyProc.C$PlotDailySumsY('Rec0',Year.i=Year)

##### Plot individual years/months to screen (of current R graphics
device)
EddyProc.C$PlotHHFluxesY('NEE', Year.i=Year)
EddyProc.C$PlotFingerprintY('NEE_f', Year.i=2013)
EddyProc.C$PlotDailySumsY('NEE_f','NEE_fsd', Year.i=Year)
EddyProc.C$PlotDiurnalCycleM('fCH4_f', Month.i=8)

##### Save results into (tab-delimited) text file in directory \out
CombinedData.F <- cbind(EddyData.F, FilledEddyData.F)
fWriteDataframeToFile(CombinedData.F,paste(Site,Year,'Results.txt',
sep=""),'out')
colnames(CombinedData.F)
fWriteDataframeToFile(FilledEddyData.F,paste(Site,Year,
'FilledResults.txt',sep=""),'out')
fWriteDataframeToFile(EddyData.F, paste(Site,Year,
'OriginalResults.txt',sep=""),'out')

```

```

##### Plotting
#### plot editing
#### source("plotstuff.R")
#### read in results dataframe
EddyData2013BF.F <- read.csv('EddyData2013BF.csv')
colnames(EddyData2013BF.F)

## remove nonsense data
EddyData2013BF.F[EddyData2013BF.F>1000000]<-(-9999)
EddyData2013BF.F[EddyData2013BF.F<(-1000000)]<-(-9999)
print("Nonsense data removed done")

#### Convert gap flags to NA
EddyData2013BF.F <- fConvertGapsToNA(EddyData2013BF.F)
EddyData2013BF.F <- fConvertGapsToNA(EddyData2013BF.F,
GapFlag.n=9999.99)
print("gap flags converted to NA done")

##### Finger print plots
xdy=(1:365)
xhr=(1:48)/2
grid <- expand.grid(x=xhr, y=xdy)
zdat<-EddyData2013BF.F$NEE_f
dim(zdat)<-c(48,365)
levelplot(zdat~x*y,grid,col.regions=HSV(h=seq(from=4/6,to=0,length=20),
s=1,v=1),
xlab="",ylab="",at=c(-20,-16,-12,-9,-6.5,-3,-2.5,-2,-1.5,-1,0,3.5,6.5,
10,15,20))
levelplot(zdat~x*y,grid,col.regions=rainbow(15,start=0,end=4/6),
xlab="Hour",
ylab="Days",at=c(-15,-12,-8,-4,-3,-2,-1,0,1,2,3,4,10))

##### Monthly Mean Diurnal cycles plots
#### create matrix and fill the dataframe in
xdy=(1:365)
xhr=(1:48)/2
grid <- expand.grid(x=xhr, y=xdy)
zdat<-EddyData2013BF.F$NEE_f
dim(zdat)<-c(48,365)

#### Plot yr1
plot(c(1:48),rowMeans(zdat[,1:31]),xlim=c(0,600),ylim=c(-25,15),
type='l', lwd=2.5,col=2,xlab="",ylab="",xaxt="n")
lines(c(50:97),rowMeans(zdat[,32:59]), lwd=2.5, col=2)
lines(c(100:147),rowMeans(zdat[,60:90]), lwd=2.5, col=2)
lines(c(150:197),rowMeans(zdat[,91:120]), lwd=2.5, col=2)
lines(c(200:247),rowMeans(zdat[,121:151]), lwd=2.5, col=2)
lines(c(250:297),rowMeans(zdat[,152:181]), lwd=2.5, col=2)
lines(c(300:347),rowMeans(zdat[,182:212]), lwd=2.5, col=2)
lines(c(350:397),rowMeans(zdat[,213:243]), lwd=2.5, col=2)
lines(c(400:447),rowMeans(zdat[,244:273]), lwd=2.5, col=2)
lines(c(450:497),rowMeans(zdat[,274:304]), lwd=2.5, col=2)
lines(c(500:547),rowMeans(zdat[,305:334]), lwd=2.5, col=2)
lines(c(550:597),rowMeans(zdat[,335:365]), lwd=2.5, col=2)

```

```

#### Plot editing
  abline(h=0,lty=2,col="lightgrey")
  abline(v=0,lty=2,col="lightgrey")
  abline(v=49,lty=2,col="lightgrey")
  abline(v=98,lty=2,col="lightgrey")
  abline(v=148,lty=2,col="lightgrey")
  abline(v=198,lty=2,col="lightgrey")
  abline(v=248,lty=2,col="lightgrey")
  abline(v=298,lty=2,col="lightgrey")
  abline(v=348,lty=2,col="lightgrey")
  abline(v=398,lty=2,col="lightgrey")
  abline(v=448,lty=2,col="lightgrey")
  abline(v=498,lty=2,col="lightgrey")
  abline(v=548,lty=2,col="lightgrey")
  abline(v=598,lty=2,col="lightgrey")
  mtext(labCO2fums,side=2,line=2.5)
  axis(1,at=ilabp5,labels=cmlab5)

##### Daily sum seasonal change
  barplot(daysum(EddyData2013BF.F$NEE_f)*60*30/1000000*12,width=1,
  ylim=c(-20,20))
  lines(c(1:365)*1.2,daysum(EddyData2013BF.F$GPP_f)*(-
  60)*30/1000000*12,col=3)
  lines(c(1:365)*1.2,daysum(EddyData2013BF.F$Reco)*60*30/1000000*12,
  col=2)
  axis(1,at=ilabp4,labels=cmlab4)
  abline(h=-20)
  abline(h=20)
  abline(v=455)
  mtext(labNEEgm2d,side=2,line=2.5)
  barplot(daysum(FilledEddyData.F$ET_f)*60*30/1000000*12,width=2,
  ylim=c(0,6),col=4)
  polygon(CombinedData.F$DATE,
  daysum(EddyData2013BF.F$NEE_f)*60*30/1000000*12,ylim=c(-5,5))

##### Cumulative plots
  plot(cumsum(EddyData2013BF.F$NEE_f)*12/1000000*1800,type="l",
  xaxt="n",xlab="",ylab="",
  main="Cumulative carbon dioxide flux",font.main=2)
  axis(1,at=ilabp3,labels=cmlab3)
  mtext(labNEEgm2,side=2,line=2.5)
  abline(h=0,lty=2,col="lightgrey")
  lines(cumsum(EddyData2013BF.F$NEE_f)*12/1000000*1800,type='l',col=2)

##### Environment factors
  plot(EddyData2013BF.F$PAR_f,EddyData2013BF.F$NEE_f,xlim=c(0,2000),
  ylim=c(-30,20))

##### Energy balance
#### EBC
  message('Linear regression results')
  plot(EddyData2013BF.F$Ein,EddyData2013BF.F$Eout,xlim=c(-150,800),
  ylim=c(-150,800),xlab=labRnwm2,ylab='',col="skyblue")

```

```

lm.r=lm(EddyData2013BF.F$Eout ~ EddyData2013BF.F$Ein)
abline(lm.r,col=2)
summary(lm.r)

##### EBC with intecept = 0
message('Linear regression results, intecept=0')
lm0.r=lm(EddyData2013BF.F$Eout ~ -1+EddyData2013BF.F$Ein)
abline(lm0.r,col=4)
summary(lm0.r)

##### adding slop and R2
a=round(as.numeric(lm.r$coefficients[1]),2)
b=round(as.numeric(lm.r$coefficients[2]),2)
if(a>0) {cv="x+"} else {cv="x"}
teq=paste("y=",b,cv,a,sep='')
r2=round(as.numeric(summary(lm.r)$r.squared),2)
tr2=bquote(bold(R^2 == .(r2)))
mtext(labLEwm2, side=2, line=2.5)
title(main="Energy balance closure - 30 minute fluxes",font.main=2)
text(0,750,teq)
text(0,700,tr2)
abline(a=0,b=1,lwd=2)

EBR1=EddyData.F$Eout/EddyData.F$Ein
plot(EBR1,ylim=c(-10,10))
plot(EddyData.F$Ein, EddyData.F$Eout,xlim=c(-150,800),ylim=c(-150,
800))
lm.m=lmodel2(Eout ~ Ein, data=EddyData.F, "interval", "interval",99)
lm.m
abline(lm.m,col=2)
plot(lm.m,"OLS",col=4)
plot(lm.m,"RMA")

##### pollutionRose
ws=EddyData.F$wsp
dd.F=as.data.frame(ws)
dd.F <- cbind(dd.F,wd=EddyData.F$wdir)
dd.F <- cbind(dd.F,fCH4=EddyData.F$fCH4)
pollutionRose(dd.F,pollutant="fCH4",breaks=c(-0.2,-0.1,-0.05,0.,0.05,
0.1,0.15,0.2,0.25))

```